Microplastics in the Weser – North Sea transitional system: Potential pathways and methodological improvements

by

Lisa Roscher

a Thesis submitted in partial fulfilment
of the requirements for the degree of

Doctor of Philosophy in Biology

Approved Dissertation Committee

Prof. Dr. Matthias Ullrich
Constructor University

Prof. Dr. Laurenz Thomsen
Constructor University

Dr. Gunnar Gerdts
Alfred Wegener Institute

Dr. Sebastian Primpke
Alfred Wegener Institute

Date of Defense: 29th of August 2022

Department of Life Sciences and Chemistry, Constructor University Bremen

Statutory Declaration

Family Name, Given/First Name	Roscher, Lisa
Matriculationnumber	20332062
What kind of thesis are you submitting: Bachelor-, Master- or PhD-Thesis	PhD-Thesis

English: Declaration of Authorship

I hereby declare that the thesis submitted was created and written solely by myself without any external support. Any sources, direct or indirect, are marked as such. I am aware of the fact that the contents of the thesis in digital form may be revised with regard to usage of unauthorized aid as well as whether the whole or parts of it may be identified as plagiarism. I do agree my work to be entered into a database for it to be compared with existing sources, where it will remain in order to enable further comparisons with future theses. This does not grant any rights of reproduction and usage, however.

The Thesis has been written independently and has not been submitted at any other university for the conferral of a PhD degree; neither has the thesis been previously published in full.

German: Erklärung der Autorenschaft (Urheberschaft)

Ich erkläre hiermit, dass die vorliegende Arbeit ohne fremde Hilfe ausschließlich von mir erstellt und geschrieben worden ist. Jedwede verwendeten Quellen, direkter oder indirekter Art, sind als solche kenntlich gemacht worden. Mir ist die Tatsache bewusst, dass der Inhalt der Thesis in digitaler Form geprüft werden kann im Hinblick darauf, ob es sich ganz oder in Teilen um ein Plagiat handelt. Ich bin damit einverstanden, dass meine Arbeit in einer Datenbank eingegeben werden kann, um mit bereits bestehenden Quellen verglichen zu werden und dort auch verbleibt, um mit zukünftigen Arbeiten verglichen werden zu können. Dies berechtigt jedoch nicht zur Verwendung oder Vervielfältigung.

Diese Arbeit wurde in der vorliegenden Form weder einer anderen Prüfungsbehörde vorgelegt noch wurde das Gesamtdokument bisher veröffentlicht.

06.08.2023, Lisa Roscher

Date, Signature

Thesis Abstract

In recent decades, microplastics (MP) raised more and more scientific, political and societal attention due to their occurrence in ecosystems around the globe, as well as their potential to harm organisms throughout all trophic levels. An overview about their occurrence in the environment, their impact as well as examples for mitigation strategies and assessment methods are presented in **Chapter 1** (General Introduction). As distribution patterns are still not entirely understood, the present work aimed at elucidating pathways (**Chapter 2**) and potential sources (**Chapter 3**) of this emerging pollutant. Furthermore, methods for the assessment of especially small MP still face challenges, especially with respect to complex samples matrices. Therefore, method adaptations have been performed in **Chapter 3**, and two MP analysis pipelines were systematically compared and evaluated for potential discrepancies in obtained outcomes, which may be useful for future standardisation efforts (**Chapter 4**).

For the work presented in **Chapter 2**, surface water samples collected in the Weser – North Sea transitional system were analysed for the presence of MP in the size range 11−5000 µm by means of Fourier Transform Infrared (FTIR) Spectroscopy, a commonly used method for the identification and quantification of MP isolated from environmental samples. Results showed that small MP (henceforth denoted as S-MP, 11-500 µm) were predominant, with polymer compositions being dominated by the polymer cluster acrylates/polyurethanes (PUR)/varnish. Large MP (L-MP, 500-5000 µm) showed significantly lower concentrations, and were mostly assigned to polyethylene (PE) and polypropylene (PP), which are amongst the most commonly produced plastic materials and often present in consumer plastics. Overall, highest MP concentrations were measured in the turbidity maximum zone (TMZ) of the Weser River, with decreasing concentrations towards North Sea waters, which may be explained by factors such as vertical or horizontal export through currents or winds, or dilution by the wider marine water body. Finally, this study contributes to the current knowledge by providing a detailed characterisation of 23 sampling locations along the Lower Weser – North Sea transect with regards to MP concentrations, polymer compositions and size distributions.

Whilst the Weser River may act as a source for MP in North Sea waters, the question arises where MPs present in the river originate from. Herein, two Waste water treatment plants were evaluated for their potential to act as point sources for riverine MP loads in the

Weser River (**Chapter 3**). Monthly samples were collected at the effluent over one year, and processed and analysed in a similar way as performed in **Chapter 2**. Due to matrix interferences by residual plant material in the processed samples, an adaptation of the FTIR reference database have been performed during this study through the inclusion of new reference material. In addition to FTIR spectroscopy, which provides item-based information, Pyrolysis gas chromatography mass spectrometry (Py-GC/MS) was performed, in order to gain complementary mass-related MP data. Results showed that both analysis techniques showed that polyolefins were generally most abundant in samples. MP concentrations over the scope of the year could be partially explained by increased precipitation (and effluent volume) or suspended matter/TOC; however, more directed studies are necessary in order to draw final conclusions regarding the influence of underlying environmental parameters. With regards to the role of WWTPs as point sources for riverine MP, it can be stated that they were shown to contain increased MP loads in the effluent, and therefore transport MP into the river system. However, no distinct imprint could be observed with regards to polymer compositions. Increased concentrations observed downstream of the facility in Bremen-Seehausen may be due to the added MP loads in effluents; however, follow-up investigations using replicates as well as a timely more synchronised sampling could further elucidate the relationship between MP pollution levels in effluents and riverine surface waters.

In the past years, efforts have been made in order to increase the degree of automation during MP analyses. This is especially of importance for small microplastics, which generally occur in high abundances in the environment. In this context, two currently used MP analysis pipelines (namely Bayreuth Particle Finder and simple/MPAPP) were compared in **Chapter 4** by applying them to two sets of aquatic samples, investigating the respective data outputs with regards to MP abundances, polymer compositions and size distributions. This comparison showed that abundances of few polymer types showed strong discrepancies, which may be due either to the pipeline-specific grouping of polymer types, or possibly overestimations by one of the pipelines. When excluding these polymer types, MP counts as well as chemical composition was generally in accordance, with the exception of some samples, which were – interestingly – characterised by specific origins (e.g., from the Jade Bay adjacent to the North Sea) and exhibited increased amounts of suspended matter, possibly influencing the results. These observations show that the two investigated pipelines show similarities, but also still differences, which should be further worked on in

future studies, with the final aim to improve comparability as well as increase standardisation of MP analysis methods.

Through the above-presented studies, the present work aimed at providing a detailed data basis for MP pollution patterns in aquatic systems, but also attempted to highlight methodological challenges in this relatively young research field. In **Chapter 5**, the results obtained and methods applied in **Chapters 2, 3 and 4** are set into the context of the current research.

Table of contents

List of Abbreviations

ABS	Acrylonitrile butadiene styrene
ATR	Attenuated total reflectance
AWI	Alfred Wegener Institute
BASEMAN	Defining the baselines and standards for microplastics analyses in European waters (*Project*)
BEPP	Basic enzymatic purification protocol
BPF	Bayreuth Particle Finder
CMC	Chemically modified cellulose
EVA	Ethylene vinyl acetate
EVOH	Ethylene vinyl alcohol
FPA	Focal plane array
FTIR spectroscopy	Fourier transform infrared spectroscopy
HNO_3	Nitric acid
H_2O_2	Hydrogen peroxide
HQI	Hit quality index
ICBM	Institute for Biology and Chemistry of the Ocean
KOH	Potassium hydroxide
L-MP	Large microplastics
MP	Microplastics
MPAPP	MicroPlastic Automated Particle/fibre analysis Pipeline
MSFD	Marine Strategy Framework Directive
NaI	Sodium iodide
NOAA	National Oceanic and Atmospheric Administration
PA	Polyamide
PAH	Polycyclic aromatic hydrocarbons
PAN	Polyacrylonitrile
PC	Polycarbonate
PCL	Polycaprolactone
PE	Polyethylene
PEEK	Polyether ether ketone
PEST	Polyester

PET	Polyethylene terephthalate
PIM	Particulate inorganic matter
PLA	Polylactic acid
PLA-PBAT	Polylactic acid/poly(butylene adipate-co-terephthalate)
PLAWES	Plastic contamination in the model system Weser – Wadden Sea: A system-wide approach (*Project*)
PMMA	Polymethyl methacrylate
POM	Particulate organic matter
PP	Polypropylene
PS	Polystyrene
PSU	Polysulfone
PUR	Polyurethane
PVC	Polyvinyl chloride
Py-GC/MS	Pyrolysis gas chromatography mass spectrometry
QA	Quality assessment
QC	Quality control
RV	Research vessel
SDS	Sodium dodecyl sulfate
SEB	Styrene ethylene butylene
SI	Supplementary Information
siMPle	Systematic identification of MicroPlastics
S-MP	Small microplastics
SPM	Suspended particulate matter
TED-GC/MS	Thermal extraction desorption-gas chromatography/mass spectrometry
TMZ	Turbidity maximum zone
TWP	Tyre wear particles
UBT	University of Bayreuth
WWTP	Waste water treatment plant
$ZnCl_2$	Zinc chloride

Chapter 1 – General Introduction

Plastic pollution is a central problem of our world society. High production rates of plastic products are accompanied by environmental pollution, which has even reached the deep sea (Chiba et al. 2018, Tekman et al. 2020), Polar regions (Eriksen et al. 2020, Bergmann et al. 2022) or remote islands (Andrades et al. 2018). Plastic litter causes harm to the biosphere, as it was reported in numerous studies on fish (Rummel et al. 2016), birds (Ryan 2018), and mammals (Moore et al. 2020). Beside large plastic items, small-sized debris is increasingly discussed as global pollutant by researchers, stake holders and policy makers. In order to develop a common discussion base, synthetic organic pollutants <5 mm were denoted `microplastics´ (MP) (Arthur et al. 2009), which received increased attention by the scientific community in recent years. Although many studies apply this suggested upper limit, variations with regards to size classification still exist, as outlined in the overview study by Hartmann et al. (2019). As stated by the authors, other upper size limits suggested in previous literature are 1 mm (Andrady 2015, Kershaw and Rochman 2015) or 2 mm (Ryan et al. 2009). With respect to lower size limits, the studies or reports referred to in Hartmann et al. (2019) suggested various values, e.g. 1 µm (Desforges et al. 2014, Kershaw and Rochman 2015), 20 µm (Wagner et al. 2014), or 335 µm (Koelmans et al. 2017), partly based on the sampling method used. An international standard which takes into account practicability, existing technical definitions and SI prefixes is highly necessary, in order to allow for comparability of data and harmonization of assessment approaches (Hartmann et al. 2019).

MP were recorded in ecosystems worldwide (Klingelhöfer et al. 2020). Early records of MP pollution were reported in marine waters, e.g. the Sargasso Sea in the 1970s (Carpenter and Smith 1972). Following studies mostly focussed on seawater (Wagner et al. 2014), but especially in recent years, also freshwater systems were investigated with respect to MP presence (Wang et al. 2021b). Herein, rivers were shown to exhibit significant levels of plastic pollution, acting as potential pathways for MPs into the ocean. Recent studies proved MP occurrence in sediments, fish or water collected in the Amazon, Nile, and Yangtze, the three largest rivers in the world (Gerolin et al. 2020, Khan et al. 2020, He et al. 2021). Based on model estimates, highest pollution levels were recorded in Asian rivers, being in the range of $10^4 - 10^5$ tons of plastics entering the oceans yearly (Lebreton et al. 2017).

Beside various records in the aquatic environment, also pollution of terrestrial (Kallenbach et al. 2021) or atmospheric (Can-Güven 2021) systems was reported. Transport mechanisms and the identification of sources and sinks receive increased attention, in empiric as well as modelling studies, allowing for a better understanding of the `plastic problem´. The gained knowledge can act as a basis for developing solutions and mitigation strategies, which require suitable assessment methods. The following sections give an overview about the current state of knowledge concerning sources, impacts and mitigation strategies for aquatic plastic and MP pollution **(section 1.1)**, as well as commonly applied assessment techniques **(section 1.2)**. In **section 1.3**, the research aims of the present work are presented, followed by an overview of the contained studies of this cumulative thesis (**section 1.4**).

1.1 Sources, impacts and mitigation of plastic and microplastics in aquatic environments

Microplastics can be distinguished into primary and secondary MP. Primary MP are intentionally produced in a small size, dependant on the application. Examples are plastic production pellets or beads used in cosmetics or medical applications. Sources for primary MP in the aquatic environment can be, e.g. spillages at industrial sites (Lechner et al. 2014, Lechner and Ramler 2015, Karlsson et al. 2018) or household wastewaters containing microbeads from product usage (Bashir et al. 2021). Secondary MP, in contrast, derive from the fragmentation of larger plastic items and were found to be generally more abundant in environmental samples than primary microplastics (Shim et al. 2018). Possible origins are e.g., discarded consumer plastics such as food wrappers or grocery bags (Chen et al. 2021). As stated by Wang et al. (2019), a detailed assessment of shape type, size and colour can help in identifying potential sources.

A further distinction can be made between land-based and sea-based sources of MP, with land-based sources being responsible for the majority of plastics and MP present in the oceans (Galafassi et al. 2019). Examples for sea-based sources are abandoned fishing nets or other fishery-related items (Zhang et al. 2021b), shipping containers with plastic pellets lost at sea (van der Molen et al. 2021, Sewwandi et al. 2022), scratched off paint coatings from ship hulls (Gaylarde et al. 2021), or grey water from ships directly released in the water (Peng et al. 2022). Land-based sources, in contrast, can be agricultural drainage (Bigalke et al. 2022), wrongly disposed consumer plastics on beaches (Piperagkas and Papageorgiou 2021), construction sites (Wang et al. 2021a) or industrial facilities. With respect to industrial sources, Karlsson et al. (2018) conducted a case study, investigating surroundings of a polyethylene (PE) production plant in Sweden. The authors recorded the release of millions of plastic pellets per year. Furthermore, Siegfried et al. (2017) developed a model addressing the largest European Rivers, and found that the efficiency of sewage treatment is an important factor for MP pollution levels, as waste water effluents are directly discharged into the river. Finally, sources of MP in aquatic environments can be highly diverse, and require detailed assessments on both spatial and temporal scales in order to better understand origins and distribution patterns.

Once in the environment, plastics and MP are available for organisms throughout the food web. Here, it can cause harm on many different levels. Physical damage by the item itself

can occur, e.g., through the entanglement of organisms in plastic bags (Ryan 2018) or internal or external injuries caused by sharp-edged fragments. Moreover, not only the polymeric material itself, but also associated chemicals can pose a problem. In this context, intentionally added compounds such as phthalates or flame retardants may leach from environmental plastics or MP and negatively impact organisms (Zhang et al. 2018a). Besides, chemicals such as Polycyclic Aromatic Hydrocarbons (PAHs), chlorobenzenes or pesticides may be adsorbed to MPs, which then act as transport vectors (Mai et al. 2018, Fu et al. 2021). Not only chemicals were shown to be transported by MP: Previous studies showed that biofilms on MP can act as carriers for pathogenic or drug resistant bacteria, amplifying their impact in the environment (Song et al. 2020, Pham et al. 2021).

With the increasing level of plastic pollution and the resulting continuous generation of MP as well as potential harm for organisms, the need for regulations and mitigation strategies increased. The Marine Strategy Framework Directive (MSFD) was adopted in 2008, providing a guidance for member states of the European Union (EU) for working towards a good environmental status of marine waters by 2020. Herein, Descriptor 10 is dedicated to the plastic pollution problem. Moreover, in the 'Strategy for Plastics', adopted in 2018 by the European Commission, especially commonly used consumer plastics such as plates, plastic bags or cigarette butts were addressed, as they are often recorded on beaches in Europe. These large plastic items can represent a direct source for secondary MP. The 'Strategy for Plastics' aims at a reduction of the negative environmental impact of these products by reducing their production and by implementing alternatives, working towards a circular and therefore more sustainable economy. The underlying law is covered in the EU Directive 2019/904. Although sea-based litter is contributing less to the global plastic pollution than land-based sources, it can have serious local environmental impacts. Derelict fishing gear e.g., is especially threatening to the marine megafauna, as shown in a review by Stelfox et al. (2016). Moreover, Wright et al. (2021) estimated that twisted or braided ropes and filaments may emit 1277±431 MP fragments per metre of beach, which then might enter the food chain of smaller organisms. Gilman et al. (2021) state that the current understanding on life span and management of non-biodegradable fishing gear is highly limited, and recommend better monitoring and surveillance, as well as improved governance frameworks, in order to reduce both ecological and socioeconomic risks.

In order to provide a solid basis for legislative decisions and risk assessments, the generation of detailed data for the occurrence and distribution of environmental MP is

indispensable. Although methodological pipelines still strongly differ between studies, some tools and protocols have proved suitable for the analysis of MP in environmental samples. In the following, an overview of the most common methods is presented.

1.2 Methods used for the assessment of microplastics

Initially, MP were assessed rather unintentionally, as bycatch of plankton or fish surveys via net sampling (Carpenter et al. 1972, Carpenter and Smith 1972). Especially in recent decades, surveys became more and more systematic, and sampling approaches became more complex, with e.g. the usage of filter cascades (Mintenig et al. 2020) or flow through centrifugation (Hildebrandt et al. 2021) in order to address smaller size classes. Previous studies also performed a combined approach, with pump-driven filtration systems with a lower mesh size of 2−44 µm to target small MPs, in addition to net sampling with mesh sizes mostly being 100-500 µm (Cai et al. 2018, Uurasjärvi et al. 2020, Zhang et al. 2021a, Zhao et al. 2022). A combination of sampling techniques was also recommended by (De-la-Torre et al. 2022). The authors performed a literature review with the focus on the comparison between bulk and trawl sampling, and highlighted the advantages and drawbacks of both methods: Small MP as well as fibres, underestimated by trawl sampling, can be better addressed with bulk sampling (e.g., by use of a 10 L bucket), whereas trawl sampling allows for the collection of larger water volumes and are more suitable for the assessment of larger MPs. Finally, the sampling design is highly dependent on the research question asked, and limitations of applied sampling techniques should be critically assessed during investigations (e.g., underestimation of small items by net sampling).

The most basic approach for analysing MP retrieved from environmental samples is the visual examination with the naked eye or under a stereomicroscope, following pre-defined criteria (Norén 2007, Hidalgo-Ruz et al. 2012). This visual approach as a preparatory step for chemical analysis is only suitable for larger MP, as smaller items are more difficult to spot and handle manually, especially when they are embedded in a complex sample matrix. Previous studies suggested size limits for visual sorting of 500 µm (Hidalgo-Ruz et al. 2012, Löder and Gerdts 2015). For the assessment of MP morphologies, microscopical inspection in combination with imaging programs such as cellSens (Frias et al. 2020) can provide data on item dimensions, shape and colour, which can be valuable indications for potential origins. A basic approach for identifying the synthetic nature of a suspected MP item is a melting test, performed by heating a needle and observing if the item is fusing or not (commonly denoted as ‘hot needle test’) (Cutroneo et al. 2020). However, a detailed analysis of polymer compositions is only possible by means of chemical analyses, and was strongly recommended in previous studies (Gago et al. 2019, Schwaferts et al. 2019,

Primpke et al. 2020a, Ivleva 2021). Kroon et al. (2018), e.g., showed that a solely visual inspection can be highly prone to human bias. In their study, only 39% of the visually isolated plastic items were actually proved to be of synthetic origin after validation through Attenuated Total Reflectance – Fourier Transform Infrared (ATR-FTIR) spectroscopy. FTIR spectroscopy is generally based on the generation of vibrational bands by radiation with an IR beam, leading to material-specific spectra. The comparison of sample spectra to reference databases leads to the identification of polymer types with a certain probability, expressed as a so-called Hit Quality Index (HQI). ATR-FTIR is a surface technique, where the IR beam penetrates the suspected particle only to a low depth of few micrometres (Primpke et al. 2020a, Ivleva 2021). It is suitable for the analysis of larger MP, as manual handling is necessary: The item of interest is placed on a diamond crystal and fixated with a stamp before measurement. Cabernard et al. (2018) applied ATR-FTIR as well as the 'Single Particle Explorer' µRaman tool for the analysis of items >500 µm. Raman spectroscopy as well generates characteristic vibrational bands within spectra, based on Raman light scattering when the laser beam meets the molecules of the sample material. The application of both ATR-FTIR and µRaman spectroscopy on the same items showed a general accordance with respect to the resulting polymer assignments and MP numbers, with a marginally higher identification rate by µRaman (Cabernard et al. 2018).

Another ATR-based technique is µATR, where items positioned on a filter, glass slide, or similar surface are brought into close contact with the germanium crystal – containing objective (Käppler et al. 2018, Szewc et al. 2021). Käppler et al. (2018) applied µATR in combination with Pyrolysis gas chromatography mass spectrometry (Py-GC/MS) on suspected MP items in the size range 500-5000 µm, isolated from river bed sediments. The complementary application of Py-GC/MS provides data on particle masses, and is based on the detection of characteristic decomposition products after pyrolysis of the sample (Fischer and Scholz-Böttcher 2017). Käppler et al. (2018) found a general accordance between both techniques especially with regards to the most common plastic types (PE, PP, PS, PET), and highlighted the advantage of their complementing character. In conclusion, for the analysis of larger MP items, the combination of a visual preparatory step together with subsequent chemical analysis via vibrational spectroscopy (ideally in combination with mass spectroscopy) can be seen as a suitable tool.

For smaller size classes, e.g., <500 µm, sample preparation as well as analysis techniques are generally more complex. The reduction of especially biogenic material from

environmental samples is of high importance, as small items are more easily overlaid by these materials, hindering an accurate detection. Different approaches for the maceration of sample material exist, ranging from alkaline or acidic digestion methods, oxidizing digestion to enzymatic digestion (Stock et al. 2019). Previous studies also applied combined protocols, e.g., enzymes in combination with one or more oxidative steps (Löder et al. 2017, Möller et al. 2022). A density separation step is often applied in addition in order to separate heavier sample material such as sediment grains from the lighter sample fraction, containing the suspected MP. Commonly applied salt solutions are e.g., NaCl or $ZnCl_2$, exhibiting densities of 1.0−1.2 g cm^{-3} and 1.6-1.8 g cm^{-3}, respectively (Gago et al. 2019), addressing polymers with a respective lower density. Important factors influencing the choice of the applied solution are cost efficiency, level of environmental hazard or achievable density, with the latter being of relevance for the targeted MP (Stock et al. 2019).

As outlined for larger MP, also for the chemical analysis of small MP vibrational spectroscopy was commonly utilized in previous studies. Prior to the measurement, putative MP items are enriched on a filter, slide or similar surface, by either pipetting or filtration. For the subsequent chemical analysis, µRaman e.g. was used for the analysis of MP >1 µm isolated from water (Cabernard et al. 2018, Fortin et al. 2019), sediment (Sobhani et al. 2019) or biota samples (Domogalla-Urbansky et al. 2019, Sevillano-González et al. 2022). Furthermore, µFTIR in combination with a focal plane array (FPA) detector has been commonly applied and recommended in previous studies (Löder et al. 2015, Simon et al. 2018, Primpke et al. 2020a), allowing for a mostly automated chemical imaging of measurement filters. Different methods are available for the subsequent processing of spectral information, including manual integration of relevant IR bands and subsequent visual evaluation based on chemical images (Löder et al. 2015), or more advanced and automated approaches based on image analysis and a comparison with an underlying reference database through spectral correlation (Primpke et al. 2018, Primpke et al. 2019, Primpke et al. 2020b). Another identification approach is the usage of Random Forest Networks, which identifies MP items based on polymer-specific spectral descriptors (Hufnagl et al. 2019). Furthermore, as stated above for large MP, a complementary analysis with Py-GC/MS can be also performed with small MP, as shown in a previous study on MP in drinking water (Kirstein et al. 2021). In summary, MP <500 µm require a more elaborate sample processing, and with respect to vibrational spectroscopy a rather automated analysis

of filters was shown to be most suitable, as manual pre-selection is not practical due to the small size.

Although the gained knowledge on MP identification processes based on vibrational spectroscopy data raised significantly within the last decade, further development and improvement is required in order to solve remaining challenges such as the analysis of smallest MP or even nanoplastics, disturbances by residual biogenic sample materials, and further automation in order to allow for high sample throughputs (Ivleva 2021). Herein, adequate QA/QC measures as well as the implementation of (and compliance to) standard protocols are highly necessary and should have priority in research projects.

1.3 Research aims

As stated in the previous sections, the distribution of MP in the environment is highly complex, and detailed data are needed as a basis for modelling studies, risk assessments, and subsequent implementation of adequate countermeasures. The investigation of aquatic environments themselves, but also of potential sources are of high relevance for a better understanding of the underlying dynamics. Being embedded in the joint FONA project PLAWES (**Pla**stic contamination in the Model system **Wes**er – Wadden Sea: A system-wide approach; https://bmbf-plastik.de/de/verbundprojekt/plawes), the present work investigated the status of pollution in surface waters in the interface between freshwater and marine waters, using the example of the Weser–Wadden Sea transitional system (Roscher et al. (2021), **Chapter 2**). By means of a sampling campaign conducted in April 2018 as well as subsequent microscopical and FTIR analysis of MP items within the size range 11-5000 µm, the status of MP pollution in surface waters from the Weser-Wadden Sea transitional system was assessed. Herein, the research objectives were **(a)** a detailed assessment of the distribution of MP along the Weser-Wadden Sea transitional system with regards to environmental concentrations and polymer compositions, as well as **(b)** a distinct morphological characterisation of detected MP (especially MP 500-5000 µm), which may provide information on possible origins, as well as a solid data basis for modelling or risk assessment studies.

Furthermore, potential point sources, namely WWTPs discharging into the river system, were investigated (Roscher et al. (2022), **Chapter 3**). Complementary approaches using both item- and mass-based MP analysis techniques are scarce in current research. The study presented in **Chapter 3**, based on a year-long sampling campaign, targeted MP loads in WWTP effluents by FTIR analysis of MP in the size range 11-5000 µm (in accordance with the approach followed in **Chapter 2**) as well as Py-GC/MS analysis for the complementary assessment of masses. Thereby, it was aimed at evaluating the role of WWTPs as potential point sources for riverine MP, through the assessment of **(a)** polymer compositions, **(b)** characterisation of MP morphologies and **(c)** both mass and item concentrations in WWTPs effluents. Besides providing a detailed data basis, this study also contained the optimisation of the underlying polymer database, and can therefore help avoiding false-positive assignments due to interfering biological material in future studies.

Especially for small MP (i.e., <500 µm down to ~10 µm), the application of a suitable analysis tool is of great importance, as this size fraction is known to be most numerous, and also most complex to analyse. Therefore, the study contained in **Chapter 4** (Moses et al. 2023) aimed at a critical comparison of two analysis pipelines applied for the assessment of MP in the framework of the joint project PLAWES, in order to evaluate their applicability and potential limitations. For this purpose, the resulting data output of both pipelines was compared with regards to the typically assessed information, being **(a)** MP abundance, **(b)** polymer composition and **(c)** size distributions. Similarities and differences were critically investigated and set into context with associated studies, working towards a better comparability of analysis pipelines and an increase of reliability of results. Finally, the knowledge gained in the studies presented in **Chapters 2-4** was set into the broader scientific context in **Chapter 5**, with a special focus on (a) the discussion of the here applied analysis techniques under consideration of currently applied methods in this research field (as well as possible improvements), (b) the contextualisation of the obtained MP data with regards to other works on aquatic systems in Germany, and c) a final conclusion drawn from the knowledge gained in the framework of this thesis.

1.4 Overview of studies

The core of this thesis consists of three scientific studies, which have been published in the peer-reviewed journals *Environmental pollution*, *Science of the Total Environment*, and *Analytical and Bioanalytical Chemistry* **(Chapter 2, 3, and 4**, respectively**).** In the following, the context and main content of the three manuscripts are outlined.

Microplastic pollution in the Weser estuary and the German North Sea (Chapter 2)

*Published in: Environmental pollution, **288:**117681 (November 2021)*
https://doi.org/10.1016/j.envpol.2021.117681

Lisa Roscher[a], Annika Fehres[a], Lorenz Reisel[a], Maurits Halbach[b], Barbara Scholz-Böttcher[b], Michaela Gerriets[b], Thomas H. Badewien[b], Gholamreza Shiravani[c], Andreas Wurpts[c], Sebastian Primpke[a], Gunnar Gerdts[a]

[a] Alfred Wegener Institute, Helmholtz Centre for Polar and Marine Research, D-27483 Helgoland, Germany

[b] Institute for Chemistry and Biology of the Marine Environment (ICBM), Carl von Ossietzky University of Oldenburg, D- 26111 Oldenburg, Germany

[c] Lower Saxony Water Management, Coastal Defence and Nature Conservation Agency (NLWKN), D-26548 Norderney, Germany

This manuscript studies the MP pollution in surface waters of the Lower Weser and transition to the North Sea, and was produced in the framework of the project FONA PLAWES. Sampling campaigns were conducted in April 2018 by the ICBM (Institute for Chemistry and Biology of the Marine Environment; RV Otzum) in the Lower Weser stretch, and by the AWI (Alfred Wegener Institute, RV Uthörn), in the case of the Outer Weser and North Sea stations. Water samples collected by the ICBM were transported to the AWI Helgoland for sample processing and analysis. Lisa Roscher, Dr. Gunnar Gerdts, Maurits Halbach, Prof. Barbara Scholz-Böttcher, Michaela Gerriets, Dr. Thomas Badewien, Gholamreza Shiravani, and Dr. Andreas Wurpts were substantially involved in the planning and/or performance of the sampling campaign. Laboratory work was conducted by Lisa Roscher, supported by Annika Fehres and Lorenz Reisel. The supervision was held by Dr. Gunnar Gerdts and Dr. Sebastian Primpke. Lisa Roscher conducted the final data analysis

and preparation of the manuscript. All authors were involved in the editing of the manuscript, and approved the final version.

This study gives a comprehensive insight into the status of MP pollution in surface waters of the Lower Weser and transition to the North Sea. Two size fractions, large MP (L-MP, 500-5000 µm) and small MP (S-MP, 11-500 µm) were analysed. Results show that the vast majority of MP items were recorded in the smaller size fraction. Herein, highest abundances were recorded in the turbidity maximum zone (TMZ) of the river. Polymer compositions differed strongly: S-MP were mostly assigned to the polymer cluster acrylates/PUR/varnish, whereas L-MP were mainly identified as PE and PP. By studying this important interface between freshwater and marine systems, this work contributes to a better understanding of MP distribution patterns, but also identifies and highlights current knowledge gaps, which can be helpful for future monitoring studies.

Microplastics in two German wastewater treatment plants: Year-long effluent analysis with FTIR and Py-GC/MS (Chapter 3)

Published in: Science of the Total Environment ***817:****152619 (April 2022)*
https://doi.org/10.1016/j.scitotenv.2021.152619

Lisa Roscher*[a], Maurits Halbach*[b], Minh Trang Nguyen[a], Martin Hebeler[c], Franziska Luschtinetz[d], Barbara Scholz-Böttcher[b], Sebastian Primpke[a], Gunnar Gerdts[a]

[a] Alfred Wegener Institute, Helmholtz Centre for Polar and Marine Research, D-27483 Helgoland, Germany
[b] Institute for Chemistry and Biology of the Marine Environment (ICBM), Carl von Ossietzky University of Oldenburg, D-26111 Oldenburg, Germany
[c] hanseWasser Bremen GmbH, D-28217 Bremen, Germany
[d] Kasselwasser, D-34125 Kassel, Germany
* *Shared first-authorship*

This study investigates the MP pollution in the effluents of two WWTPs, located in Bremen-Seehausen and Kassel. As stated for **Chapter 2**, also this work was performed in the framework of the project FONA PLAWES, in cooperation with the ICBM, as well as the WWTP operators (Bremen: Hansewasser GmbH, Kassel: KasselWasser). Sampling was conducted from July 2018 – June 2019. After an initial instruction on-site by Lisa Roscher, staff of the WWTPs performed a monthly sampling at the effluent outlet. Samples were

transported to the AWI Helgoland for sample processing and analysis. Dr. Martin Hebeler and Dr. Franziska Luschtinetz were substantially involved in the supervision of sampling activities at the WWTP sites, and in regular discussions about obtained findings with respect to WWTP background parameters. Laboratory work was performed by Lisa Roscher, supported by Minh Trang Nguyen, and supervised by Dr. Gunnar Gerdts and Dr. Sebastian Primpke. In addition to FTIR analysis at the AWI Helgoland, also Py-GC/MS analyses were conducted. Therefore, shares of the samples were transferred to the PLAWES project partners at the ICBM and analysed by Maurits Halbach under the supervision of Prof. Dr. Barbara Scholz-Böttcher. This cooperation led to the shared first authorship of Lisa Roscher and Maurits Halbach, allowing a complementary assessment of MP item and mass concentrations using FTIR and Py-GC/MS. All authors were involved in the reviewing and editing of the manuscript.

Results showed a general dominance of polyolefins in both mass and item values. Morphology and polymer composition were similar in both WWTP; however, the WWTP in Bremen-Seehausen showed higher item and mass concentrations, possibly due to the characteristics of inflowing wastewater or shorter settling and pre-clarification times in Bremen. Furthermore, high MP levels were often accompanied by increased effluent volumes, but also elevated turbidity. On the whole, this study gives a comprehensive overview of MP pollution in WWTPs over a whole year. It hereby contributes to the current MP research with a solid data basis, and allows for an initial evaluation of the role of WWTPs as sources for riverine MP pollution.

Comparison of two rapid automated analysis tools for large FTIR microplastic data sets (Chapter 4)

Published in: Analytical and Bioanalytical Chemistry 1-13 (2023)
https://doi.org/10.1007/s00216-023-04630-w

Sonya Moses*[a], Lisa Roscher*[b], Sebastian Primpke[b], Benedikt Hufnagl[c,d], Martin G. J. Löder[a], Gunnar Gerdts[b#], Christian Laforsch[a#]

[a] Department of Animal Ecology I, University of Bayreuth, Universitätsstr. 30, 95440 Bayreuth, Germany
[b] Alfred-Wegener-Institute Helmholtz Centre for Polar and Marine Research, Biologische Anstalt Helgoland, Kurpromenade 201, 27498 Helgoland, Germany
[c] Institute of Chemical Technologies and Analytics, Vienna University of Technology, A 1060 Vienna, Austria
[d] Purency GmbH, A 1010 Vienna, Austria
* *Shared first-authorship*
[#] *Shared senior authorship*

This study aimed at evaluating the comparability of the two MP analysis tools siMPle and Bayreuth Microplastic Finder (BPF), which were applied for MP analyses within the project PLAWES. Being based on different mathematical principles and algorithms as well as QA/QC approaches, discrepancies in data outputs can be expected to a certain degree. In order to compare both pipelines, a selection of samples obtained during the MP assessments in PLAWES for Middle and Upper Weser (initial analysis performed by University of Bayreuth, in the following abbreviated as UBT) as well as Lower and Outer Weser (initial analysis by AWI, cf. **Chapter 2**) were re-analysed with the respective other analysis pipeline, and results were evaluated for similarities and differences with regards to polymer composition, MP counts and size distributions. Dr. Sebastian Primpke and Benedikt Hufnagl were substantially involved in the development of the software tools and contributed with the respective expertise to the study. Dr. Martin Löder, Prof. Christian Laforsch and Dr. Gunnar Gerdts were involved in the conceptualisation and supervision of the study. The cooperation between AWI and UBT led to a shared first authorship of Sonya Moses and Lisa Roscher, who performed the data analysis and wrote the original manuscript.

Chapter 2 – Microplastic pollution in the Weser estuary and the German North Sea

Lisa Roscher[a], Annika Fehres[a], Lorenz Reisel[a], Maurits Halbach[b], Barbara Scholz-Böttcher[b], Michaela Gerriets[b], Thomas H. Badewien[b], Gholamreza Shiravani[c], Andreas Wurpts[c], Sebastian Primpke[a], Gunnar Gerdts[a]

[a] Alfred Wegener Institute, Helmholtz Centre for Polar and Marine Research, D-27483 Helgoland, Germany

[b] Institute for Chemistry and Biology of the Marine Environment (ICBM), Carl von Ossietzky University of Oldenburg, D- 26111 Oldenburg, Germany

[c] Lower Saxony Water Management, Coastal Defence and Nature Conservation Agency (NLWKN), D-26548 Norderney, Germany

Corresponding author: Lisa Roscher (lisa.roscher@awi.de)

Keywords: Microplastics**,** Plastic pollution, Freshwater system, River system, Infrared spectroscopy

Citation:

Roscher, L., Fehres, A., Reisel, L. *et al.* Microplastic pollution in the Weser estuary and the German North Sea. *Environ Pollut* 288 (2021):117681.
https://doi.org/10.1016/j.envpol.2021.117681

Abstract

Microplastics (MP) are defined as synthetic organic pollutants sized <5 mm and have been recorded in various environments worldwide. Due to their small size, they pose a potential risk for many organisms throughout the food web. However, little is known about MP distribution patterns and associated transport mechanisms. Rivers may act as pathways for MP into marine environments. In this study, we investigate the occurrence of MP in the estuary and lower stretch of the second-largest German River, the Weser, representative of a significant interface between fresh water and marine environments. The aim of the study was to enhance the general understanding by providing novel, comprehensive data and suggestions for future studies on estuarine systems. Surface water samples of two different size classes were collected by ship using an on-board filtration system (11–500 µm fraction) and net sampling (500–5000 µm fraction). After a thorough sample preparation, all samples were analysed with Focal Plane Array (FPA) Fourier Transform Infrared (FTIR) spectroscopy and Attenuated Total Reflection (ATR) FTIR spectroscopy in order to obtain information on MP concentrations, polymer composition and size distribution. Our findings show highest concentrations in the 11–500 µm fraction ($2.3 \times 10^1 - 9.7 \times 10^3$ MP m^{-3}), with the polymer cluster acrylates/polyurethanes(PUR)/varnish being dominant. The >500 µm fraction was dominated by polyethylene. Estimated MP concentrations generally increased in the Turbidity Maximum Zone (TMZ) and decreased towards the open sea. This study contributes to the current research by providing novel insights into the MP pollution of the estuary and lower stretch of an important European river and provides implications for future MP monitoring measures.

2.1 Introduction

The increasing plastic production and consumption in previous decades was accompanied by rising amounts of plastic waste, entering the environment either accidently or intentionally (van Emmerik and Schwarz 2020). Once there, plastic items pose a potential threat to organisms, e.g., by entanglement in plastic ropes, damage by the ingestion of sharp-edged items or starvation through intestinal blockage. The smaller the plastic debris, the higher the potential for ingestion by organisms at the lower size-range of the food web, leading to an increased ecotoxicological risk (Ma et al. 2019). In order to address this small-sized plastic debris, 'microplastics' (MP) were defined as synthetic polymers sized <5 mm during the 'International Research Workshop on Occurrence, Effects and Fate of Microplastics Marine Debris' (Arthur et al. 2009). Furthermore, studies distinguished between primary and secondary MP, with relation to their source: primary MP are intentionally produced in a small dimension, e.g., in plastic production (virgin pellets) or in the cosmetics industry (abrasives in body cleansers). Secondary MP derive from the fragmentation of plastic items, e.g. through environmental factors such as wave action or UV radiation (Barnes et al. 2009). Yet, the distinction between primary and secondary MP is not always possible with regard to environmental samples, as e.g. fragment-like items are often intuitively assigned to secondary MP fragmented by environmental factors, although primary MP could also be designed intentionally in this form (Hartmann et al. 2019).

MP have been recorded in various ecosystems, and were detected even in remote locations, e.g., in water, ice, snow and sediment of the Polar regions (Waller et al. 2017, Peeken et al. 2018, Bergmann et al. 2019, Tekman et al. 2020). Whilst initial studies focused on small-sized plastic debris in marine ecosystems (Carpenter et al. 1972, Carpenter and Smith 1972, Colton et al. 1974), recent studies follow a more holistic approach. Distribution patterns are systematically investigated including the attempt to identify potential sources and sinks of MP (Kataoka et al. 2019, van Emmerik and Schwarz 2020), including taking into account modelling approaches (Siegfried et al. 2017, van Wijnen et al. 2019). Herein, rivers were considered as potential pathways for MP from land-based sources into the oceans and received more attention in recent years (Dris et al. 2015, Hitchcock and Mitrovic 2019, Mani and Burkhardt-Holm 2020, Mintenig et al. 2020).

The River Weser, being the subject of the present study, is the second-largest river in Germany. It passes industrial and urban areas, before discharging into the North Sea at the

port of Bremerhaven, a hotspot of shipping activity. Thus, being an aquatic system with strong anthropogenic pressure, the Weser estuary represents an ideal model system for the analysis of transitional MP distribution patterns. To our knowledge, no comprehensive data are available and published yet on MP pollution in this system.

The aim of the present study is to provide insights into the status of MP pollution in surface waters of the Weser estuary and the adjacent German North Sea. Herein, the following research questions were addressed: i. Do MP abundances and polymer compositions change along the transitional system? ii. What are the morphological characteristics of detected MP? By addressing these questions, we attempt to evaluate the potential of the lower stretch of the River Weser as a pathway for MP into the North Sea, hypothesizing higher pollution levels in proximity to areas with increased anthropogenic activity. For this purpose, FTIR (Fourier Transform Infrared) spectroscopy was chosen as analytical tool, having been proved suitable for the chemical identification and assessment of item concentrations of environmental MP (Haave et al. 2019, Lorenz et al. 2019).

2.2 Material and Methods

2.2.1 Sampling site

The River Weser originates in Lower Saxony by the confluence of the rivers Werra and Fulda, yielding a total length of 733 km and catchment area of 46,300 km^2 (Zhao et al. 2015b). Adjacent land use is dominated by agricultural activities, with grassland/pasture being the main land use type in the northern catchment area (Hirt et al. 2008).

The focus of the present study is the transitional zone between the estuarine part of the River Weser, and the German North Sea (**Fig. 2.1 A**). The channel-like Lower Weser is situated between the cities of Bremen and Bremerhaven and is highly influenced by the tides, with a tidal range of 3.6–4 m (Grabemann and Krause 2001, Papenmeier et al. 2014). The official starting point of the Lower Weser is located approx. 5 km downstream of the Weser Weir (Bremen), which separates the tidal zone from the Middle Weser stretch (for better legibility, also sampling stations located <5 km downstream the Weir will be assigned to the Lower Weser in the following). The funnel-like Outer Weser starts at Bremerhaven and forms the transitional zone towards North Sea waters. Lower and Outer Weser form an important waterway, linking the ports of Bremen and Bremerhaven to the Southern North Sea (Krämer et al. 2019). The mean freshwater discharge into the North Sea amounts to approx. 330 $m^3 s^{-1}$ (Zorndt et al. 2012, Stanev et al. 2019). Furthermore, the River Weser exhibits a pronounced Turbidity Maximum Zone (TMZ) between Brake and Bremerhaven. It is approx. 15–20 km long and characterized by increased suspended sediment concentrations (Grabemann and Krause 2001, Schrottke et al. 2006, Hesse et al. 2019).

2.2.2 Sample collection

Surface water samples were taken in April 2018 with the RV Otzum and the RV Uthörn at 23 sampling stations. Nine stations were located in the Outer Weser and at the North Sea margin. Thirteen sampling stations were situated in the Lower Weser and the adjacent Jade Bay, and one station upstream of the Weser Weir (station 53) (**Table S1, Fig. 2.1**). Sampling started approx. 30 min after high tide, aiming at riverine water flowing towards the North Sea. Two sampling stations were sampled consecutively. Environmental parameters recorded during sampling are documented in **Table S2**. For the assessment of suspended particulate matter (SPM), triplicate station water samples were filtered on-board using glass fibre filters (GF/F, Whatman, UK). Filters were stored frozen until the determination of particulate inorganic and organic matter (PIM and POM).

2.2.2.1 Small microplastics (S-MP, 11–500 µm)

An in-house designed filtration system was used for sampling MP in the 11–500 µm size range (**Fig. S1**), allowing surface water sampling within a depth of approx. 1 m. It consisted of a stainless steel floating suction basket (Wolftechnik, Germany; mesh size: 500 µm), two membrane pumps (Xylem, USA), and a stainless-steel filter stand (Sterlitech, USA). Polyvinyl chloride (PVC) hoses connected the different elements, with an outlet flowmeter (Gardena, Germany) measuring sample volumes. This set-up allowed for the on-board filtration of surface water onto 15 µm filter screens (Ø 293 mm; GKD, Germany). The screens were transferred into 2 L glass jars, containing 500 mL of 1% sodium dodecyl sulfate (SDS; w/v; Carl Roth, Germany), and stored at 4 °C until further analysis.

2.2.2.2 Large microplastics (L-MP, 500–5000 µm)

MP in the 500–5000 µm size range were sampled with a microplastic net (**Fig. S1**; mesh size: 300 µm; Hydro-Bios Apparatebau GmbH, Germany), having a net opening of 0.4 × 0.7 m. It was towed for up to 20 min at approx. 3 knots. A mechanical flowmeter attached to the net allowed for the assessment of sampling volumes (Table S1). Sample material from the net beaker was transferred into 1.5 L glass jars (RV Uthörn) or 1 L PVC containers (RV Otzum). Remaining material attached to the inner wall of the net beaker was flushed into the sampling containers using station water. A total of 10 g of SDS pellets (Carl Roth, Germany) was added to the samples in order to obtain an approx. SDS concentration of 1% (w/v), preserving the samples from fungal growth and allowing a pre-digestion of the

sample material. For samples collected with the RV Uthörn, SDS had been prepared in the glass jars beforehand, whereas samples taken with the RV Otzum underwent the SDS treatment after transfer of the sample material into glass jars. Prior to further processing, samples were either stored at 4 °C (glass jars) or frozen at −4 °C (PVC bottles).

2.2.3 Isolation of MP from the sample matrix

2.2.3.1 Small microplastics (S-MP, 11–500 µm)

Purification of the 11–500 µm sample fraction followed the enzymatic-oxidative protocol introduced by Löder et al. (2017) and applied by Lorenz et al. (2019), with slight modifications. First, the sample material collected on the stainless-steel filters was subjected to a 10% SDS solution (w/v, Carl Roth), and incubated for 24 h at 50 ◦C. The sample material was then concentrated on 47 mm stainless-steel screens (mesh size: 18 µm, Haver&Boecker OHG, Germany). These were mounted to the lower part of our in-house developed MP-Reactors, which allow for a reduction of processing steps and reduce the risk of sample loss or contamination (Gerdts 2018). As described in Lorenz et al. (2019), the technical enzymes protease, cellulose, and chitinase (ASA Spezialenzyme GmbH 2005a, 2005b, 2005c) as well as hydrogen peroxide were added sequentially in order to further macerate the biogenic material.

Subsequently, a density separation with $ZnCl_2$ was performed (density: approx. 1.7 g cm^{-3}) to remove heavy inorganic material. The upper phase, containing potential MP, was recovered and concentrated on stainless steel gauzes (mesh size: 15 µm; GKD, Germany). For accompanying investigations within the joint project PLAWES (Microplastic Contamination in the Weser-Wadden Sea – National Park Model System: an Ecosystem-Wide Approach), the filters were cut into two halves using stainless steel scissors. One filter half was transferred to the Institute for Chemistry and Biology of the Marine Environment (ICBM; for further Pyrolysis-GC/MS analysis). The other half of the sample material was concentrated on aluminium oxide filters (Ø 25 mm; 0.2 µm pore size; Anodisc, Whatman, UK) in preparation for the µFTIR measurement. Depending on the residual material load in the processed samples, between 1 and 11 Anodisc filters were prepared per sample (**Table S3**). This was necessary, as overlaying sample material would hamper an accurate measurement. The approach to analyse the entire purified sample material designated for µFTIR analyses was based on a recent study by Abel et al. (2021), showing the risk of over- and underestimation of MP when extrapolating from small

subsamples. Anodisc filters were stored in petri dishes and dried for at least 24 h at 37 °C or in a desiccator.

2.2.3.2 Large microplastics (L-MP, 500–5000 µm)

Before further treatment, net samples containing approx. 1% SDS were incubated for approx. 24 h at 50 °C in order to pre-digest organic material. Samples were filtered onto a stainless-steel sieve (mesh size: 500 µm) and rinsed with filtered tap water (pre-filtered over 5 µm stainless-steel screens; Haver&Boecker OHG, Germany). Sample material >500 µm was investigated using a stereomicroscope (Olympus SZX16, Olympus, Germany). Putative MP items were selected based on the following criteria: the lack of cellular structures, bright and even coloration, and a solid texture (Norén 2007). Each putative MP item was photographed with a microscope camera (Olympus DP26 Digital Camera, Olympus), coupled to the imaging software CellSens (Olympus, Germany). With the same software, the major and minor dimension of the putative MP items were measured, following the approach of Simon et al. (2018). Here, the major axis was defined as the longest continuous axis passing the centre of the item, and the minor axis as the longest dimension perpendicular to the major axis (henceforth denoted as length and width). Putative MP were assigned to specific shape-related groups: pellets, fragments, films, spheres, foams, fibres and lines/filaments. This followed the standardized monitoring protocol presented by Gago et al. (2019), with slight modifications. Discrimination between fibres and filaments has been shown to be challenging in previous studies (Baldwin et al. 2016). In this study, fibres were defined as threads with a diameter up to 50 µm, whereas the diameter of lines/filaments was defined as >50 µm (Tanaka and Takada 2016, Kühn et al. 2020). Selected fibres were analysed, but finally excluded from the assessment, as they represent the shape type most prone to airborne contamination (Song et al. 2021b).

2.2.4 Spectroscopic analysis

2.2.4.1 Small microplastics (S-MP, 11–500 µm)

Putative S-MP, concentrated on Anodisc filters, were measured with a FTIR microscope (Hyperion 3000, connected to a Tensor 27 spectrometer; Bruker Optik GmbH, Germany), using a Focal Plane array (FPA) detector and the software OPUS 7.5 (Bruker Optics GmbH, Germany). Before the measurement, Anodisc filters were covered with a BaF_2 window, maintaining all items within the focal plane of the FTIR microscope, which especially

enhances the assessment of fibre-like MP (Primpke et al. 2019). A 3.5x IR objective was used, resulting in a reduced measurement time of approx. 4 h. A spectral range of 3600−1250 cm^{-1} was chosen, with 32 scans for MP measurements (background: 64 scans). Further settings were a spectral resolution of 8 cm^{-1}, Blackman-Harris 3-term apodization and a zero-filling factor of 2. A grid of 20–22 measurement fields was applied in order to cover the whole filtration area. The lower detection limit provided by the instrument was 11 µm. Resulting infrared spectra were processed with the software OPUS 7.5, followed by the polymer identification tool siMPle (Primpke et al. 2020b) coupled to the reference database designed by Primpke et al. (2018). The image analysis via MPAPP (Primpke et al. 2019) was performed based on the spectral matching thresholds presented in Lorenz et al. (2019), providing data on MP numbers, sizes and assigned polymer cluster (in the following denoted as 'polymer type').

2.2.4.2 Large microplastics (L-MP, 500–5000 µm)

Putative L-MP were measured with Attenuated Total Reflection (ATR)-FTIR (Bruker Tensor 27 coupled to diamond platinum ATR unit, Bruker Optik GmbH, Germany). Selected items were placed on the diamond crystal, and three replicate spectra were recorded with a resolution of 4 cm^{-1} and 32 co-added scans (spectral range: 400-4000 cm^{-1}). Further settings were a Blackman-Harris 3-term apodization and a zero filling factor of 2. This was followed by a comparison to our inhouse reference polymer database (Primpke et al. 2018). Spectral similarity of 70–100% led to identification of the polymer. When obtaining hit qualities of 60–70%, the spectrum was validated or rejected based on visual re-evaluation (Kroon et al. 2018). Measurements with hit qualities below 60% were defined as 'not identified'. A share of 2.4% of MP items was assigned to polymer types which are not included in the clusters defined by Primpke et al. (2018), but clearly showed a synthetic appearance (ethylene/propylene, SEB, EVOH). These polymer types are included in L-MP estimates and denoted as 'others'. The handling of small-sized or very thin fibres proved challenging during FTIR-ATR measurements. Instead, potential MP fibres were placed on an Anodisc filter, covered with a BaF2 window and analysed in the same way as S-MP. A visual re-evaluation step of spectra was added whenever necessary.

2.2.5 Contamination mitigation

In order to avoid contamination during sample handling, several safety measures were followed. These are presented in **Section S1**.

2.2.6 Data evaluation

Based on MP numbers and sampling volumes, MP item concentrations [n (MP) m^{-3}] were estimated for both S-MP and L-MP separately (in the following denoted as MP concentrations).

For statistical analyses, both fractions were combined. In order to relate MP distribution patterns to the environmental and geographical context, regression analyses were conducted based on MP concentrations, conductivity and the location along the sampling transect. The latter was denoted as 'distance from Weser Weir' and determined using the distance measurement tool in ArcGIS Pro 2.4.0 (reference point: 53.0604087° North, 8.8601435° East). Station 20 and 45 were excluded from statistical analyses, as referring data points had been identified as outliers through studentized residual diagnostics in SigmaPlot 11.0. Regression analysis of the variables MP concentration and 'distance from Weser Weir' was based on data collected in the whole investigated riverine-estuarine transect, whereas linear regression of the variables MP concentration and conductivity, illustrating the transition towards the North Sea, was performed using conductivity data from station 41 on (**Table S2**). Furthermore, correlation analyses were performed in Statistica 13 based on MP concentrations and SPM, PIM and POM. Spearman Rank Correlation was chosen (significance level: $p < 0.05$), as data were not normally distributed.

In order to identify specific groupings of sampling stations regarding polymer compositions, a non-hierarchical kR clustering coupled to a similarity profile test (SIMPROF, significance level: 5%, permutations: 999) was performed in Primer 7 (Primer-e, New Zealand). This was based on square root transformed data arranged in a Hellinger distance matrix, which does not put a strong weighting on rare polymers (Legendre and Gallagher 2001, Lorenz et al. 2019). In order to identify the most important polymer types representing the corresponding groups, a Kolmogorov-Smirnov test was performed in Statistica (significance level: $p < 0.05$).

2.3 Results

2.3.1 Microplastic abundance and polymer composition

2.3.1.1 Small microplastics (S-MP, 11–500 µm)

As stated in **section 2.2.3**, the entire purified sample material designated for µFTIR analyses was concentrated on 1–11 Anodisc filters per sample prior to the measurements (**Table S3**). By adding up the results of the individual subsamples before relating them to the sample volume, the estimated S-MP concentrations and polymer compositions were assessed.

Estimated S-MP concentrations in the transitional zone Weser-North Sea ranged from 2.3 × 10^1 MP m^{-3} at station 19 (North Sea margin) to 9.7 × 10^3 MP m^{-3} at station 45 (TMZ) (**Fig. 2.1B**). Elevated concentrations were recorded in proximity to the port of Bremerhaven, decreasing steadily along the Outer Weser transect. Station 20, situated at the North Sea margin, showed an exception here, yielding the second highest estimated MP concentration (**Fig. 2.1B**).

The dominant polymer type was acrylates/polyurethanes/varnish (acrylates/PUR/varnish), accounting for 66.7% of all detected MP items, and being the only polymer type present in all sampling stations (**Fig. 2.1A**, **Fig. S2**). Second-most polymer type was Rubber type 3 (9.8%), followed by polypropylene (PP; 6.0%), which was only absent in stations 19 and 30 d. In total, twenty different S-MP polymer types were detected. Polymer diversity varied from 3 to 17 different types detected (station 41 and 45, respectively) (**Fig. S3**). Highest diversity was recorded in the sampling station with the highest estimated S-MP concentration (station 45). Sampling stations at the North Sea margin (stations 19 and 30 d) showed low MP diversities and equally low estimated concentrations compared to most of the Lower Weser stations.

The consideration of the entire sample material for MP estimates, as applied here, proved appropriate: a theoretical extrapolation of MP concentrations based on individual subsamples revealed strong variations in the extent of over- or underestimation (**Fig. S4**, **Table S4**). Subsample 1/3 obtained for station 20, e.g., yielded a MP concentration of 1.8 × 10^3 MP m^{-3} after extrapolation based on total MP numbers in this share of the sample. However, when calculating the MP concentrations based on the whole sample material available for µFTIR (i.e. all three subsamples added up), it yielded 5.4 × 10^3 MP m^{-3}. Thus, extrapolation from a single subsample would lead to a severe underestimation of −68%. Vice versa, when basing the calculations only on subsample 3/3 of station 20 (sample share:

27%), an overestimation of +85% is occurring (these methodological observations are further discussed in **section 2.4.3**).

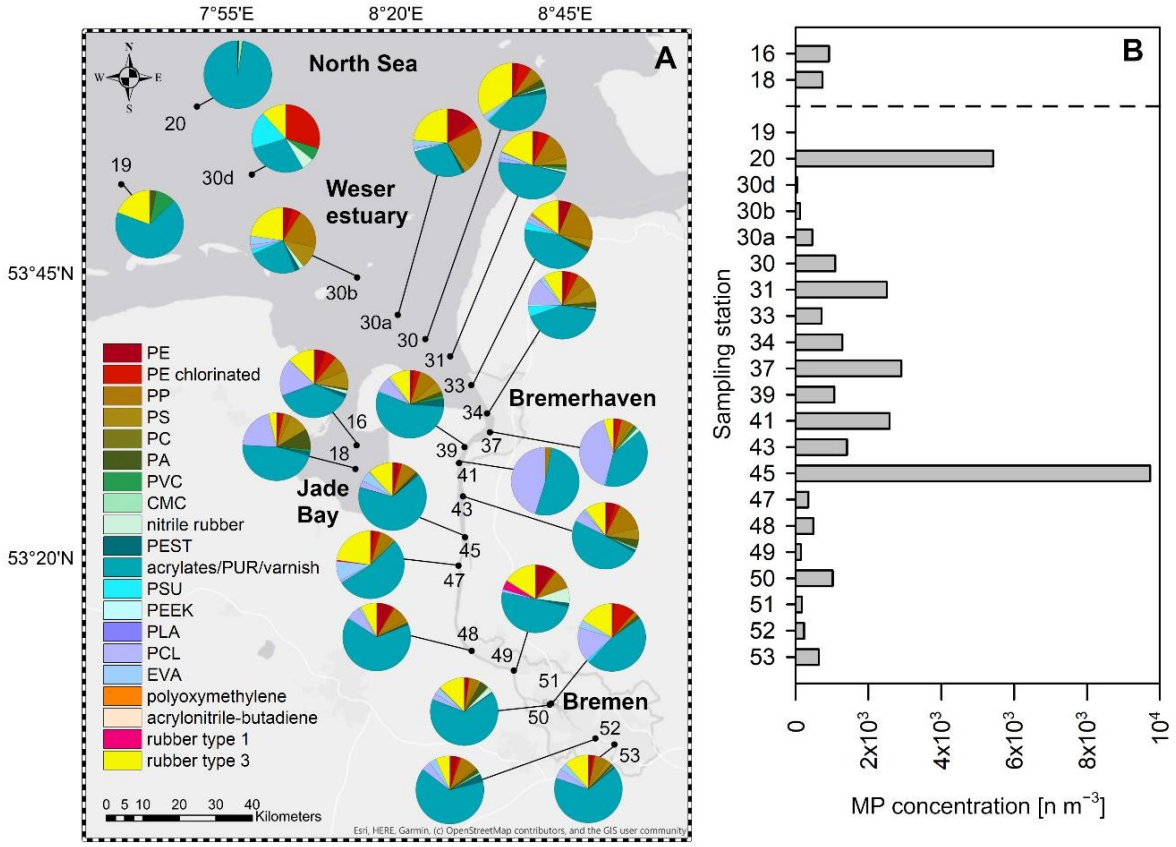

Fig. 2.1: Polymer composition (A) and estimated concentrations (B) of S-MP, detected in the transitional zone Weser-North Sea. PE: polyethylene; PP: polypropylene; PS: polystyrene; PC: polycarbonate; PA: polyamide; PVC: polyvinylchloride; CMC: chemically modified cellulose; PEST: polyester; PSU: polysulfone; PEEK: polyether ether keton; PLA: polylactide acid; PCL: polycaprolactone; EVA: ethylene vinyl acetate.

2.3.1.2 Large microplastics (L-MP, 500–5000 µm)

A total of 943 putative L-MP items were pre-selected by visual sorting. Of these, 89.1% were identified as MP, whereas 0.8% were assigned to natural polymers and 9.1% were defined as 'not identified' (cf. **section 2.2.4**). A low proportion of 1.0% of putative MP was lost before FTIR-ATR measurement.

L-MP were present in all sampling stations other than station 30 d (**Fig. 2.2**). Estimated concentrations range from 1×10^{-2} MP m^{-3} to 9.8×10^{-1} MP m^{-3} (station 20 and 53, respectively) (**Fig. 2.2B**). Polyethylene (PE) accounted for 63.1% of all detected MP and was detected in all MP containing stations except 30 b (**Fig. 2.2A**). Second- and third-most abundant polymer types were PP (24.6%) and polystyrene (PS; 5.8%), being present in stations along the Middle and Lower Weser and in the Jade Bay, and mostly absent in the Outer Weser and at the North Sea margin (**Fig. 2.2, Fig. S5**).

Thirteen different MP polymer types were detected in total. Highest polymer diversities were recorded in proximity to Bremen (n = 8, station 53) and Bremerhaven (n = 7, station 39), and in the Jade Bay (n = 6, station 18) (**Fig. S6**).

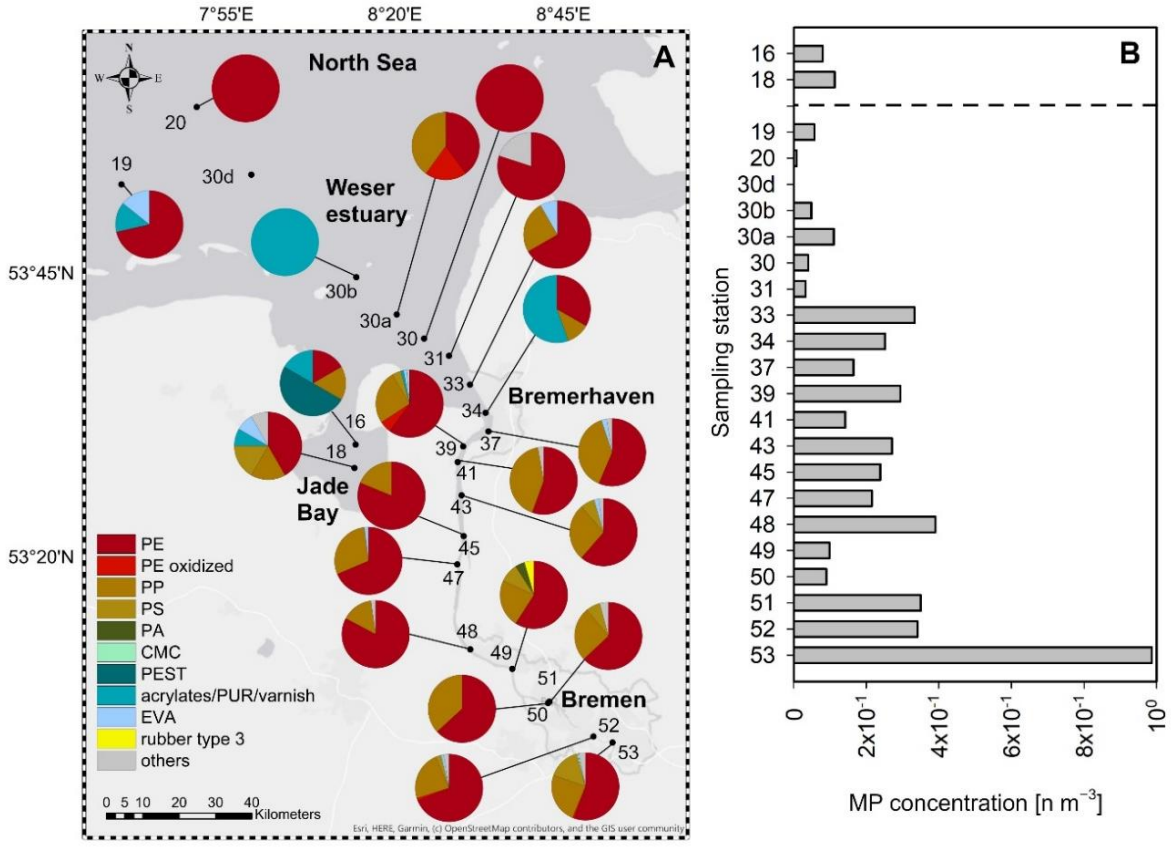

Fig. 2.2: Polymer composition (A) and estimated concentrations (B) of L-MP, detected in the transitional zone Weser-North Sea.

2.3.2 Morphology of microplastic items

2.3.2.1 Small microplastics (S-MP, 11–500 µm)

Within the S-MP fraction, the automated analysis revealed a predominance of small size classes, with 94.5% of the items being <100 µm. This trend was visible in both fibre-like MP and MP particles (**Fig. S7, A+B**). MP particles were the main driver of estimated concentrations, accounting for 87.8% of all detected MP items. Few MP items >500 µm were recorded in the S-MP fraction, which likely had a width <500 µm allowing for passing through the 500 µm pre-filtration during sampling.

2.3.2.2 Large microplastics (L-MP, 500–5000 µm)

A share of 72.9% of the detected L-MP were <2000 µm in size. Particles were dominated by small size classes, whereas this was not observed in lines/filaments (**Fig. S7, C+D**). Particles were dominant compared to lines/filaments, yielding a total relative abundance of 94.0%. Few MP items <500 µm were recorded in the L-MP fraction, likely due to clogging of the 500 µm mesh during sample processing.

The majority of L-MP were fragments (84.9%) (**Fig. 2.3**). Other detected shapes were lines/filaments (6.0%) and foams (3.9%). Spheres, films, and pellets made up for the remaining share. Highest diversities of shape types were recorded in proximity to the city of Bremen and Bremerhaven (station 34 and 53, respectively), whereas most stations situated in the Jade Bay, Outer Weser and at the North Sea margin only showed one shape type (**Fig. 2.3I**).

Fragments were mostly composed of PE or PP (68.9% and 21.9%, respectively). Various morphological subtypes were present, e.g., transparent sheets (**Fig. 2.3A**), amorphous fragments (**Fig. 2.3B**) or paint chips (**Fig. 2.3C**). Moreover, a noticeable amount of twisty, frayed fragments with blue or white coloration was recorded in the majority of sampling stations upstream of station 37 (n = 99; polymer type: PE; Fig. S8).

Lines/filaments were present along the Lower Weser and in three Outer Weser stations close to Bremerhaven (Fig. 2.3I) and were identified as PP (92.0%) and PE (8.0%). Foams were predominantly detected in proximity to the city of Bremen and mostly composed of expanded PS (93.9%). Twenty-one synthetic fibres were detected, mostly made of polyester (PEST; 33.3%) and PP (38.1%), but were excluded from further analyses (cf. **Section 2.2.3**).

2.3.2.3 Plastic items >5000 µm

The majority of plastics recorded in this study was assigned to MP (99.5%), whereas plastic items >5000 µm only accounted for 0.5%. These were detected in 82.6% of the samples. More information is presented in the Supplementary material (**Section S2**, **Fig. S9**).

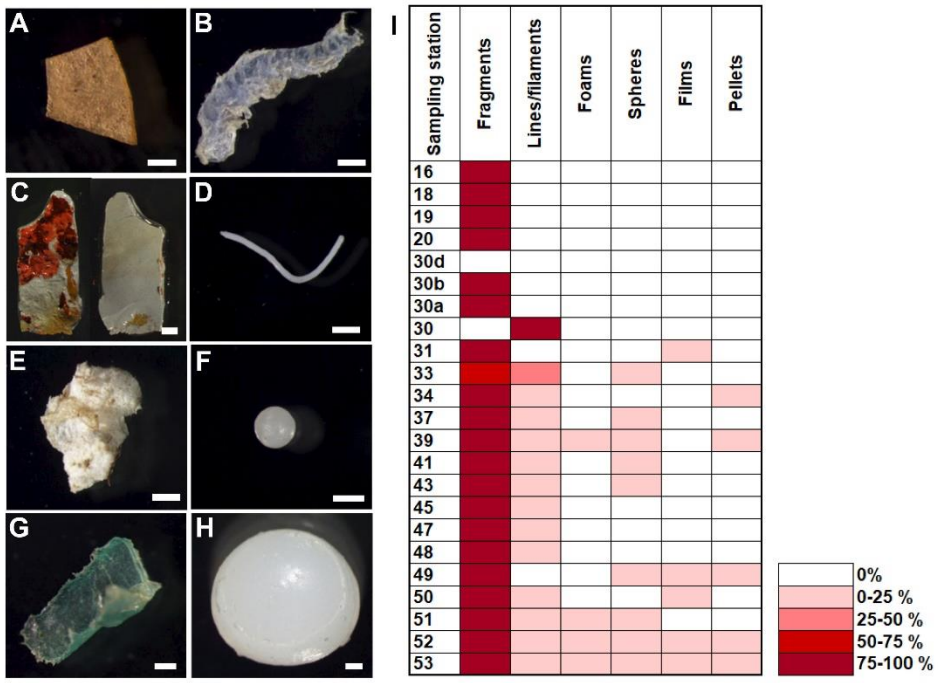

Fig. 2.3: A–H: L-MP shape types detected in surface water samples. A: Fragment, PE, station 34; B: Fragment, PE, station 39; C: Fragment, Acrylates/PUR/Varnish, station 30 b; D: Line/filament, PP, station 43; E: Foam, PS, station 53; F: Sphere, PE, station 39; G: Film, PE, station 53; H: Pellet, PE, station 39. Scale bar: 500 µm. I: Relative abundances of shape types within sampling stations.

2.3.3 Spatial MP patterns and environmental factors

For statistical analysis, data obtained for S-MP and L-MP were combined (in the following denoted as total estimated MP concentration and total MP polymer composition). Correlation and regression analyses were performed under exclusion of data recorded for station 20 and 45, which had been identified as outliers (cf. **Section 2.2.6**).

Correlation analyses revealed a strong relationship between total MP concentrations and SPM, with a Spearman's rank correlation coefficient of $r_s = 0.83$. This was mainly driven by the strong correlation with PIM ($r_s = 0.81$), which showed maximum values in the TMZ (station 37, 39, and 41; **Table S2**). Nonlinear regression of the variables 'distance from Weser Weir' and total MP concentrations revealed a Gaussian distribution as best fitting

model (R^2 = 0.58) (**Fig. 2.4A**), illustrating the peak concentrations of MP in the TMZ. The subsequent decreasing trend towards marine waters was underlined through linear regression of total MP concentration and conductivity (**Fig. 2.4B**; R^2 = 0.67).

The application of kR Clustering revealed two groups with respect to polymer composition. Sampling stations situated at the North Sea margin (stations 19, 20, 30 d) and station 41 (Lower Weser) were classified as group B. All remaining stations were summarised as group A (**Fig. S10**). A Kolmogorov-Smirnov test showed that relative abundances of PE, PP, PS, PEST and EVA were significantly different between group A and B (**Table S5**). These polymer types were mostly present in the Lower Weser and the direct riverine plume, but rare or absent in stations with higher influence of marine water, exhibiting a conductivity of >50 mS cm^{-1} (with the exception of station 41).

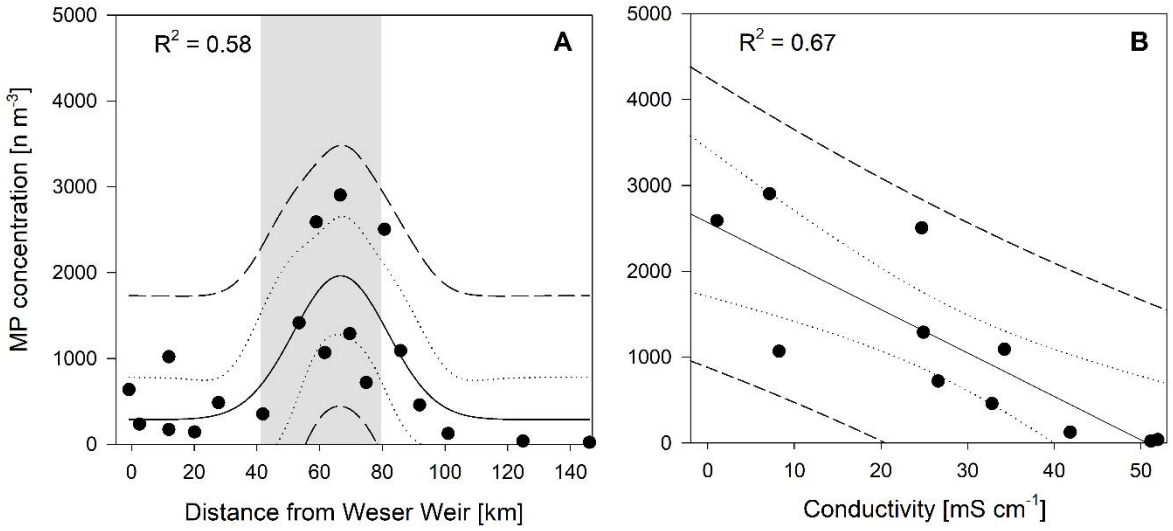

Fig. 2.4: Regression analysis of estimated MP concentration with distance from Weser Weir (A, Gaussian distribution; solid line) and conductivity (B, linear regression; solid line). Dotted lines: 95% prediction interval; dashed lines: 95% confidence interval. The grey background in (A) displays the TMZ.

2.4 Discussion

2.4.1 Microplastic abundance and polymer composition

2.4.1.1 The river mouth as microplastic hotspot

Riverine MP concentrations recorded in this study were in the same dimension as those found by Mintenig et al. (2020) (**Table S6**), who investigated MP in surface waters of Dutch river systems using similar analytical methods. The present study revealed strong variations of MP abundances and polymer composition along the transitional zone Weser-North Sea. Total estimated MP concentrations were driven by S-MP, with highest values around the port of Bremerhaven and a decreasing trend along the Outer Weser transect towards the North Sea margin (**Fig. 2.1**). Items assigned to the polymer cluster acrylates/PUR/varnish contributed strongly to increased estimated concentrations. This cluster comprises a broad range of synthetic polymers, used in a plethora of applications (e.g. medical sector, construction and surface coatings, and packaging) which cannot be further distinguished from each other due to the limited spectral range available for the μFTIR measurement using Anodisc filters (Primpke et al. 2018). A definition of a distinct source of pollution is therefore not possible at this stage. However, exemplary visual inspections of S-MP showed that single items with the appearance of paint flakes were assigned to the cluster acrylates/PUR/varnish. Furthermore, in the L-MP fraction, few paint-like items assigned to the same cluster were detected (e.g., **Fig. 2.3**). These observations suggest that also assignments in smallest size classes might be due to the presence of paint flakes, especially when considering their brittleness and therefore high fragmentation rates (Imhof et al. 2016). Accordingly, Dibke et al. (2021) revealed increased abundances of methyl-methacrylate-based and other potentially shipping-related polymers in water samples collected in the Southern North Sea and adjacent coastlines, applying Pyrolysis-GC/MS. Other studies have also recorded paint flakes in aquatic systems (Turner 2010, Song et al. 2014, Imhof et al. 2016). Turner (2010) emphasized the need for a systematic assessment of paint pollution, especially anti-fouling-paints, as they often contain heavy metals and other biocides, posing an additional threat to aquatic organisms. Therefore, a holistic approach assessing both the polymeric matrix and other potential harmful components is highly recommended.

Besides the potential anthropogenic sources (including shipping) in proximity to the port city of Bremerhaven, the specific hydrodynamic conditions in the TMZ of the River Weser

may also influence MP distribution patterns in this area. Tidal estuaries are known to accumulate fine sediments as SPM, mostly appearing as flocs and larger aggregates (Winterwerp 2002, Papenmeier et al. 2014), and often have extended particulate resident times. Likewise, MP might accumulate in the TMZ and get bound into SPM aggregates. Furthermore, vertical mixing leads to a transport of sediment to surface layers (Papenmeier et al. 2014), which was underlined by increased local concentrations of PIM at stations 37, 39 and 41 (**Table S2**). MP present in the sediment might equally underlie these suspension/resuspension dynamics.

2.4.1.2 Transition to the North Sea

The decreasing trend of MP estimates in the transition to the North Sea is in accordance with previous studies on transitional aquatic systems (Cohen et al. 2019, Lam et al. 2020). A possible explanation for the decrease is a dilution effect, occurring when MP-rich riverine water enters the wider marine water body (**cf. Fig. 2.4B**). As previously discussed, the TMZ of tidal estuaries might additionally act as accumulation zones, steadily releasing low concentrations of MP. Previous studies suggested that estuarine sediments might act as reservoirs for MP before entering the ocean (Defontaine et al. 2020, Xu et al. 2020). Potential drivers of this vertical export might be wind-mixing events, entrapment in aggregates or biofouling (Kukulka et al. 2012, Kooi et al. 2017, Möhlenkamp et al. 2018, Porter et al. 2018). Transport through currents or wind drift should also be considered (Lam et al. 2020). With respect to the present study, the anti-clockwise circulation in the Southern North Sea might be crucial for a better understanding of the fate of riverine MP. These complex dynamics should be addressed in future studies.

With the exception of station 20, total estimated MP concentrations at the North Sea margin are similar to those recorded in adjacent North Sea locations (Lorenz et al. 2019), yielding values between 5 and 40 MP items m^{-3}. Regarding polymer composition comparison, the contribution of items assigned to acrylates/PUR/varnish was generally higher in the present study. However, a direct quantitative comparison between studies is hampered due to differences in sampling methodology. Lorenz et al. (2019) applied net sampling (mesh size: 100 µm), whereas the present study performed an additional on-board filtration (mesh size: 10 µm), therefore reducing the underestimation of small-sized MP.

Interestingly, station 20 showed strikingly high estimated MP concentrations, with most of the S-MP items assigned to the polymer cluster acrylates/PUR/varnish. This station is

located in the intersect of several important shipping routes, representing a potential source (Dibke et al. 2021). Previous studies have highlighted that MP distribution patterns in aquatic environments can be vastly heterogeneous, with local scale MP hot spots forming through specific hydrodynamic conditions (Cohen et al. 2019) or the presence of point sources such as ship wrecks (Jones 2007, Avio et al. 2017).

In the adjacent Jade Bay, total estimated MP concentrations were similar to those recorded in Lower Weser stations, and significantly higher than measured at the North Sea margin (stations 19 and 30 d). The semi-enclosed character may lead to a temporary accumulation of MP, as shown for PIM and POM (**Table S2**). Hydrodynamics in the embayment are mainly influenced by tidal seawater inflow and outflow (Grabemann et al. 2004), which is in accordance with the recorded salinity during sampling (**Table S2**). In previous studies, land-based sources (e.g., industrial facilities, urban areas) were suggested as important drivers for MP pollution in the Jade Bay (Dubaish and Liebezeit 2013, Stolte et al. 2015). However, these studies used visual identification techniques, leading to a possible human bias. The present study provides comprehensive data based on chemical-analytical identification methods and can act as valuable reference for future assessments. Cluster analysis revealed that sampling stations situated at the North Sea margin differed from the other stations regarding their polymer composition (**Fig. S10**). Yet, one Lower Weser station (41) was assigned to the 'marine' kR group B. This station is characterised by a comparatively low sample volume (44 L), possibly due to the strongly elevated PIM content (**Table S2**), which may explain the differences in polymer composition in comparison to adjacent stations. Differences between the kR groups were driven by PE, PP, PS, PEST, and EVA. Interestingly, both in S-MP and L-MP PP and PS were absent in stations with higher influence of seawater, and predominant in Middle and Lower Weser stations or in the direct riverine plume (**Figs. 2.1 and 2.2**). This underlines the potential of the River Weser as a source of MP, but also stresses the need for further investigating the fate once entering the North Sea.

2.4.1.3 Pollution with large microplastics

L-MP items tend to degrade under environmental conditions, acting as a source for numerous small-sized MP (Barnes et al. 2009, ter Halle et al. 2016, Gerritse et al. 2020). Therefore, despite a low contribution to total concentrations, the relevance of L-MP items should not be overlooked. L-MP concentrations were in accordance with previous studies,

investigating the same or similar size range (Frère et al. 2017, Lorenz et al. 2019). Mani et al. (2015), however, recorded values up to 15–20 items m^{-3} in the Rhine-Ruhr metropolitan area. The authors explain the increased pollution with high population densities and elevated industrial activity. Yet, the authors used a lower size limit for MP of 300 µm (this study used 500 µm), hindering a direct comparison. A general trend of higher estimated concentrations in the Lower Weser than in the Outer Weser and North Sea margin is visible (**Fig. 2.2**). The maximum was recorded at station 53, situated upstream from the Weser Weir, seemingly representing an accumulation zone for L-MP. Several industrial facilities are located here, suggesting potential localised land-based pathways of MP into the river.

In contrast to S-MP composition in this study, L-MP items were mainly made from PE, PP, and PS, which is in accordance with previous studies (Zhao et al. 2015a, Frère et al. 2017, Kataoka et al. 2019, Lorenz et al. 2019). These polymer types were predominantly recorded in the Lower Weser, with the sudden absence of PP and PS in the transition to the North Sea being of additional interest.

2.4.2 Morphological characterization

The dominance of small size classes is in accordance with previous studies (Enders et al. 2015, Lorenz et al. 2019). These numerous small-sized MP may disintegrate further, acting as a potential source of nanoplastics. The smaller the size, the higher the bioavailability to a broad range of organisms, posing an increased ecotoxicological risk (Ma et al. 2019). Ideally, nanoplastic analysis should be implemented into monitoring programs, allowing a holistic risk assessment.

Furthermore, MP particles were the dominant shape type in this study. However, S-MP and L-MP received different characterisation approaches with a more detailed differentiation for L-MP (c.f. **section 2.2.3 and 2.2.4**). The highest diversities regarding shape types were found in sampling stations around the city of Bremen, whereas most of the stations situated in the Outer Weser and at the North Sea margin only exhibited one shape type (Fig. 2.3). The dominance of fragments is in accordance with previous studies on MP occurrence in surface waters, being attributed to the fragmentary breakdown of larger plastic items (Frère et al. 2017, Heß et al. 2018, Koongolla et al. 2018, Kataoka et al. 2019, Mani and Burkhardt-Holm 2020). Lines/filaments were the second-most abundant shape type and mostly assigned to PP. Previous studies also found PP as one of the most common polymer type for lines/filaments in environmental samples, with PA, PET and PE also

recorded (Tanaka and Takada 2016, Yin et al. 2019, Saeed et al. 2020). The third-most common shape type was foam, mostly assigned to expanded PS, widely used for packaging or isolation purposes (Koongolla et al. 2018, Mani and Burkhardt-Holm 2020).

In this study a notable number of frayed PE-fragments of a similar morphology was recorded (**Fig. S8**) in the tidal Lower Weser stretch, as well as upstream of the Weser Weir. Whether these stem from one specific point source, or if they are a general industrial by-product, remains unclear. In previous studies, specifically shaped MP recorded in aquatic systems were assigned to industrial sources (Lechner et al. 2014, Ballent et al. 2016). Helm (2017) coined the term 'commercial-activity-related fragments'. The author stressed the need for an improved source apportionment as a basis for better management strategies, but also acknowledged the subjectivity during visual identification. The use of a standardized morphological key combined with chemical identification methods was suggested. Accordingly, recent studies proposed classification systems based on the morphology of putative MP items (Wang et al. 2019, Lusher et al. 2020). In combination with chemical identification methods, a high spatial and temporal resolution of sampling points (e.g., in proximity of a suspected point source) is suggested.

2.4.3 Discussion of methods and implications for future studies

This study provides an overview of MP pollution in the transitional zone Weser-North Sea, using state-of-the-art analysis methods. Sampling stations were located along a transect, attempting to cover all important sections in the transitional zone. The on-board filtration allowed an assessment of MP down to 15 µm, which is less prone to underestimation of small-sized MP than the application of nets with larger mesh sizes (Lindeque et al. 2020). For addressing L-MP, net sampling was applied, which proved suitable in former studies (Mani and Burkhardt-Holm 2020). An alternative to the use of two different sampling techniques is the filter cascade approach as applied by Mintenig et al. (2020). With regards to minimum sampling volumes, Koelmans et al. (2019) proposed 500 L for surface water samples, which was achieved for 52% of the samples collected by on-board filtration (**Table S1**). Especially in the TMZ, lower sample volumes were collected, likely due to high SPM content hampering the filtration. Considerably higher volumes were sampled for the L-MP fraction, with 91% of the samples being >35 m^3, a minimum volume suggested by Bruge et al. (2020) for net sampling.

S-MP samples were collected with 15 µm stainless steel filters, followed by sample processing using 18 µm screens. This might have caused a potential loss of items below these size limits, leading to an underestimation of MP < 18 µm. Yet, using µFTIR spectroscopy (lower detection limit: 11 µm), we recorded numerous MP items in the smallest size classes (**Fig. S7**). This might be due to clogging of filters or temporal aggregation of small particles. Finally, the high records in smallest size classes, occurring despite an assumed underestimation, underline the relevance of studying this size fraction, as stated by Lorenz et al. (2019).

The small MP fraction was split into half after processing, in order to obtain complementary chemical-analytical information by Pyrolysis-GC/MS analysis within the joint project PLAWES (publication in preparation). Yet, the entire remaining 50% of the sample were distributed on 1–11 filters per sample and measured with µFTIR spectroscopy, so that the proportion analysed was still high compared to other studies (Frei et al. 2019, Tekman et al. 2020). Theoretical extrapolations of the individual subsamples showed strong over- and underestimations of MP concentrations (**Tab S4, Fig. S4**) of up to +121% (sample 16, subsample 2/11) and produced underestimations of polymer diversities. Hence, the applied approach to consider the entire sample material available − instead of single extrapolated subsamples − proved appropriate. These observations is in accordance with recent studies (Abel et al. 2021, Hildebrandt et al. 2021), and underlines the need to analyse the highest proportion possible in order to generate reliable MP datasets.

2.5 Conclusion

The aim of the present study was to elucidate MP pollution in surface water of the transitional zone Weser – German North Sea, with regard to abundances, polymer composition and morphological characteristics. MP were present in all analysed sampling stations, with S-MP (11–500 µm) being the main driver for total estimated concentrations. This emphasises the need of adequate sampling in order to avoid severe underestimations. Furthermore, estimated MP concentrations varied over the sampled transect, with a decreasing trend towards the North Sea and highest values in proximity to the port of Bremerhaven, suggesting anthropogenic activity as a potential source. Moreover, the estuarine circulation appears to influence MP distribution patterns, likely through vertical mixing and accumulation, and should be the focus of future monitoring programs utilising holistic sampling approaches (i.e. from the surface layer to the sediment).

Although L-MP showed significantly lower estimated concentrations, we emphasize the need of analysing this sample fraction, as it represents a potential source for S-MP. The dominant polymer type in L-MP was PE, which contrasts with small-sized MP, where most of the items were assigned to the polymer cluster acrylates/PUR/varnish. These differences again highlight the need of assessing a broad size range and suggest that the two MP size fractions might stem from different sources. This study provides comprehensive data on MP pollution in an important German river and estuary system and elucidates general trends in distribution patterns. Yet, it also highlights existing knowledge gaps, with implications for future monitoring programs. It hereby contributes to the current research on MP pollution in aquatic systems and may serve as a reference point for future MP assessments in estuarine systems similar to the transitional zone Weser-North Sea.

Declaration of competing interest

The authors declare that they have no known competing financial interests or personal relationships that could have appeared to influence the work reported in this paper.

Acknowledgements

This study was funded by the German Federal Ministry of Education and Research (Project PLAWES, 'Microplastic Contamination in the Weser- Wadden Sea – National Park Model System: an Ecosystem-Wide Approach'; grant numbers: 03F0789B, 03F0789E, 03F0789F). We thank the crew of the RV Uthörn and RV Otzum for their help during sampling, Hannah Jebens for laboratory assistance and S. Abel and N. Mackay-Roberts for proofreading.

Chapter 3 – Microplastics in two German wastewater treatment plants: Year-long effluent analysis with FTIR and Py-GC/MS

Lisa Roscher*[a], Maurits Halbach*[b], Minh Trang Nguyen[a], Martin Hebeler[c], Franziska Luschtinetz[d], Barbara Scholz-Böttcher[b], Sebastian Primpke[a], Gunnar Gerdts[a]

[a] Alfred Wegener Institute, Helmholtz Centre for Polar and Marine Research, D-27483 Helgoland, Germany

[b] Institute for Chemistry and Biology of the Marine Environment (ICBM), Carl von Ossietzky University of Oldenburg, D-26111 Oldenburg, Germany

[c] hanseWasser Bremen GmbH, D-28217 Bremen, Germany

[d] Kasselwasser, D-34125 Kassel, Germany

* *Shared first-authorship*

Corresponding author: Lisa Roscher (lisa.roscher@awi.de)

Keywords: Spectroscopic analysis, Microplastic pollution, Point source, Aquatic environment, Microplastic masses, Polymer database

Citation:

Roscher, L., Halbach M., Nguyen, M. T. *et al.* Microplastics in two German wastewater treatment plants: Year-long effluent analysis with FTIR and Py-GC/MS. *Sci Total Environ* (2022) 817:152619.

https://doi.org/10.1016/j.scitotenv.2021.152619

Abstract

Microplastics (MP) have been recorded in various environments around the globe. For a better understanding of distribution patterns and for providing a basis for risk assessments, detailed data on MP concentrations and polymer compositions are required. This study investigated the effluents of two German wastewater treatment plants (WWTP) monthly over one year, in order to better understand their temporal input of MP into the receiving river systems. MP item data down to 11 µm were obtained by means of Fourier Transform Infrared (FTIR) spectroscopy under the application of an improved polymer database. Complementary mass data were obtained by pyrolysis gas chromatography–mass spectrometry (Py-GC/MS) (for one WWTP). Both FTIR and Py-GC/MS analysis revealed a homogeneous polymer composition over the year, with a general dominance of polyolefins. Elevated MP item and mass concentrations (maximum: 3×10^4 items m^{-3} and 3.8×10^3 µg m^{-3}) were observed during winter months and were accompanied by either heavy rainfall (increased discharge and total organic carbon) or elevated turbidity values. These observations emphasize the need for the assessment of background parameters in future MP monitoring studies. By providing monthly data over one year on MP items and masses in WWTP effluents, this study helps enhancing the understanding of temporal MP dynamics and can act as a valuable reference point for future assessments.

3.1 Introduction

Microplastics (MP) have been recorded ubiquitously all over the globe, in terrestrial as well as aqueous environments. Especially small MP are considered as potentially harmful for organisms throughout the food web. For a holistic risk evaluation of this pollutant, it is crucial to investigate distribution patterns, but also to determine the pathways into the environment. In recent years, several studies investigated waste water treatment plants (WWTPs) as potential point sources of MP pollution in receiving aquatic systems (Sun et al. 2019). Possible origins of MP in wastewater are from both industrial and domestic sources. The latter includes MP released during washing of clothes, as well as the application of cosmetics (such as facial cleansers or toothpaste) and the improper disposal of hygiene products (Carr et al. 2016, Napper and Thompson 2016, Hernandez et al. 2017). In the review by Sun et al. (2019), polyethylene (PE), polyamide (PA), and polyester (PEST; often dominated by its main representative polyethylene terephthalate, PET) were identified as the most common polymer types in WWTP influents and effluents. All are frequently used in synthetic clothing, personal care products or as packaging material.

Most WWTPs consist of several treatment stages, including a mechanical treatment, followed by a biological and frequently chemical treatment. Although not specifically designed for retaining MPs, a significant reduction of MP was shown in previous studies (Murphy et al. 2016, Talvitie et al. 2017b). Nevertheless, the final effluent still contains MP that enter the adjacent aquatic system from many WWTPs (Liu et al. 2021). Within Germany, 9166 WWTPs are connected to major river systems, which discharge into North Sea, Baltic Sea or Black Sea (Schmidt et al. 2020), and therefore potentially transporting a considerable amount of MP into the aquatic environment.

In studies to date, limited data are available on seasonal MP output and the underlying factors mitigating MP concentrations in WWTP effluents (Michielssen et al. 2016, Conley et al. 2019, Ben-David et al. 2021). Furthermore, MP modelling studies demand information on MP polymer composition, MP morphology (size, shape) and MP mass (Siegfried et al. 2017, van Wijnen et al. 2019). Regarding MP polymer compositions, this is especially important for modelling as the polymer-specific density can influence the sinking behavior during transportation in aquatic systems (Waldschläger and Schüttrumpf 2019). MP morphology is not only important for the toxicological assessment, but also greatly affects MP retention and transport time within the environment. Finally, the assessment of MP mass

is crucial to estimate the total input of MP into the environment and its potential to degrade and fragment into smaller MP (Harris 2020).

In order to generate the afore-mentioned MP data, suitable analysis techniques are required. Fourier Transform Infrared (FTIR) Spectroscopy has been shown to be a strong tool for the chemical analysis of MP items, whereas pyrolysis gas chromatography-mass spectrometry (Py-GC/MS) has been highly recommended for the assessment of MP masses (Primpke et al. 2020a, Kirstein et al. 2021). By use of both FTIR and Py−GC/MS, we aimed to evaluate the role of WWTPs as point sources for MP pollution by complementarily assessing (a) the MP composition, (b) the MP item morphology (size, shape) and (c) MP item−/mass concentration at the effluent of two German WWTPs along the Weser river system. This evaluation was performed by sampling the effluents monthly over one year. By providing these novel and comprehensive data, the dynamic impact of two exemplary WWTPs along a major German river system with respect to MP pollution is highlighted. The given dataset provides a valuable reference for future studies, in particular regarding modelling approaches.

3.2 Methods

3.2.1 Study sites

Samples were collected at the effluents of two municipal wastewater treatment plants (WWTPs) in Bremen and Kassel, Germany (**Supplementary Data 1, Fig. S1**). Treated wastewater from the WWTP in Bremen-Seehausen is discharged into the Lower Weser, i.e., the tidally influenced stretch of the River Weser. The plant processes the wastewater of the city of Bremen as well as neighbouring communities (population equivalent: 820,000). The WWTP in Kassel is discharging the processed wastewater into the Fulda, one of the two headstreams of the River Weser. The plant is receiving wastewater from the city area of Kassel, serving a population equivalent of 340,000. Both plants have a mechanical purification, followed by a biological and final treatment step. Further details on the examined WWTPs are presented in Table S1 (**Supplementary Data 1**).

3.2.2 Sampling

The effluents of the WWTPs in Kassel and Bremen-Seehausen were sampled monthly over one year (July 2018–June 2019). Samples were concentrated on stainless-steel cartridge filters (mesh size: 10 µm; filtration area: approx. 250 cm^2) (Wolftechnik Filtersysteme, Germany), sitting in a housing composed of styrene-acrylonitrile (SAN) and polypropylene (PP) (Wolftechnik Filtersysteme, Germany). Effluent water was pumped into the cartridge filter units using a custom-made pumping station. This consisted of a stainless-steel suction weight (positioned approx. 5−10 cm below the water surface), polyvinyl-chloride (PVC) hosing and two membrane pumps (JABSCO EMG-590-8023; Toplicht, Germany), and was based on the pumping system applied by Mintenig et al. (2017). The sampled volume was assessed by use of a digital flowmeter (Water Smart Flow Meter, Gardena, Germany), which was connected to the outflow of the cartridge filter unit. After priming the system for 5 min with treated wastewater, sampling was conducted. The targeted sampling volume was 1000 L; the maximum sampling duration was limited to 2 h. Whenever the filter clogged before reaching the targeted volume, the sampling was stopped beforehand. In Bremen-Seehausen, filtered volumes ranged from 136 to 1000 L, with one sample (November 2018) reaching the targeted volume of 1000 L. In Kassel, volumes ranged from 200 to 1000 L, and four samples reached the targeted volume (September and October 2018, February and April 2019) (**Table S2**). Samples were stored at 4 °C until further treatment. In order to

account for any contamination by the sampling system, procedural blanks were run, and detected MP were subtracted from the results (cf. **section 3.2.5**).

3.2.3 Sample processing

In order to isolate the MP fraction from the samples, an enzymatic protocol was applied, following the approach presented in previous studies, with slight modifications (Löder et al. 2017, Mintenig et al. 2017). All processing steps are summarised in a flow chart presented in the **Supplementary Data 1, Fig. S3**. Briefly, sodium dodecyl sulphate (SDS; 10% *w/v*; Carl Roth, Germany), Protease and Cellulase (ASA Spezialenzyme GmbH, Germany) were transferred successively as independent treatments into the cartridge units and samples were incubated in a shaking incubator after each treatment (InforsHT, Einsbach, Germany) (for more details on sample handling see **Supplementary Data 1, Section S1**). After the Cellulase treatment, the stainless-steel cartridge filters were removed from the housing and transferred to a glass beaker. Sample material attached to the filter was rinsed off with a wash bottle of Milli-Q water, and subsequently split into two size fractions using a 500 µm stainless-steel filter screen (HAVER & BOECKER OHG, Germany) and a glass vacuum filtration unit. Sample material <500 µm was concentrated on an 18 µm stainless-steel filter screen (HAVER & BOECKER OHG).

In order to isolate putative large MP items (L-MP, 500−5000 µm) for the subsequent spectroscopic measurements, the sample material collected on the 500 µm stainless-steel filter screen was inspected visually with a stereomicroscope (Olympus SZX16, Olympus, Germany). Suspected MP items were transferred to custom-made metal sorting plates using a pair of forceps. During sorting, we followed the criteria presented in Norén (2007), and sizes as well as shape types were assigned in the same way as presented in a recent study (Roscher et al. 2021).

The sample fraction containing potential small MPs (S-MP, <500 µm) underwent further purification steps (**Supplementary Data 1, Fig. S2**), in order to reduce the amount of natural organic and inorganic matter and therefore facilitate the subsequent chemical analyses. An initial treatment with H2O2 (30%, Carl Roth; 24 h) was applied, followed by a chitinase treatment (ASA Spezialenzyme GmbH, 96 h, 37 °C) and a second H_2O_2 step (5 h) (Löder et al. 2017). In order to remove any inorganic compounds (e.g., sand grains), a density separation using a $ZnCl_2$ solution (approx. 1.7 g cm^{-3}) was performed in separation funnels. The upper phase, containing the putative MP fraction, was recovered and

concentrated on a stainless-steel filter gauze (mesh size: 15 µm, Ø 47 mm, GKD, Germany). For the application of the two different measurement techniques, µFTIR and Py-GC/MS, filter gauzes were split in two halves with a pair of surgical scissors. One half was stored in a glass petri dish and kept frozen before being transferred to the ICBM, Oldenburg, for pyrolysis measurements. The sample material on the other filter half was resuspended by rinsing it into 100 mL glass bottles with Milli-Q water, followed by storage at 4 °C until further analysis. Further preparation steps for the respective analysis methods are explained in **sections 3.2.4.2 – 3.2.4.4**.

3.2.4 Chemical identification of microplastics

For both WWTP, MP item data were assessed using µFTIR (for S-MP) and Attenuated Total Reflection (ATR)-FTIR (for L-MP) (cf. **sections 3.2.4.1.-3.2.4.3**). For the WWTP in Bremen-Seehausen, mass data were also obtained through Py-GC/MS for S-MP (cf. **section 3.2.4.4**). The following sections provide details on the chemical-analytical methods used.

3.2.4.1 ATR-FTIR-analysis of large microplastics (L-MP, 500-5000 µm)

ATR-FTIR analysis of putative L-MP items from the WWTPs in Bremen-Seehausen and Kassel was performed using a Tensor 27 coupled to a diamond platinum ATR unit (Bruker Optik GmbH, Germany). Three replicate spectra were recorded per item, covering a spectral range of 400−4000 cm^{-1} (resolution: 4 cm^{-1}; scans: 32). Further settings related to the Fourier Transformation of spectra were a zero filling factor of 2, and a Blackman-Harris 3-term apodization (Andrade et al. 2020). Comparison to our in-house database (Primpke et al. 2018) allowed the assessment of spectral similarity based on the underlying reference polymers. Hit qualities of 70−100% resulted in the identification of the polymer type. When yielding 60−70%, a manual re-evaluation of the spectra was performed, leading to a confirmation or rejection. Spectral hits <60% were marked as ‘not identified’. Potential MP fibres were measured with ATR-FTIR whenever possible, however, the handling of very thin or short fibres proved challenging. These fibres were instead transferred to an aluminium oxide filter (Ø 25 mm, pore size: 0.2 µm; Anodisc®, Whatman, UK), covered with a BaF_2 window and analysed in the same way as S-MPs (cf. **section 3.2.4.2**). Spectra were re-evaluated manually, whenever necessary.

3.2.4.2 µFTIR measurements of small microplastics (S-MP, <500 µm)

In preparation for the µFTIR analysis of the S-MP fraction, a maximum of three representative aliquots of each sample was concentrated on aluminium oxide filters (Ø 25 mm, pore size: 0.2 µm; Anodisc®, Whatman, UK). The 100 ml bottles containing the digested and resuspended sample were manually shaken for homogenisation, and aliquots were pipetted onto Anodisc® filters (Lorenz et al. 2019). These were dried in a drying oven (37 °C, >12 h) or in a desiccator. Splitting the samples into aliquots is necessary in order avoid overloading Anodisc® filters, which would hamper the µFTIR analysis due to absorption effects. A maximum of three aliquots was chosen in order to reduce the measurement time (in comparison with analysing the whole sample) whilst increasing the representativeness of data. In seven out of 24 samples, 100% of the sample material designated for µFTIR was covered by 1−3 aliquots (Kassel WWTP: Samples 07/2018−11/2018; Bremen-Seehausen WWTP: Samples 07/2018 and 11/2018). All other samples exhibited a generally higher load of solids, so that the analysed percentage range between 15 and 69%. More details on the representative aliquots are provided in the **Supplementary Data 1** (**Fig. S3**) and **Supplementary Data 2.1−2.6**.

Measurements were performed using a Hyperion 3000 µFTIR microscope, coupled with a Tensor 27 spectrometer (Bruker Optik GmbH) and a 64 × 64 focal plane array detector (lower detection limit: 11 µm). OPUS 7.5 (Bruker Optik GmbH) was applied as measurement software. Anodisc® filters were covered with a BaF_2 window prior to the measurement, allowing for the assessment of particles as well as fibre-like MP (Primpke et al. 2019). Spectra were recorded in the wavenumber range 3600−1250 cm^{-1} with a spectral resolution of 8 cm^{-1} (32 scans; background: 64 scans). Furthermore, a Blackman-Harris 3-term apodization and a zero-filling factor of 2 were applied. A grid of 21 × 21 measurement fields was selected, covering the whole filtration area. After the processing of spectra in OPUS 7.5, the polymer identification software siMPle (version 1.1.β) (Primpke et al. 2020b) was used. Pixels assigned to the PP edge of the Anodisc® filter were removed using the circular mask function within the heat map feature application within siMPle. In order to obtain the final data on MP numbers, sizes and assigned polymer cluster, an image analysis in MPAPP (version 1.1.1) was performed (Primpke et al. 2019). An overview of µFTIR polymer clusters is given in **Table 3.1**. The obtained results were examined, and spectral assignments re-evaluated. This re-evaluation revealed the necessity of adapting our in-house reference database, as stated in the following.

3.2.4.3 Database adaptation for the µFTIR analysis of small microplastics

The MP results obtained through MPAPP showed numerous assignments to the polymer cluster acrylates/polyurethanes (PUR)/varnish. Polyacrylamide-based flocculation agents, widely used in WWTPs, were assumed to be potentially assigned to this relatively broad µFTIR cluster. In order to test this, a comprehensive selection of these agents, stemming from different manufacturers (**Table S3**), were measured with ATR-FTIR. Spectra were then included into our in-house reference database. Furthermore, a detailed inspection of the Anodisc® filters using the stereomicroscope often showed the presence of residual plant material, which apparently have not been fully macerated during the enzymatic-oxidative digestion. FTIR-spectra of this material showed similarities to spectra of plant cuticles (Heredia-Guerrero et al. 2014), but also similar spectral bands as certain reference spectra within the acrylates/PUR/varnish cluster. Since cuticle spectra were not included in the reference database so far and in order to investigate possible misassignments, plant cuticles of holly (*Ilex aquifolium*), tomato (*Solanum lycopersicum*) and Avocado (*Persea sp.*) were subjected to the enzymatic digestion protocol and density separation, and measured via ATR-FTIR (**cf. section 3.2.4.1**) and in transmission with a HTS-XT Multiplate reader using silicon-based plates (96 sample positions, Bruker Optik GmbH). After addition of the polyacrylamide and cuticle spectra to the reference database, polymer identification through siMPle 1.1.β and MPAPP 1.1.1 was repeated (for the adapted database file as well as spectral matching thresholds, see **Supplementary Data 2**). Thorough inspection of the resulting polyacrylamide assignments, however, showed no satisfactory matches. Hence, these assignments were excluded from the results.

3.2.4.4 Py-GC/MS measurements of small microplastics (S-MP, <500 µm)

The polymer mass concentrations of all monthly S-MP samples from the WWTP in Bremen-Seehausen were measured with Py-GC/MS. The assigned analysis with Py-GC/MS is based on the analysis by Fischer and Scholz-Böttcher (2017) and its improvements Fischer and Scholz-Böttcher (2019). Prior to the measurement, the respective sample moieties representative for half of the sampled volume were thoroughly rinsed from the stainless-steel filters onto a muffled glass fibre filter (Ø 15 mm, pore size 1 µm, Pall Life Sciences, USA). The filter was subsequently folded into a pyrolysis cup. The sample was spiked with 20 µl internal standard ($ISTD_{py}$, **Supplementary Data 1, Table S4**) and 20 µl tetramethylammonium hydroxide (TMAH, 25% in methanol, Sigma Aldrich, Germany).

The samples were measured in accordance to Fischer and Scholz-Böttcher (2019). Detailed information on the Py-GC/MS method and respective specifications are given in the supplementary information (**Supplementary Data 1, Table S5**).

The identification and quantification are performed using indicator ions. These ions are indicative for specific pure polymer types and represent clusters that relate to these specific polymers. This clustering is necessary since thermal detection principles like Py-GC/MS are not able to distinguish between pure polymers, copolymers or composites (Primpke et al. 2020c, Dibke et al. 2021). The selection of indicator ions is derived from former published studies (Fischer and Scholz-Böttcher 2017, Fischer and Scholz-Böttcher 2019) and displayed in the **Supplementary Data 1, Table S6**. Resulting calibrations curves and the associated linear regressions are given in the **Supplementary Data 1, Table S7**.

3.2.5 Contamination mitigation

In order to avoid contamination with synthetic polymers, plastic-free laboratory material, such as glass or metal, was used whenever possible. Most of the sample processing was conducted in a laminar flow bench (ScanLaf Fortuna, Denmark), and room air was filtered using dust boxes equipped with a HEPA14 filter (Möcklinghoff Lufttechnik, Germany). All chemicals and enzymes were pre-filtered before usage (pore size: <1 µm). In parallel to the effluent samples, procedural blanks (n = 3) were run. Therefore, 10 L of filtered tap water, prepared in a stainless-steel bucket, was run through the pumping system used for effluent sampling (**cf. section 3.2.2**) for approx. 2 h. Blank samples concentrated on the 10 µm cartridge filters were processed and analysed in the same way as effluent samples. Averaged S-MP counts (**Supplementary Data 2.1 to 2.6**) and masses (**Supplementary Data 1, Table S8**) detected in the blanks were subtracted from the results. In the L-MP fraction, only one transparent PEST fibre was recorded. Fibre counts with the same polymer type and coloration were subtracted from L-MP results (**Supplementary Data 2.7**).

3.2.6 Data handling

Information on MP item and mass concentrations are given per cubic meter (n m^{-3} and µg m^{-3}, respectively). Presented S-MP item concentrations represent the sum of MP items detected in the 1−3 aliquots (**Supplementary Data 2.1 to 2.6**). In order to allow the comparison between FTIR and Py-GC/MS analyses, a harmonisation of polymer clusters was performed after Primpke et al. (2020c) with slight modifications (**Table 3.1**). This step is obligatory for any data comparison generated with two different detection and quantification principles. The resulting harmonised clusters can represent, in some cases, fusions of different (but chemically similar) polymer groups. Furthermore, MP masses were estimated based on µFTIR data, by following two different approaches: Firstly, the mass calculation based on the reference surface area of detected items and their assumed density (previously introduced by Primpke et al. (2020c)), and secondly the mass calculation approach by Simon et al. (2018), which is assuming an ellipsoid shape as a basis.

For the comparison of item concentrations between the initial and adapted database analysis (cf. **section 3.2.4.3**) as well as between the two WWTPs (after database adaptation), a Mann-Whitney-U Test was performed in Statistica 13, as normality of data was rejected by means of a Shapiro-Wilk-Test beforehand. Further, correlations between MP data and background parameters were tested with the non-parametric Kendall-Tau-b correlation coefficient embedded in SPSS (IBM Corp., USA). Background parameters like total organic carbon (TOC), chemical oxygen demand (COD), suspended matter (SPM), turbidity and effluent volume were provided by the WWTPs. Turbidity and effluent volume values were averaged over 3 h spanning the sampling period.

The effluent sample collected in the WWTP in Bremen-Seehausen in October 2018 (S-MP items) showed comparatively high MP concentrations combined with a strong degree of variation between the three sample aliquots after µFTIR measurements (see **Supplementary 1, Fig. S3**). This was possibly due to an insufficient homogenisation prior to filtration onto Anodisc© filters. Due to the lack of representativeness of this sample, it was excluded from further statistical analyses.

Table 3.1: Harmonised polymer types for the comparison between FTIR and Pyrolysis-GC/MS (modified after Primpke et al. (2020c)). PE: polyethylene; EVA: ethylene vinyl acetate; PP: polypropylene; PET: polyester; PBT: polybutylene terephthalate; PS: polystyrene; PVC: polyvinyl chloride; PC: polycarbonate; PUR: polyurethane; PMMA: poly (methyl methacrylate); MDI: methylene diisocyanate; PA: polyamide; CMC: chemically modified cellulose; PSU: polysulfone; PEEK: polyether ether ketone, PLA: polylactide acid; PCL: polycaprolactone; POM: polyoxymethylene; EVOH: ethylene vinyl alcohol.

Harmonised (h-) polymer cluster	**Polymer cluster Pyrolysis-GC/MS**	**Polymer cluster FTIR**
h-PE	PE and copolymers	PE, PE oxidized, rubber type 3, EVA
h-PP	PP and copolymers	PP
h-PET	PET/PBT	PEST
h-PS	PS and copolymers	PS
h-PVC	PVC/PE chlorinated, polychloroprene	PVC, PE chlorinated, polychloroprene
h-PC	PC	PC
h-PUR/PMMA	MDI-PUR, PMMA and all poly (alkyl-methacrylate)s	Acrylates/PUR/varnish including PMMA
h-PA	PA6	PA
Others (only FTIR)		CMC, nitrile rubber, PSU, PEEK, PLA, PCL, polyimide, POM, polybutadiene, acrylonitrile-butadiene, rubber type 1, rubber type 2, EVOH, ethylene propylene, styrene-butadiene copolymer, styrene ethylene butylene
Not included (minerals, coal, natural polymers)		Natural polyamides, natural cellulose, quartz, chitin, charcoal, coal

3.3 Results

The following section introduces the database adaptation performed during the analysis of S-MP items (**3.3.1**), of which the outcomes are then used for the following sections presenting MP item and mass data for WWTP effluent samples (**3.3.2 and 3.3.3**).

3.3.1 Database adaptation for µFTIR analysis of small microplastics

As stated in **section 3.2.4.3**, we performed a database adaptation in order to counteract false-positive assignments due to interference by residues of the sample matrix (i.e. waxy substances in plant cuticles). Indeed, the addition of plant cuticles to the database and the re-analysis of data led to a significant decrease of MP item concentrations, especially within the harmonised clusters h-PUR/PMMA, h-PE and h-PVC (**Supplementary Data 1, Table S9** and **S10**). Accordingly, false colour images generated through MPAPP showed that the suspected plant residuals on the Anodisc© filters were identified as cuticles by use of the adapted database (**Fig. 3.1A+B**), and that initial assignments to MP (in this case acrylates/PUR/varnish) decreased strongly (**Fig. 3.1C+D**). This effect is also illustrated in **Fig. S4**. Based on these findings and the acceptance of the newly adapted database, the MP item-based results presented in the following sections are generated, with improved confidence that there has been a reduction of the potential bias by matrix interferences.

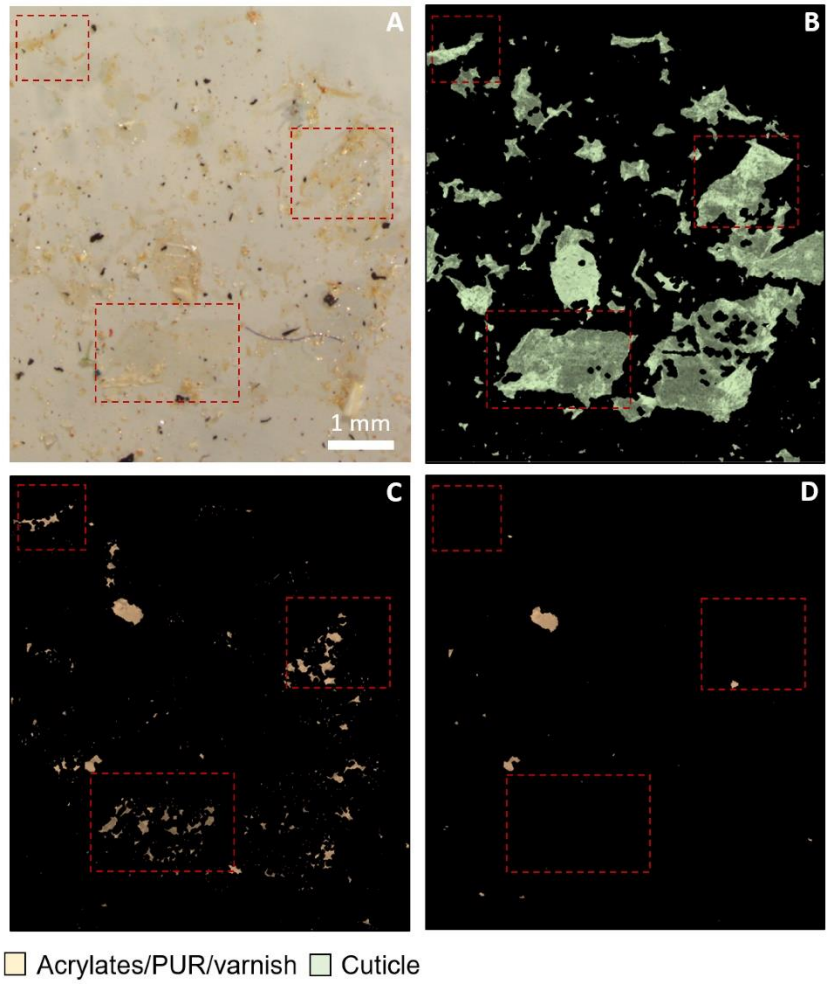

Fig. 3.1 A: Light microscopy image of Anodisc filter surface with sheet-like, transparent plant material (exemplarily marked in red). B-D: False colour image obtained through MPAPP software, B: showing the assignments to the newly added FTIR cluster "cuticle", C: Assignments to the FTIR cluster acrylates/PUR/varnish after initial database run, D: Assignments to the FTIR cluster acrylates/PUR/varnish after re-analysis with adapted reference database (sample collected in 04/2019 at the Bremen-Seehausen WWTP).

3.3.2 Monthly assessment of MP items and masses in WWTP effluents

MP were detected in all effluent samples collected monthly at the WWTPs in Bremen-Seehausen and Kassel (**Fig. 3.2**). Item concentrations for L-MP were generally below 10^2 items m^{-3}, whereas S-MP were several magnitudes higher (max. Values: 3×10^4 items m^{-3}) (**Fig. 3.2 A-D**). Mass concentrations measured in Bremen-Seehausen were ranging from $0.3 \times 10^3 – 3.8 \times 10^3$ µg m^{-3} (**Fig. 3.2 E**).

Considering the L- and S-MP concentrations over the year, the Bremen-Seehausen WWTP showed minimum item and mass concentrations (S-MP) in November 2018, whereas samples collected in February and March 2019 yielded increased values (**Fig. 3.2 A, C, E**). In contrast to L-MP item concentrations (**Fig. 3.2 A**) and S-MP mass concentrations (**Fig. 3.2 E**), the S-MP item concentration of the sample taken in October 2018 was increased. As stated in **section 3.2.6**, this sample had been identified as an outlier. In Kassel, increased concentrations were recorded from December 2018 onward. S-MP concentrations were highest in January and March 2019, whereas L-MP concentrations showed a maximum in December 2018 (**Fig. 3.2 B+D**).

Concerning polymer compositions, polyolefins (PE, PP) were most abundant throughout the samples, regardless of the applied analytical method. The harmonised cluster h-PE was more prominent for L-MP items and S-MP masses, whereas h-PP was dominant for S-MP items (**Fig. 3.2 A, B, C, D**). Beside polyolefins, h-PUR/PMMA was prominent in S-MP items (**Fig. 3.2 B**). This was however not reflected in the mass data (**Fig. 3.2 E**), where instead h-PET was the third-most polymer type recorded. In general, the polymer composition, for both FTIR and Py-GC/MS data, indicated no clear seasonal changes over the year.

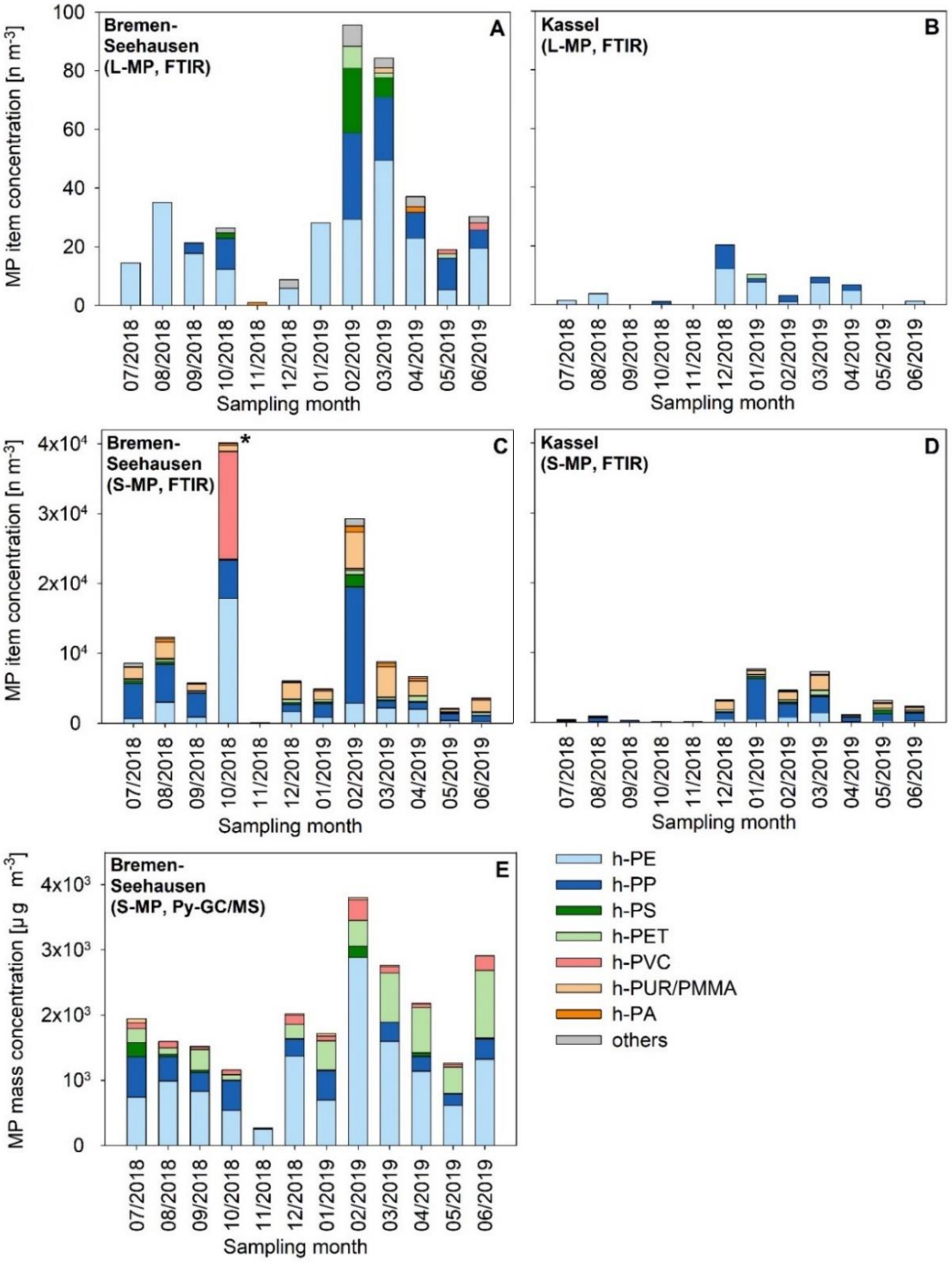

Fig. 3.2: MP item concentrations (A-D) and mass concentrations (E) detected in the effluents of the WWTPs in Bremen-Seehausen and Kassel. A: Bremen-Seehausen, L-MP items. B: Kassel, L-MP items. C: Bremen-Seehausen, S-MP items. D: Kassel, S-MP items. E: Bremen-Seehausen, S-MP masses. Polymer cluster abbreviations are given in Tab. 1 (*note: the sample collected in October 2018 showed strikingly high variations between the analysed aliquots and was considered as an outlier).

3.3.3 Comparison of two WWTPs: MP item concentrations, polymer composition and morphology

3.3.3.1 Large microplastics (L-MP)

Monthly MP item concentrations in the L-MP fraction were significantly higher in Bremen-Seehausen (median: 2.7×10^1 items m^{-3}) than in Kassel (median: 0.2×10^1 items m^{-3}) (**Fig. 3.3 A**) ($p = 0.001$). In both WWTPs, polyethylene (h-PE) and polypropylene (h-PP) were dominant polymer types (Bremen-Seehausen: 85%, Kassel: 97%) (**Fig. 3.3 B**). Bremen-Seehausen showed a higher polymer diversity, with assignments to all investigated clusters. The third-most abundant polymer type here was polystyrene (h-PS; 5%), whereas h-PET, h-PVC, h-PUR/PMMA, h-PA, and 'others' made up for the remaining 10%. Furthermore, with regards to morphology, particles were dominant over fibres/lines/filaments in both WWTPs, accounting for 88% (Bremen-Seehausen) and 90% (Kassel) of all detected items (**Fig. 3.3 C**). Regarding more specific shape type assignments, Kassel only showed two types (fragments: 90%, fibres and lines/filaments: 10%), whereas a higher diversity was recorded in Bremen-Seehausen (fragments: 80%, fibres and lines/filaments: 12%, films: 6%, foams: 1%). For illustration of the shape types recorded, a selection of L-MP items is presented in the **Supplementary Data 1, Fig. S5**. Size class distributions of particles from the two WWTPs were similar, with 77% being <2000 µm. As stated above, fibres/lines/filaments were scarce (Bremen-Seehausen: n = 19, Kassel: n = 4), and did not show a clear trend of increased abundances in small size classes.

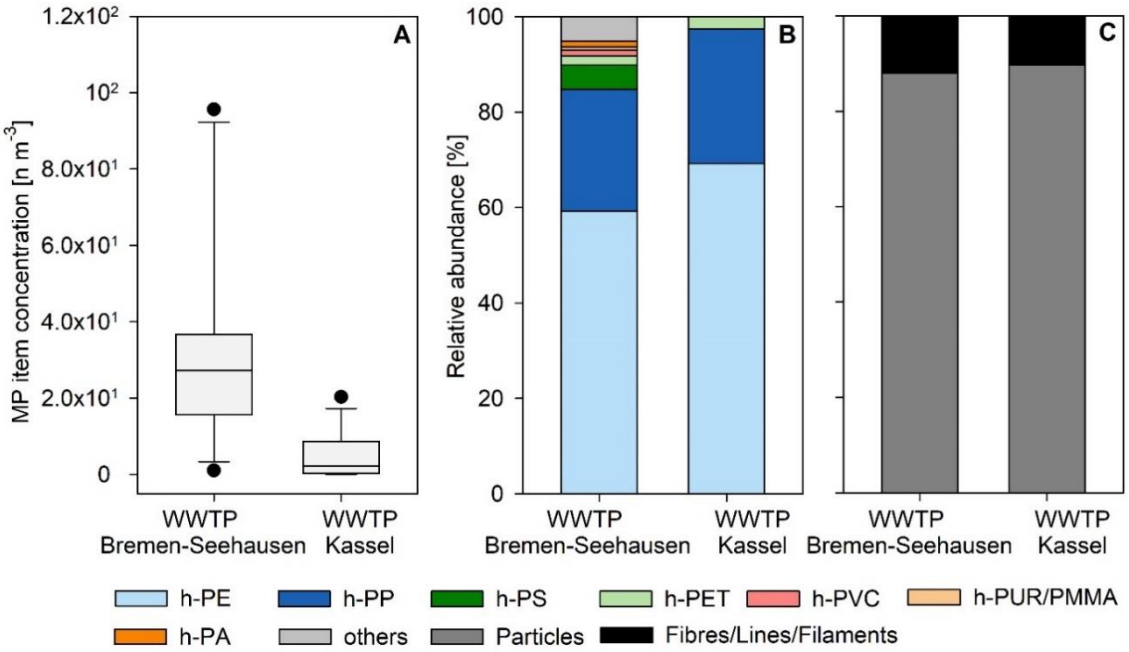

Fig. 3.3: Comparison of L-MP occurrence in the effluents sampled from the WWTPs in Bremen-Seehausen and Kassel. A. Item concentrations. B: Relative abundance of polymer types. C: Relative abundance of particles and fibres/lines/filaments. Polymer cluster abbreviations are given in Tab. 3.1.

3.3.3.2 Small microplastics (S-MP)

In accordance with the L-MP results, item concentrations in the S-MP fraction were significantly higher in Bremen-Seehausen (median: 6.0×10^3 items m^{-3}) than in Kassel (median: 1.7×10^3 items m^{-3}) ($p = 0.02$) (**Fig. 3.4 A**). The two WWTPs showed similar polymer compositions, with h-PP and h-PUR/PMMA being the dominant polymer types (Bremen-Seehausen: 42% and 25%, Kassel: 47% and 21%, respectively) (**Fig. 3.4 B**). The third-most abundant polymer type was h-PE (Bremen-Seehausen: 17%, Kassel: 12%). Regarding the morphology of detected MP items, as with the L-MP results, a clear dominance of particles over fibres was recorded in both WWTPs (**Fig. 3.4 C**). Additionally, the vast majority of particles was <100 µm (Bremen-Seehausen: 93 ± 15%, Kassel: 93 ± 24%). In contrast to the L-MP fraction, S-MP fibres showed a distinct trend of high abundances occurring in small size classes.

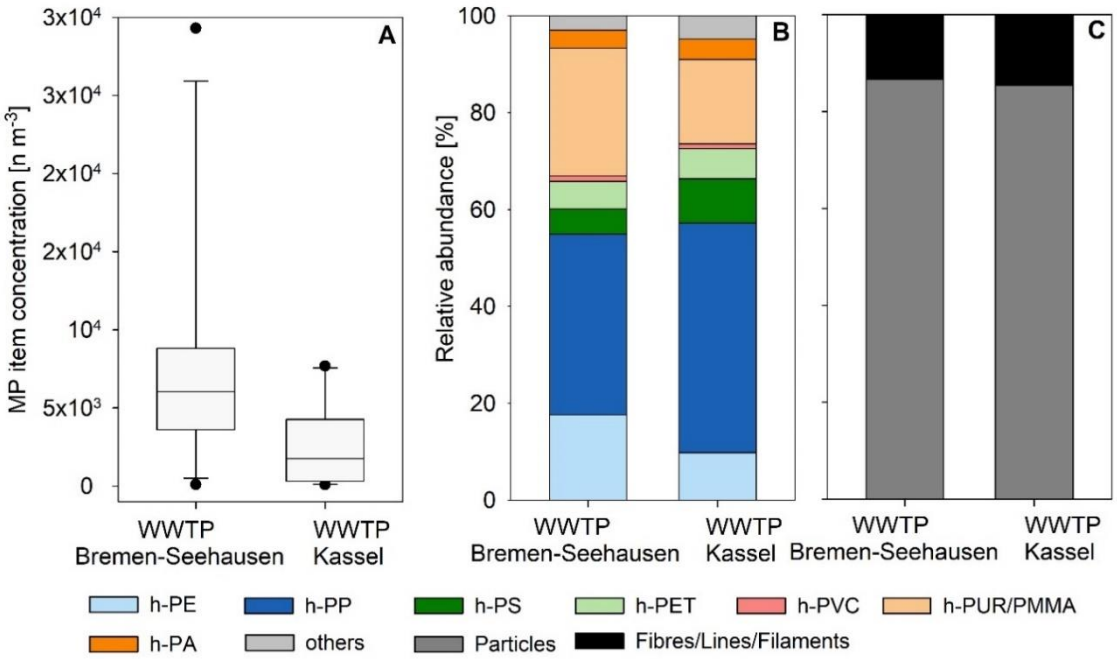

Fig. 3.4: Comparison of S-MP occurrence in the effluents sampled from the WWTPs in Bremen-Seehausen and Kassel. A. Item concentrations. B: Relative abundance of polymer types. C: Relative abundance of particles and fibres/lines/filaments. Polymer cluster abbreviations are given in Tab. 3.1.

3.4 Discussion

3.4.1 MP concentration, polymer composition and morphology: Inter-study comparison

This study provides detailed information on MP concentrations in the effluents of two German WWTPs over one year. In the following, our results on MP items and masses are set into context with the current research.

FTIR imaging allowed the detailed assessment of S-MP items down to 11 µm and revealed concentrations in the range $8.8 \times 10^1 – 2.9 \times 10^4$ items m^{-3}, with medians of 1.7×10^3 items m^{-3} (Kassel WWTP) and 6.0×10^3 items m^{-3} (Bremen-Seehausen WWTP). This was comparable to values previously reported for geographically relevant effluents of WWTPs in Northern Germany, following a similar approach for MP analysis (Mintenig et al. (2017), Primpke et al. (2020c); maximum: approx. 2×10^4 items m^{-3}). Comparable counts (average: 3.7×10^3–17.6×10^3 items m^{-3}) were also recorded by Conley et al. (2019), investigating the effluents of secondary WWTPs in South Carolina. Differences in analysis techniques, however, hamper a direct comparison: MP identification was performed solely visually, and the lower size limit of 60 µm possibly caused underestimations of smaller items. Simon et al. (2018) investigated the effluents of ten WWTPs in Denmark via FTIR imaging (size range 10–500 µm), and recorded roughly tenfold higher concentrations than presented in our study (median: 54×10^3 MP m^{-3}). Regarding their methodological approach, small sample volumes (median: 23.8 L) in combination with small individual aliquots (2–6% per sample) might have influenced the representativity of results, possibly causing overestimation. In our study, the application of mostly three representative aliquots enabled us to identify an outlier with strong variability between aliquots (Bremen-Seehausen, sample October 2018; Fig. S3). This approach represents a good compromise if the analysis of the whole sample is not possible. Finally, in accordance with previous studies (Sun et al. 2019, Primpke et al. 2020a), we emphasize the need for standardised protocols, including chemical identification, automation and harmonised sample handling, in order to set certain quality standards and allow a better comparability of datasets.

L-MP items were significantly less abundant than S-MP, representing <1% of all items. Concentrations of L-MP (on average < 20 items m^{-3}) were in a similar range as presented in Mintenig et al. (2017), who also applied ATR-FTIR for chemical identification. Similar concentrations of MP >500 µm were detected in previous studies, also applying visual pre-

sorting in combination with FTIR-ATR on effluent samples from WWTP in China (Lv et al. 2019) and Sweden (Rasmussen et al. 2021). In accordance with our findings, Rasmussen et al. (2021) also recorded significantly higher concentrations in the size fraction 10-500 µm (2300 and 5300 items m^{-3}) than in the fraction >500 µm (4 and 14 items m^{-3}). Despite these low concentrations often measured for MP >500 µm, their assessment can add valuable information, as these items can be considered as a potential source of smaller MP due to fragmentation processes and are also important contributors to overall mass loads.

The recorded mass concentrations of total MP were in the range of mg per cubic meter and are comparable to values presented by Primpke et al. (2020c). Furthermore, Funck et al. (2020) detected PS concentrations of 3 µg m^{-3}, using 10 µm meshes to concentrate WWTP effluent samples. This value was significantly lower than our results for PS masses (53 ± 71 µg m^{-3}). In general, comparable data on mass concentrations in WWTP effluents are scarce (Sun et al. 2019), and more research is required in order to fill this knowledge gap.

Chemical identification through FTIR and Py-GC/MS analyses revealed comparable results with a general dominance of polyolefins (h-PE and h-PP) in the WWTP effluent samples. These polymer types are amongst the most commonly used plastic materials worldwide (PlasticsEurope 2020), and were shown to be present in waste water effluents in several former studies, despite differences in analysis methods (Bayo et al. 2020, Tagg et al. 2020, Rasmussen et al. 2021). Beside h-PE and h-PP, h-PUR/PMMA was often present in the S-MP fraction with respect to MP items, but this trend was not reflected in the mass data. Polymers of this cluster (e.g., acrylate or alkyd-based) had been recorded in WWTPs in former studies (Murphy et al. 2016, Simon et al. 2018, Bayo et al. 2020). These compounds are commonly used for surface coatings, but also in various other applications (e.g. biomedical sector, cosmetics) (Ajekwene 2020). In contrast, the third-most abundant polymer type recorded in the mass assessment was h-PET, which was not prominent in MP item data. The much lower relative proportion when considering particle-based data could be caused by differences in polymer clustering. The µFTIR analysis, e.g., categorises polyesterurethanes in the Acrylates/PUR/varnish cluster (which corresponds to the h-PUR/PMMA cluster), while polyesterurethanes might be detected as PET in the Py-GC/MS. This difference in clustering would explain the diverging third-most abundant clusters in µFTIR (h-PUR/PMMA) and Py-GC/MS (h-PET) analysis. Further observed discrepancies

regarding polymer compositions obtained by both complementary detection principles are further discussed in **section 3.4.4**.

The clear dominance of particle over fibre items (**Fig. 3.3 B, Fig. 3.4 B**) contrasts with previous studies, which predominantly detected fibres in WWTP effluent samples (Gündoğdu et al. 2018, Conley et al. 2019, Ben-David et al. 2021). However, Bayo et al. (2020) and Simon et al. (2018) as well recorded less fibres compared to particles in effluents. It remains unclear if these discrepancies are due to differences in WWTP treatment processes or rather caused by differences in methodological approaches, which again emphasizes the need of standardised methods to allow for a solid comparison. Within the L-MP fraction, particles were further distinguished into fragments, films and foams, with fragments being most abundant. Within the fragment-like items, many different colorations, and shapes (e.g., irregularly frayed, or with straight edges) were recorded, suggesting various different origins.

3.4.2 Influencing factors of microplastic pollution in WWTPs

3.4.2.1 Seasonal variation

The twelve-month sampling had the advantage of covering various effluent states, which can be further evaluated for effects on MP pollution levels in WWTP effluents. The assessment of relevant basic effluent parameters like effluent discharge rate, suspended matter (SPM), chemical oxygen demand (COD), total organic carbon (TOC) and turbidity revealed no clearly visible correlation with MP item and mass concentration in the Bremen-Seehausen WWTP (**Supplementary Data 1, Table S11, Table S12**). Nonetheless, the effluent sample with the highest level of MP pollution from this site (February 2019) was sampled during heavy rainfall (11.8 L m^{-2}), and thus has the highest discharge in combination with high SPM and TOC. This trend was also reflected in high mass concentrations in June 2019. In Kassel we could identify a correlation between turbidity and total MP item concentration (r^2 = 0.545; p = 0.014) (**Supplementary Data 1, Tab. S13, Tab. S14**). This correlation is particularly brought out by the samples collected from December 2018 until March 2019 with the highest turbidity values. The two most polluted samples are from January and March 2019, which also hold the highest turbidity values. Furthermore, the March sample has the highest discharge values for this site due to rainfall, similarly to the February sample from Bremen-Seehausen.

The general trend that high discharge or high organic loads are accompanied by high MP item and mass concentrations underlines the current theory that extreme events like heavy rainfalls remobilise MP and therefore are a main vector in MP transport (Veerasingam et al. 2016, Gündoğdu et al. 2018b, Hitchcock 2020). Thus, more MP might enter the WWTP during heavy rains and therefore pass it, assuming the WWTP maintains the same clearance rate. Furthermore, a reduction in the clearance rate could be assumed due to shorter residence times, pre-clearance or higher turbulences in the WWTPs and might therefore lead to diminished particle settling. The reduction of settling MP might then induce a higher MP load in the effluent.

In conclusion, our data underline the need for a comprehensive background parameter analysis in MP environmental analysis with a special focus on rainfall events. The aspect that rain events lead to an increasing discharge paired with an increased MP concentration suggest that they can be seen as a major driver for MP pollution levels in effluents.

3.4.2.2 Site-specific influences

The analysis of the effluents from the WWTPs in Bremen-Seehausen and Kassel allowed for the direct comparison of MP item concentrations and polymer compositions between these two sites over the course of a year. Polymer composition and MP morphology were shown to be very similar in both WWTPs. The S-MP fraction was dominated by h-PP, h-PUR/PMMA and h PE (**Fig. 3.4**), consisting out of 93% particles over fibres. The L-MPs were mainly identified as h-PE and h-PP (**Fig. 3.3**). The lower polymer diversity in the L-MP fraction in Kassel is most likely caused by the lower total number of particles which induces a relative underrepresentation of rarer polymer types. The morphology of L-MP items again is very similar with 88% (Bremen-Seehausen) and 90% (Kassel) particles over fibres/lines/filaments.

The similarities in polymer composition and item morphology are in contrast with the significant differences in MP concentrations. However, with respect to polymer composition, polyolefins are omnipresent in household as well as industry, and are therefore likely to be detected in WWTP despite having different proportions of wastewater influxes. Accordingly, Mintenig et al. (2017) showed a dominance of polyolefins in 12 investigated Northern German WWTPs, regardless of the varying proportions of municipal, industrial or touristic wastewater they received.

The WWTP in Bremen-Seehausen showed consistently higher L-MP and S-MP item concentrations in the annual comparison of the effluent (**Fig. 3.4, Fig. 3.3**) than the Kassel WWTP. The annual mean discharge is 7-fold higher in Bremen than in Kassel. This significant difference most likely results from different wastewater inputs or clearance rates. Concerning the wastewater input, both WWTPs differ in the relative proportion of industrial wastewater they receive. The WWTP in Bremen-Seehausen receives 39% industrial inputs, while Kassel receives only 22%. Another input factor is the admixture of extraneous water within the sewage system potentially inducing a dilution of the MP pollution prior to the WWTP, which accounts for 30% for the Kassel WWTP, and only 10% in Bremen-Seehausen.

Furthermore, a difference in the clearance efficiency could be caused by multiple variations in the subsequent clean-up stages. The major differences between the two WWTPs were the unequal residence times in the pre-clearance stage and the extent to which each WWTP used flocculation agents. The residence time in pre-clearance in Kassel is comparably longer (Kassel: 4.4 h, Bremen-Seehausen: 3.1 h) which might cause a higher settling rate of MP and therefore a better clearance. Furthermore, Kassel uses more flocculation agent (personal communication) which could result in a higher MP retention through the incorporation of MP into flocs (Lapointe et al. 2020). Accordingly, a higher residence time and flocculation agent usage might be responsible for the lower MP count in the Kassel WWTP effluent.

The afore-mentioned factors can be seen as possible explanations for the observed MP pollution levels in effluents, although the major factors on MP transport within the sewage system are still lacking scientific insights.

3.4.3 Impact on receiving water body

The two WWTPs investigated in this study are potential point sources for MPs in the receiving water bodies. These are the Lower Weser, which discharges into the German North Sea, as well as one of its two headstreams, the river Fulda. The Lower Weser has been assessed for MP occurrence (item-based) in a recent study (Roscher et al. 2021). When contextualising the results, temporal differences in sampling have to be taken into account (Lower Weser: April 2018, WWTP: July 2018 to June 2019). In the following, we attempt a conservative comparison of pollution patterns for MP items in effluent and surface water samples from the receiving water body.

For both S-MP and L-MP, mean item concentrations were higher in the effluent of the Bremen-Seehausen WWTP than in adjacent riverine surface water (**Supplementary Data 1, Table S15**), e.g. averaged S-MP concentrations in the effluent were 8 to 40 times higher than S-MP in the river surface. Thus, the WWTP Bremen-Seehausen can be seen as a MP source for the Weser River. Furthermore, the S-MP river concentrations were higher at the downstream station, whereas L-MP were slightly lower, but yet in the same order of magnitude, downstream.

Regarding the absence/presence of polymer types, both size fractions showed that h-PE, h-PP and h-PUR/PMMA were present in effluent samples as well as in upstream and downstream surface water stations (even upstream the Weser Weir) (**Supplementary Data 1, Fig. S6**). Considering the absence/presence of polymer types, no distinct influence of the WWTP effluent is visible in the available river sample data. Thus, we suggest that the WWTP feeds into the already existing pollution patterns of the Weser River.

Only few studies systematically investigated the direct impact of WWTPs on MP pollution levels in the receiving water bodies (item-based). Kay et al. (2018) studied six WWTPs and adjacent riverine locations in England and recorded that MP item concentrations were highest downstream of the WWTPs at all locations. Recent studies focused on WWTPs discharging into marine systems (Ramírez-Álvarez et al. 2020, Franco et al. 2021), recording significantly higher item concentrations in the WWTP effluents (8.1×10^{1}–1.6×10^{3} MP m^{-3} and 16.4×10^{3}–13.1×10^{4} MP m^{-3}, respectively) than in adjacent surface waters (1×10^{-2}–7×10^{-1} MP m^{-3} and 0.8×10^{3}–6.6×10^{3} MP m^{-3}, respectively). Ramírez-Álvarez et al. (2020), in addition, showed that accumulation of MP occurs in nearby sediments. The authors conclude that WWTPs effluents are relevant pathways for MPs in the Mexican Todos Santos Bay, but also suggest the presence of other sources, such as agricultural activities or beach littering, emphasizing the importance of currents or winds for MP distribution patterns as well.

Although analytical methods and locations of WWTPs differ strongly in the afore-mentioned studies, all have in common that WWTPs steadily discharge MPs into the environment. Despite the high potential removal rates of MP by WWTPs observed in previous studies (Bayo et al. (2020): 90%; Conley et al. (2019): 85-98%; Talvitie et al. (2017b): 98%), they should be still seen as a considerable pathway of MP into river systems (Iyare et al. 2020, Schmidt et al. 2020), in particular, since removal rates can vary severly

(Akarsu et al. (2020): 55-97%). Finally, WWTPs can be seen as constant point sources of MP into the receiving water bodies, especially when considering the high input of treated waste water per day (this study: Bremen-Seehausen WWTP: 84,000-297,000 m^3; Kassel WWTP: 46,000-113,000 m^3; cf. **Table S11 and S13**). Resulting estimated MP fluxes amount to $1.1 \times 10^9 \pm 1.7 \times 10^9$ items/day and $2.5 \times 10^8 \pm 2.0 \times 10^8$ µg/day in Bremen-Seehausen, and $1.9 \times 10^8 \pm 2.5 \times 10^8$ items/day in Kassel.

3.4.4 Analytical methods used for MP assessment

3.4.4.1 Complementary analysis techniques

This study provides detailed information on MPs in WWTP effluents over one year, including the complementary application of µFTIR and Py-GC/MS for item and mass assessments for one of the sample sets (S-MP fraction, Bremen-Seehausen WWTP). In the following, we attempt to elucidate general similarities and differences between mass and item data. Here, it has to be kept in mind that the processed sample material was split in half prior to the two analysis approaches, and a maximum of three representative aliquots per sample were measured via µFTIR. Though this hampers a one-to-one comparison of individual samples, the approach of splitting the samples in half provides a general overview about MP item and mass data and represented the most time-efficient way for a complementary analysis.

As stated in **section 3.4.1**, both MP mass and item data resulted in a general dominance of polyolefins (h-PE and h-PP). Although highly abundant in all S-MP size classes from 11 to 500 µm, these polymers become even more prominent in larger size classes of the S-MP fraction, with h-PE and h-PP accounting for approx. 80% of the polymer types between 200 and 500 µm (**Supplementary Data 1, Fig. S7**). Thus, these large h-PE or h-PP items are most likely responsible for their elevated mass data. The second-most abundant polymer type within the S-MP item data was h-PUR/PMMA, however it was much less prominent in the mass data. Compared to h-PE and h-PP, particle sizes assigned to h-PUR/PMMA were much smaller, which might be reflected by their smaller mass impact.

In order to evaluate this assumption, the mass calculation suggested by Simon et al. (2018) and Primpke et al. (2020c) were applied on the S-MP item data (cf. **section 3.2.6**). The results showed that both mass calculations did not influence the overall polymer composition despite the higher percentage of h-PE particles in the bigger size classes. The h-PUR/PMMA cluster remained equally dominant, respectively (**Supplementary Data 1,**

Fig. S8). The absence of relative changes in the polymer composition is probably attributed to the very low number of items in the bigger size classes. Thus, their relative influence on the calculated mass is negligible. The observed differences in polymer compositions might be due to method-specific polymer identification techniques, producing differences in polymer clustering as already observed by Primpke et al. (2020c).

Interestingly, the area-based mass calculations suggested by Primpke et al. (2020c) and applied to our data led to significantly lower masses in comparison to Simon et al. (2018) and the measured masses (**Supplementary Data 1, Fig. S9**). This was in contrast to the findings by Primpke et al. (2020c) (however, Primpke et al. (2020c) did not perform a sample splitting but measured exactly the same sample material with µFTIR and Py-GC/MS, so that a direct comparison is hampered). Further, in the present study the area-based mass data calculation underestimated the directly measured Py-GC/MS data by a factor of four, or often more. The mass calculation based on Simon et al. (2018) lays in the same order of magnitude, while it highly overestimates the mass of one sample (August 2018) by a factor of five. However, the overall concentration trend of both mass-calculations generally reflected the measured masses almost consistently, with a minimum value in the November 2018 sample, and a maximum in the February 2019 sample.

In conclusion, the application of MP mass calculations based on MP item counts can support data interpretation and comparability, although limitations of this theoretical approach must be considered. The adequate conversion of item data in to mass data still needs further investigation. As stated by Primpke et al. (2020c), the Py-GC/MS mass calculation based on the calibration of pure polymers should be the preferred approach for systematic studies focussing on MP mass concentrations.

3.4.4.2 Database adaptation for µFTIR analysis

To our knowledge, this study is the first to prove the potential of waxy plant cuticles to be mistaken for synthetic polymers in µFTIR analyses. This was due to interfering spectral bands at 2920 cm^{-1} and 2850 cm^{-1} (asymmetric and symmetric CH_2 stretching; cutin waxes), 1730 cm^{-1} (C=O stretching; cutin) and 1450 cm^{-1} (CH_2 scissoring, cutin waxes) (Heredia-Guerrero et al. 2014). As stated in **section 3.2.4.3**, a database adaptation was performed in order to counteract these false-positive assignments. This approach significantly reduced MP item counts, especially within the µFTIR clusters acrylates/PUR/varnish, PE-chlorinated, and EVA (cf. **section 3.3.1; Supplementary**

Data 1, Table S8 and S9). Our original in-house designed polymer database already contained several natural reference materials, such as cellulose, quartz or chitin (Primpke et al. 2018), aiming at an accurate assessment of materials present in environmental samples. However, a thorough re-inspection of µFTIR data, as performed in this study, is crucial for the identification of missing links in terms of other potentially disturbing matrix compounds. This necessity of the inclusion of natural materials to polymer databases has also been pointed out in other studies (Renner et al. 2018, Kedzierski et al. 2019), and so has the requirement for validating and calibrating polymer databases before usage (Cowger et al. 2020).

Beside advancements of polymer databases, the application of a broader wavenumber range for MP measurements has potential to increase differentiation of materials. The Anodisc© filters used in this study already cover a relatively wide wavenumber range (3600−1250 cm^{-1}) and proved suitable for MP analysis (Löder et al. 2015), but are not IR-transparent below 1250 cm^{-1}. This range is known to contain important additional spectral information. Materials like silicon oxide, in contrast, are IR-transparent below 1250 cm^{-1} (Käppler et al. 2015). Disadvantages are higher costs and longer processing times due to an increased data output, however, it can be seen as a promising alternative filter material for MP analysis.

In addition to adaptations to the chemical-analytical approaches, sample preparation methods should also be reconsidered. We chose to apply an enzymatic-oxidative protocol, representing a less destructive alternative to treatments with strong acids or alkaline solutions. The 3-day-treatment with technical cellulase likely macerated plant material to a certain extent, but was obviously not suited to digest the more complex wax-containing cuticle residues. The implementation of another digestion step, targeting these waxy compounds, could provide remedy for this issue. Cutinases have been described as versatile enzymes, which are stable in the temperature range 20−50 °C and applicable together with other enzymes and H_2O_2 (Chen et al. 2013). Hence, the addition of a cutinase step, subsequent to the cellulase treatments, could be promising to target any remaining cutin-rich material. Systematic studies should be performed in order to evaluate its efficacy. Furthermore, the ability of cutinases to break down the ester bonds of PEST fibre surfaces, reported in previous studies (Kawai et al. 2017, Sooksai et al. 2019), should be critically investigated in order to better evaluate any detrimental effects that the cutinases may have on MP contained within the samples.

3.5 Conclusion

This study provides comprehensive MP item and mass data of the effluents of two German WWTPs, sampled monthly over one year. The analysis of MP composition and MP item morphology (size, shape) revealed high similarities between the two WWTPs and within the monthly samples. Both WWTP effluents were dominated by polyolefins and particles below 100 µm. This implies similar MP inputs passing through the WWTPs. The MP item concentration, on the other hand, was significantly different between both WWTPs, which might be linked to differences in treatment processes, admixture ratio of extraneous water or industrial inputs.

The complementary application of Py-GC/MS on effluent samples from the Bremen-Seehausen WWTP confirmed the dominance of polyolefins, as well as the similarities in polymer composition between sampling events. In contrast, both MP mass and item concentrations showed variations over the course of the year. High MP levels mainly occurred with increased total organic carbon, turbidity or effluent discharge volumes, caused by heavy rainfall. These observations highlight that the parallel assessment of background parameters should be implemented in future studies, in order to better understand MP dynamics and variances in pollution levels in WWTPs.

The combined analysis using both Py-GC/MS and FTIR provided a detailed insight into MP pollution levels with regards to items and masses, as well as respective polymer compositions. Herein, we still see potential to further improve the comparability of both analysis methods, to strengthen the complementary character. With regards to FTIR, our findings emphasize the importance of including valid natural materials within polymer reference databases used in MP analyses, in order to improve data quality and avoid false-positive assignments due to matrix effects.

Finally, the comprehensive dataset obtained here provides a reference for upcoming studies on MP in WWTP effluents and can act as a baseline for future toxicological or modelling studies.

Declaration of Competing Interest

The authors declare that they have no known competing financial interests or personal relationships that could have appeared to influence the work reported in this paper.

Funding: This work was supported by the German Federal Ministry of Education and Research (Project PLAWES, ʻMicroplastic Contamination in the Weser- Wadden Sea – National Park Model System: an Ecosystem-Wide Approachʼ; grant numbers: 03F0789B, 03F0789E).

Acknowledgements

We thank the staff members at the WWTP in Bremen-Seehausen and Kassel for implementation of the monthly sampling and for kindly providing technical background data and functional knowledge of the facilities. We further thank H. Jebens and S. Dirksen for laboratory assistance, and N. Mackay-Roberts for proof-reading of the manuscript.

Chapter 4 – Comparison of two rapid automated analysis tools for large FTIR microplastic data sets

Sonya Moses[a]*, Lisa Roscher[b]*, Sebastian Primpke[b], Benedikt Hufnagl[c,d], Martin G. J. Löder[a], Gunnar Gerdts[b#], Christian Laforsch[a#]

[a] Department of Animal Ecology I, University of Bayreuth, Universitätsstr. 30, 95440 Bayreuth, Germany

[b] Alfred Wegener Institute Helmholtz Centre for Polar and Marine Research, Biologische Anstalt Helgoland, Kurpromenade 201, 27498 Helgoland, Germany

[c] Institute of Chemical Technologies and Analytics, Vienna University of Technology, A 1060 Vienna, Austria

[d] Purency GmbH, A 1010 Vienna, Austria

* *Shared first-authorship*

[#] *Shared senior authorship*

Corresponding authors:

Gunnar Gerdts (gunnar.gerdts@awi.de)

Christian Laforsch (christian.laforsch@uni-bayreuth.de)

Sebastian Primpke (sebastian.primpke@awi.de)

Martin Löder (martin.loeder@uni-bayreuth.de)

Keywords: automated microplastic analysis, FTIR, siMPle, Bayreuth Particle Finder (BPF), water samples

Citation:

Moses, S.R., Roscher, L., Primpke, S. *et al.* Comparison of two rapid automated analysis tools for large FTIR microplastic datasets. *Anal Bioanal Chem* (2023). https://doi.org/10.1007/s00216-023-04630-w

Abstract

One of the biggest issues in microplastic (MP, plastic items < 5 mm) research is the lack of standardization and harmonization in all fields, reaching from sampling methodology to sample purification, analytical methods and data analysis. This hampers comparability as well as reproducibility among studies. Concerning chemical analysis of MPs, Fourier-transform infrared (FTIR) spectroscocopy is one of the most powerful tools. Here, focal plane array (FPA) based micro-FTIR (µFTIR) imaging allows for rapid measurement and identification without manual preselection of putative MP and therefore enables large sample throughputs with high spatial resolution. The resulting huge data sets necessitate automated algorithms for data analysis in a reasonable time frame. Although solutions are available, little is known about the comparability or the level of reliability of their output. For the first time, within our study, we compare two well-established and frequently applied data analysis algorithms in regard to results in abundance, polymer composition and size distributions of MP (11 – 500 µm) derived from selected environmental water samples: a) the siMPle analysis tool (**s**ystematic **i**dentification of **M**icro**Pl**astics in the **e**nvironment) in combination with MPAPP (**M**icro**P**lastic **A**utomated **P**article/fibre analysis **P**ipeline) and b) the BPF (**B**ayreuth **P**article **F**inder). The results of our comparison show an overall good accordance but also indicate discripancies concerning certain polymer types/clusters as well as the smallest MP size classes. Our study further demonstrates that a detailed comparison of MP algorithms is an essential prerequisite for a better comparability of MP data.

4.1 Introduction

While the microplastic (MP, plastic items < 5 mm) contamination of the environment is constantly growing, MP has meanwhile been detected in all ecosystems reaching from aquatic (Cole et al. 2011, Lebreton et al. 2017, Primpke et al. 2017) to aerial (Dris et al. 2016, Gasperi et al. 2018, Kernchen et al. 2021) to terrestrial systems (Rillig 2012, Weithmann et al. 2018, Rillig and Lehmann 2020) and has also been found in remote areas far from population centres such as Arctic ice (Obbard et al. 2014, Peeken et al. 2018) and remote mountain lakes (Free et al. 2014, Negrete Velasco et al. 2020) but also in biota (Sanchez et al. 2014, Scherer et al. 2018). For an accurate risk assessment reliable analytical methods are thus urgently required to appropriately identify MP isolated from environmental matrices qualitatively and quantitatively (Kögel et al. 2020). The field of MP research arose from MP detected in coastal waters in the 70s, initially focusing on rather large MPs (sampled with plankton tow nets (mesh size: 333 µm)) (Carpenter et al. 1972, Carpenter and Smith 1972). Due to their size, manual handling of prospective large MP items for analysis is possible and is common practice. Commonly applied methods for larger MP particles are visual identification (Norén 2007), Nile red staining (Cole 2016, Shim et al. 2016), the hot needle method (Devriese et al. 2015) or through Attenuated Total Reflectance (ATR)-Fourier transform-infrared (FTIR) spectroscopy (Löder and Gerdts 2015, Primpke et al. 2020a, Ivleva 2021) which allows for chemical identification of the respective polymer. However, most of these methods are prone to human bias, leading to an over- or underestimation of the MP abundance. While analysis with ATR-FTIR also requires a manual preselection of prospective MP and is thus also susceptible to bias, the chemical identification of polymers is reliable which makes this method favourable for the analysis of larger MP.

Recent studies have shown that the abundance of small MP (S-MP, < 500 µm) in the environment is much higher and thus should not be neglected when evaluating the environmental MP contamination (Hildebrandt et al. 2021, Huang et al. 2021), especially when considering the increased potential toxicity of small MP (Yong et al. 2020). Due to their miniscule size and high abundance, manual analysis of S-MP is not feasible. Thus rapid, automated and highly accurate analytical methods are required that allow for a high throughput rate of samples. Well established analytical methods include pyrolysis-gas chromatography (py-GC) coupled with mass spectrometry (MS) (Fischer and Scholz-

Böttcher 2017, Gerdts et al. 2017, Fischer and Scholz-Böttcher 2019) or thermal extraction desorption (TED) GC-MS (Dümichen et al. 2015, Mansa and Zou 2021) which, however, only give information on polymer composition and polymer masses in a sample. In contrast, spectroscopic methods such as focal plane array (FPA) based micro-Fourier-transform infrared (µFTIR) imaging (Löder et al. 2015, Primpke et al. 2020a, Ivleva 2021) and µRaman mapping (Lenz et al. 2015, Käppler et al. 2016, Ivleva 2021) have proven to be highly efficient methods for MP analysis of sample filters, yielding information not only on polymer type but also on item count, shape and size distributions.

This study focuses on FPA-µFTIR analysis of S-MP derived from environmental samples as this technique facilitates chemical imaging by simultaneously recording thousands of spectra within one measurement in a reasonable timeframe, which makes it a powerful tool in MP analysis of whole sample filters (Löder et al. 2015). Previously, the IR-spectra of each item on the filter containing the purified sample were compared manually to reference spectra, which is prone to human bias. Due to the prevalence of non-plastic residues post purification and the potentially high abundance of S-MP in environmental samples, this, however, is extremely time-consuming and therefore not practical, especially for monitoring studies where a high number of samples need to be analysed. To facilitate a rapid analysis without manual screening, a broad range of algorithms have been developed to automate the process of spectroscopic MP data analysis. As explained by Hufnagl et al. (2022), these can be categorized into model-based (Serranti et al. 2018, Hahn et al. 2019, Hufnagl et al. 2019, Paul et al. 2019, Shan et al. 2019, da Silva et al. 2020, Weisser et al. 2021) and instance-based (Primpke et al. 2017, Renner et al. 2017, Primpke et al. 2018, Zhang et al. 2018b, Kedzierski et al. 2019, Liu et al. 2019, Renner et al. 2019, Brandt et al. 2020, Primpke et al. 2020b) machine learning approaches. Model-based approaches are based on a statistical model from spectroscopic reference data which is then applied to unknown spectra. These are then assigned to predefined classes which may include anything from polymer types to matrix components such as sediment, plant or animal debris. Instance-based approaches, in contrast, directly apply the reference data (i.e. the "instance") to identify unknown spectra based on similarity measures. Here, hit quality indices (HQIs) are computed, e.g. by measures such as the Pearson correlation coefficient (Primpke et al. 2020b, Hufnagl et al. 2022). The advantage of this approach is that the spectroscopic reference data can easily be enhanced or adapted, e.g. by adding relevant spectra to the existing library (Roscher et al. 2022). For model-based learning, however, a high degree of

expert knowledge is required which make application-specific changes more difficult. On the other hand, it has the advantage of much shorter analysis time which allows for a higher analytical throughput (Hufnagl et al. 2022).

In the field of MP research, it is well recognised that the comparison of results from different studies is often hampered by the lack of standardization concerning sampling methods, sample processing and analytical methods. Discrepancies can of course also arise from different automated data evaluation algorithms at the end of the analytical pipeline. Thus, as a first step towards harmonization in this regard, the aim of our study is a comprehensive comparison of the output of two frequently used and well-established FPA-µFTIR data analysis algorithms: (1) siMPle (systematic identification of MicroPlastics in the environment) (which is freely accessible on www.simple-plastics.eu) (Primpke et al. 2020b) in combination with the image analysis tool MPAPP (MicroPlastic Automated Particle/fibre analysis Pipeline), with its script having been published by Primpke et al. (2019) (available for download as executable here: https://drive.google.com/drive/folders/1fWIGp7MgJZJcy7NWI5Vri0eUYJw0Qvrz?usp=share_link), and (2) the Bayreuth Particle Finder (BPF), which is based on the methodology presented in Hufnagl et al. (2019) and is an integrated module in the Epina ImageLab Engine (www.imagelab.at). BPF is the preliminary version of the Microplastic Purency Finder developed by the Purency GmbH, which is commercially available (https://www.purency.ai/microplastics-finder). The main difference between both approaches is that siMPle is an instance-based machine learning approach and relies on a dual database search using two different similarity measures. HQIs are computed through Pearson correlation (Primpke et al. 2020b). BPF on the other hand is a model-based machine learning approach. Here a combination of spectral descriptors and random decision forest (RDF) classifiers is applied [42]. Both pipelines allow for the analysis of whole filters, avoiding the bias which would occur during extrapolation of results obtained from randomly preselected subareas of a filter (Schymanski et al. 2021). Furthermore, they have been applied frequently in a multitude of different studies, analyzing MP from various environmental matrices. BPF has for instance been applied in different studies focusing on MP contamination in freshwater environments, such as Frei et al. (2019) and Schrank et al. (2022). It has further been applied in studies focusing on the analysis of airborne MP (Kernchen et al. 2021), MP in soil (Möller et al. 2022) but also MP in animal tissue (Teichert et al. 2021). Over the course of the years, the approach based on RDF classifiers after

Hufnagl et al. (2019) has undergone different development stages to improve on certain aspects of the classification, resulting in the latest version which was released in 2021 (Hufnagl et al. 2022) and applied in Dong et al. (2021). For the present study, the version released in 2019 was chosen, as it had been applied in the above-mentioned previous studies. The analysis software siMPle also finds a broad range of applications, e.g. in the analysis of drinking water (Kirstein et al. 2021), wastewater (Rasmussen et al. 2021) or marine waters (Rist et al. 2020). In combination with MPAPP or its precedent version APA (Automated Particle Analysis, after Primpke et al. (2017)) siMPle has been applied in recent studies on river surface water (Mintenig et al. 2020, Roscher et al. 2021), wastewater effluents (Primpke et al. 2020c, Roscher et al. 2022), and deep sea sediments (Abel et al. 2021).

Within this study we have analysed two sample sets containing ten measurement files each, which were both analysed by the algorithms siMPle/MPAPP and BPF. The resulting data output was compared with respect to (a) MP abundance, (b) polymer composition and (c) size distribution. Hereby, the present work can enhance the understanding of similarities and differences of MP analysis pipelines, with the ultimate goal of forming a basis for a better comparability of MP data sets from different studies. It is to be noted that the two sample sets used for the comparison of the two aforementioned analysis algorithms are based on environmental samples. Thus, the actual amount of MP in the samples is unknown but the comparison of the output data is nevertheless valid. We chose to work with environmental samples in order to demonstrate the complexity of the analysis of these samples, representing all environmentally relevant polymer types, shapes and sizes as well as environmentally aged MP, potentially containing matrix residue and remains of biofilm. As mentioned above, S-MP is much more abundant in the environment and poses a higher ecotoxicological risk. Thus, the importance of evaluating methods suitable for the analysis of S-MP is enhanced and our study aims at shedding light on this matter.

4.2 Materials & Methods

In order to compare the output of the two analysis pipelines, two MP sample sets (size range: 11 - 500 µm) – sample set A containing ten riverine samples and sample set B containing ten estuarine samples - were analysed with the BPF (Hufnagl et al. 2019) and in parallel with the MP analysis tools siMPle and MPAPP (Primpke et al. 2019, Primpke et al. 2020b). The measurement files re-analysed in the present work had been generated in the framework of the joint project PLAWES (Micro**pla**stic Contamination in the We**s**er-Wadden Sea – National Park Model System: an Ecosystem-Wide Approach), which aimed at a comprehensive assessment of MP in the river system Weser-Wadden Sea. Herein, sample set A contains water samples from the Upper and Middle Weser, and is subject of a study by Moses et al. (unpublished data). Sample set B contains water samples collected in the Lower/Outer Weser and Jade Bay and was initially analysed by Roscher et al. (2021) (**Tab. S1**).

After enzymatic-oxidative sample purification based on the protocol presented in Löder et al. (2017), all samples had been filtered onto Anodisc^{TM} filters (aluminium oxide, pore size: 0.2 µm, diameter: 25 mm, Whatman, UK). Measurements using µFTIR imaging (Bruker Hyperion 3000, Bruker Optik GmbH, Germany) were performed with a 64x64 FPA detector in transmission mode with a 3.5 x IR lens in the wavenumber range 3600−1250 cm^{-1} (spectral resolution: 8 cm^{-1}) using 32 co-added scans (background on pure filter: 32 and 64 scans, respectively), resulting in a pixel resolution of 11 µm. Data were saved as OPUS-measurement files (operating software OPUS 7.5, Bruker Optik GmbH, Germany). Details on the subsequent data analysis through siMPle/MPAPP and BPF are provided in the following sections.

4.2.1 siMPle/MPAPP

OPUS-measurement files of sample set A and B were first processed with the software OPUS 7.5 (Bruker Optik GmbH, Germany), in order to transfer spectral data into the file format .dx in preparation to the following analysis steps (Primpke et al. 2020b). In siMPle (version 1.1.β), the .dx files were converted into the .spe format, allowing for the subsequent automated comparison to our in-house polymer database (Primpke et al. 2018). Within this process, each spectrum is compared twice with the database (siMPle_database_Version 1.0.1), first using the untreated spectra and a second time using the 1st derivatives for

spectral correlation calculation. Only if both processes determine the spectrum of the same polymer type, it is labelled as correctly identified for later image analysis, following the approach from Primpke et al. (2017). The data processing in siMPle was followed by the final image analysis via MPAPP. Here, the determined image containing the x,y coordinates on the filter, the combined hit quality and assigned polymer type are first analysed against polymer-specific quality control threshold values (Lorenz et al. 2019) for each polymer type. This is followed by a majority voting filter analysis and a series of image analysis tools to separate fibre like items from particles (see Primpke et al. (2019) for the exact details of the procedure). Sample set B underwent an additional processing step, where the pixels assigned to the polypropylene (PP) support ring of the Anodisc filters containing the sample were removed in OriginPro.2017G (OriginLab Corporation, USA) (size of measurement field: 20 × 20 – 22 × 22 FPA tiles). This step was not necessary for sample set A, as a smaller measurement field had been applied (17 × 17 FPA tiles), which did not cover any border area of the filter. The final analysis using MPAPP provided information on numbers, sizes and polymer composition of particle and fibre-like MP items Primpke et al. (2019).

4.2.2 Bayreuth Particle Finder (BPF)

Both datasets analysed with BPF were also first processed with the software OPUS 7.5 (Bruker Optik GmbH, Germany), in order to transfer spectral data into the file format .hdr while the optical image was extracted as .jpeg file. The .hdr file containing the spectral data and the infrared image of the analysed filter were then imported to the program ImageLab (Epina GmbH) (Hufnagl et al. 2019). The optical image was then aligned with the infrared image and carefully adjusted manually. After calibration with measurement parameters from the OPUS measurement file, the BPF algorithm was applied to the measurement data. The database used to train the machine learning model contained 22 polymer types (for details see **Tab. 4.1**). In the classification step each pixel is classified by the machine learning model resulting in the assignment to either a polymer type or a class describing the matrix (“non-plastic”) or the filter surface (“background”). MP items are detected as neighboring pixels of the same polymer class. The results are presented in a list containing their properties such as the size (longest and shortest dimension), polymer type, position on the filter etc. All material identified and categorized as “non-plastic” and “background” were deselected. The spectra of the remaining items were checked twice by experts. This conservative step is optional but was included in our routine for QA/QC and more reliable

results. In Hufnagl et al. (2022) cases are dicussed, where expert intervention can significantly improve questionable results, e.g. coming from total absorption and overlapping MP items. For this the spectra of items identified as plastic were compared using a built in reference database. Furthermore, the size of the identified polymer was verified with the optical and infrared image and if necessary adapted using the editing tools. This allowed to correctly assing items that are partially covered with organic material post-purification that may mistakenly be registered as smaller items. Furthermore, due to the round cross section of synthetic fibers and resulting distorted IR spectra, oftentimes only individual pixels of fibers are identified as plastic. Therefore, the entire length and width of the fibres were audited to allow an exact size measurement. The generated output file delivers information on polymer type, shape, length and width of the identified items.

4.2.3 Data evaluation

In order to compare the datasets generated by the siMPle/MPAPP and BPF analysis, MP polymer data were harmonised. For this, comparable polymer types (e.g. containing same functional groups, such as therephthalates or styrenes) were identified, and grouped into clusters whenever necessary (**Tab. 4.1**). For instance, the therephthalates Polybutylene terephthalate (PBT) and Polyethylene terephthalate (PET) are identified separatly in the BPF. The siMPle output data, however, shows results on the cluster polyester (PEST), which includes both aforementioned therephthalates (Primpke et al. 2018). This resulted in the harmonised polymer cluster PEST, which for the BPF output data includes PET and PBT. In contrast, some polymer types were only present in one of the analysis pipelines (e.g. Polyacrylonitrile (PAN), polyimide or polychloroprene; (**Tab. 4.1**)), and were therefore excluded from the comparison.

Tab. 4.1: Harmonised polymer types compared in this study, as well as excluded ones, which were only present in one of the analysis pipelines. Abbreviations: A: acrylates, CA: cellulose acetate; CMC: chemically modified cellulose; EVA and EVAc: ethylene vinyl acetate; PA: polyamide; PC: polycarbonate; PP: polypropylene; POM: polyoxymethylene; PEEK: polyether ether ketone; PVC: polyvinylchloride; PUR/PU: polyurethane; PMMA: polymethyl methacrylate; PS: polystyrene; ABS: acrylonitrile butadiene styrene; PEST: polyester; PET: polyethylene terephthalate; PBT: polybutylene terephthalate; PSU: polysulfone; PLA: polylactic acid; PLA-PBAT: polylactic acid/poly(butylene adipate-co-terephthalate) blend; PE: polyethylene, V: varnish

Polymer type	**BPF**	**siMPle/MPAPP**
Harmonised polymer types/clusters		
CA	CA	CMC
EVA	EVAc	EVA
PA	PA	PA
PC	PC	PC
PP	PP	PP
POM	POM	POM
PEEK	PEEK	PEEK
PVC	PVC	PVC
A/PUR/V	PU, PMMA	A/PUR/V
PS	PS, ABS	PS
PEST	PET, PBT	PEST
PSU	PPSU, PSU	PSU
PLA	PLA, PLA-PBAT	PLA
PE	PE	PE, PE-oxidized
Polymer types only present in one pipeline (excluded from analysis)		
	EVOH	-
	PAN	-
	SIL	-
	-	PE-chlorinated
	-	nitrile rubber
	-	polyimide
	-	polychloroprene
	-	polyisoprene-chlorinated
	-	PCL
	-	polybutadiene
	-	acrylonitrile-butadiene
	-	rubber type 1
	-	rubber type 2
	-	rubber type 3

4.3 Results

4.3.1 Exclusion of further polymer clusters from analysis

When comparing the data output of BPF and siMPle/MPAPP, we noticed that the polymer type ethylene vinyl acetate (EVA) was relatively prominent in the siMPle/MPAPP data (n = 55 in both sample set A and B, respectively), whereas no assignments to EVA were reported after BPF analysis (see **Tab. S2** and **S4**). The same was true for cellulose acetate (CA), with no detections after BPF analysis, but 14 assignments (sample set B) after siMPle/MPAPP analysis. With respect to EVA, 10 exemplary spectra assigned to EVA by siMPle were re-inspected together and rejected in agreement of both operators, due to poor hit quality. Furthermore, strong discrepancies in the data output were also recorded for the acrylates/polyurethanes/varnish (A/PUR/V) cluster, with much higher counts after siMPle/MPAPP analysis (n = 1086 and n = 1016 in sample set A and B, repectively) compared to after BPF analysis (n = 4 and n =108 in sample set A and B, respectively) (**Fig. 4.1**). Thus, the clusters EVA, CA and A/PUR/V were excluded from further analysis. Reasons for the differences will be discussed in detail in **section 4.4.3**.

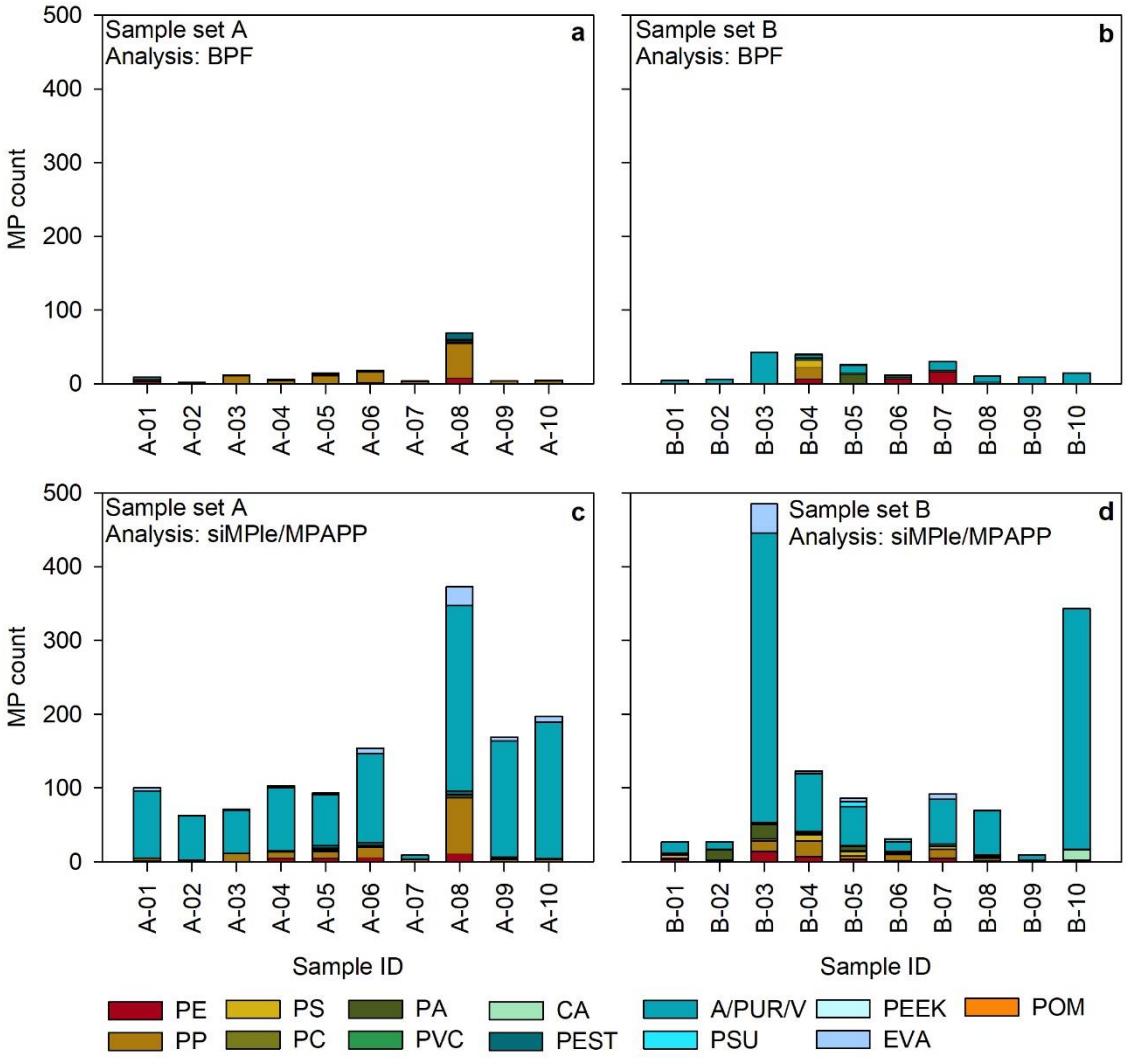

Fig. 4.1: Data output after BPF (a, b) and siMPle/MPAPP (c, d) analyses of sample set A and B before exclusion of EVA, CA, and A/PUR/V (cf. section 4.3.1). For abbreviations refer to Tab. 4.1.

4.3.2 MP abundance, polymer composition and size distribution

Comparison of the analysis output of siMPle/MPAPP and BPF after exclusion of previously mentioned polymer types/clusters (EVA, CA and A/PUR/V) revealed similar results for sample set A (Fig. 2a+c), with a difference in polymer count detected by both pipelines being on average $\Delta n \sim 6$ (mean ± standard deviation (SD) = 6 ± 8), with Δn ranging from 0 for A-02 and A-03 to 27 for A-08. Samples with a difference of $\Delta n > 6$ were A-04 ($\Delta n = 10$), A-05 ($\Delta n = 7$), A-06 ($\Delta n = 8$) and A-08 ($\Delta n = 27$). Within both pipelines, PP and PE were identified as dominant polymer types and maximum item counts were recorded for sample A-08 (**Fig. 4.2a+c**). Furthermore, in all remaining samples (except for sample A-04) a similar trend was observed.

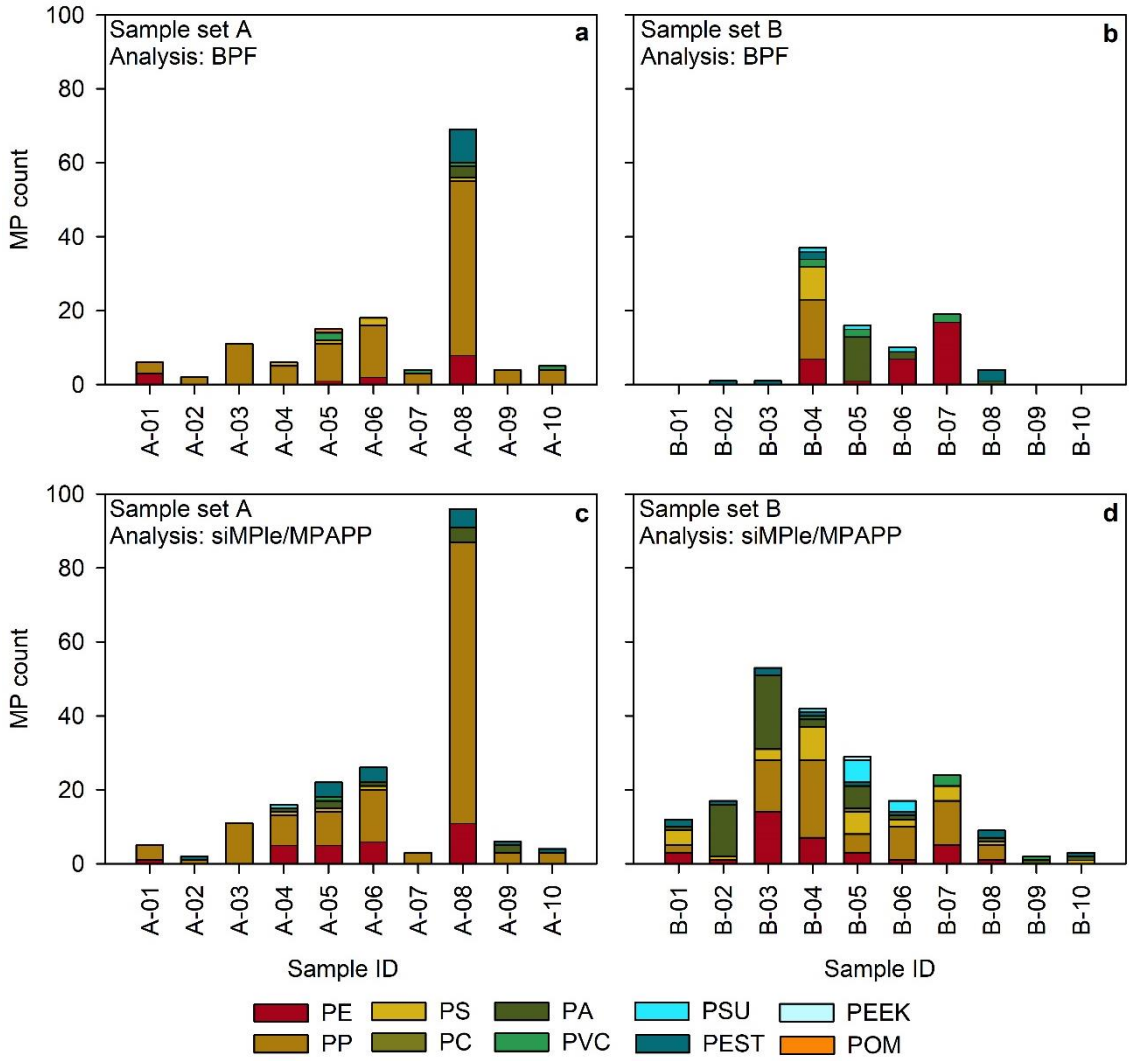

Fig. 4.2: Data output after BPF (a, b) and siMPle/MPAPP (b, c) analyses of sample set A and B, under exclusion of EVA, CA and A/PUR/V (cf. section 4.3.1). For abbreviations refer to Tab. 4.1.

Generally, in the riverine sample set A, the siMPle/MPAPP pipeline detected more PA (present in five samples, 1 – 4 items per sample) and PEST (present in six samples, 1 – 5 items per sample) than the BPF pipeline (PA present in one sample containing 3 items; PEST present in one sample containing 9 items). Slight differences were also recorded with regard to PE: In samples A-04, A-05 and A-06, siMPle/MPAPP detected more PE than BPF (**Fig. 4.2**, $\Delta n = 5$, 4, and 4, respectively). On the other hand side, BPF detected more PVC (four samples, 1 – 2 items per sample) than siMPle (one sample containing 1 item). Details can be found in **Tab. S2** and **Tab. S3**. The differences in PE in the aforementioned samples were especially recorded for items <100 µm (**Fig. 4.3**), and herein the majority of MP detected by siMPle/MPAPP had a size <25 µm (85%). A similar observation was made for items identified as PA (70% < 25 µm, n = 7) and PEST (100% < 25 µm, n = 16) by

siMPle/MPAPP within sample set A, which were rather present in larger size classes based on BPF results.

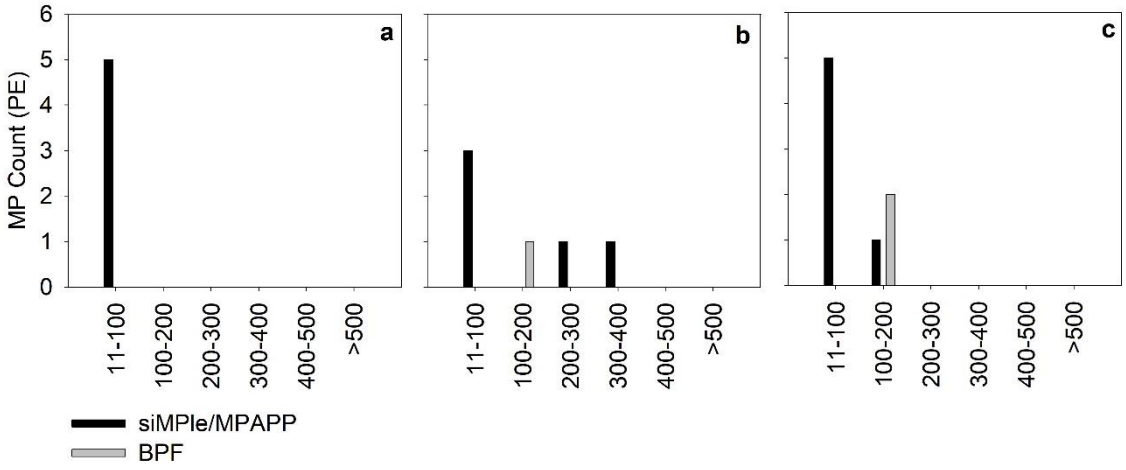

Fig. 4.3: Assignments to PE in samples A-04 (a), A-05 (b) and A-06 (c) by siMPle/MPAPP (black) and BPF (grey), shown for different size classes. A share of 85% of the assignments to the 11-100 µm size class refers to MPs <25 µm.

With respect to the estuarine sample set B, a decreasing trend in the MP counts was recorded from sample B-04 to B-10 with both analysis pipelines (**Fig. 4.2b+d**). The other samples, however, showed a stronger variation between pipelines: samples B-01, B-02 and B-03 showed 0 - 1 MP item after BPF analysis, whereas siMPle detected >10 MP (B-01 and B-02), and >50 MP (B-03). Concerning polymer compositions, sample B-04 showed a high degree of similarity after BPF and siMPle/MPAPP analysis, with PE, PP, and PS being predominant polymer types. The results of the remaining samples, however, showed higher discrepancies. For samples B-06 and B-07, e.g., BPF detected more PE, whereas after siMPle analysis PP was predominant. Details can be found in **Tab. S4** and **Tab. S5**. Here too, with regards to PE, the differences were mainly driven by the smallest size class 11 – 25 µm, with n = 6 (sample B-06) and n = 13 (sample B-07) MP items detected by BPF, while 0 and 3, respectively, were detected by siMPle/MPAPP. This contrasted with the findings for sample set A, where more small PE items were detected by siMPle/MPAPP (**Fig. 4.3**). **Fig. 4.4** confirms the impression of size-related discrepancies, which were already stated above for PE, PEST and PA. For sample set A, few counts in small size classes were recorded in the BPF results, and most MP were assigned to the 50-75 µm size range (**Fig. 4.4a**). In contrast, siMPle results were clearly dominated by MP items in the size class 11 - 25 µm (**Fig. 4.4c**), with PP, PEST and PE being dominant. With regard to

sample set B, both analyses showed highest counts in the smallest size class (**Fig. 4b+d**). However, especially in this size class, polymer compositions differed strongly with PE being dominant in the BPF results, whereas PP but also PA were dominant in siMPle/MPAPP results.

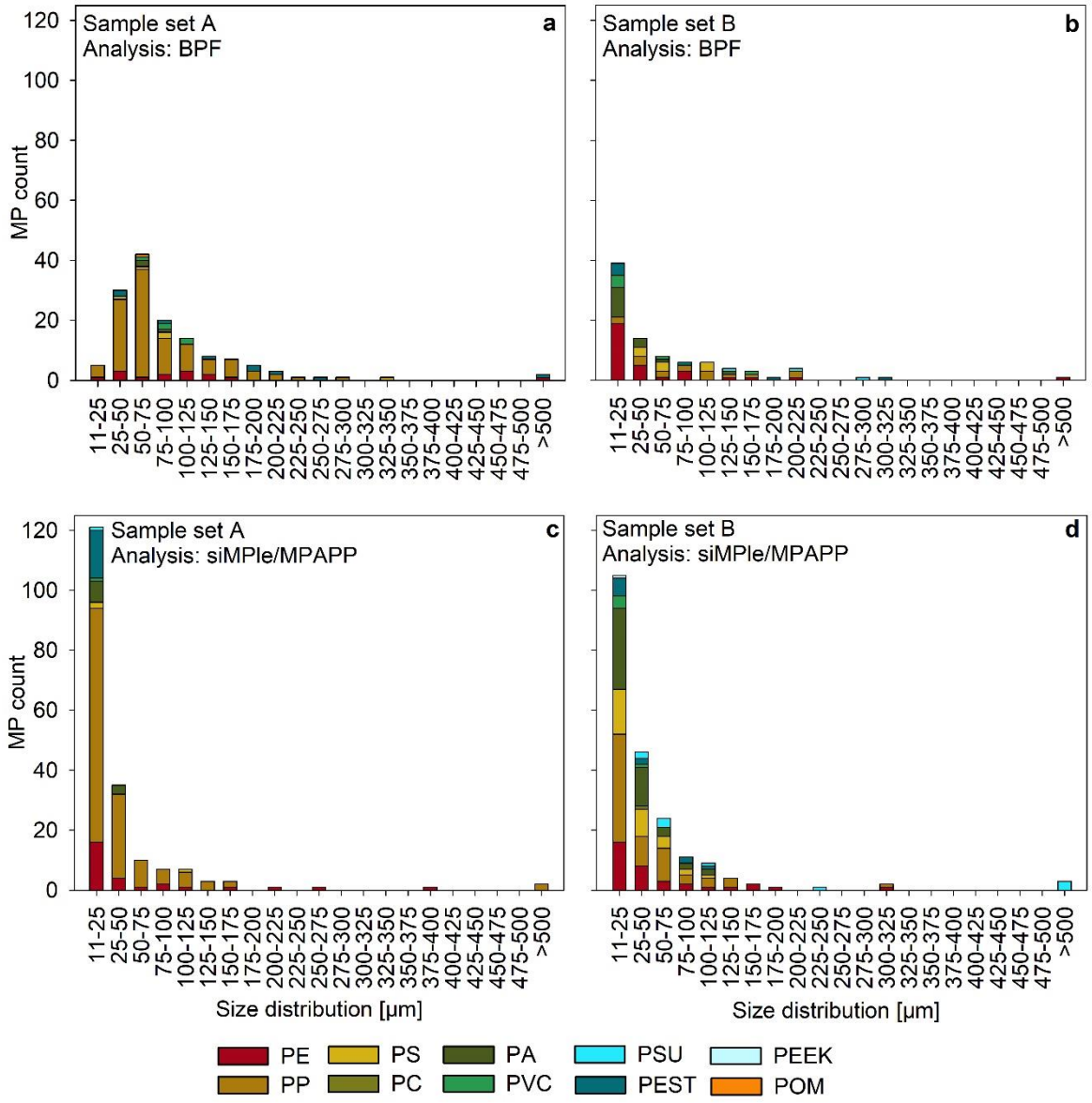

Fig. 4.4: Overall size distributions (length of detected MP in µm) recorded for sample set A and B through BPF (a, b) and siMPle/MPAPP (c, d) analysis. It is to be noted that all size bins cover 25 µm, except for the smallest category. The latter starts at 11 µm which is equivalent to the size of one FPA detector pixel.

4.4 Discussion

4.4.1 Effects of MP size on spectral quality and automated analysis

This study provides a detailed comparison of two MP analysis pipelines, i.e. siMPle/MPAPP and BPF. It is to be noted that this comparison was conducted with environmental samples, containing an unknown amount and composition of MP items. Thus, it remains unclear which results of the aforementioned analysis pipelines are closer to the actual MP occurrence. However, this approach was chosen to shed some light on the complexity of the analysis of environmental samples. Working with internal standards or spiked samples has multiple limitations in terms of representativeness due to the limited availability of commercially available reference material in regard to polymer types, shapes and sizes. Additionally, the preparation of spiked MP samples is challenging, especially using S-MP < 100 µm (Mári et al. 2021). As this size range, however, appears to be the most abundant in environmental samples and poses an increased ecotoxicological risk, it is especially important to represent this size class. The aim of our study, however, was to demonstrate the complexity of the analysis of environmental samples in its full spectrum, containing all relevant polymer types, shapes and sizes, as well as the interplay of matrix residues with aged microplastic being the real challenge for both algorithms. Furthermore, a well established approach in other domains of chemometrics for comparing algorithms is the use of expert-annotated training data (Demšar 2006, Westad and Marini 2015). However, within the considered size range experimental difficulties (e.g. the handling of small virgin MP items) make it very challenging to ensure a correct assignment of the ground truth of spectra, which is why, as a first step, this study was limited to a relative comparison of results. Nevertheless, our study highlights the similarities and differences in results obtained with both tools which is essential for further efforts towards method optimization and harmonization.

Despite of the use of state-of-the-art methods, our results, however, also underline the uncertainties in MP analysis concerning polymer identification, especially at the lower end of the detection limit in terms of size. Depending on morphology and thickness of MPs in a size range below 50 µm, IR-spectra can be influenced by effects such as diffraction and Mie scattering (Hufnagl et al. 2019), in tandem with low intensity of the original polymer signal. Thus, the interplay of these phenomenons potentially results in low quality spectra and a low signal-to-noise ratios. Due to a more conservative, time-intensive approach with BPF,

possibly such low-quality polymer spectra were manually rejected. While for sample set A between 17 to 50% (mean ± SD = 37% ± 9%) of all items identified as MP were accepted after manual re-inspecting the data, only between 0 and 39% (mean ± SD = 13% ± 15%) of all MP hits were accepted for sample set B. For siMPle/MPAPP such a process was performed former to this study in previous work on surface water samples collected in the North Sea (Lorenz et al. 2019), setting the minimum threshold to be reached per polymer type. Nevertheless, during application of siMPle/MPAPP a fraction of such low quality spectra may have been included automatically. Although the problem of classification of MPs with low quality spectra at the lower end of the detection limit of IR spectroscopy has been demonstrated in our case on the example of two automated analysis algorithms, it also holds true for other automated classification solutions or pure manual classification. The severity of this phenomenom may differ between studies as it also depends on the specifications of the respective µFTIR system, filter type, etc. used for MP sample measurement.

4.4.2 Potential reasons for differences in MP abundance, polymer composition and size distribution

Our results showed a high similarity between MP counts and polymer composition especially with respect to sample set A (average difference: Δn ~ 6, maximum difference: A-08, Δn = 27), where PP and PE were recorded as most abundant polymer types (**Fig. 4.2a+c**). Slight differences in polymer compositions, however, were observed: more PE and PEST, e.g. were detected by siMPle/MPAPP than with BPF (samples A-04, A-05, and A-06). As stated above, these differences were mostly driven by the spectral features occuring in the smallest size classes.

With regards to sample set B, most samples showed similar MP counts after BPF and siMPle/MPAPP analysis (average difference: Δn ~ 12). Additionally, sample B-04 showed strikingly high similarities also with regards to polymer compositions (**Fig. 4.2b+d**). Discrepancies in MP counts, however, were observed in samples B-01 to B-03, (maximum difference: B-03, Δn >50). For B-01 and B-02, this is possibly due to a matrix effect: these samples were rich in very fine sediments that could not be effectively eliminated during sample purification, which was underlined by high content of suspended particulate matter (SPM) (details in **Tab. S1**) recorded during sampling in the semi-enclosed Jade Bay (German North Sea) (Roscher et al. 2021). These characteristics, potentially resulting in

matrix interferences, were in contrast to the other samples from sample set B, and might have negatively affected the automated polymer identification by either under- or overestimation by the respective analysis pipelines. This problem can only be solved in future by further adjustments in the extraction and purification methodology. Sample B-03, however, did not show any obvious specific matrix-related characteristics which would explain the observed differences between both pipelines. Concerning the remaining samples of sample set B (B-04 to B-10), a general trend of decreasing MP counts was observed for both pipelines. However, differences in polymer compositions became evident especially in B-06 and B-07, where BPF detected more PE, whereas siMPle/MPAPP detected more PP. Randomly selected PP spectra detected through siMPle analysis were visually checked (exemplary spectra shown in **Fig. S1**) and accepted, as characteristic bands were present (i.e. stretching vibrations of CH_3 and CH_2 between ~2830 and 2950 cm^{-1}, and bending vibrations of mainly CH_3 at ~1450 and ~1370 cm^{-1}). However, existing noise in the spectra might have resulted in manual rejection during the quality check after BPF analysis while it was considered valid due to double spectral confirmation within the siMPle process, as described in Primpke et al. (2020b). The differences in PE counts, however, could not be explained in the framework of this study. Finally, our analysis showed that for the polymer clusters considered, BPF and siMPle/MPAPP generally are in accordance with regards to MP counts and polymer compositions, with exceptions likely caused by residues of complex sample matrixes post sample purification on the sample filters and discrepancies regarding the detection of small MP items <25 µm.

Both pipelines found an overall dominance of MP in the smaller size classes. However, especially for sample set A the overall size distribution differed between BPF and siMPle/MPAPP results, with the latter showing much higher counts in the smallest size class. Next to low quality spectra resulting from diffraction, Mie scattering and low signal intensity that may have led to an under- (BPF) or overestimation (siMPle/MPAPP) in the smallest size classes by the respective methods as described above, these discrepancies are potentially also due to different assessment approaches with regards to size classification in both algorithms. After the application of BPF, a manual QA/QC was performed for each classified MP item, and whenever necessary adjacent pixels were combined retrospectively if they clearly belong to the same item. During siMPle/MPAPP analysis, a closing step is implemented, where neighboured pixels are combined automatically (Primpke et al. 2017, Primpke et al. 2019). Thus, if the surface of an item is not uniform, potentially due to organic

residues i.e., the closing step may not be successful. This may lead to the detection of multiple counts in smallest size classes instead of the detection of one large item, which could be the reason for the observed differences in size classification.Nevertheless, a general high occurrence of small MP items was confirmed by Primpke et al. (2020d) using QCL-IR measurements and Cabernard et al. (2018) with both µFTIR and Raman, with the latter showing even higher counts in the exact same sample. Thus it remains unclear, to what extent the aforementioned effect is relevant for the differences in size distributions observed in the present study.

Consequently, the observed differences between BPF and siMPle/MPAPP concerning size distributions underline the necessity of further comparative studies, and should be focus of future harmonisation efforts with the final goal of a reliable assessment of environmental MP concentrations in all detectable size classes.

4.4.3 Effects of differences in the general methodological approach

To our knowledge, this is the first study to compare a model-based to an instance-based algorithm with respect to resulting MP abundances, polymer compositions and sizes, by applying both analysis pipelines on the data of the same two MP sample sets. For an accurate comparison of BPF and siMPle/MPAPP, a restructuring of the data output was performed, including the harmonisation of polymer types and the exclusion of those which are not targeted in both pipelines (e.g. silicone, which is only addressed by BPF, or polyimide, which is only included in siMPle/MPAPP; **Tab. 4.1**). This data handling step resulted in the data output presented in **Fig. 4.1**, showing that especially A/PUR/V was much more frequently detected by siMPle/MPAPP. Both, the PUR and PMMA class of the BPF approach was trained using only PUR and PMMA spectra. In siMPle/MPAPP the individual spectra of different polymers were assigned by a label to polymer type clusters of similar substances (Primpke et al. 2018) including for example other types of acrylate substances for A/PUR/V. While the former approach tries to mimic the real structure of the underlying polymer data by deriving a statistical model, the latter uses a combination of hierarchal cluster analysis and expert knowledge to generate generalized polymer type clusters separable in the available spectral range. The harmonization step should thus be observed critically, as different design philosophies, with very different mathematical characteristics are compared. This potentially leads to a broader coverage of polymers by siMPle/MPAPP,

while the BPF database allows that certain polymer types such as PUR and PMMA are differentiated.

Interestingly, BPF detected items falling into the A/PUR/V cluster especially in sample set B (Weser-Wadden Sea transitional zone), but almost none in sample set A (Upper and Middle Weser) (**Fig. 4.1**). Sample set B originates from sampling stations situated in an area with relatively high shipping activity, which represents a potential source for varnish-like items (Roscher et al. 2021). In this study, also L-MP items with a varnish-like morphology were recorded in this area. Sample set A, however, stems from an area less influenced by shipping activity in the middle and upper part of the Weser River, which is in accordance with very few (n = 4) validated assignments to the cluster A/PUR/V by BPF, but contrasts with the extremely high abundances after siMPle/MPAPP analysis (n = 1086). Beside the possibility of potential underestimation of this polymer cluster by BPF due to conservative manual rejection of low-quality spectra, another explanation could be an overestimation by siMPle/MPAPP, e.g. due to the missing awareness of specfic natural materials causing systematic false positive assignments. This cluster was addressed with an extensive QA/QC procedure in a previous study on MP in WWTP effluents. It was found, that this polymer cluster is strongly affected by a spectral interference with plant cuticles in sample matrixes present in high amounts of residual biological material (Roscher et al. 2022) resulting in false positives with a high spectral match. Hence, in sample set A an overestimation in samples with a high organic load by siMPle/MPAPP in the A/PUR/V cluster cannot be ruled out. Also, the polymer cluster EVA showed significant discrepancies, with relatively high abundances after siMPle/MPAPP analysis (sample set A: n = 55, sample set B: n = 55), and no counts after BPF analysis. As stated in **section 4.3.1**, respective siMPle-Spectra were rejected after visual re-inspection by both operators as false positives. Also here, the manual inspection of the analysis results as routinely implemented after BPF analysis leads to exclusion and more conservative results with regards to this polymer type. Especially the lack of the ethylene signal at approx. 1370 cm^{-1} in the sample spectra (**Fig. S2**) led to rejection of most spectra assigned to EVA. Moreover, similar to the siMPle cluster A/PUR/V, also EVA was affected by matrix interferences in the study by Roscher et al. (2022), further hinting towards the assumption that respective counts in the present study might also be due to false positive identification. Indeed, the two samples with highest EVA counts (A-08: n=25; B-03: n=39) showed high amounts of potentially biogenic material on Anodisc^{TM} filters (**Fig. S3**) in comparison to other samples. These observations show that

despite the high benefit of automated or semi-automated analysis pipelines, expert knowledge and manual QA/QC processes are highly necessary in order to allow for solid and unbiased datasets, as previously stated by Song et al. (2021a). In siMPle/MPAPP, a QA/QC on the individual spectral level is implemented on a regular basis (see Lorenz et al. (2019) and Primpke et al. (2020b)), whereas in BPF the manual check of MP assignments was performed routinely for each data set. Although the latter may provide a high certainty, it can also be time consuming, depending on the amount of potential MPs detected. For example, as stated above, in sample set A 50 – 73% (mean ± SD = 63% ± 9%) and in sample set B 61 – 100% (mean ± SD = 87% ± 15%) of all items identified as MP by the BPF algorithm were rejected after manual reinspection of the spectra. Here, especially samples with a high content of residual matter post-purification (such as fine sand or non-digestible matter such as plant pollen) appear to be critical. Due to an increased amount of material remaining on the filter, the time required for manual re-inspection of all spectra assigned to MP increases. These observations underline the great importance of an effective purification approach to produce final MP samples with as little sample matrix as possible present (Löder et al. 2017).

Due to the IR- transparency features of the filter material (aluminum oxide, Anodisc) used as substrate for FTIR imaging in this study only the wavenumber range 3600−1250 cm^{-1} could be measured, where synthetic and biogenic substances partly share similar bands and discrimination can be challenging (Roscher et al. 2022). Thus, the additional assessment of data in the spectral fingerprint range <1250 cm^{-1} should be further pursued for better distinguishing materials. In the case of µFTIR imaging in transmission mode, which results in the highest spectral quality (Löder et al. 2015) this is only possible if the used filter material aluminium oxide is replaced by material like silicon that is also IR transparent in the fingerprint region (Käppler et al. 2015). This filter substitute could help to improve classification especially for acrylate- and PUR-based polymers as well as EVA which would enhance the comparability of results as well as the general detection success and reliability of data.

4.4.4 Future implications

By comparing two currently well established and frequently applied MP analysis tools, this study can act as a basis for future harmonisation and standardisation efforts in MP analysis. In general, BPF and siMPle/MPAPP showed similar results, with some

discrepancies likely caused by matrix effects, and others explainable by the chemical characteristics of certain polymers which could be improved by a broader measurement range including the fingerprint region. On the whole, both pipelines are rapid and generate a detailed data output, and therefore show great potential for a broad application in MP assessments. This study further underlines the importance of QA/QC, e.g. implemented by manual counter-checking by experts, in order to allow for the generation of high quality datasets and underlines the importance of purification approaches that reduce the present sample matrix effectively. Additionally, our study also shows that all studies on MP contamination should be interpreted with caution, especially with respect to smaller size classes, since it remains unclear for all currently applied methods how correct the generated results are with respect to the actual occurrence of MP in the environment. Keeping this in mind, as a final consequence, we have to admit, that even by the use of state-of-the-art methodology the determination of the real environmental MP number is still a challenge which needs to be addressed by further research efforts. In order to have a clearer picture of how close the obtained results are to the actual numbers, it may perhaps be beneficial to work with spiked samples – although one has to be aware of the limitations in regard to available polymer types, shapes and sizes. Nevertheless, through the current ongoing development and improvement of the here applied analysis tools, both usability and reliability are being enhanced, e.g. by adaptations of underlying reference databases (siMPle) or optimized follow-up versions ("Purency Microplastic Finder" derived from BPF). These improvements and further optimisations will lead to analysis tools that – in the best case – produce data with high reliability without additional manual re-evalution efforts.

Conflict of interests

Benedikt Hufnagl reports that he is a co-founder and shareholder of Purency GmbH, a software company which specializes in the automated data analysis of MP measurements using machine learning. The herein used version of the machine learning approach "BPF", however, is not a commercial product of that company but a very early-stage prototype developed during Mr. Hufnagl's PhD studies. Sebastian Primpke served as Guest Editor at the time of manuscript submission but was not involved in peer review of this manuscript. The remaining authors declare they have no conflict of interest.

Acknowledgements and Funding Information

This study was funded by the German Federal Ministry of Education and Research (Project PLAWES, 'Microplastic Contamination in the Weser- Wadden Sea – National Park Model System: an Ecosystem-Wide Approach'; grant numbers: 03F0789A, 03F0789B). Furthermore, we kindly thank Heghnar Martirosyan and Ursula Wilczek for laboratory assistance.

Chapter 5 – General Discussion

Although the awareness for MP pollution has been rising in recent decades, knowledge gaps still exist, especially concerning distribution patterns in aquatic systems. Especially before 2014, the vast majority of studies focussed on MP pollution in marine environments (Kasavan et al. 2021). According to Kasavan et al. (2021), this changed in the time between 2014 and 2020, with a high share of studies focussing on MP in freshwater systems. Especially rivers have been identified as pathways for land-based MP into marine waters (Talbot and Chang 2022). In order to evaluate the potential of the German river Weser as a pathway for MP into marine waters of the North Sea, surface water samples were collected and analysed for concentrations, polymer compositions, and size distributions (**Chapter 2**). This is the first study providing detailed data in MP pollution patterns in this river system, analysing MP items down to 11 µm. spatial differences were revealed especially for small size classes, with highest MP abundances in the TMZ of the river.

Going one step further, the question arises where the riverine MP originate from. Diffuse sources such as atmospheric input (e.g., wind force or precipitation) or runoff have been investigated in previous studies (Mani and Burkhardt-Holm 2020, Wong et al. 2020, Kernchen et al. 2021). More localized pathways could be WWTP effluents, which likewise have gained more attention by the research community in recent years (Azizi et al. 2022). Nonetheless, it is still a rather young research field, and especially data collected in longer timespans are required in order to understand MP dynamics in WWTPs, as emphasized by Barchiesi et al. (2021). By performing a one year-long sampling campaign with monthly sampling events, the work presented in **Chapter 3** provides a comprehensive overview of the MP pollution level of the investigated WWTP effluents. These discharge into the Fulda River, as well as into the Lower stretch of the Weser. Although it was not possible to conduct sampling of effluent and river surface water in the same time frame, an attempt was made to set the MP findings of **Chapter 2 and 3** into context (cf. **Chapter 3**, **section 3.4.3**).

In the broad and developing field of MP research, still a lot of variability exists with regard to methodological approaches throughout all analysis steps. Standardization is the key challenge at this point in time, and was more and more demanded in recent years (Zhao et al. 2018, Andrade et al. 2020, Provencher et al. 2020). Within the project PLAWES, also the Upper and Middle Weser and its tributaries were investigated. This was conducted by the coordinating institute UBT. As mentioned in **section 1.4**, a different approach for the

final MP data evaluation was performed by the UBT, being based on random forest analyses, whereas the analysis pipeline applied in **Chapter 2 and 3** of the present work was based on Pearson correlation of FTIR spectra. In **Chapter 4**, both approaches underwent a detailed comparison. This study revealed differences and similarities, and may provide a basis for further standardisation of MP analysis methods.

In the following sections, the methods for sampling, sample processing, and chemical analysis applied in **Chapters 2-4** are discussed in the framework of an inter-study comparison (**section 5.1**), followed by a contextualisation of the results obtained, based on recent literature on geographically relevant aquatic environments (**section 5.2**).

5.1 Discussion of applied methods

The studies presented in **Chapter 2 and 3** were both based on the collection of water samples from different compartments (riverine/estuarine surface water and wastewater effluent), targeting an overall size range of ~10−5000 µm **(Fig. 5.1)**. The set-up used for sample collection was different in a way that the two sampling approaches for estuarine surface water already targeted different sample fractions (L-MP: net with a mesh size of 300 µm; S-MP: filtration system with membrane pumps, mesh sizes of 500 and 15 µm). The sampling of wastewater effluent, in contrast, aimed at both L-MP and S-MP at the same time by use of cartridge filter units (mesh size 10 µm), with a size fractionation later on in the laboratory **(Fig. 5.1)**. This approach was already successfully applied by Mintenig et al. (2017), and was chosen in order to increase the comparability between studies. Overall, sampling of wastewater was comparable to estuarine S-MP sampling, as in both cases membrane pumps were forwarding the sample liquid to a filtration unit for concentration of the sample material, with a similar final mesh size. Furthermore, both studies presented in **Chapters 2 and 3** included a thorough sample processing using an enzymatic-oxidative digestion protocol (incl. density separation step) before further analysis, in order to carefully isolate the MP fraction. The sample fractions resulting from sample processing were subjected to spectroscopic analyses for polymer identification, with L-MP being analysed with FTIR-ATR, whilst S-MP items were assessed with µFTIR **(Fig. 5.1)**. Within **Chapter 3**, also complementary MP mass data obtained through Py-GC/MS measurements were included. Besides, a database adaptation for µFTIR data and re-evaluation was performed, as the presence of plant residues in processed effluent samples was shown to induce false-positive assignments (cf. **section 3.2.4.3**). The following sections provide a detailed discussion of methods used in sample collection, sample processing, chemical analysis and data evaluation.

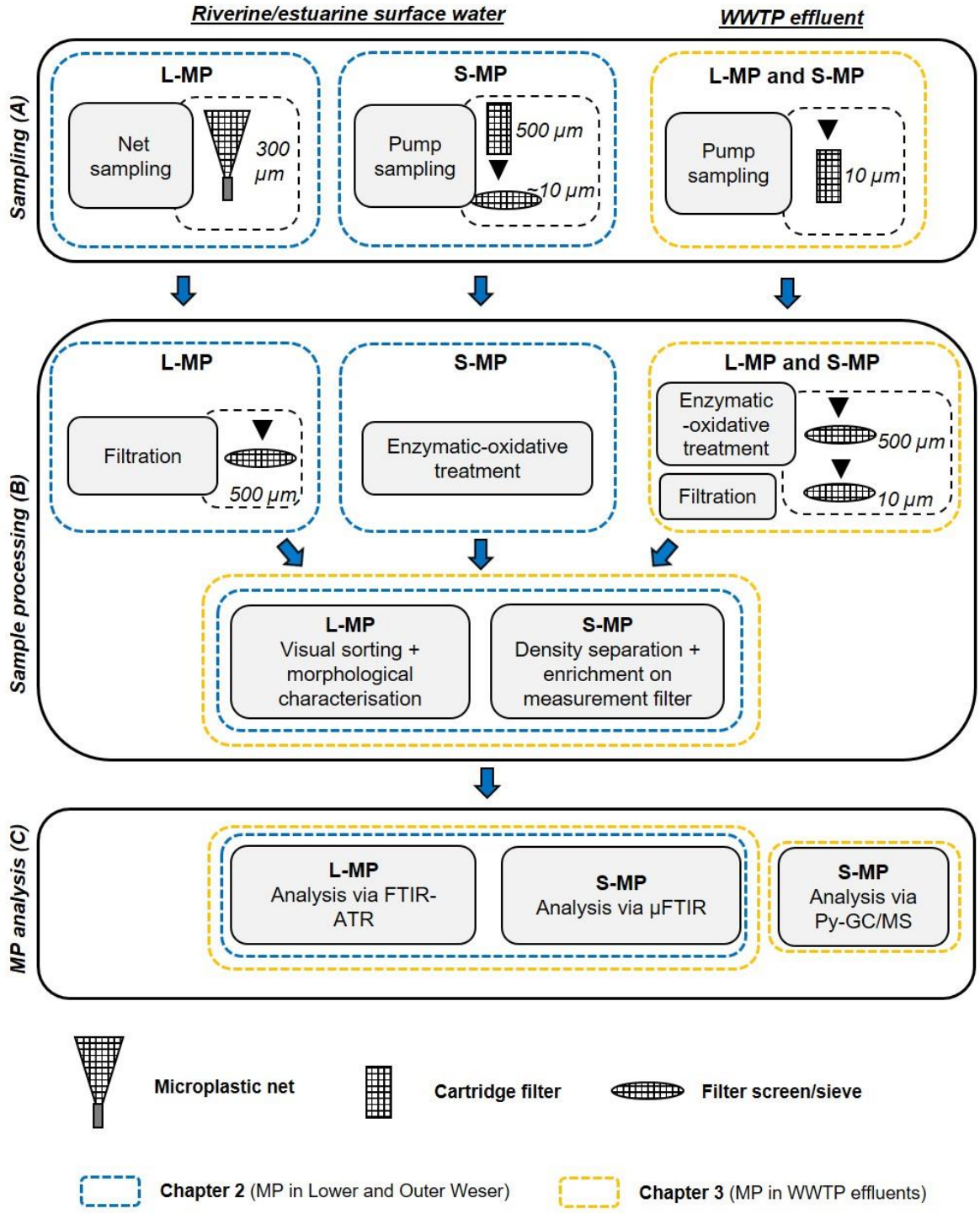

Fig. 5.1: Overview of methods applied in Chapter 2 and 3 of the present work, including sampling (A), sample processing (B) and MP analysis (C).

As stated above, the study presented in **Chapter 4** was based on the data output of the study presented in **Chapter 2**, as well as data provided by the UBT **(Fig. 5.2)**. It critically evaluated the MP analysis tools siMPle/MPAPP and BPF used in PLAWES, aiming at identifying current challenges in identification techniques. These are further discussed in **section 5.1.3**.

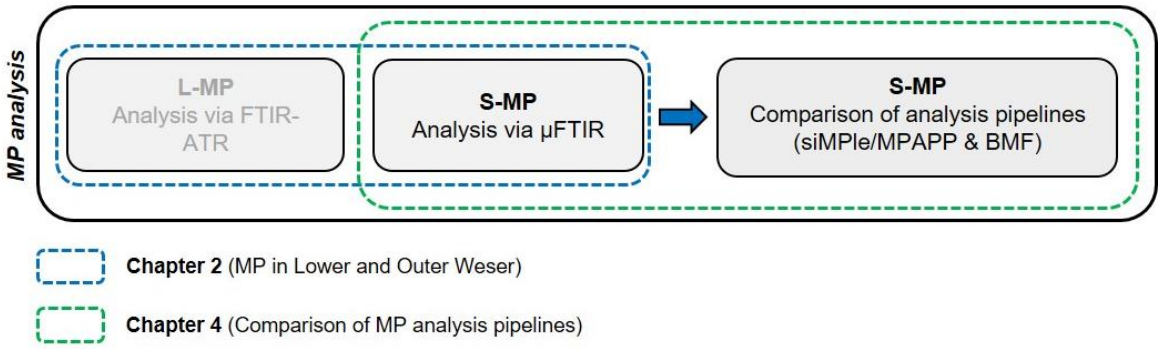

Fig. 5.2: Comparison of MP analysis pipelines performed in Chapter 4 was based on S-MP data output of Chapter 2, as well as S-MP data obtained from studies conducted by the project partner UBT.

5.1.1 Sample collection

Many different approaches for surface water sampling in freshwater and marine environments exist, and each MP sampling method bears advantages and disadvantages. Grab sampling, using a bucket or comparable containers is frequently applied (Han et al. 2020, Wang et al. 2020, Bian et al. 2022), and exhibits a relatively easy handling. However, small sample volumes might not be representative with regards to MP concentrations and polymer type compositions (Koelmans et al. 2019, Brander et al. 2020). Net sampling, in contrast, allows for the collection of significantly higher sample volumes, as shown in **Table 5.1**. Net sampling has especially been applied for the assessment of larger MP, with common mesh sizes of ~300 or ~100 µm, as it was the case in the study presented in **Chapter 2** (300 µm). Recent studies which applied nets for the collection of surface water samples are listed in **Table 5.1**, with reported sampling volumes in the range 0.4−557 m^3, being mostly in a similar order of magnitude as in the present work.

Table 5.1: Overview of recent studies which applied net sampling for the assessment of MP in surface waters.

Reference	Sampling location	Sampling device	Mesh size [µm]	Sample volume [m^3]
Roscher et al. (2021) (***Chapter 2***)	Weser estuary, Germany	Microplastic net	300	16−252
Zhang et al. (2020)	Qin river, China	Plankton net	300, 75	7.9−160.5
Wong et al. (2020)	Tamsui river & tributaries, Taiwan	Manta net	300	0.4−6.5 [a)]
Mani and Burkhardt-Holm (2020)	Rhine river catchment,	Manta trawl	300	25.2−200.9
Park et al. (2020b)	Han river, South Korea	Manta net	100	3−5
Scherer et al. (2020)	Elbe river, Germany	Plankton net	150	3.2−32.7
Russell and Webster (2021)	Marine waters around Scotland	Neuston catamaran	335	16−557
Suaria et al. (2020)	Southern Ocean	Neuston net	200	292.5 ±78.5
Silvestrova and Stepanova (2021)	Atlantic Ocean	Manta net	500	260
Lorenz et al. (2019)	Southern North Sea	Neuston net	100	15.3−51.3

[a)] At each sampling station 3−5 replicates were collected.

Reviewed studies which applied pumping systems for sample collection in riverine or marine environments generally used smaller sampling volumes (mostly <1 m^3) (range: 0.02−3.8 m^3), as presented in **Table 5.2**. This approach mainly addresses smaller MP, with minimum sizes defined by the mesh/pore size of filters used for subsequent concentration of the sampled water. Especially studies which applied filter cascades by use of sieves with different mesh sizes achieved sample volumes >1 m^3 (Mintenig et al. 2020, Schönlau et al. 2020, Carlsson et al. 2021) (**Table 5.2**). The study presented in **Chapter 2** did not apply a sieve stack, but had a pre-filtration step deployed in a floating cartridge filter with a mesh size of 500 µm (**Supplementary Material for Chapter 2, Fig. S1A**). This led to a selective filtration of items < 500 µm and avoided instant clogging of the 15 µm meshes.

Table 5.2: Overview of recent studies which applied pump sampling for the assessment of MP in surface waters. The lower size limit [µm] refers to final mesh/pore size where pumped surface water was concentrated on.

Reference	Sampling location	Lower size limit [µm]	Sample Volume [m^3]
Roscher et al. (2021) **(*Chapter 2*)**	Weser estuary, Germany	15	0.04−1
Napper et al. (2021)	Ganges, India/Bangladesh	330	0.03
Mintenig et al. (2020)	Various rivers, Netherlands	20 [a)]	0.03−2.25
Liu et al. (2020)	Haihe river, China	1.2	0.02
Mao et al. (2020)	Yulin river, China	64	0.05
Zhang et al. (2020)	Qin river, China	25	0.03 [b)]
Jiang et al. (2020)	Southern Yellow Sea, China	50	0.1
Zheng et al. (2021)	Jiaozhou Bay, China	20	0.2
Schönlau et al. (2020)	Skagerrak/Kattegat, Baltic Sea, Gulf of Bothnia	50 [c)]	0.8−3.8
Carlsson et al. (2021)	Western Svalbard, Arctic	100 [d)]	2.6−3.0

[a)] Sieve stack: 300, 100, 20 µm. Presented sampling volume refers to volume filtered over 20 µm sieve.
[b)] At each sampling station, 3−5 replicates were collected.
[c)] Sieve stack: 500, 300, 50 µm. Presented sampling volume refers to volume filtered over 50 µm sieve.
[d)] Sieve stack: 500, 300, 100 µm.

In order to target a broad MP size range from ~10 µm to 5000 µm, both net sampling as well as pump sampling was used for the riverine/estuarine samples in the present work (cf. **Chapter 2**, **section 2.2.2**). With regards to optimisation of the sampling design, the collection of replicate samples could help to better assess variations between samples and estimate a potential bias, as discussed in **Chapter 2**, **section 2.4.3**, and conducted in Wong et al. (2020) (**Table 5.1**) and Zhang et al. (2020) (**Table 5.2**). This was, however, out of the scope of the present work. Concerning replication, the focus was laid on the actual analysis step of S-MP, attempting to overcome the current approach of taking small sample percentages of processed samples for MP measurements (**cf. section 5.1.3**).

Sampling at WWTP effluents (**Chapter 3**) was initially planned in parallel to Lower Weser sampling in April 2018, in order to increase the comparability of both studies. Due to logistical reasons, the sampling campaign at the WWTPs had to be postponed and was

performed from July 2018–June 2019. Nonetheless, the year-long campaign gave interesting insights into MP pollution and potential influencing background conditions, and the relatively high temporal resolution of the assessment is in accordance with suggestions made in recently published studies (Kang et al. 2020, Ben-David et al. 2021). Furthermore, the study targeted MP down to 11 µm, which is in contrast to the majority of studies in this field of research (Koelmans et al. 2019), and therewith reduces the risk of underestimating important size fractions. The sampling technique chosen for the study presented in **Chapter 3** was based on the study by Mintenig et al. (2017), and the suggested targeted volume for the pump sampling (1000 L) was aimed at in both Roscher et al. (2021) and Roscher et al. (2022) (**Chapter 2 and 3**). In **Table 5.3**, recent publications with a similar sampling set-up are presented. Effluent water obtained by pump sampling ranged from 0.01–1 m^3 in these studies, with Naji et al. (2021) taking samples in triplicates. The selected studies often analysed 1–2 WWTP facilities, with the exception of Park et al. (2020a), who conducted a nation-wide monitoring study with 50 WWTP investigated.

Table 5.3: Overview of recent studies which applied pump sampling for the assessment of MP in WWTP effluents. The lower size limit [µm] refers to final mesh/pore size where pumped surface water was concentrated on.

Reference	Sampling location	Lower size limit [µm]	Sample Volume [m^3]
Roscher et al. (2022) ***(Chapter 3)***	2 municipal WWTPs, Germany	10 µm	0.1–1
Rasmussen et al. (2021)	1 municipal WWTP, Sweden	10 µm	>0.55
Naji et al. (2021)	2 municipal WWTPs, Iran	333	0.035 [a)]
Tagg et al. (2020)	1 municipal WWTP, United Kingdom	5 µm	0.01
Park et al. (2020a)	50 municipal WWTPs, Korea	100 µm [b)]	1
Menéndez-Manjón et al. (2022)	1 municipal WWTP, Spain	20 µm [c)]	0.2–0.3

[a)] At each site three replicates were collected.
[b)] Sieve stack: 5000, 1000, 300, 100 µm.
[c)] Sieve stack: 500, 250, 100, 20 µm.

Possible advancements of the study design are a higher number of investigated WWTPs, a focus on even lower size ranges as well as the analysis of other treatment steps and waste water types (e.g., influent water). Furthermore, 24-h composite samples can further

elucidate diurnal dynamics, as shown by Cao et al. (2020). The authors revealed intra-day variations in MP concentrations in accordance with human activity, with gradually increasing values between 9:30 a.m. and 5:30 p.m., as well as variations in polymer compositions. However, limitations of the study were an applied minimum size of 100 µm, as well as a sample collection on one single day, which might hamper the representativeness of the study. Overall, the sampling design applied depends on the research question asked, and is often a compromise with respect to spatial and temporal resolution as well as practicability.

Finally, both studies in **Chapters 2 and 3** applied a minimum MP size limit at the lower range, decreasing the degree of underestimation of small MP (e.g., compared to studies with minimum sizes >100 µm). The methods used (pump and net sampling) proved successful for the assessment of MP over a broad size range, and are in accordance with approaches applied in the current literature.

5.1.2 Sample processing

Various approaches exist for sample processing in preparation to MP analysis. With respect to the studies which used net sampling listed in **Table 5.1**, the majority applied at least a filtration or sieving step for the concentration of samples, as well as visual examination of the samples. Especially studies applying small mesh sizes during sampling (~100 µm) performed sample digestion steps for the maceration of biogenic material. Herein, a commonly used chemical is H_2O_2 (Park et al. 2020b, Wong et al. 2020, Zhang et al. 2020), which was combined with a KOH treatment in Scherer et al. (2020). In Roscher et al. (2021) (**Chapter 2**), SDS was used for a gentle pre-treatment of samples before sieving over 500 µm. Some studies also applied a density separation step, e.g., with sodium chloride (Zhang et al. 2020), castor oil (Mani and Burkhardt-Holm 2020) or potassium formate (Scherer et al. 2020). This is especially useful in the case of high amounts of sediment grains in samples. Ideally, the sample processing method should be adapted to the characteristics of the sample material.

For the visual examination of samples, often performed by help of a stereomicroscope, approx. 50% of studies above did not state which protocol was followed. For the distinction of MP from biogenic material, Mani and Burkhardt-Holm (2020) and Scherer et al. (2020) followed the protocols by Masura et al. (2015) and/or Norén (2007), with the latter having been followed in **Chapters 2 and 3**. Applied protocols for the categorisation into different

shape types were the guidelines published by the MSFD technical group on marine litter (Directive 2013) and BASEMAN (Gago et al. 2019), with the latter having been applied in the present work. As discussed in **section 2.4.2**, a thorough reporting of MP morphology can increase the chance of identifying potential sources, and herein a further standardisation is highly suggested for a better comparability of data on a global scale.

The samples collected with pump sampling required a more complex sample treatment (cf. **section 2.2.3** and **section 3.2.3**). Accordingly, 7 out of 10 studies listed in **Table 5.2** and all studies listed in **Table 5.3** applied digestion steps, mostly using either H_2O_2, Fenton's Reagent or KOH. A high degree of sample purification is especially necessary when the final analysis is targeting smallest size classes, e.g., by use of FTIR imaging in transmission mode. For the studies presented in **Chapters 2 and 3**, the basic enzymatic purification protocol (BEPP) after Löder et al. (2017) was chosen, which uses technical enzymes and H_2O_2 for the maceration of biogenic sample material. It is a comparatively mild treatment, in contrast to protocols with strong acidic or alkaline solutions. Acid-based protocols using HNO_3, for example, were shown to have a destructive effect especially on nylon, but also other polymer types such as PS, PE or PET (Claessens et al. 2013, Catarino et al. 2016). Alkaline digestion, e.g., using NaOH, was shown to have a negative impact on CA, PC and PET in previous studies (Dehaut et al. 2016, Hurley et al. 2018, Pfeiffer and Fischer 2020). With regards to oxidative treatments, Pfeiffer and Fischer (2020) generally found a low impact on the tested synthetic polymers. For H_2O_2, a significant weight loss was observed for PA only at higher temperatures (60-70 °C). The low temperature during H_2O_2 treatments applied in the present study (35 °C) in combination with a moderate percentage (35%) suggests a neglectable impact on synthetic polymers present in the samples, whilst the digestion efficiency (in combination with the technical enzymes) had been shown to be very good in the study by Löder et al. (2017) (reduction of sample matrix by 98.3 ± 0.1%). Although a systematic evaluation of the digestion success was out of the scope of the present work, the applied treatment generally appeared to reduce the sample matrix visibly. However, during the analysis of WWTP effluent samples, it became evident that this was not the case for residual plant cuticles (cf. **Chapter 3**, **section 3.2.4.3**). The persistent characteristics of this waxy material suggests the need for another digestion step with appropriate reagents, as discussed in **section 3.4.4.2**.

Zinc chloride was used for the separation of the microplastic fraction from remaining heavier material such as sediment grains, as suggested by Löder et al. (2017) and applied in

numerous previous studies (Imhof et al. 2012, Lorenz et al. 2019, Mani et al. 2019, Mintenig et al. 2020, Cunsolo et al. 2021). Based on a recent review which included 50 publications, $ZnCl_2$ is amongst the most commonly used salts for density separation within microplastic studies (Cutroneo et al. 2021). Its high density (1.7 g cm^{-3}) allows for the isolation of highly dense synthetic polymers such as PVC, and thus reduces the bias of underestimating these polymers. Moreover, the here used approach of recycling the $ZnCl_2$ solution as often as possible by filtering it in several steps before reusing, reduces the negative environmental impact of this chemical. Another frequently applied salt solution is NaCl, despite the drawback of a significantly lower density (1.2 g cm^{-3}). According to the review by Cutroneo et al. (2021), it was identified as the most commonly used salt, being applied by 45.6% of the considered studies. Its strength is the low cost, as well as the neglectable environmental impact, which made it a preferred solution for monitoring studies with high sample throughput. Herein, it was recommended in the BASEMAN guidelines for monitoring microplastics in seawater (Gago et al. 2019). Yet, the authors acknowledge the limitation with regards to its density, and suggest NaI as an alternative (1.6 g cm^{-3}).

In conclusion, the here applied methods for sample processing in preparation to the spectroscopic identification are generally in accordance with the current research. In general, their application proved successful, and matrix compounds of the samples were reduced significantly during sample processing. Yet, enhancements should be performed, especially with regards to the digestion success of residual plant material in the sample matrix, in order to avoid complications during µFTIR analysis. Here, further investigation on the level of laboratory experiments is highly recommended, ideally resulting in an adapted digestion protocol for samples rich in residual cuticle material.

5.1.3 Chemical analysis and data evaluation

In the here presented work, FTIR-ATR and µFTIR imaging were applied for the analysis of L-MP and S-MP items, respectively. This approach proved practical in several previous studies (Haave et al. 2019, Lorenz et al. 2019, Mintenig et al. 2020). In order to gain information on MP masses, which is of relevance e.g., for mass budgeting in modelling studies, thermoanalytical methods such as Py-GC/MS can be applied (cf. **Chapter 3**). By the use of specific indicator ions, a detailed characterisation of individual polymer types in environmental samples can be performed (Primpke et al. 2020a). The complementary application of both FTIR-based and Py-GC/MS analysis is a strong approach for identifying

both MP item and mass concentrations in environmental samples, as applied in **Chapter 3**, as well as Kirstein et al. (2021), Primpke et al. (2020c), Chouchene et al. (2022), or Saliu et al. (2022). In the following, a special focus will be laid on the discussion of the applied FTIR spectroscopy methods.

FTIR-ATR offers an easy handling for larger MP items, and spectral information of measured items is provided within seconds and can be directly compared to a spectral library. It is noteworthy that documentation of the morphology of items (ideally with a microscope camera) should be performed before the FTIR-ATR measurement, as it is a contact analysis which may damage especially brittle MP (Shim et al. 2017). In the present work, FTIR-ATR analyses were performed on all suspected MP items in triplicate measurements, being in total >1000 items and therefore >3000 individual measurements conducted in Roscher et al. (2021) (**Chapter 2**) and Roscher et al. (2022) (**Chapter 3**). Previous studies stated that – for samples with >50 suspected MP items – the analysis of a subset of n=50 per sample is sufficient to represent the overall polymer and shape compositions (Koelmans et al. 2019, Mintenig et al. 2020). Especially for samples with several hundreds of suspected MP items (e.g., sampling station 53, **Chapter 2**, n=276), this subsampling could have been a valid option in order to reduce the time demand, and should be considered for future works and specifically for monitoring studies with a high sample throughput. On the other hand, the complete analysis conducted in the present work gives the most accurate picture of the L-MP polymer composition, providing a valuable dataset also in combination with the reporting of morphological features, which can be used e.g., for associated modelling studies.

Challenges eventually occurring during FTIR-ATR analyses were residual biofilms on the selected items, which can hamper an accurate chemical identification. An extreme example for this occurred during the analysis of a MP item isolated from a surface water sample collected in proximity to the city of Bremerhaven (sampling station 34; **Chapter 2**): It was covered by a thick layer of biofilm, and – in the initial measurement – showed a HQI of <600 and was thereby not identifiable (more specifically, it was assigned to algae material, *Fucus serratus*, with a HQI <400 out of 1000) (**Fig. 5.3A**). The similarity of the sample spectrum to the reference spectrum of *Fucus serratus* is based on different matching spectral bands: The wavenumber regions ~1630 cm^{-1}, e.g., was related to uronic acids (Chale et al. 2014), sugar acids which are common in brown algae (January et al. 2019). The band at ~1015 cm^{-1} has been described as a characteristic for carbohydrates of polysaccharides,

whereas the bands at ~2850 cm^{-1} and ~2920 cm^{-1} refer to lipids (Bartošová et al. 2015). Although the appearance (together with the low HQI) disproves the assignment to the rather solid, up to 2 m long *Fucus serratus*, it is suggested that the biofilm might be constituted of other algae material such as microalgae, which share similar IR bands (Manjunatha and Girisha 2021), or residues of colonizing phyla such as the brown algae *Ectocarpus*. Due to the distinct pellet-like appearance, it was suspected that the item was of synthetic nature. Therefore, another cleaning step was introduced for removing the biofilm: The surface was thoroughly scratched off with a scalpel, and the item measured again – this time resulting in the assignment to PE with a maximum HQI of 902 out of 1000 (**Fig. 5.3B**). This example underlines the importance of a thorough examination of morphological features of suspected MP, and that adaptations of sample handling needs to be performed whenever necessary.

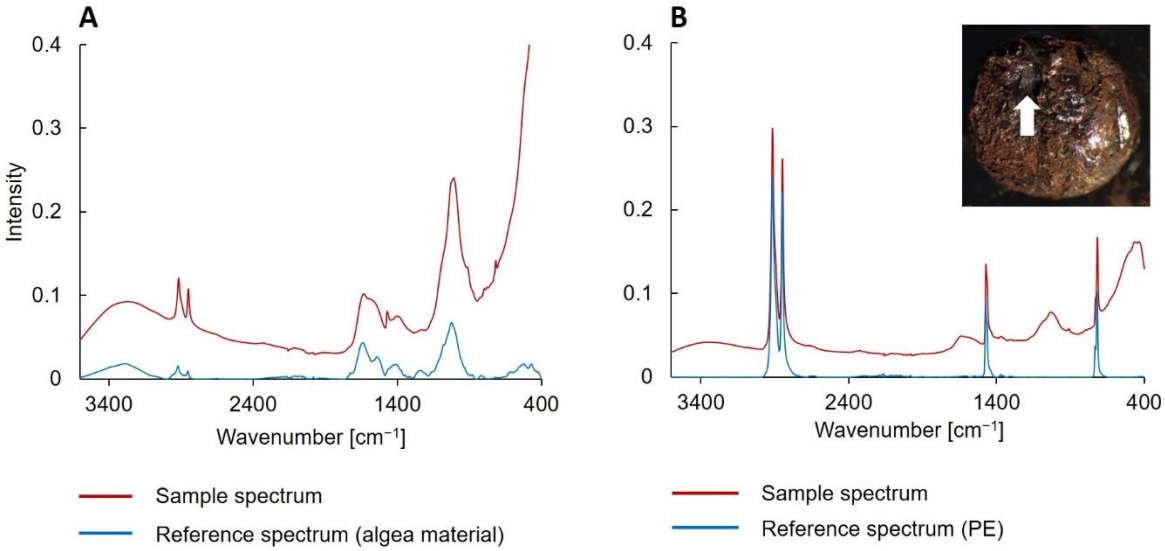

Fig. 5.3: Analysis of pellet-shaped item, with initial assignments to biological material based on comparison to reference spectrum (A), additional preparation step for removal of biofilm and repeated measurement of respective area, now resulting in the assignment to PE (B).

In contrast to FTIR-ATR, where each L-MP item is measured individually, the µFTIR imaging of S-MP runs automatically (after the selection of measurement area and manual setting of parameters), and requires currently approx. 4 h per filter (Primpke et al. 2020a). In the present work, it was attempted to provide a most accurate picture for the pollution with S-MP items, by measuring either the whole sample material available for µFTIR analyses (**Chapter 2**), or three filters per sample (**Chapter 3**). This approach was based on former observations by Abel et al. (2021), showing that the analysis of only one subsample can lead to severe under- or overestimations. This was especially reassured in **Chapter 2**,

as presented in **Table S4 (Supplementary Material for Chapter 2)** and discussed in **section 2.4.3**. Based on these findings and in accordance to Hildebrandt et al. (2021), it is highly recommended to analyse replicate samples, if it is not feasible to measure the whole sample material.

As shown in **Chapter 3**, challenges can occur during µFTIR imaging, when the biological matrix is not completely removed during sample processing. In this specific case, residues of plant cuticles present on measurement filters hindered the analysis, and were falsely identified as synthetic polymers (**cf. sections 3.2.4 and 3.4.4.2**). The adaptation of the existing polymer database performed in Roscher et al. (2022) (**Chapter 3**) was increasing the assignments to cuticle material, and seemingly reducing false positive assignments to synthetic polymers (cf. **Chapter 3**, **Fig. 3.1; Supplementary Material for Chapter 3, Fig. S4**). Moreover, this example highlights the need of regular QA/QC assessments (i.e., by manual investigation of assigned spectra and critical assessments of particle morphologies on measurement filters). As mentioned in **section 3.4.4.2**, another enhancement could be the broadening of the investigated wavenumber range, as spectral interferences especially occur in the wavenumber range >1250 cm^{-1}. Aluminium oxide-based filters, as applied in the present work, hold the advantage of being relatively cheap in purchasing (Primpke et al. 2020a), show in general a good IR transparency >1250 cm^{-1} (Löder et al. 2015), and provide the possibility of MP mass analysis by Py-GC/MS measurements subsequent to the µFTIR analysis, as shown in Primpke et al. (2020c). However, especially the wavenumber range below is not covered, as the filter material itself is responding to IR radiation in this range. As several polymer-specific peaks are present in this area, the application of silicon membranes in the wavenumber range 4000–600 cm^{-1} has been suggested by Käppler et al. (2015). Another IR-transparent alternative is the usage of zinc selenide transmission windows, applied e.g., by Kirstein et al. (2021) in the wavenumber range 3750–800 cm^{-1}, or Simon et al. (2018) in the range 3750–950 cm^{-1}. However, both silicon membranes and IR-transparent windows are rather cost-intensive, with 10–30 US$ and 50–100 US$, respectively (Primpke et al. 2020a). Finally, the identification of a suitable and affordable filter material should be the focus of future efforts, in order increase the reliability of data and avoid complications due to biogenic residual material.

Beside the purification success during sample processing and the choice of measurement filters, also the subsequent analysis of obtained IR spectra can have an influence on the

quality of data. As stated above, automation of analysis procedures are necessary in order to allow for a high sample throughput, as well for reducing a human bias which especially occurs during e.g. hand picking of small MP items. Of specific interest here is the choice of the polymer database, against which sample spectra are compared. It should include a broad set of natural materials, assuming that no sample processing protocol can guarantee the complete maceration of all natural residues. The database applied in **Chapter 2**, first introduced by Primpke et al. (2018), includes natural materials such as cellulose, natural polyamide or quartz. Through the adaptation performed in **Chapter 3**, the matrix-specific challenges specifically occurring in this study (i.e., interferences by plant residuals in effluent samples) were tackled by adding respective reference spectra to the database. Similar plant structures were not observed on measurement filters of the river water samples in **Chapter 2**, so that respective false-positive assignments are improbable here. Nonetheless, a special focus should be laid on interferences by persistent biogenic materials such as waxy substances in future studies, as especially carbohydrate bands at wavenumber 2920 cm^{-1} and 2850 cm^{-1}, or bands reflecting ester compounds at ~1730 cm^{-1} can be present in both synthetic as well as natural substances.

In the context of automated analysis procedures, a comparison of two MP analysis pipelines was performed in **Chapter 4**, aiming at revealing similarities and differences between a) siMPle/MPAPP, which is mainly based on database comparisons through Pearson correlation (and subsequent image analysis), and b) the BPF pipeline, which uses spectral descriptors and Random Forest classifiers for the assignment to different polymer classes (cf. **Chapter 4**, **section 4.1**). For this comparison, two sample sets were analysed with both pipelines: Sample set A was obtained from a related study in the framework of PLAWES (samples from Middle/Upper Weser), and sample set B from the study presented in **Chapter 2** (transect Lower Weser – North Sea). Initial assessments of the resulting data output already showed strong discrepancies with regards to certain polymer types. Especially the polymer cluster acrylates/PUR/varnish was highly abundant after siMPle/MPAPP analysis, but less prominent after BPF analysis (cf. **Fig. 4.1**). One possible explanation could be that the respective polymer cluster used in BPF only comprises PUR and PMMA, whereas the siMPle/MPAPP contains a broader range of different polymers, including PUR and PMMA, but also polyester urethanes, styrene butyl methacrylate and other acrylate-based compounds (Primpke et al. 2018). Another explanation could be an overestimation through siMPle/MPAPP or underestimation through BPF with regards to

this polymer cluster, possibly also in association with the analytical challenges posed by residual biogenic material, as discussed in **section 4.4.3**. This, however, could not be fully clarified in this study, as it was limited to a comparison of output data based on the analysis of environmental samples, and the actual 'true' MP values in the samples were not known. A systematic laboratory study including the measurement of known (MP) reference items and subsequent analysis with both discussed pipelines could shed light on this question.

After exclusion of respective polymer clusters, the obtained data revealed that both pipelines were in general in good accordance with each other, but also showed certain discrepancies. Especially MP counts in samples with 'challenging' sample matrixes, such as those retrieved from surface waters of the Jade Bay bearing high sediment loads, varied severely (e.g., samples B-01 and B-02, **Fig. 4.2**). Furthermore, especially in small size classes polymer assignments differed. In the framework of this study, the exact reasons for these differences could not be revealed; however, it is – to our knowledge – the first study drawing a detailed comparison of the data output the two MP analysis pipelines siMPle/MPAPP and BPF. The observations made based on the results directs into further optimisation with regards to especially smallest MP classes, but also highlights the need for further standardisation with respect to clustering of polymer types, as well as further investigation of the influence of residual sample material on MP data.

5.2 Assessment of microplastics in an important German river system: Inter-study comparison

5.2.1 Status of pollution in riverine and marine systems

As stated in **section 5.1**, applied methods for the assessment of MP still vary strongly between studies, and although the attempt for standardization exists and gained more and more attention in recent years, a direct comparison between studies is not yet feasible. Nonetheless, in the following an overview will be given about MP studies in comparison to the present work, with a focus on assessments in German river systems and adjacent marine waters. Respective peer-reviewed studies were mainly published between 2019 and 2022, whereas the underlying sampling campaigns were conducted between 2014 and 2020 (**Table 5.4**). In these studies, either nets (mesh sizes: 100−300 µm), filtration systems (mesh sizes: 15 and 50 µm) or a centrifugal separator were applied for mainly surface water sampling. Analysis techniques were either item-based (FTIR-ATR, µFTIR, Raman) or mass-based (Py-GC/MS), but were mostly performed on a subset of visually identified MP. With respect to larger MP items collected in the rivers Elbe, Rhine and Weser via net sampling, percentages of analysed items varied strongly, with e.g., 7% analysed in Scherer et al. (2020), 41% in Mani and Burkhardt-Holm (2020), and 100% in Roscher et al. (2021) (cf. **Chapter 2**), respectively. Eibes and Gabel (2022), analysing MP samples collected in the Ems river, chose the approach of the hot needle test in order to identify synthetic polymers, and performed a qualitative FTIR-ATR analysis on selected items with a size >1 mm. Smaller MP, in contrast, are often concentrated on analysis filters in preparation for chemical mapping, although only rarely a whole sample fits on one filter, making subsampling and/or the distribution on several filters necessary (cf. **section 5.1.3**). With regards to the studies listed in **Table 5.4**, approaches for subsampling varied, including the measurement of one filter per sample, the analysis of triplicate samples, or the distribution of the whole available sample material on several analysis filters (Lorenz et al. 2019, Hildebrandt et al. 2021, Roscher et al. 2021) (as discussed in **section 5.1.3**). These differences in methodology should be kept in mind for the following comparison of resulting MP concentrations.

As already stated in several MP studies worldwide, small MP items are vastly more abundant in the environment than larger ones (Enders et al. 2015, Cabernard et al. 2018, Lindeque et al. 2020, Tekman et al. 2020). This was also shown in **Chapter 2**, where pump

samples, targeting items <500 µm, showed significantly higher MP abundances than net samples (size range 500-5000 µm). Similar findings were presented by Laermanns et al. (2021), detecting MP concentrations of approx. 50–100 MP m^{-3} in the Elbe River via pumping water into a filter cascade (lower size limit: 50 µm), and values <10 MP m^{-3} for samples collected with 150 and 300 µm nets (**Table 5.4**). Due to these differences, studies applying net sampling and sampling with filtration systems are discussed separately in the following.

Studies which applied nets for sample collection in the rivers Weser, Elbe, Trave, Rhine, and Ems generally revealed concentrations ≤10 MP m^{-3} (**Table 5.4**). In the Trave, similar concentrations as in the Weser River were recorded (0-1 MP m^{-3}, size fraction: 300-5000 µm). In contrast, assessments in the Elbe (Piehl et al. 2020, Scherer et al. 2020, Laermanns et al. 2021) and Rhine river (Mani and Burkhardt-Holm 2020), higher concentrations were found. Both show larger catchment areas and strong industrial activity along the rivers, which may cause stronger MP pollution. However, differences in concentrations could also be influenced to a certain degree by the lower minimum sizes applied for MP analysis (Elbe and Rhine: 150 µm and 300 µm; Weser: 500 µm), again underlining the importance of method standardisation for a more accurate comparison.

With regards to spatial trends revealed by assessments via net sampling, the Trave River – similar to the Weser – showed higher concentrations within the river, decreasing towards the Baltic Sea (Piehl et al. 2020). In contrast, in their campaign in August 2015 in the Elbe River, concentrations were increasing from the river mouth towards the North Sea. The authors suggest additional MP input from sea-based sources as an explanation for this increase. An interesting aspect with this respect could be the horizontal export of MP items from the Weser mouth, located at the south-west of the Elbe, potentially influencing MP concentrations in the Outer Elbe. Surveys with a higher spatial resolution, spanning over both estuaries, could be of high value to better understand MP distribution patterns.

Table 5.4: Overview of geographically relevant MP studies on rivers and marine waters in Germany, sorted by sampling method. Abbreviations: SWIR spectroscopy – short-wave infrared spectroscopy.

Reference	Sampling area / Sampling time	Sampling method (incl. lower size limit)	Chemical analysis and size range targeted with analytical detection	MP concentration [n m^{-3}]	MP concentration [µg m^{-3}]
Net sampling					
Roscher et al. (2021) (*Chapter 2*)	Weser estuary[1] / Apr. 2018	Microplastic net (300 µm)	FTIR-ATR (500–5000 µm)	0 – 1	–
Laermanns et al. (2021)	Elbe River[1] / Jan. 2020	Plankton nets (150, 300 µm)	Py-GC/MS (>150 µm)	~10	~300 – 700
Scherer et al. (2020)	Elbe River[1] / Jul./Aug. 2015	Plankton net (150 µm)	FTIR-ATR (150–5000 µm)	0.88 – 13.24 (5.57±4.33)	–
Piehl et al. (2020)	Elbe estuary[1] / May 2014, June + Aug. 2015	Manta net (300 µm)	FTIR-ATR (500–5000 µm)	0 – 11 [3]	–
Piehl et al. (2020)	Trave estuary[2] / May 2014	Manta net (300 µm)	FTIR-ATR (500–5000 µm)	0 – 1 [3]	–
Mani and Burkhardt-Holm (2020)	Rhine River[1] / Apr. 2016 – Feb. 2017	Manta trawl (300 µm)	FTIR-ATR (300–5000 µm)	2.7 ± 0.4 – 6.3 ± 2.6	–
Eibes and Gabel (2022)	Ems River[1] / Mar.+ Apr. 2014	Driftnet (250 µm)	FTIR-ATR (>1 mm)	0 – 5.28 (1.54±1.54)	–
Wagner et al. (2019)	Parthe River (close to the city of Leipzig) Nov. 2015 – Jan. 2016; Oct. 2016 – Feb. 2017	Driftnet (500 µm)	Raman (500 µm–10 mm)	74 ± 67 [4]	60 ± 60 [5]
Lorenz et al. (2019)	Southern North Sea / Jul. – Aug. 2014	Neuston net (100 µm)	µFTIR (10–500 µm) FTIR-ATR (500–5000 µm)	0.1–245 [3]	–

1) Discharges into the North Sea.
2) Discharges into the Baltic Sea.
3) Value refers to total MP abundances, not differentiating between small and large MP fractions.
4) Includes MP items >5mm; however, respective counts are negligible compared to numbers obtained for the <5 mm fractions.
5) Mass was only determined for items with a size between 1 – 5 mm.

Table 5.4 – continued: Overview of geographically relevant MP studies on rivers and marine waters in Germany, sorted by sampling method. Abbreviations: SWIR spectroscopy – short-wave infrared spectroscopy.

Reference	Sampling area / Sampling time	Sampling method (incl. lower size limit)	Chemical analysis and size range targeted with analytical detection	MP concentration [n m^{-3}]	MP concentration [µg m^{-3}]
Filtration systems					
Roscher et al. (2021) (***Chapter 2***)	Weser estuary[6] / Apr. 2018	Pumping system (15 µm)	µFTIR (11–500 µm)	23 – 9700	–
Laermanns et al. (2021)	Elbe River[6] / Jan. 2020	Pump + Filter cascade (50 µm)	Py-GC/MS (>50 µm)	~50 – 100	~700 – 1.200
Piehl et al. (2021)	Warnow River[7]/ Sep. – Oct. 2018; May – Mar. 2019	Filtration system (50 µm)	Raman (>50 µm)	57 – 388 (226.79±119.	–
Dibke et al. (2021)	German Bight, North Sea / Oct. 2016, Oct. 2017	Pump + Filter cascade (20/40 µm)	Py-GC/MS (20/40 µm–1 mm)	–	2 – 1396
Other sampling methods					
Hildebrandt et al. (2021)	Elbe estuary[6] / Nov. 2018	Centrifugal separators	FTIR-ATR (500–5000 µm) µFTIR (10–500 µm)	193 – 2072[8] (800 ±1700)	
Schmidt et al. (2018)	Teltow canal (city of Berlin) / May – Aug. 2015	Niskin bottle	SWIR imaging spectroscopy (450–5000 µm)	10 – 96.000	–

6) Discharges into the North Sea.
7) Discharges into the Baltic Sea.
8) Value refers to total MP abundances, not differentiating between small and large MP fractions.

Filtration systems driven by pumps were less frequently used for sampling than nets (**Table 5.4**). Sampling campaigns with such set-ups in the Rivers Weser, Elbe and Warnow revealed concentrations of several magnitudes higher than recorded for net sampling. The two studies which applied a lower size limit of 50 µm for assessments in the rivers Elbe and Warnow detected concentrations between approx. 50-100 and 57-388 MP m^{-3}, respectively (Laermanns et al. 2021, Piehl et al. 2021). Maximum concentrations in the Weser River were of one magnitude higher, which, however, is possibly influenced again by the lower minimum mesh size used (15 µm). The application of centrifugal separators for MP sampling in the Elbe estuary by Hildebrandt et al. (2021), followed by µFTIR analysis with the sample detection limit (11 µm) as applied in the present work, led to S-MP concentrations similar to those detected in the Weser estuary. With respect to the studies listed in **Table 5.4**, highest MP concentrations (max. value: 96.000 m^{-3}) were recorded by Schmidt et al. (2018) in the surface layer of an urban waterway in the city of Berlin. Grab samples were collected with Niskin bottles directly at the water surface (sample volume: ~100 L). Rain events, likely remobilising MP, in combination with the influence of highly urbanised areas may be responsible for these elevated MP pollution levels (Schmidt et al. 2018). Finally, as stated above, a standardisation of MP analysis is indispensable in order to allow an accurate comparison between studies.

Although assessment techniques within the mentioned studies differ, the outcome with regards to polymer compositions shows similarities. In the majority of studies, PE, PP, and PS are vastly detected polymers (Schmidt et al. 2018, Mani and Burkhardt-Holm 2020, Scherer et al. 2020, Laermanns et al. 2021, Piehl et al. 2021), reflecting the strong production and usage. These polymers were often recorded in the form of secondary MP, indicating that they were generated during breakdown of larger plastic items. In this regard, Schöneich-Argent et al. (2020) recorded significant shares of consumer plastics as well as suspected polystyrene pieces during their macrolitter survey in Ems, Weser and Elbe. In order to allow for a more detailed source apportionment, it could be beneficial to link both MP and macroplastic assessments in future assessments. Macrolitter surveys often only refer to the morphology of items or derive the underlying polymer type from it (e.g., a piece of foamy material is assigned to polystyrene, although also other synthetic foams are available on the market). A more detailed analysis at least of a subset of macroplastic items, by means of FTIR or Raman spectroscopy, might be beneficial especially for the linkage to fragmented MP.

Beside PE, PP and PS, also PUR- or acrylate-based polymers were detected in significant amounts in the S-MP fraction especially in the North Sea as well as estuarine waters (Lorenz et al. 2019, Dibke et al. 2021, Hildebrandt et al. 2021, Roscher et al. 2021). Although these polymers are used in a plethora of applications, these records suggest paint fragments as a potential origin, possibly stemming from ship hulls (cf. **Chapter 2**, **section 2.4.1.1**). Finally, the assessment of paint debris and related polymer types should be systematically included in future MP studies, as stated by Hartmann et al. (2019), as they were more and more shown to contribute strongly to MP pollution (Dibke et al. 2021, Turner 2021).

5.2.2 Potential sources of MP in aquatic systems: Contextualisation of findings

In the past years, an increasing number of studies investigated WWTPs, in order to evaluate their potential as point sources for MP in aquatic environments. Wolff et al. (2019) investigated a WWTP in the federal state of Hessen, Germany, using a similar size range for MP (minimum size: 10 µm; also sampled with cartridge filters), and spectroscopic analysis (Raman) for polymer identification. Minimum concentrations in the effluent were at approx. 2000 MP m^{-3}, maximum concentrations at approx. 10.500 MP m^{-3}, which is roughly in the same order of magnitude as values recorded in the effluents of the Bremen-Seehausen WWTP (cf. **Chapter 3**, **Fig. 3.2 C**). Commonly detected polymer types were PET, PE, PP, and PS, which were also prominent in the effluent samples analysed in Roscher et al. (2022), **Chapter 3**. Especially PE, PP and PS were also predominantly detected by Mintenig et al. (2017), analysing 12 WWTPs in Northern Germany. Funck et al. (2021) investigated three German WWTPs (locations anonymised), which were – contrary to the WWTPs studied in **Chapter 3** – equipped with sand filters in the final treatment stage. Analysis with TED-GC/MS aimed at the detection of PE, PS, PP and PET, with PE being again identified as dominant polymer type. Mass assessments of samples taken before the sand filtration step showed concentrations of PE similar to the ones recorded for the Bremen-Seehausen WWTP (cf. **Supplementary Material for Chapter 3, Tab. S8**), being in the range 100-200 µg m^{-3} (Funck et al. 2021). The study showed that the application of sand filters is highly efficient, with MP retentions of 60-95%. Accordingly, Wolff et al. (2020) recorded MP retentions of >99% in municipal WWTPs as well as in a PVC manufacturing plant, both equipped with sand filters. Also other technologies were shown to be highly efficient, such as activated carbon filters (dos Santos and Daniel 2020), membrane bioreactors (Talvitie et al. 2017a, Rögener et al. 2021), or ozone-based

technologies (Hidayaturrahman and Lee 2019). Finally, the application of an additional treatment step for conventional WWTPs could help to further reduce MP input into aquatic systems, and should be further pursued.

As observed for the assessment of MP in river systems, also studies in WWTPs require further standardisation, in order to allow for a better comparability. Nonetheless, as outlined above for riverine samples, available data clearly show that polyolefins as well as PS and PET are commonly present in WWTP effluents, reflecting our daily usage of these plastic types. When it comes to the role of WWTPs as a source of MP for aqueous systems, no clear impact with regards to polymer compositions or MP abundances was observed for the Lower Weser (**Chapter 3, section 3.4.3**). In contrast to L-MP, increased MP item and mass concentrations were measured for S-MP in the downstream station in comparison to the upstream station; however, it has to be taken into account that sampling of the riverine stations and sampling of the WWTP was not conducted in the same timeframe, hampering a direct comparison. Increased MP values in proximity to WWTP were also recorded in Piehl et al. (2020), analysing different locations in the Trave River, Germany. For the Warnow River, also discharging into the Baltic Sea, the total contribution of WWTPs to riverine MP loads was estimated to only account for 1.4% for (Piehl et al. 2021). For this river system, a stronger influence was attributed to combined sewer overflow (6.1%) and especially storm water runoff (43.1%). In the scope of the WWTP sampling campaign conducted in the present work, we exemplary sampled storm water at a pumping station in Bremen four times after rain events. The analysis revealed total MP item and mass concentrations in the range 0.8–4.0 × 10^3 MP items m^{-3} and 0.8–2.7 × 10^3 µg MP m^{-3}, respectively (**Fig. 5.4**), and thus showed no stronger MP pollution than the WWTP effluents. However, due to the small number of samples, these data should be considered preliminary, and should be reaffirmed in future studies. Furthermore, the applied methodology was not tailored to the assessment of tire wear particles (TWP), a currently strongly discussed type of MP (Knight et al. 2020, Goßmann et al. 2021, Werbowski et al. 2021), likely leading to an underestimation of actual MP numbers: Firstly, the applied density separation during sample processing might have removed the relatively dense TWP, as discussed by Goßmann et al. (2021). The application of denser solutions such as Sodium Polytungstate might provide remedy here, as shown by Klöckner et al. (2019). Secondly,

TWP most often show a rather dark coloration, potentially leading to total absorption in FTIR analyses and therefor hampering an accurate detection.

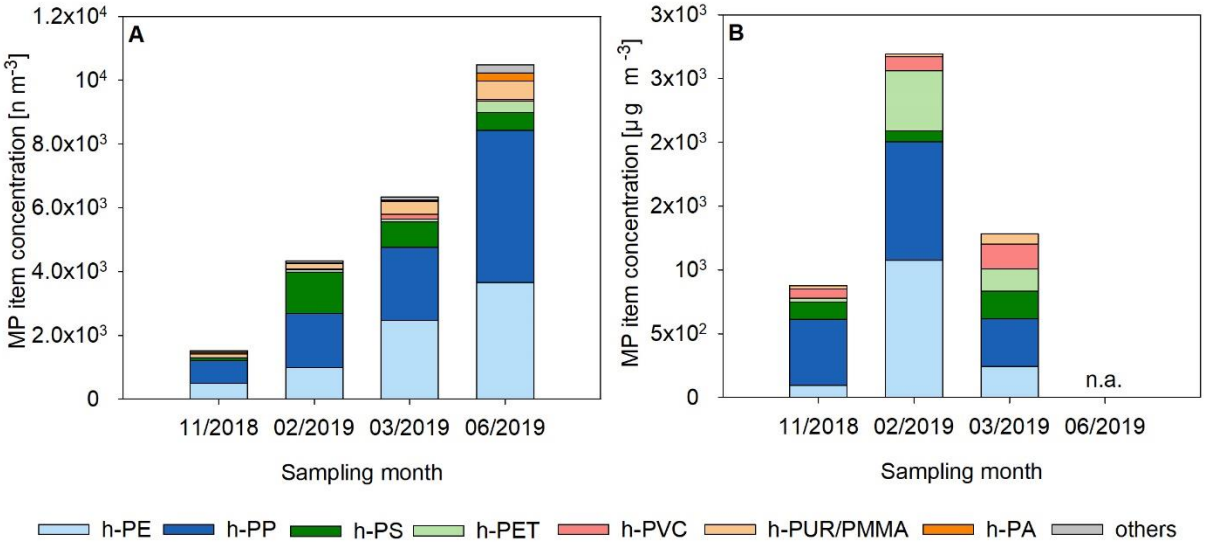

Fig 5.4: S-MP item (A) and mass (B) concentrations detected in storm water samples collected in Bremen after rain events, using the same methods as the here presented WWTP study (for abbreviations of harmonized polymer clusters see Tab. 3.1).

A retrospective analysis of Py-GC/MS data using suitable reference pyrograms might provide more insights in the TWP loads in the storm water samples at least at a qualitative level; however, this was out of the scope of the present work. Finally, future studies should aim at systematically assessing pollution with TWP, in order to better evaluate their contribution to total MP loads in the environment.

Beside municipal WWTPs, also industrial WWTP have been discussed as MP source in former literature. In waters and sediments of the Rhine and Elbe Rivers, primary MP in the form of PS beads have been detected in significant amounts, and were suggested to stem from ion exchange resin applications used in industrial wastewater treatment (Mani and Burkhardt-Holm 2020, Scherer et al. 2020, Laermanns et al. 2021). Also plastic production sites have been suggested as point source for riverine MP in Germany, e.g. in the case of transparent PMMA spherules in the Rhine River (Mani et al. 2015). In the context of primary MP spillages, Mani and Burkhardt-Holm (2020) emphasize the need for rigorous emission controls in production and transport processes, usage and waste management in order to reduce MP pollution. For the Weser River, records of spherules were especially close to urban areas, but generally rather low in comparison to secondary MP in the form of fragments (**Chapter 2**, **cf. Fig. 2.3**). This indicates that these primary MP played a minor role for the sampling locations along the Weser River within the chosen timeframe.

Another possible MP source are construction sites situated along rivers. Wagner et al. (2019) applied driftnet sampling (mesh size: 500 µm; cf. **Table 5.4**) and detected increased numbers of expanded PS beads with a similar morphology of insulation material in the Parthe River in the southeast of the city of Leipzig, Germany, hypothesizing that they were stemming from larger PS pieces used on active construction sites located close to the sampling stations. PS foam was also detected in the present study, but the origin remained unclear. A more directed assessment, e.g., along a transect in proximity to construction activities or other suspected MP sources, could further elucidate their potential for introducing MP into aquatic environments.

In conclusion, sources for MP in riverine systems can be highly diverse and vary from river to river, depending on adjacent land use, local riparian construction activity, urbanisation or density of industrial sites. The exact contribution of each source type is not yet fully understood, and require further in-depth analysis with high temporal and spatial resolution, implemented e.g., in future monitoring efforts.

5.3 Conclusion & Outlook

The present work aimed at elucidating MP distribution patterns and potential point sources in and adjacent to the Weser River system, Germany, by assessing MP in a broad size range of 11−5000 µm. Another important aspect was the adaptation and evaluation of analysis methods, including the optimisation of the reference database applied in the analysis of spectral data, and the comparison of two currently applied MP analysis pipelines.

The results of the field studies showed a clear dominance of S-MP (especially <100 µm) in both riverine locations and waste water effluents. This finding reaffirms previous research but also emphasizes again the need of suitable sampling and analysis strategies, in order to not underestimate these small size fractions, which are most relevant in the context of ecotoxicology. Due to ongoing fragmentation processes, an even higher number of items is to be expected in size classes below <11 µm. Although their analysis was out of the scope of the present work, it is highly recommended to implement them into future studies, including the optimization of respective analysis techniques.

Polymer compositions showed a prominence of polyolefins (PE, PP) in riverine surface waters as well as in WWTP effluents. This is in accordance with numerous previous studies, and mirrors their high production and consumption. The fact that the majority of items were in the form of fragments suggests that they derived from the breakdown of larger plastic items. Especially for riverine surface water, also the polymer cluster acrylates/PUR/varnish was highly abundant (S-MP fraction). Together with the observation of paint flakes also in the L-MP fraction of the samples, it can be hypothesized that paint coatings, potentially stemming from ship hulls, are a possible origin. However, further improvements of the underlying analysis are required in order to better distinguish paint fragments from other acrylate/PUR-based materials, especially for very small items, where a visual confirmation based on shape or colour is not possible. Future research should further address this issue as associated heavy metals or other additives pose a threat to aquatic wildlife.

Based on the characterisation with respect to MP concentrations, polymer compositions, and morphological features performed in the present work, it was attempted to evaluate the potential of WWTPs as point sources for riverine MP loads. Based on the findings, no major influence of the effluent on the riverine MP polymer compositions was observed. Regarding general pollution levels, downstream concentrations for S-MPs items and masses were higher in comparison to upstream concentrations, suggesting an influence by MP loads in

the WWTP effluent. However, it has to be taken into account that river and WWTP sampling campaigns could not be conducted in the exact same time frame, and that no replicate samples were taken. Therefore, these first observations should be further validated, e.g., in the form of more regular monitoring with a higher spatial and temporal resolution. Although the exact influence of WWTP effluents could not be fully elucidated in the present work, the yearlong analysis showed MP occurrence in all analysed effluent samples, implying that MP is transported from the investigated WWTP into the receiving river system.

With regards to MP concentrations in the Weser River, elevated amounts (especially of S-MP) were observed in the TMZ. The accumulation in the TMZ might be caused by inclusion into flocs or aggregates composed of SPM, followed by a slow release into North Sea waters following the tidal dynamics. Another factor could be suspension/resuspension dynamics, where MP in sediment is released again to the water column or surface. Decreasing MP loads along the North Sea transect may be related to different factors, such as dilution, or vertical/horizontal export. In the context of distribution patterns, this work gives an initial insight into MP down to 11 µm in surface waters of the Weser-North Sea transitional system, and suggests – based on the observations made – further investigations on MP dynamics along a vertical transect in the water column and a detailed analysis of the fate of riverine MP once entering the North Sea.

Concerning the methodological background, the automation of MP analysis procedures is highly necessary, especially for the assessment of smallest MP. Although great improvements have been made especially in the last decade, there is still room for development and optimisation within the rising field of MP research. The present work aimed at contributing to the methodological development, by providing an adapted reference database for the analysis of samples with a high degree of residual plant material, developed during analysis of the WWTP effluent samples. The observation of false-positive assignments due to biogenic material can be a valid information for future studies, and the database adaptation may reduce the resulting error. However, the development is still ongoing and future studies should stay aware of the interfering impact also other biogenic materials may have. Further improvements in this context could be the optimisation of the purification protocol, as well as the usage of an alternative filter material with a broader applicable wavenumber range, covering the important finger print region of polymers in the range $<1250\ cm^{-1}$. Herein, a cost-efficient solution with similar benefits (such as the

possibility of subsequent Py-GC/MS measurements) is still to be identified and implemented into current research.

Another methodological aspect of this work was the comparison of two currently applied analysis pipelines for the assessment of S-MP. Results showed a general accordance between the approaches in most of the samples. However, also differences have been observed with respect to certain polymer clusters, such as acrylates/PUR/varnish or EVA, but also assignments to PE and PP especially in small size classes were not always consistent. These outcomes suggest that further standardisation and harmonisation is required especially with regards to these discrepancies, in order to increase the comparability of results obtained from different analytical approaches. For this, the analysis of reference materials with known chemical compositions with both analysis pipelines and a subsequent evaluation of their recovery/misidentification rates would be suitable.

Overall, the present work provides a detailed data basis of MP pollution levels in the Weser – North Sea transitional system as well as in the effluents of two German WWTPs, with regards to MP concentrations, polymer compositions and size class distributions. Furthermore, the above-mentioned methodological improvements as well as the comparative study may be implemented and considered in future MP research, leading towards increased data quality and highlighting aspects which should be further investigated and standardised.

Appendix

The following sections contain the Supplementary Material for the studies presented in **Chapters 2, 3 and 4**.

Supplementary Material for Chapter 2

Microplastic pollution in the Weser estuary and the German North Sea

Lisa Roscher[a], Annika Fehres[a], Lorenz Reisel[a], Maurits Halbach[b], Barbara Scholz-Böttcher[b], Michaela Gerriets[b], Thomas H. Badewien[b], Gholamreza Shiravani[c], Andreas Wurpts[c], Sebastian Primpke[a], Gunnar Gerdts[a]

[a] Alfred Wegener Institute, Helmholtz Centre for Polar and Marine Research, D-27483 Helgoland, Germany

[b] Institute for Chemistry and Biology of the Marine Environment (ICBM), Carl von Ossietzky University of Oldenburg, D- 26111 Oldenburg, Germany

[c] Lower Saxony Water Management, Coastal Defence and Nature Conservation Agency (NLWKN), D-26548 Norderney, Germany

Corresponding author: Lisa Roscher (lisa.roscher@awi.de)

Keywords: Microplastics**,** Plastic pollution, Freshwater system, River system, Infrared spectroscopy

Content

Figures

Tables

Tab. S5: Results of Kolmogorov-Smirnov-Test performed based on kR Cluster analysis

Table S6: Overview of microplastic item concentrations [n m^{-3}] in riverine, estuarine and marine surface waters recorded in previous studies, which also applied net sampling as well as pumping systems for sample collection

Sections

Section **S2:** Records of plastic items >5000 µm

Tab. S1: Background information on the sampling campaign performed in April 2018 in the transitional zone Weser-Wadden Sea (cf. sections 2.2.1 and 2.2.2). Presented coordinates associated with the RV Otzum refer to sampling of S-MP by on-board filtration (coordinates for net sampling events differed slightly). For Lower Weser samples, the approx. river width and distance from river bank is indicated (l=left, r=right, indicated in brackets behind distance values).

Area	Sampling station	Research vessel	Sampling date	North	East	Approx. river width [km]	Approx. distance from river bank [km]	Sample volume [L] (S-MP)	Sample volume [L] (L-MP)
Jade Bay	16	Otzum	05.04.2018	53°29.94	008°14.18	-	-	577	112,560
	18	Otzum	05.04.2018	53°27.87	008°14.00	-	-	478	132,510
North Sea margin	19	Uthörn	18.04.2018	53°52.78	007°39.42	-	-	900	116,046
	20	Uthörn	19.04.2018	53°59.53	007°50.61	-	-	800	122,976
	30d	Uthörn	17.04.2018	53°53.62	007°58.70	-	-	871	16,128
Outer Weser	30b	Uthörn	16.04.2018	53°44.65	008°14.26	-	-	700	40,740
	30a	Uthörn	15.04.2018	53°41.38	008°20.26	-	-	476	45,108
	30	Uthörn	15.04.2018	53°39.27	008°24.32	-	-	487	24,864
	31	Uthörn	14.04.2018	53°37.75	008°28.01	-	-	357	153,468
	33	Uthörn	14.04.2018	53°35.22	008°31.12	-	-	490	42,000
	34	Uthörn	13.04.2018	53°32.74	008°33.43	-	-	280	67,494

Tab. S1 - continued

Area	Sampling station	Research vessel	Sampling date	North	East	Approx. river width [km]	Approx. distance from river	Sample volume [L] (S-MP)	Sample volume [L] (L-MP)
Lower Weser	37	Otzum	09.04.2018	53°31.10	008°33.87	1.23	0.29 (r)	127	247,800
	39	Otzum	09.04.2018	53°29.78	008°30.12	0.83	0.06 (l)	499	238,308
	41	Otzum	10.04.2018	53°28.39	008°29.31	1.10	0.28 (l)	44	252,336
	43	Otzum	10.04.2018	53°25.46	008°29.88	0.83	0.11 (r)	410	162,288
	45	Otzum	11.04.2018	53°21.86	008°30.19	0.79	0.20 (r)	517	200,844
	47	Otzum	11.04.2018	53°19.35	008°29.23	0.50	0.07 (l)	966	236,292
	48	Otzum	12.04.2018	53°11.82	008°31.18	0.30	0.06 (r)	1000	222,726
	49	Otzum	12.04.2018	53°10.08	008°37.41	0.36	0.00 (r) *)	951	223,146
	50	Otzum	13.04.2018	53°07.05	008°42.71	0.27	0.02 (l)	943	210,966
	51	Otzum	13.04.2018	53°07.17	008°42.90	0.30	0.01 (r)	913	211,260
	52	Otzum	14.04.2018	53°04.07	008°49.44	0.13	(midstream)	973	225,582
Middle Weser	53	Otzum	14.04.2018	53°03.53	008°52.26	0.15	(midstream)	1000	218,820

*) Station 49 was located in a port entrance, lining up with the shore line.

Tab. S2: Environmental parameters recorded during the sampling campaign in April 2018 in the transitional zone Weser-Wadden Sea (cf. sections 2.2.1 and 2.2.2). Conductivity, Temperature and Salinity were recorded during SPM sampling.

Area	Sampling station	Conductivity [mS cm^{-1}]	Temp. [°C]	Salinity [psu]	SPM [mg L^{-1}]	PIM [mg L^{-1}]	POM [mg L^{-1}]
Jade Bay	16	n.a.	7.1	29.1	147.6	116.4	31.2
	18	n.a.	5.7	29.5	85.6	68.6	17.0
North Sea margin	19	51.2	6.95	n.a.	0.8	0.5	0.3
	20	52.0	6.15	n.a.	12.8	8.5	4.3
	30d	52.0	5.5	n.a.	2.1	1.4	0.8
Outer Weser	30b	41.9	8.6	n.a.	13.5	10.6	2.9
	30a	32.8	9.4	n.a.	29.7	27.1	2.6
	30	34.3	8.95	n.a.	29.9	25.1	4.9
	31	24.7	8.85	n.a.	35.7	30.2	5.6
	33	26.6	8.8	n.a.	14.3	14.3	0.00
	34	24.9	n.a.	n.a.	54.0	44.6	9.4
Lower Weser	37	7.2	10.5	8.7	146.0	114.9	31.0
	39	8.2	9.3	8.6	143.3	111.8	31.5
	41	1.1	10.8	2.1	431.8	358.3	73.4
	43	n.a.	10.8	2.3	47.1	35.4	11.8
	45	n.a.	12.0	0.5	29.7	19.1	10.6
	47	n.a.	11.9	0.1	16.4	8.4	7.9
	48	n.a.	12.5	0.5	12.0	4.7	7.3
	49	n.a.	12.1	0.4	12.5	3.9	8.7
	50	n.a.	13.0	0.5	16.6	8.2	8.4
	51	n.a.	13.0	0.5	15.4	3.7	11.7
	52	n.a.	12.4	0.5	16.3	7.7	8.6
Middle Weser	53	n.a.	11.5	0.6	14.8	7.0	7.7

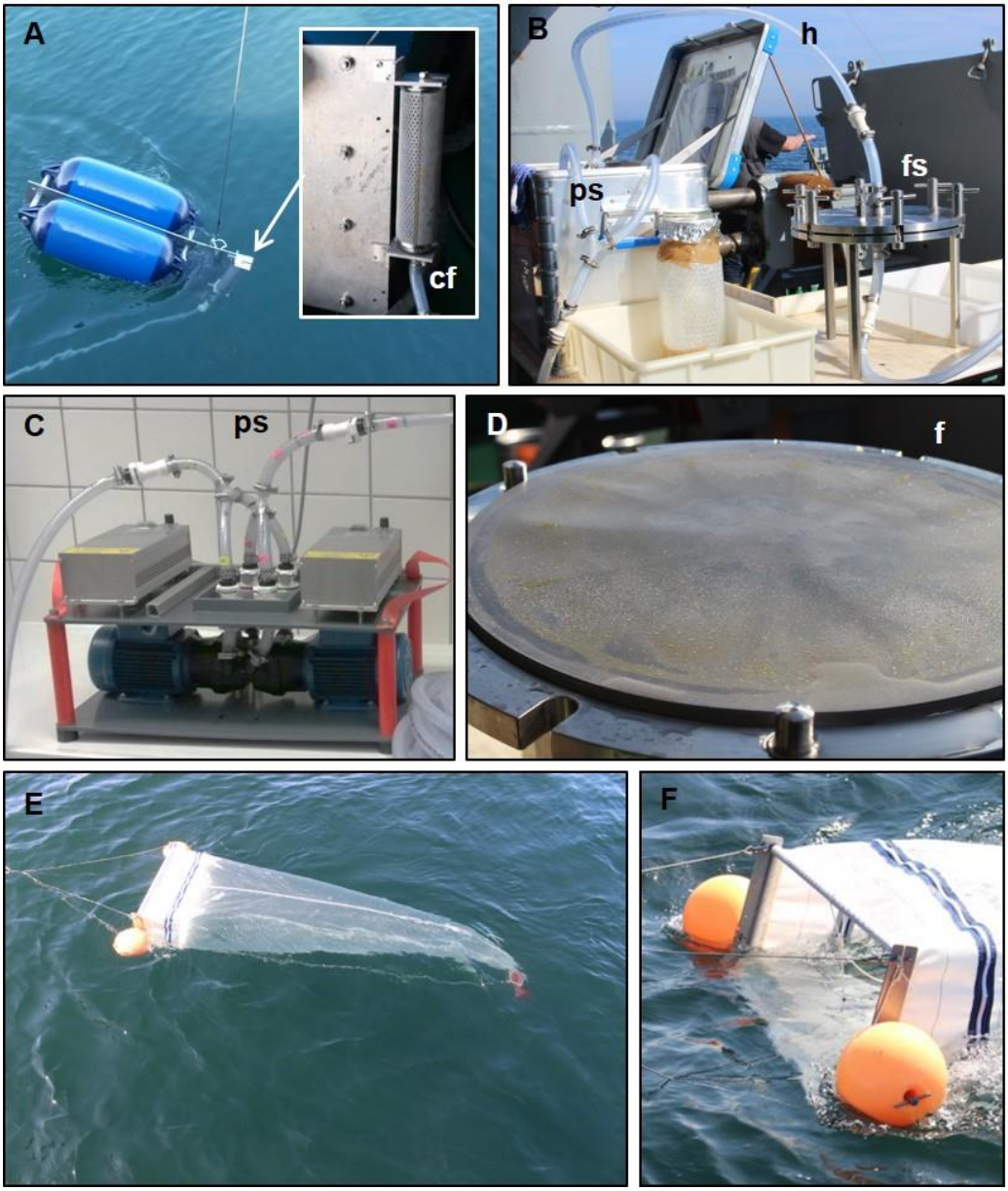

Fig. S1: Sampling devices used during the sampling campaign in April 2018. A-D: Filtration set-up used for surface water sampling of (S-MP). C: floating suction basket (cf). D: Pumping station (ps), PVC hosing (h) and filter stand (fs). E: pumping station (ps) with two membrane pumps. F: 15 µm stainless steel filter screen. E-F: Manta net (mesh size: 300 µm; net opening: 0.4 x 0.7 m) used for surface water sampling (L-MP).

Tab. S3: Total number of Anodisc filters analysed per sample via µFTIR (S-MP), range of sample shares used for the respective subsamples, and total sample share analysed. * Percentages refer to the sample material obtained after splitting the sample in half and used for µFTIR measurements (cf. section 2.2.3)

Sampling station	Total number of Anodisc filters used	Range of analysed sample shares used for subsamples [%] *	Final sample share analysed [%] *
16	11	5.9 − 10.2	100.0
18	7	14.0 − 15.2	100.0
19	1	100.0	100.0
20	3	25.0 − 48.1	100.0
30d	1	100.0	100.0
30b	3	19.9 − 42.3	100.0
30a	3	21.2 − 46.8	100.0
30	3	19.4 − 54.0	100.0
31	3	19.1 − 58.1	100.0
33	4	12.3 − 28.9	100.0
34	2	36.6 − 63.4	100.0
37	1	100.0	100.0
39	4	n.a.[1)]	100.0
41	1	100.0	100.0
43	3	n.a.[1)]	100.0
45	9	8.1 − 13.9	100.0
47	2	28.1 − 71.9	100.0
48	1	100.0	100.0
49	1	100.0	100.0
50	2	n.a.[1)]	100.0
51	1	100.0	100.0
52	1	100.0	100.0
53	2	22.7 − 77.3	100.0

[1)] Data were excluded, as documentation on exact proportions was incomplete.

Section S1: Contamination mitigation

Whenever possible, laboratory material made of glass or stainless steel was used, which was rinsed with Milli-Q water beforehand in order to remove potential contaminants. Sample containers were covered either with stainless steel/glass lids or aluminium foil. Sample processing was performed in a laminar flow bench whenever possible (ScanLaf Fortuna, Denmark), and dust boxes were used for filtering the room air (DustBox1000, Möcklinghoff

Lufttechnik, Germany). In order to remove potential particle contamination, SDS (Carl Roth, Germany) and technical enzymes were filtered through cellulose nitrate filters (0.45 µm, Sartorius, Germany). All other chemicals were filtered through polycarbonate filters (0.2 µm; GTTP, Merck Millipore GmbH, Germany). If necessary, pre-filtrations were performed using glass fibre filters (Whatman, UK).

Six procedural blanks were run in parallel to samples in the S-MP fraction in order to assess a possible contamination. Therefore, 10 L of Milli-Q water was concentrated, processed and analysed in the same way as the environmental samples and the averaged MP counts subtracted from environmental samples. As no contamination control was performed for L-MP, fibres were excluded from results (cf. **section 2.2.3**).

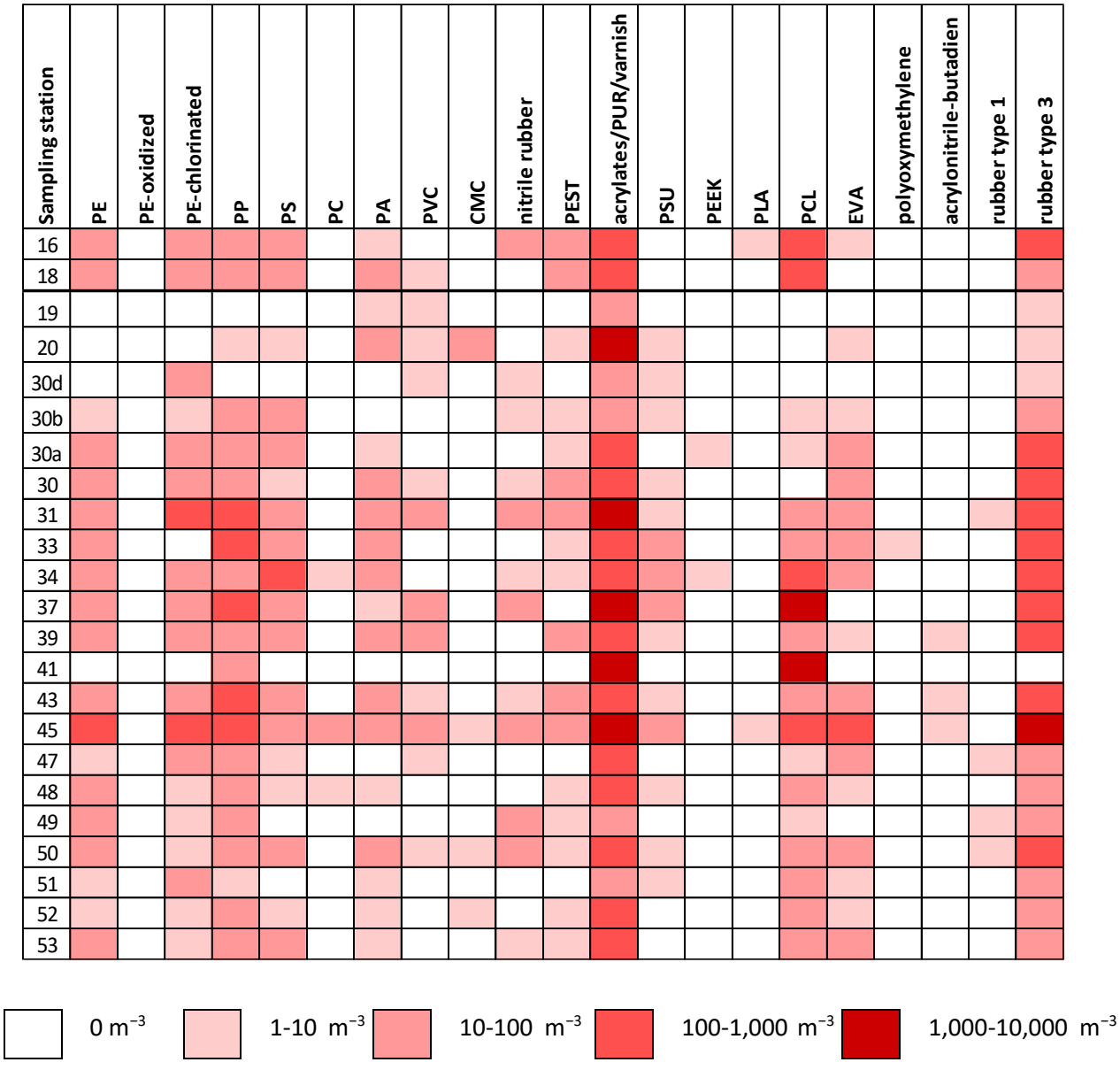

Fig. S2: Heat map showing ranges of estimated S-MP polymer concentrations detected in Lower Weser, Weser estuary and Jade Bay detected by µFTIR

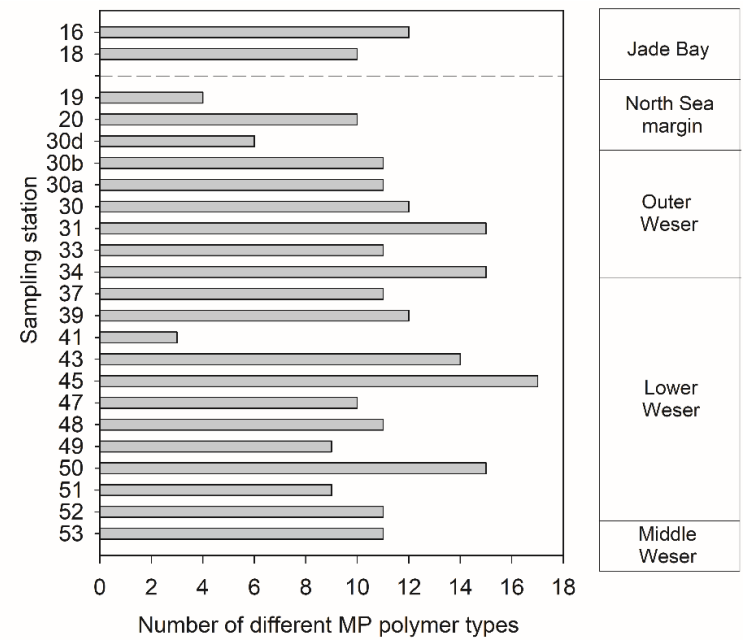

Fig. S3: Polymer diversity displayed as total number of different MP polymer clusters detected in the transitional zone Weser-Wadden Sea (S-MP).

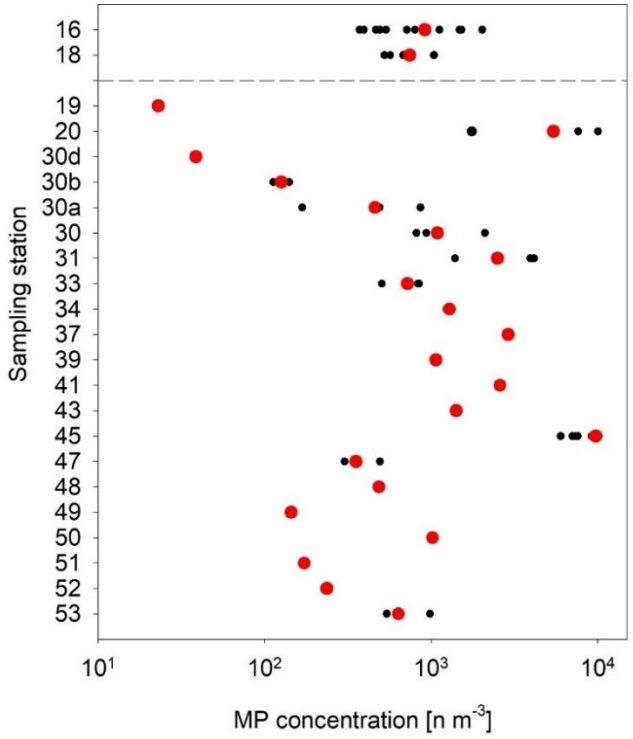

Fig. S4: Estimated S-MP concentrations obtained for the subsamples (black dots) and totalled samples (red dots) of the 23 analysed sampling stations in the transitional zone Weser-Wadden Sea. *) Note: for station 39, 43 and 50 several subsamples were taken, yet data were excluded, as documentation was incomplete (cf. Tab. S 3)

Tab. S4: Overview of subsamples prepared prior to µFTIR measurements, including replicate number, proportion of subsample in relation to totalled sample [%], over- and underestimation with regard to total sample [%] based on estimated MP concentrations (MP conc.) of subsamples, number of polymer types and absence/presence matrix of polymer types detected. Results of totalled samples are depicted in bold letters and originate from the cumulative addition of results obtained for subsamples. Presented are the data referring to samples collected in Jade Bay and North Sea margin. Modified after Abel et al. (2021).

Sampling station	Subsample	Proportion [%]	Over-/ under-estimation [%]	MP conc. [n m^{-3}]	n (polymer types)	PE	PE-chlorinated	PP	PS	PC	PA	PVC	CMC	nitrile rubber	PEST	acrylates/PUR//varnish	PSU	PEEK	PLA	PCL	EVA	polyoxymethylene	acrylonitrile-butadiene	rubber type 1	rubber type 3
16	1/11	8	+62	1481	10	x	x	x	x		x			x	x	x				x					x
	2/11	10	+121	2029	9	x	x	x	x					x		x				x	x				x
	3/11	10	-13	800	5	x		x								x				x					x
	4/11	10	-42	536	5	x	x	x						x		x									
	5/11	10	+66	1520	7		x	x	x							x			x	x					x
	6/11	10	-57	395	6		x	x	x							x				x					x
	7/11	9	-59	371	5		x	x	x							x				x					
	8/11	10	-22	715	8	x	x	x	x						x	x				x					x
	9/11	10	-46	493	7	x	x	x	x		x					x									x
	10/11	10	+22	1123	8		x	x	x		x				x	x				x					x
	11/11	6	-49	466	5			x	x						x	x									x
	Σ	**100**	**-**	**917**	**12**	**x**	**x**	**x**	**x**		**x**			**x**	**x**	**x**			**x**	**x**	**x**				**x**
18	1/7	14	+40	1037	7	x			x		x				x	x				x					x
	2/7	14	-24	568	4				x						x	x				x					
	3/7	14	-29	524	0							x													
	4/7	14	-6	696	6			x	x		x					x				x					x
	5/7	14	-9	679	6		x	x	x		x					x				x					
	6/7	14	-8	687	5	x	x		x							x									x
	7/7	15	+40	1043	6			x	x						x	x				x					x
	Σ	**100**	**-**	**743**	**10**	**x**	**x**	**x**	**x**		**x**	**x**			**x**	**x**				**x**					**x**
19	**1/1**	**100**	**-**	**23**	**4**						**x**	**x**				**x**									**x**
20	1/3	49	-68	1757	5				x		x		x		x	x									
	2/3	24	+41	7641	6			x					x			x	x				x				x
	3/3	27	+85	10051	7			x	x		x	x	x		x	x									
	Σ	**100**	**-**	**5428**	**10**			**x**	**x**		**x**	**x**	**x**		**x**	**x**	**x**				**x**				**x**
30d	**1/1**	**100**	**-**	**39**	**6**		**x**					**x**		**x**		**x**	**x**								**x**

Tab. S4 – continued: Presented are the data referring to samples collected in the Outer Weser.

Sampling station	Subsample	Proportion [%]	Over-/ under-estimation [%]	MP conc. [n m^{-3}]	n (polymer types)	PE	PE-chlorinated	PP	PS	PC	PA	PVC	CMC	nitrile rubber	PEST	acrylates/PUR/varnish	PSU	PEEK	PLA	PCL	EVA	polyoxymethylene	acrylonitrile-butadiene	rubber type 1	rubber type 3
30b	1/3	42	+11	140	7			x	x						x	x				x	x				x
	2/3	38	-11	112	8	x	x	x	x		x			x		x	x								x
	3/3	20	+2	129	5	x		x	x							x									x
	Σ	**100**	-	**126**	**11**	x	x	x	x		x			x	x	x	x			x	x				x
30a	1/3	47	+7	491	6	x	x	x								x					x				x
	2/3	21	+88	863	8		x	x	x		x					x				x	x				x
	3/3	32	-63	168	7	x		x	x						x	x		x							x
	Σ	**100**	-	**459**	**11**	x	x	x	x		x				x	x	x	x		x	x				x
30	1/3	54	-25	817	9	x	x	x	x		x				x	x					x				x
	2/3	27	-14	936	7	x	x	x							x	x					x				x
	3/3	19	+93	2106	12	x	x	x	x		x	x		x	x	x	x				x				x
	Σ	**100**	-	**1091**	**12**	x	x	x	x		x	x		x	x	x	x				x				x
31	1/3	58	-44	1391	10	x	x	x	x			x			x	x				x	x			x	x
	2/3	19	+58	3949	10	x	x	x	x		x			x		x				x	x				x
	3/3	23	+66	4159	12	x	x	x	x		x	x		x	x	x	x			x					x
	Σ	**100**	-	**2505**	**14**	x	x	x	x		x	x		x	x	x	x			x	x			x	x
33	1/4	30	-30	506	10	x		x	x		x				x	x	x			x	x				x
	2/4	29	+18	847	8	x		x	x							x	x				x	x			x
	3/4	29	+16	835	9	x		x	x		x					x	x			x	x				x
	4/4	12	+1	728	4	x		x								x									x
	Σ	**100**	-	**720**	**11**	x		x	x		x				x	x	x			x	x	x			x
34	1/2	63	+4	1335	14	x	x	x	x	x	x			x	x	x	x	x		x	x				x
	2/2	37	-4	1238	9	x	x	x	x						x	x	x			x					x
	Σ	**100**	-	**1289**	**14**	x	x	x	x	x	x			x	x	x	x	x		x	x				x

Tab. S4 – continued: Presented are the data referring to samples collected in the Lower and Middle Weser.

Sampling station	Subsample	Proportion [%]	Over-/ underestimation [%]	MP conc. [n m^{-3}]	n (polymer types)	PE	PE-chlorinated	PP	PS	PC	PA	PVC	CMC	nitrile rubber	PEST	acrylates/PUR/varnish	PSU	PEEK	PLA	PCL	EVA	polyoxymethylene	acrylonitrile-butadiene	rubber type 1	rubber type 3
37	**Σ**	**100**	**-**	**2903**	**11**	**x**	**x**	**x**	**x**		**x**	**x**		**x**		**x**	**x**			**x**					**x**
41	**Σ**	**100**	**-**	**2590**	**3**			**x**								**x**				**x**					
45	1/9	13	+62	1579	12	x	x	x	x		x			x	x	x				x	x		**x**		x
	2/9	14	-28	7051	11	x	x	x	x		x		x		x	x				x	x				x
	3/9	11	-6	9201	10	x	x	x	x	x		x				x				x	x				x
	4/9	11	-1	9673	10	x	x	x	x		x				x	x				x	x				x
	5/9	11	-22	7603	13	x	x	x	x	x	x			x	x	x	x			x	x				x
	6/9	11	-38	6001	9	x	x	x	x	x						x				x	x				x
	7/9	11	+4	1016	10	x	x	x	x						x	x			x	x	x				x
	8/9	11	-25	7315	10	x	x	x	x		x	x				x				x	x				x
	9/9	8	+61	1563	13	x	x	x	x	x		x	x		x	x	x			x	x				x
	Σ	**100**	**-**	**9738**	**17**	**x**	**x**	**x**	**x**	**x**	**x**	**x**	**x**	**x**	**x**	**x**	**x**		**x**	**x**	**x**		**x**		**x**
47	1/2	72	-15	302	10	x	x	x	x			x				x				x	x			x	x
	2/2	28	+39	493	7	x	x	x	x							x					x				x
	Σ	**100**	**-**	**354**	**10**	**x**	**x**	**x**	**x**			**x**				**x**				**x**	**x**			**x**	**x**
48	**Σ**	**100**	**-**	**486**	**12**	**x**	**x**	**x**	**x**	**x**	**x**				**x**	**x**	**x**			**x**	**x**				**x**
49	**Σ**	**100**	**-**	**144**	**9**	**x**	**x**	**x**						**x**	**x**	**x**				**x**				**x**	**x**
51	**Σ**	**100**	**-**	**173**	**9**	**x**	**x**	**x**			**x**					**x**	**x**			**x**	**x**				**x**
52	**Σ**	**100**	**-**	**236**	**11**	**x**	**x**	**x**	**x**		**x**		**x**		**x**	**x**				**x**	**x**				**x**
53	1/2	78	-15	542	8	x	x	x	x							x				x	x				x
	2/2	22	+54	983	9	x		x	x		x			x	x	x				x					x
	Σ	**100**	**-**	**636**	**11**	**x**	**x**	**x**	**x**		**x**			**x**	**x**	**x**				**x**	**x**				**x**

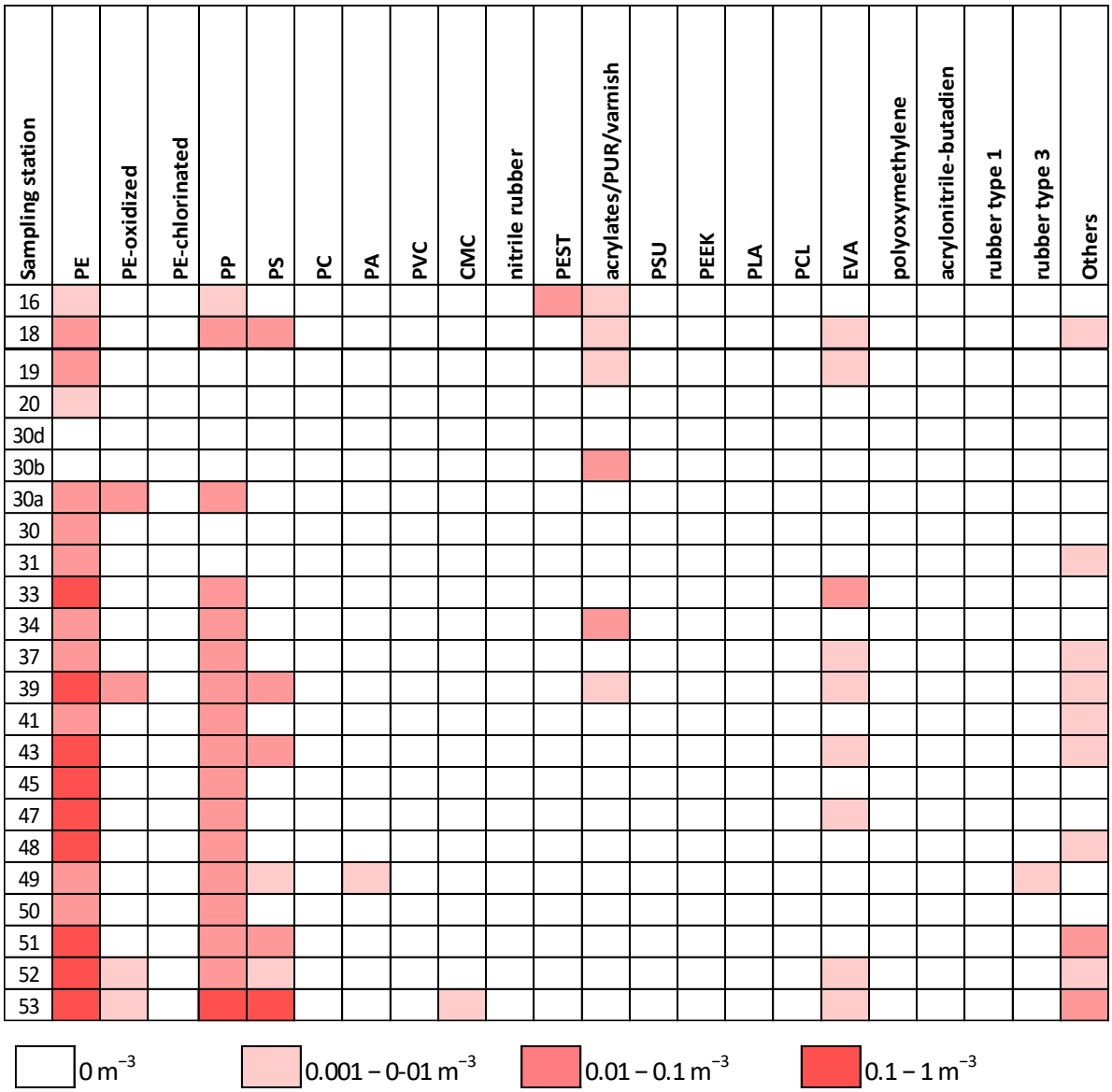

Fig. S5: Heat map showing ranges of estimated L-MP polymer concentrations detected in Lower Weser, Weser estuary and Jade Bay by FTIR-ATR. 'Others' refer to polymer types which were not assignable to the polymer clusters after Primpke et al. (2018)

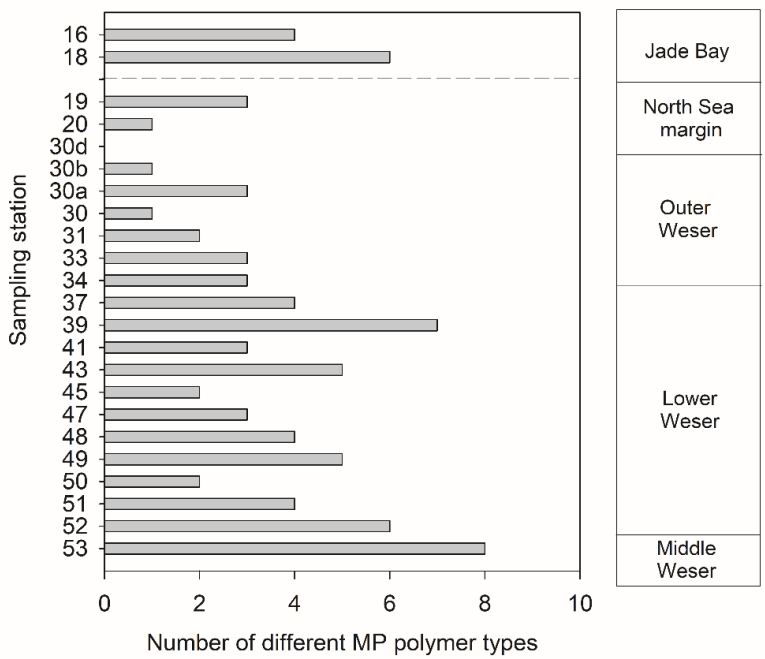

Fig. S6: Polymer diversity displayed as total number of different MP polymer clusters detected in the transitional zone Weser-Wadden Sea (L-MP).

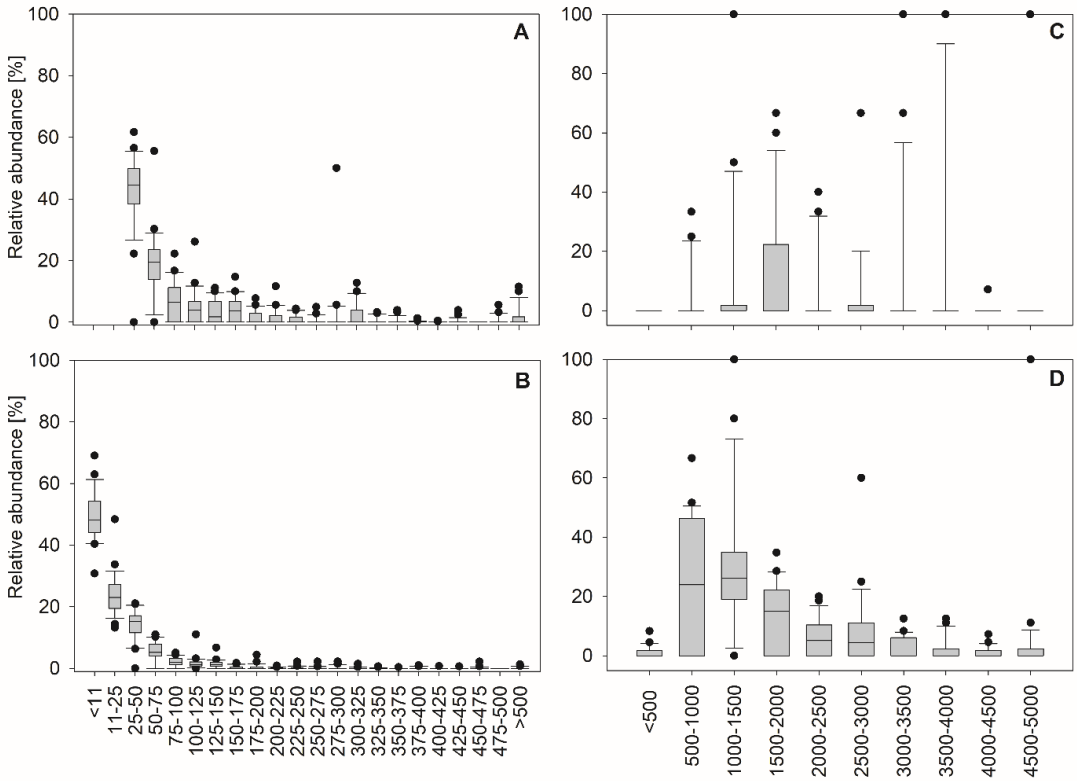

Fig. S7: Size class distribution of MP in the transitional zone Weser-Wadden Sea. Boxplots display variations of relative abundances across sampling stations. A: fibre-like S-MP; B: S-MP particles; C: L-MPlines/filaments; D: L-MP particles

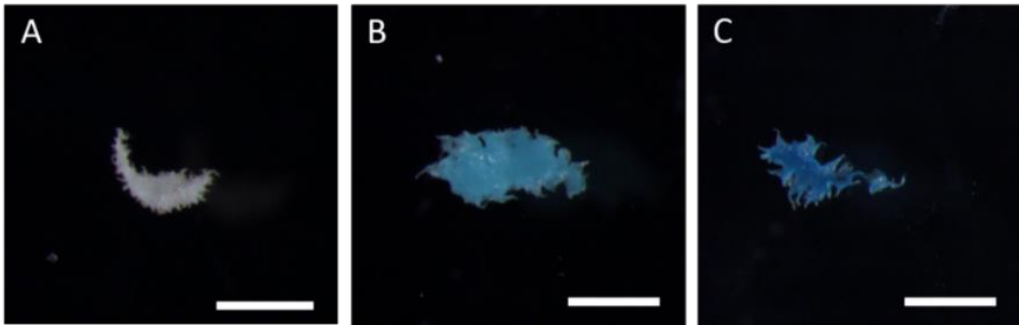

Fig. S8: PE-fragments with characteristic frayed edges, recorded in Lower Weser stations. A: station 43; B: station 41; C: station 48. Dimension of scale bar: 500 µm.

Section S2: Records of plastic items >5000 µm

The majority of plastic items >5000 µm was identified as PP (47.9%), followed by PE (31.3%) and PS (8.3%) (**Fig. S 8**). Fragments were the dominant shape type (45.8%), followed by lines/filaments (35.4%). The majority of fragments were made of PE and PP (68.2%), with the remaining 31.8% comprised of PS, PE-oxidized, EVA, Poly (diallyl phthalate) and PA. Lines/filaments were mainly made from PP (76.5%).

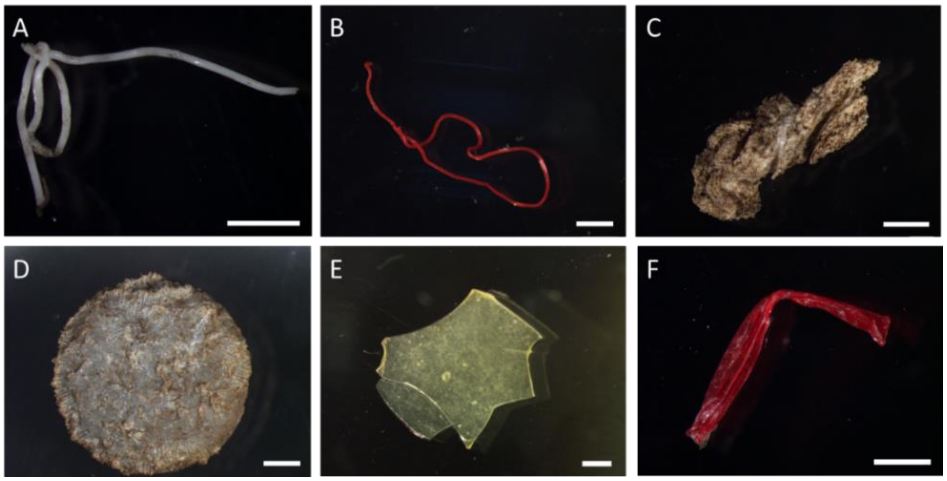

Fig. S9: Plastic items >5000 µm, isolated in sampling stations in the transitional zone Weser-Wadden Sea. A: Line/filament, PP, station 52; B: Line/filament, PP, station 34; C: Foam, PS, station 53; D: Pellet, PE, station 52; E: Fragment, EVA, station 19; F: Film, PE, station 45. Dimension of scale bar: 1 mm

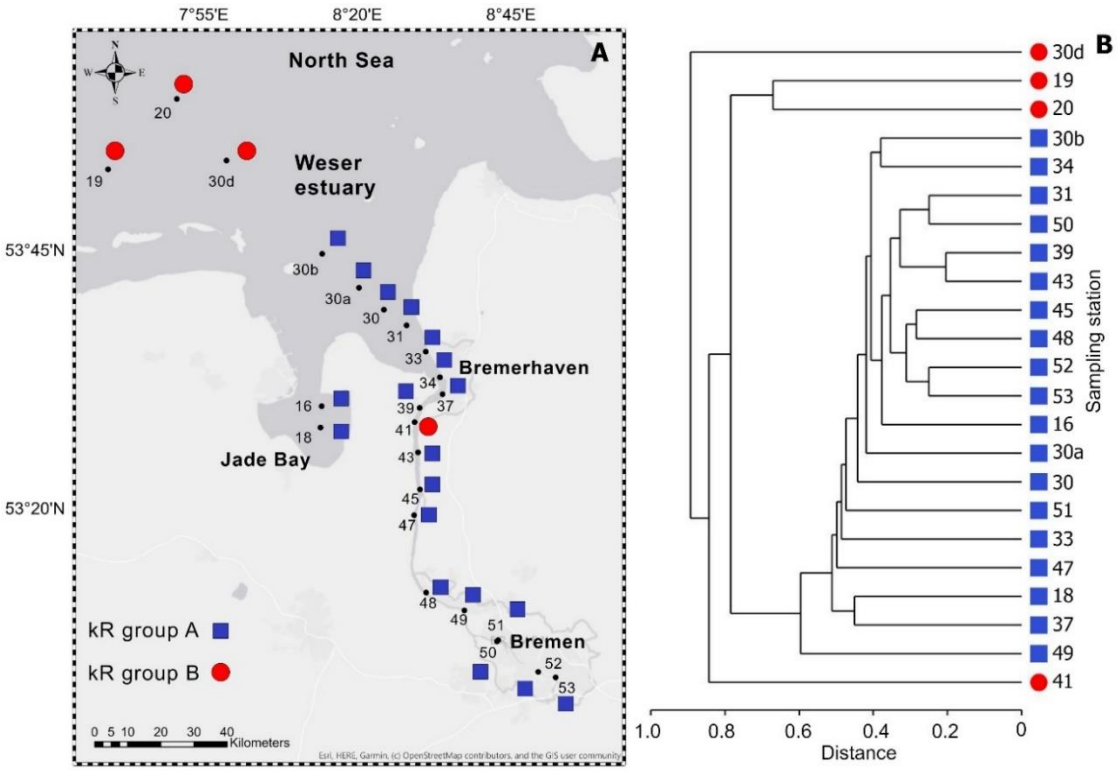

Fig. S10: Results obtained by kR Clustering based on relative abundances of polymer types detected in the transitional zone Weser-Wadden Sea (L-MP and S-MP combined)

Tab. S5: Results of Kolmogorov-Smirnov-Test performed based on kR Cluster analysis (cf. Fig. S10)

	p-value	Mean	Mean	Std.Dev.	Std.Dev.
PE	**< .005 ***	0.04	0.00	0.03	0.00
PE-oxidized	> .10	0.00	0.00	0.00	0.00
PE-chlorinated	< .10	0.03	0.07	0.02	0.15
PP	**< .01 ***	0.09	0.01	0.06	0.01
PS	**< .025 ***	0.04	0.00	0.03	0.00
PC	> .10	0.00	0.00	0.00	0.00
PA	> .10	0.02	0.01	0.02	0.02
PVC	> .10	0.00	0.04	0.01	0.05
CMC	> .10	0.00	0.00	0.00	0.01
nitrile rubber	> .10	0.01	0.01	0.02	0.03
PEST	**< .025 ***	0.01	0.00	0.01	0.00
acrylates/PUR/varnish	> .10	0.49	0.61	0.12	0.29
PSU	> .10	0.01	0.04	0.01	0.09
PEEK	> .10	0.00	0.00	0.00	0.00
PLA	> .10	0.00	0.00	0.00	0.00
PCL	< .10	0.08	0.11	0.10	0.23
EVA	**< .025 ***	0.03	0.00	0.02	0.00
polyoxymethylene	> .10	0.00	0.00	0.00	0.00
acrylonitrile-butadiene	> .10	0.00	0.00	0.00	0.00
rubber type 1	> .10	0.00	0.00	0.01	0.00
rubber type 3	> .10	0.14	0.08	0.07	0.09

Table S6: Overview of microplastic item concentrations [n m^{-3}] in riverine, estuarine and marine surface waters recorded in previous studies, which also applied net sampling as well as pumping systems for sample collection (mostly followed by spectroscopic analysis via FTIR). Abbreviations: N: North, E: East, S: South, W: West.

Location	MP concentration[n m^{-3}]	Sampling Method	Chemical identification	Reference
Lower Weser and S. North Sea (German Bight)	$2.3 \times 10^{1} – 9.7 \times 10^{3}$ $1.0 \times 10^{-2} – 9.8 \times 10^{-1}$	Pumping system (500, 10 µm filters) Microplastic net (300 µm)	µFTIR (10-500 µm) FTIR-ATR (500-5000 µm)	This study
S. North Sea (German Bight)	$1.0 \times 10^{-1} – 2.5 \times 10^{2}$	Neuston net (100 µm)	µFTIR (10-500 µm) FTIR-ATR (500-5000 µm)	Lorenz et al. (2019)
Jade Bay (German Bight)	6.4×10^{4}	Bulk sampling (100 mL PE bottles)	None (Visual identification)	Dubaish and Liebezeit (2013)
Meuse river basin (Denmark)	$6.7 \times 10^{1} – 1.2 \times 10^{4}$	Pumping system with filter stack (300, 100 and 20 µm)	FTIR-ATR (>300 µm) µFTIR (<300 µm)	Mintenig et al. (2020)
Rhine River (Switzerland/Germany)	$0.8 \times 10^{0} – 1.7 \times 10^{1}$	Manta trawl (300 µm)	FTIR-ATR	Mani et al. (2015)
Rhine River and tributaries (Switzerland/Germany)	$4.0 \times 10^{-2} – 1.0 \times 10^{1}$	Manta trawl (300 µm)	FTIR-ATR	Mani and Burkhardt-Holm (2020)
Delaware Bay (NE United States)	$1.9 \times 10^{-1} – 1.2 \times 10^{0}$	Plankton net (200 µm)	FTIR-ATR	Cohen et al. (2019)
Pearl river estuary, (S China)	$6.9 \times 10^{-1} – 8.2 \times 10^{0}$	Manta net (333 µm)	FTIR-ATR	Lam et al. (2020)
Bay of Brest (France)	$1 \times 10^{-2} – 1.4 \times 10^{0}$	Manta net (335 µm)	Raman	Frère et al. (2017)
Jiaojiang, Oujiang and Minjiang Estuaries (SE China)	$1.0 \times 10^{2} – 4.1 \times 10^{3}$	Teflon Pump and 333-µm sieve	Raman	Zhao et al. (2015a)
Various Japanese river systems	$0 – 1.2 \times 10^{1}$	Plankton nets (100, 335 µm)	FTIR	Kataoka et al. (2019)
Marine waters (S Sri Lanka)	$0 – 2.9 \times 10^{1}$	Plankton net (80 µm)	FTIR	Koongolla et al. (2018)

Supplementary Material for Chapter 3

Microplastics in two German Wastewater Treatment Plants: year-long effluent analysis with FTIR and Py-GC/MS

Lisa Roscher*[a], Maurits Halbach*[b], Minh Trang Nguyen[a], Martin Hebeler[c], Franziska Luschtinetz[d], Barbara Scholz-Böttcher[b], Sebastian Primpke[a], Gunnar Gerdts[a]

[a] Alfred Wegener Institute, Helmholtz Centre for Polar and Marine Research, D-27483 Helgoland, Germany

[b] Institute for Chemistry and Biology of the Marine Environment (ICBM), Carl von Ossietzky University of Oldenburg, D-26111 Oldenburg, Germany

[c] hanseWasser Bremen GmbH, D-28217 Bremen, Germany

[d] Kasselwasser, D-34125 Kassel, Germany

* *Shared first-authorship*

Corresponding author: Lisa Roscher (lisa.roscher@awi.de)

Keywords: Spectroscopic analysis, Microplastic pollution, Point source, Aquatic environment, Microplastic masses, Polymer database

Note:

The Supplementary Material of Chapter 3 consists of two parts: Supplementary Data 1, containing graphs and tables presented in the following, and the (electronic) Supplementary Data 2, which contains files in the formats .xlsx, .txt, and .csv (an overview of the Supplementary Data 2 is presented on page 159; the respective data files are stored on the CD submitted with this thesis).

Supplementary Data 1 for Chapter 3

Content

Figures:

Tables:

Tab. S7: Overview of different measurement sequences and accompanied calibrations for Py-GC/MS.

Tab. S8: Polymer mass derived from monthly samplings and sampling blanks at the WWTP in Bremen.

Tab. S9: Results of Mann-Whitney U test applied on MP data generated with initial ('Group 1') and adapted ('Group 2') database (WWTP Bremen).

Tab. S10: Results of Mann-Whitney U test applied on MP data generated with initial ('Group 1') and adapted ('Group 2') database (WWTP Kassel).

Tab. S11: Additional environmental, sampling and WWTPs parameter for Bremen-Seehausen.

Tab. S12: Correlation analysis Bremen-Seehausen – microplastic and basic effluent parameters.

Tab. S13: Additional environmental, sampling and WWTPs parameter for Kassel.

Tab. S14: Correlation analysis Kassel – microplastic and basic effluent parameters.

Tab. S15: MP concentrations in WWTP effluents (Bremen) and adjacent riverine surface water, obtained by FTIR and Pyrolysis-GC/MS analysis.

Sections:

Section S1: SDS, Protease and Cellulase treatments

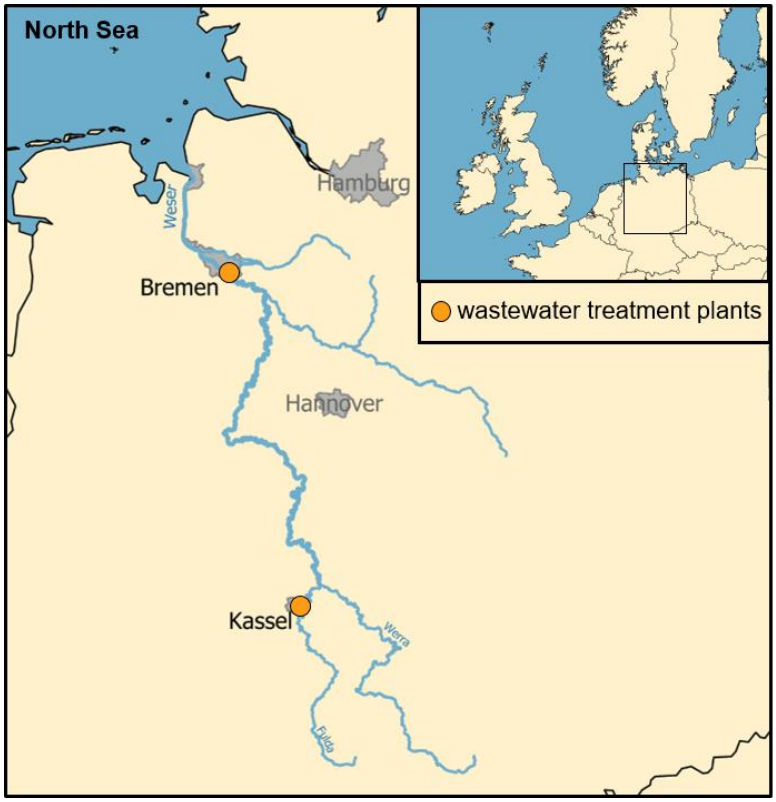

Fig. S1: Location of WWTPs analysed in this study.

Tab. S1: Background information on WWTPs, analyzed for MP occurrence in effluent samples.

	WWTP Bremen-Seehausen	**WWTP Kassel**
Catchment area	39 km²	35 km²
Population equivalent	820,000	340,000 (April 2018)
Daily discharge *)	84,000-207,000 m^3	46,000-113,000 m^3
Maximum retention capacity	270,000 m^3	260,000 m^3
Waste water processing	Primary, secondary, tertiary	Primary, secondary, tertiary
Influx	Domestic (61 %)/ industrial (39 %)	Domestic (78%)/ industrial (22 %)

*)The daily discharge refers to the values recorded during the sampling year.

Tab. S2: Volumes of effluent samples collected in the WWTPs in Kassel and Bremen-Seehausen.

	Sample volume [L]	
Sampling month	**WWTP Bremen-Seehausen**	**WWTP Kassel**
07/2018	207	732
08/2018	256	819
09/2018	282	1000
10/2018	567	1000
11/2018	1000	980
12/2018	340	493
01/2019	249	780
02/2019	136	1000
03/2019	605	536
04/2019	566	1050
05/2019	738	200
06/2019	463	914

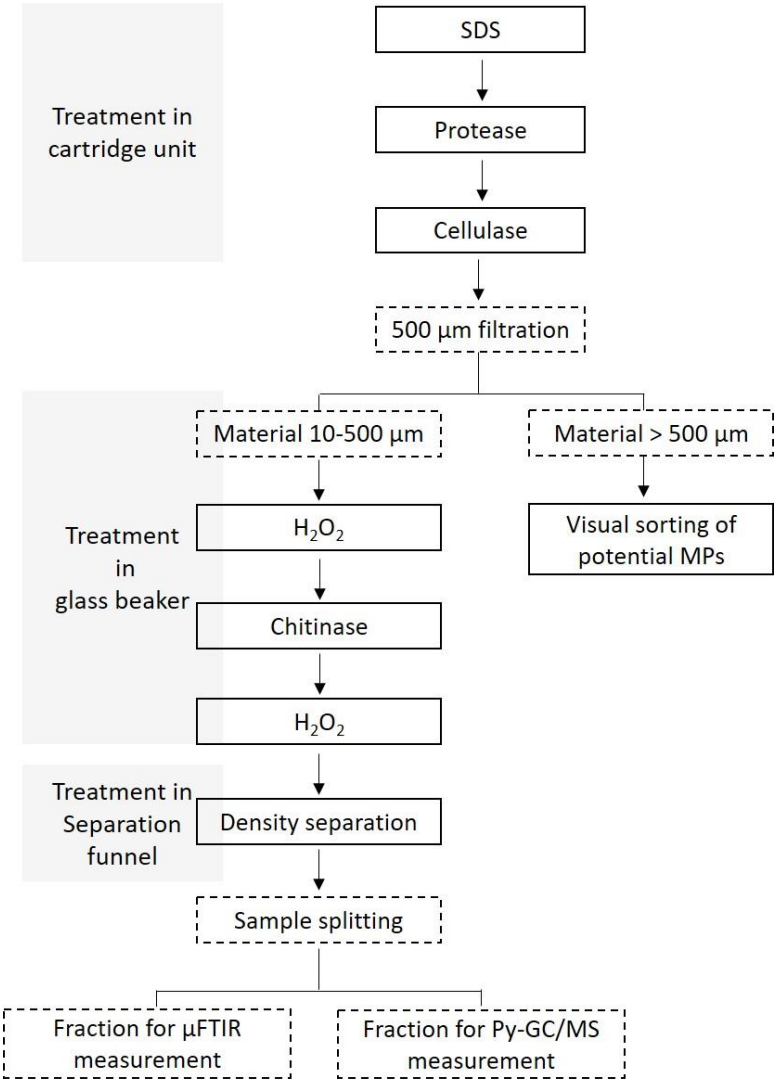

Fig. S2: Workflow of the sample processing applied for the isolation of MP from the sample matrix (cf. section 3.2.3, sample processing).

Section S1: SDS, Protease and Cellulase treatments

SDS, Protease and Cellulase were transferred as independent treatments into the cartidge filter units by use of a glass funnel and a silicone hose (cf. **section 3.2.3**). Incubation took place at 50 °C (SDS, Protease; 24 h each) and 40 °C (Cellulase; three times 24 h). After each treatment step, the treatment solution was removed using compressed air (LABOPORT© diaphragm pump; KNF Neuberger GmbH, Germany), which was pre-filtered through 1 µm polytetrafluoroethylene (PTFE) filter, Merck Millipore, USA). Samples were then rinsed with 5 µm-filtered tap water (stainless-steel filter, Haver&Boecker, Germany) in order to remove any macerated material <10 µm. Compressed air was used again in order to remove the rinsing water.

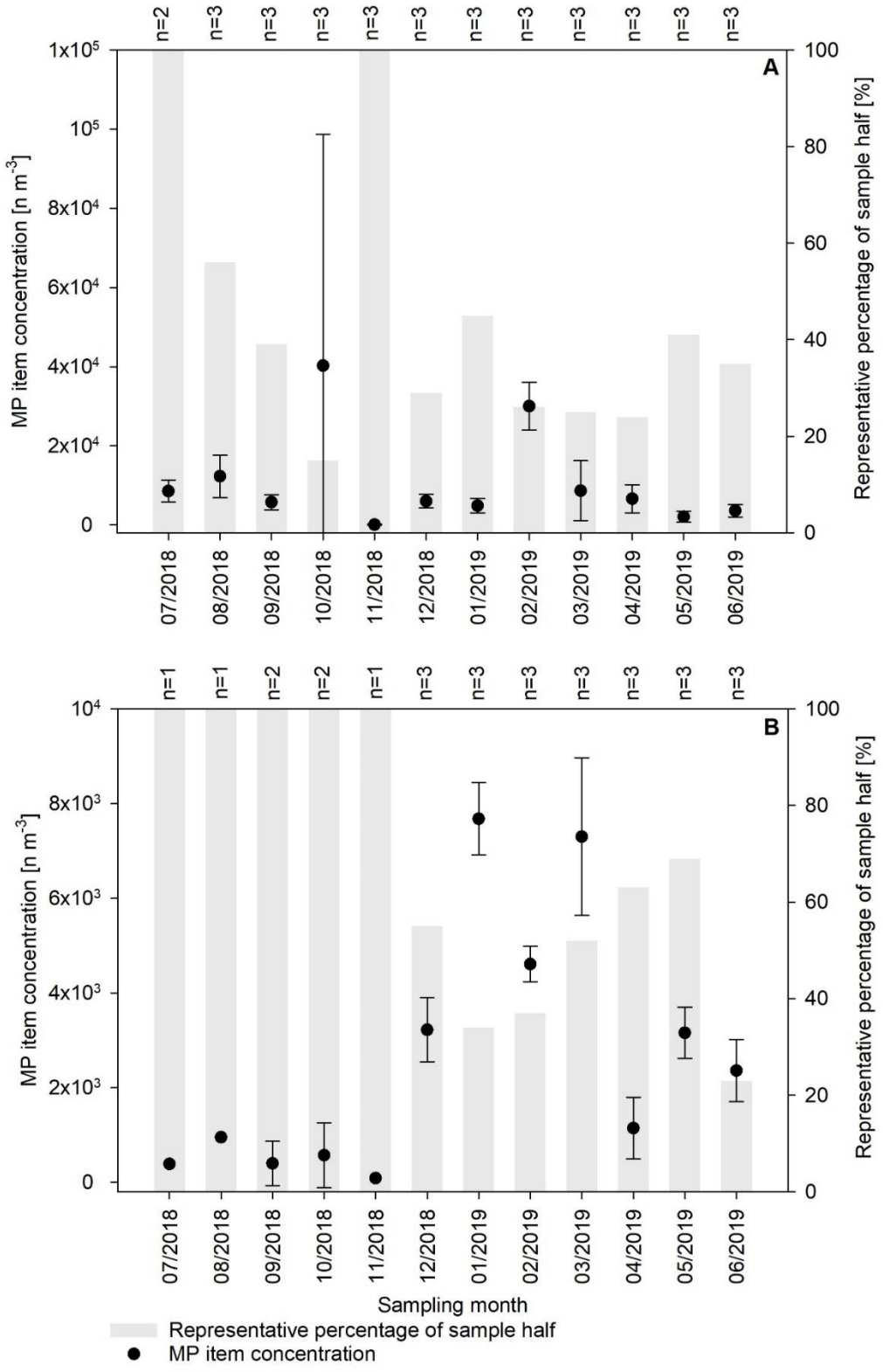

Fig. S3: Variability (Mean and standard deviation) of calculated S-MP item concentrations (left axis), and representative percentage of sample analysed (right axis), displayed for the Bremen-Seehausen (A) and Kassel (B) WWTP. The representative percentages are summed up for the 1-3 aliquots, showing how much of the sample material available for µFTIR was analysed. The number of aliquots analysed per sample is displayed in the upper part of each graph.

Tab. S3: Overview of flocculation agents added to the FTIR database used for the polymer identification of S-MP items (cf. section 3.2.4.3).

Flocculation agent	Manufacturer
NeudosF804	Ochsmann Chemie GmbH
NeudosF805	Ochsmann Chemie GmbH
NeudosF814	Ochsmann Chemie GmbH
Flopam CP 68 U	PolyChemie
CT27x	PolyChemie
CT27T	PolyChemie
CP66U	PolyChemie
CL25 T	PolyChemie

Tab. S4: Injection Standards used for Py-GC/MS measurement.

$ISTD_{PY}$	Injection (µg)
9-tetradecyl-1,2,3,4,5,6,7,8-octahydro cholanic acid	0.5
anthracene (d_{10})	1
polystyrene (d_8)	1

Tab. S5: Conditions for Pyrolysis-GCMS/Thermochemolysis measurements.

Micro furnace pyrolyzer	**EGA/PY-3030D (FrontierLabs)**
carrier gas	Helium
curie temperature	590°C
pyrolysis time	1 min
transfer line temperature	320°C
Gas chromatograph	**7890B (Agilent)**
injector	split/split less
mode	split 15:1
temperature	300°C
pre-column	Trajan P/N 064062; 10 m x 250 µm/ 363 µm VSPD Tubing
column	DB5 (J&W); 30 m x 0.25 mm ID, film thickness 0.25 µm
flow (const.)	1.2 ml/min
temperature program	35°C (2 min) → 310 °C (30 min) at 3°C/min
transfer line temperature	280°C
Mass spectrometer	**MSD 5977A (Agilent)**
ionization energy	70 eV
scan rate	2.48 scans/s
scan range	50-650 amu
EI-Source temperature	230 °C
quadrupole temperature	150 °C

Tab. S6: List of polymers and their respective specific indicator ions.

Polymer	Abbre-viation	Characteristic decomposition product(s)	RI [a]	M	Indicator ions
				(*m/z*)	(*m/z*)
Polyethylene	PE	Alkanes (e.g. C_{20})	2000	282	85
		α-Alkenes (e.g. C_{20})	1994	280	83
		α,ω-Alkenes (e.g. C_{20}**)**	1987	278	**82**
Polypropylene	PP	**2,4-Dimethylhept-1-ene**	832	126	126, **70**
		2,4,6,8-Tetramethyl-1-undecenes[b]	1306	210	100, 69
		2,4,6,8-Tetramethyl-1-undecenes[c]	1315	210	100, 69
		2,4,6,8-Tetramethyl-1-undecenes[d]	1323	210	100, 69
Polystyrene	PS	Styrene	890	104	104
		2,4-Diphenyl-1-butene	1720	208	91
		2,4,6-Triphenyl-1-hexene	2440	312	**91**
Polyvinyl chloride	PVC	**Benzene**	738	78	**78**
		Naphthalene	1187	128	128,102,64
Poly(methyl methacrylate)	PMMA	Methylacrylate	726	86	55
		Methyl methacrylate	775	100	**100**, 69
Polyamide	PA6	**ε-Caprolactam**	1257	113	**113**
		N-methyl caprolactam[e]	1224	127	**127**
Polyethylene terephthalate	PET	**Dimethyl terephthalate**[e]	1504	194	**163**
Polycarbonate	PC	p-Methoxy-tert-butylbenzene[e]	1240	242	164, 149
		2,2-Bis(4'-methoxy-phenyl) propane[e]	2065	256	256**, 241**
MDI-Polyurethane	MDI-PUR	4,4'-Methylenbis(N-methylaniline) [e]	2330	226	226
		N,N-Dimethyl-4-(4-methylamino)benzylanilin[e]	2341	240	240
		4,4'-Methylenbis(N,N-dimethylaniline) [e]	2354	254	253, **254**

[a]RI = Retention index calculated after van Den Dool and Kratz (1963), DB-5 column; M = molecular ion, m/z = mass to charge ratio; [b]Isotactic. [c]Heterotactic. [d]Syndiotactic. [e]Only after TMAH teatment; bold: indicator ions used for calibration

Tab. S7: Overview of different measurement sequences and accompanied calibrations for Py-GC/MS (for abbreviations see Tab. 3.1).

	PE	**PP**	**PET**	**PS**	**PVC**	**PC**	**PMMA**	**PA6**	**PUR**
Sequence 1									
$ISTD_{py}$	TOHA	none	anthracen-d10	TOHA	none	-	TOHA	-	-
b	-6,90E-03	1,44E+05	-3,41E-01	6,82E-01	9,09E+05	-	-1,28E-01	-	-
slope	5,48E-03	9,12E+04	3,60E-01	1,88E+00	8,96E+05	-	2,15E-01	-	-
r^2	0,99	0,97439	0,90983	0,97919	0,91622	-	0,98187	-	-
s_{x0} [µg]	1,28	3,508	1,862	1,264	2,441	-	1,071	-	-
n	9	8	6	10	8	-	10	-	-
Sequence 2									
$ISTD_{py}$	area	area	area	area	area	-	d-PS	-	-
b	-8,89E+04	2,27E+04	-3,08E+06	-2,31E+06	-9,80E+04	-	1,35E-02	-	-
slope	2,08E+04	7,72E+04	1,68E+06	1,71E+06	7,26E+05	-	4,52E-02	-	-
r^2	0,94269	0,97686	0,61621	0,85008	0,87075	-	0,77677	-	-
s_{x0} [µg]	4,517	2,704	4,787	1,731	6,341	-	1,818	-	-
n	7	7	6	6	7	-	7	-	-
Sequence 3									
$ISTD_{py}$	d-PS	TOHA	d-PS	TOHA	d-PS	-	area	-	-
b	0.01753	-8.21E-01	-2.74E+00	-3.15E-01	9.82E+00	-	1.31E+06	-	-
slope	0.00881	1.90E-01	1.64E+00	5.73E-01	4.73E+00	-	6.53E+05	-	-
r^2	0.94022	0.92149	0.96278	0.99296	0.98258	-	0.66061	-	-
s_{x0} [µg]	3.244	4.527	0.734	0.393	2.021	-	5.603	-	-
n	8	7	5	6	6	-	8	-	-
Sequence 4									
$ISTD_{py}$	d-PS	d-PS	d-PS	d-PS	d-PS	-	d-PS	-	-
b	2.78E-04	5.68E-03	-1.74E-02	-1.04E-01	1.51E-01	-	1.35E-02	-	-
slope	-6.45E-04	4.18E-03	3.36E-02	8.44E-02	8.75E-02	-	4.52E-02	-	-
r^2	0.8574	0.91835	0.8964	0.89081	0.81592	-	0.77677	-	-
s_{x0} [µg]	5.9	5.0	4.453	2.903	3.465	-	1.818	-	-
n	8	9	4	9	7	-	7	-	-

Tab. S8: Polymer masses derived from monthly samplings and sampling blanks at the WWTP in Bremen (for abbreviations see Tab. 3.1).

	PE	PP	PET	PS	PVC	PC	PMMA	PA6	PUR	MP total	Sample volume [1)]
	[µg]	[µg]	[µg]	[µg]	[µg]	[µg]	[µg]	[µg]	[µg]	[µg]	[L]
07/2018	76.6	74.3	25.5	22.9	9.8	-	6.5	-	-	215.6	104
08/2018	126.7	57.6	15.6	5.3	13.4	-	0.0	-	-	218.6	128
09/2018	116.6	51.0	48.0	5.6	6.0	-	2.0	-	-	229.2	141
10/2018	152.0	139.7	26.1	3.3	22.0	-	0.0	-	-	343.1	284
11/2018	123.8	12.9	4.7	0.7	6.3	-	0.0	-	-	148.4	500
12/2018	233.6	53.6	39.1	2.5	25.2	-	4.1	-	-	358.1	170
01/2019	86.9	65.0	58.3	3.2	10.2	-	4.8	-	-	228.4	125
02/2019	196.0	5.2	29.7	12.9	22.6	-	2.0	-	-	268.4	68
03/2019	481.9	99.2	230.8	0.0	32.2	-	6.0	-	-	850.1	303
04/2019	322.3	73.8	199.7	16.4	17.7	-	2.1	-	-	632	283
05/2019	226.3	74.4	153.1	3.8	16.3	-	6.6	-	-	480.5	369
06/2019	306.8	81.4	242.6	4.6	51.5	-	1.4	-	-	688.3	232
BL1	0.0	14.8	3.2	1.4	1.9	-	0.1	-	-	21.4	
BL2	0.0	4.4	2.0	1.20	0.2	-	0.0	-	-	7.8	

[1)] Refers to representative sample volume for Py-GC/MS, which takes into account that digested samples were split in half.

Tab. S9: Results of Mann-Whitney U test applied on MP data generated with initial ('Group 1') and adapted ('Group 2') database (Bremen-Seehausen WWTP; cf. section 3.3.1). Polymer clusters with significantly different ($p<0.05$) concentrations after database adaptation are marked in red (for abbreviations of polymers see Tab. 3.1).

Harmonised polymer clusters / underlying FTIR clusters	Rank Sum Group 1	Rank Sum Group 2	U	Z	p-value	Z adjusted	p-value	exact p 2*1sided
h-PE	165.0000	88.0000	22.0000	2.4953	0.0126	2.4953	0.0126	0.0104
PE	131.0000	122.0000	56.0000	0.2627	0.7928	0.2627	0.7928	0.7969
PE oxidized	147.0000	106.0000	40.0000	1.3133	0.1891	1.6733	0.0943	0.1932
rubber type 3	155.0000	98.0000	32.0000	1.8386	0.0660	1.8386	0.0660	0.0652
EVA	179.0000	74.0000	8.0000	3.4146	0.0006	3.4184	0.0006	0.0002
h-PP	134.5000	118.5000	52.5000	0.4925	0.6224	0.4926	0.6223	0.6063
PP	134.5000	118.5000	52.5000	0.4925	0.6224	0.4926	0.6223	0.6063
h-PET	130.5000	122.5000	56.5000	0.2298	0.8182	0.2300	0.8181	0.7969
PEST	130.5000	122.5000	56.5000	0.2298	0.8182	0.2300	0.8181	0.7969
h-PS	122.0000	131.0000	56.0000	-0.2627	0.7928	-0.2627	0.7928	0.7969
PS	122.0000	131.0000	56.0000	-0.2627	0.7928	-0.2627	0.7928	0.7969
h-PVC	173.0000	80.0000	14.0000	3.0206	0.0025	3.0206	0.0025	0.0014
PE-chlorinated	178.0000	75.0000	9.0000	3.3489	0.0008	3.3527	0.0008	0.0003
PVC	126.5000	126.5000	60.5000	-0.0328	0.9738	-0.0419	0.9666	1.0000
polychloroprene	122.0000	131.0000	56.0000	-0.2627	0.7928	-0.2695	0.7875	0.7969
h-PUR/PMMA	174.0000	79.0000	13.0000	3.0863	0.0020	3.0863	0.0020	0.0010
acrylates/PUR/ varnish	174.0000	79.0000	13.0000	3.0863	0.0020	3.0863	0.0020	0.0010
h-PA	132.0000	121.0000	55.0000	0.3283	0.7427	0.3285	0.7425	0.7477
PA	132.0000	121.0000	55.0000	0.3283	0.7427	0.3285	0.7425	0.7477
others	154.0000	99.0000	33.0000	1.7730	0.0762	1.7730	0.0762	0.0759
CMC	126.0000	127.0000	60.0000	0.0000	1.0000	0.0000	1.0000	1.0000
nitrile rubber	126.5000	126.5000	60.5000	0.0328	0.9738	0.0381	0.9696	1.0000
PSU	127.0000	126.0000	60.0000	0.0000	1.0000	0.0000	1.0000	1.0000
PEEK	126.5000	126.5000	60.5000	-0.0328	0.9738	-0.0659	0.9475	1.0000
PLA	125.5000	127.5000	59.5000	-0.0328	0.9738	-0.0419	0.9666	0.9487
PCL	168.5000	84.5000	18.5000	2.7251	0.0064	2.7259	0.0064	0.0041
POM	126.5000	126.5000	60.5000	-0.0328	0.9738	-0.0489	0.9610	1.0000
acrylonitrile-butadiene	128.5000	124.5000	58.5000	0.0985	0.9215	0.1011	0.9195	0.8977
rubber type 1	136.5000	116.5000	50.5000	0.6238	0.5327	0.7001	0.4839	0.5190
Total MP	168.0000	85.0000	19.0000	2.6923	0.0071	2.6923	0.0071	0.0052

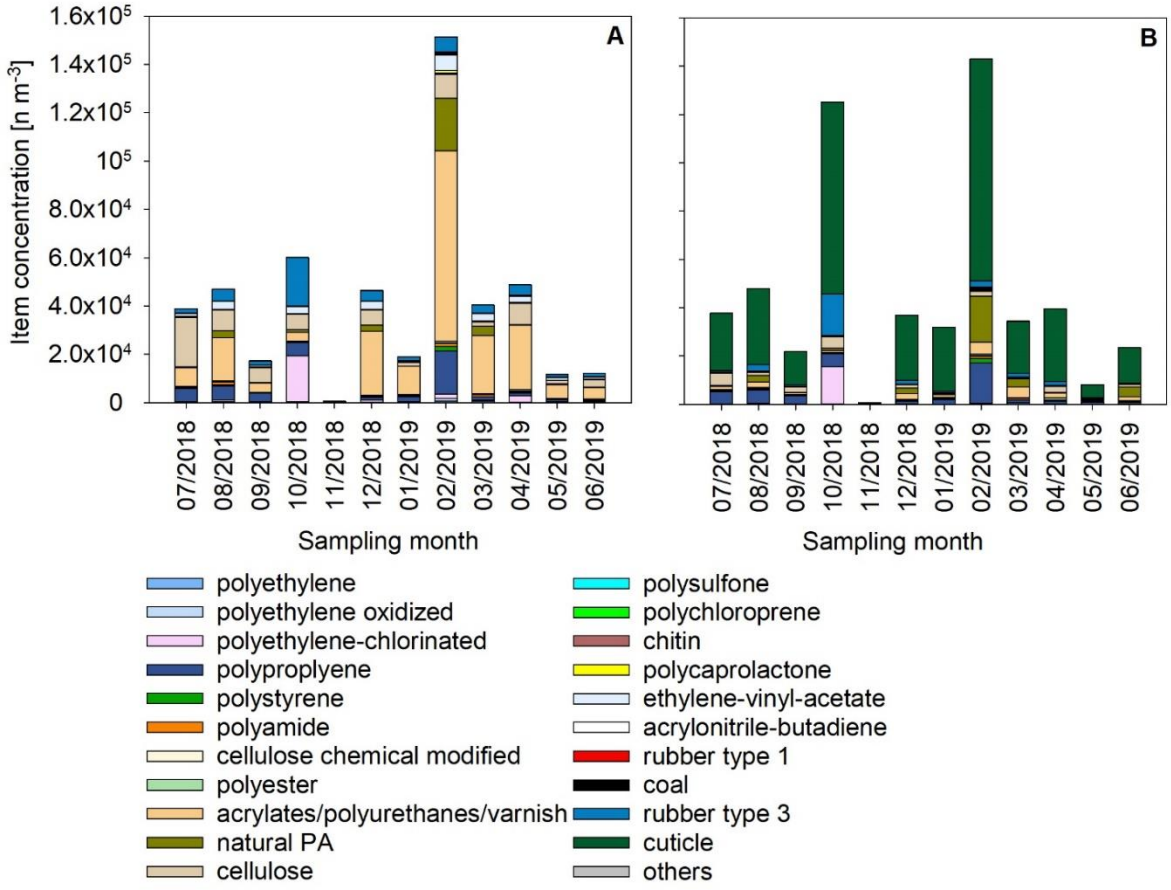

Fig. S4: Assignments to µFTIR clusters after initial database run (A) and re-analysis with adapted database (B), exemplarily shown for the Bremen-Seehausen WWTP (cf. section 3.3.1).

Tab. S10: Results of Mann-Whitney U test applied on MP data generated with initial ('Group 1') and adapted ('Group 2') database (Kassel WWTP; cf. section 3.1). Polymer types with significantly different ($p<0.05$) concentrations after database adaptation are marked in red (for abbreviations of polymers see Tab. 3.1).

Harmonised polymer clusters / underlying FTIR clusters	Rank Sum Group 1	Rank Sum Group 2	U	Z	p-value	Z adjusted	p-value	exact p 2*1sided
h-PE	175.0000	125.0000	47.0000	1.4145	0.1572	1.4145	0.1572	0.1600
PE	156.5000	143.5000	65.5000	0.3464	0.7290	0.3474	0.7283	0.7125
PE oxidized	162.0000	138.0000	60.0000	0.6640	0.5067	1.3844	0.1662	0.5137
rubber type 3	171.0000	129.0000	51.0000	1.1836	0.2366	1.1836	0.2366	0.2415
EVA	192.0000	108.0000	30.0000	2.3960	0.0166	2.4257	0.0153	0.0145
h-PP	153.0000	147.0000	69.0000	0.1443	0.8852	0.1443	0.8852	0.8874
PP	153.0000	147.0000	69.0000	0.1443	0.8852	0.1443	0.8852	0.8874
h-PET	158.5000	141.5000	63.5000	0.4619	0.6442	0.4622	0.6440	0.6297
PEST	158.5000	141.5000	63.5000	0.4619	0.6442	0.4622	0.6440	0.6297
h-PS	151.0000	149.0000	71.0000	0.0289	0.9770	0.0289	0.9770	0.9774
PS	151.0000	149.0000	71.0000	0.0289	0.9770	0.0289	0.9770	0.9774
h-PVC	188.5000	111.5000	33.5000	2.1939	0.0282	2.2040	0.0275	0.0242
PE-chlorinated	189.0000	111.0000	33.0000	2.2228	0.0262	2.2645	0.0235	0.0242
PVC	143.0000	157.0000	65.0000	-0.3753	0.7075	-0.4095	0.6822	0.7125
polychloroprene	157.0000	143.0000	65.0000	0.3753	0.7075	0.5284	0.5972	0.7125
h-PUR/PMMA	173.0000	127.0000	49.0000	1.2990	0.1939	1.2990	0.1939	0.1978
acrylates/PUR/ varnish	173.0000	127.0000	49.0000	1.2990	0.1939	1.2990	0.1939	0.1978
h-PA	156.0000	144.0000	66.0000	0.3175	0.7508	0.3180	0.7505	0.7553
PA	156.0000	144.0000	66.0000	0.3175	0.7508	0.3180	0.7505	0.7553
others	158.5000	141.5000	63.5000	0.4619	0.6442	0.4622	0.6440	0.6297
PC	157.0000	143.0000	65.0000	0.3753	0.7075	0.5289	0.5969	0.7125
CMC	151.0000	149.0000	71.0000	0.0289	0.9770	0.0309	0.9754	0.9774
nitrile rubber	152.0000	148.0000	70.0000	0.0866	0.9310	0.1139	0.9093	0.9323
polysulfone	150.5000	149.5000	71.5000	0.0000	1.0000	0.0000	1.0000	0.9774
PEEK	156.0000	144.0000	66.0000	0.3175	0.7508	0.9167	0.3593	0.7553
PLA	149.5000	150.5000	71.5000	0.0000	1.0000	0.0000	1.0000	0.9774
PCL	172.5000	127.5000	49.5000	1.2702	0.2040	1.2760	0.2020	0.1978
POM	149.5000	150.5000	71.5000	0.0000	1.0000	0.0000	1.0000	0.9774
acrylonitrile-butadiene rubber type 1	161.5000	138.5000	60.5000	0.6351	0.5254	0.6434	0.5200	0.5137
	152.5000	147.5000	69.5000	0.1155	0.9081	0.1518	0.8794	0.8874
Total MP	170.0000	130.0000	52.0000	1.1258	0.2602	1.1258	0.2602	0.2657

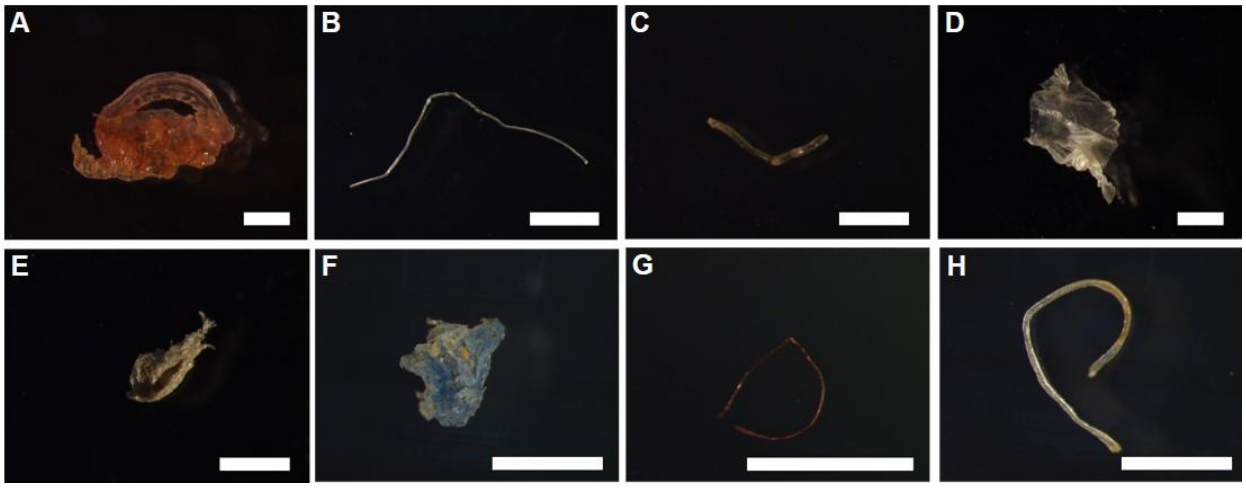

Fig. S5: L-MP items recorded in the effluent samples from Bremen-Seehausen (A-E) and Kassel (F-H). A: PE, fragment. B: PP, fibre. C: PP, line/filament. D: PE, film. E: PS, foam. F: PE, fragment. G: PEST, fibre. H: PP, line/filament. Dimension of scale bar: 1 mm

Tab. S11: Additional environmental, sampling and WWTPs parameter for Bremen-Seehausen. TOC=total organic carbon, SPM=suspended particulate matter, COD=chemical oxygen demand, BOD=biological oxygen demand.

Sampling date	Weather	TOC [mg/L]	SPM [mg/L]	COD [mg/L]	BOD [mg/L]	Turbidity - 3h average	Effluent discharge - 3 h average [m^3/h]	Effluent discharge [m^3/d]
17/07/18	Dry	17.5	11	59	n.a.	4.8	2933	86,700
14/08/18	Rain	16.4	7	49	n.a.	2.7	5110	141,200
11/09/18	Dry	17.8	7	52	n.a.	1.7	3113	84,200
09/10/18	Dry	17.9	8	57	n.a.	2.7	2861	85,800
08/11/18	Dry	20.6	8	58	n.a.	2.6	2331	89,000
05/12/18	Rain drainage	15.1	7	42	n.a.	8.8	2768	92,300
03/01/19	Rain drainage	18.5	6	55	n.a.	2.4	2740	88,700
07/02/19	Rain	23.3	13	60	n.a.	4.6	8178	207,400
07/03/19	Rain	16.9	8	53	n.a.	2.8	2550	106,400
09/04/19	Dry	17.7	5	48	n.a.	6.4	2433	102,800
09/05/19	Rain drainage	19.4	8	50	n.a.	3.0	7816	171,600
04/06/19	Rain	22.5	14	64	n.a.	3.0	4099	110,100

Colouring intensity indicates relative parameter level.

Tab. S12: Correlation analysis Bremen-Seehausen – microplastic and basic effluent parameters. TOC=total organic carbon, SPM=suspended particulate matter, COD=chemical oxygen demand.

Bremen-Seehausen - Kendall-Tau-b - correlation														
		MP item concentration						MP mass concentration						
		Total	h-PE	h-PP	h-PET	h-PS	h-PUR/PMMA	Total	h-PE	h-PP	h-PET	h-PS	h-PUR/PMMA	h-PVC
TOC	τ	-	-	-	-	-	-	-	-	-	0.121	-	-	-
	p	0.114	0.075	0.493	0.583	0.337	0.131	0.784	0.337	0.273	0.583	0.681	0.729	0.493
	n	12	12	12	12	12	12	12	12	12	12	12	12	12
SPM	τ	0.033	-	0.016	-	0.016	0.049	0.114	0.082	-	0.049	-	0.050	0.310
	p	0.887	0.621	0.944	0.525	0.944	0.832	0.621	0.724	0.724	0.832	0.621	0.831	0.179
	n	12	12	12	12	12	12	12	12	12	12	12	12	12
COD	τ	-	-	0.061	-	0.000	-	0.091	-	0.091	0.091	0.000	0.078	0.121
	p	0.945	0.273	0.784	0.493	1.000	0.784	0.681	0.583	0.681	0.681	1.000	0.729	0.583
	n	12	12	12	12	12	12	12	12	12	12	12	12	12
Turbidity [1]	τ	0.015	0.212	-	0.424	0.212	0.394	0.424	0.394	-	0.182	0.212	0.264	0.394
	p	0.945	0.337	0.891	0.055	0.337	0.075	0.055	0.075	0.411	0.411	0.337	0.240	0.075
	n	12	12	12	12	12	12	12	12	12	12	12	12	12
Effluent volume[1]	τ	0.137	0.000	0.364	0.152	0.303	0.121	0.091	0.182	0.030	0.091	0.242	0.109	0.303
	p	0.536	1.000	0.100	0.493	0.170	0.583	0.681	0.411	0.891	0.681	0.273	0.628	0.170
	n	12	12	12	12	12	12	12	12	12	12	12	12	12

* $p < 0.05$
** $p < 0.01$

[1]average over 3 hours

Tab. S13: Additional environmental, sampling and WWTPs parameter for Kassel. TOC=total organic carbon, SPM=suspended particulate matter, COD=chemical oxygen demand, BOD=biological oxygen demand.

Sampling date	Weather	TOC [mg/L]	SPM [mg/L]	COD [mg/L]	BOD [mg/L]	Turbidity - 3h average	Effluent discharge - 3 h average [m³/h]	Effluent discharge [m³/d]
18.07.2018	Dry	n.a.	3	34	<5	1.7	1583	47,424
15.08.2018	Dry	n.a.	1	23	<5	6.1	1921	49,412
20.09.2018	Dry	n.a.	19	39	<5	2.2	2233	46,270
19.10.2018	Dry	n.a.	19	27	<5	3.8	1428	46,270
19.11.2018	Rain	n.a.	3	23	<5	3.7	2022	63,023
19.12.2018	Rain	n.a.	10	35	<5	9.5	2313	51,330
22.01.2019	Dry	n.a.	9	38	5.4	11.2	2064	58,997
18.02.2019	Dry	n.a.	5	30	<5	10.3	2205	60,890
18.03.2019	Rain drainage	n.a.	4	26	8.9	16.9	4577	112,730
17.04.2019	Dry	n.a.	1	34	<5	2.4	2397	56,413
27.05.2019	Rain	n.a.	1	37	<5	3.5	3611	98,037
24.06.2019	Dry	n.a.	1	40	5.1	2.8	2649	57,549

Colouring intensity indicates relative parameter level.

Tab. S14: Correlation analysis Kassel – microplastic and basic effluent parameters. TOC=total organic carbon, SPM=suspended particulate matter, COD=chemical oxygen demand.

Kassel - Kendall-Tau-b - correlation								
		MP item concentration						
		Total	**h-PE**	**h-PP**	**h-PS**	**h-PVC**	**h-PET**	**h-PUR/PMMA**
SPM	τ	-0.032	0.033	-0.097	-0.162	0.055	-0.097	-0.097
	p	0.888	0.888	0.673	0.482	0.821	0.673	0.673
	n	12	12	12	12	12	12	12
COD	τ	0.185	0.109	0.277	0.308	0.018	0.062	0.031
	p	0.408	0.629	0.215	0.168	0.941	0.783	0.890
	n	12	12	12	12	12	12	12
Turbidity[1]	τ	0.545*	0.565*	0.455*	0.364	0.396	0.455*	0.515*
	p	0.014	0.011	0.040	0.100	0.090	0.040	0.020
	n	12	12	12	12	12	12	12
Effluent volume[1]	τ	0.394	0.351	0.485*	0.455*	-0.052	0.485*	0.485*
	p	0.075	0.114	0.028	0.040	0.825	0.028	0.028
	n	12	12	12	12	12	12	12
* p < 0.05								
** p < 0.01								

[1]average over 3 hours

Tab. S15: MP concentrations in WWTP effluents (Bremen) and adjacent riverine surface water, obtained by FTIR and Pyrolysis-GC/MS analysis.

	MP item concentration [n m^{-3}]		**MP mass concentration [µg m^{-3}]**
	S-MP	**L-MP**	**S-MP**
Effluent [1)]	**8.0×10^3** ± 3.3×10^3	**28.8×10^0** ± 20.9×10^0	**2.0×10^3** ± 0.9×10^3
River Weser, upstream [2)]	0.2×10^3	0.3×10^0	1.6×10^1
River Weser, downstream [2)]	1×10^3	0.1×10^0	1.6×10^2

1) MP concentrations averaged over sampling year (July 2018−June 2019); assessed in this study

2) Sampling stations investigated in Roscher et al. (2021) and Halbach et al. in prep.

A

	Sampling station	h-PE	h-PP	h-PS	h-PA	h-PVC	h-PEST	h-PMMA/PUR	others
up-stream	53 *)	present	present	present	present	present	present	present	present
	52	present	present	present	present	present	present	present	present
	51	present	present	absent	present	present	absent	present	present
	WWTP averaged	present	present	present	present	present	present	present	present
down-stream	50	present	present	present	present	present	present	present	present
	49	present	present	absent	absent	present	present	present	present
	48	present	present	present	present	present	present	present	present

B

		h-PE	h-PP	h-PS	h-PVC	Others
up-stream	53 *)	present	present	present	absent	present
	52	present	present	present	absent	present
	51	present	present	present	absent	present
	WWTP averaged	present	present	present	present	present
down-stream	50	present	present	absent	absent	absent
	49	present	present	present	absent	absent
	48	present	present	absent	absent	present

absent present

Fig. S6: Absence/presence matrix of polymer types (A: S-MP, B: L-MP) detected in the Bremen-Seehausen WWTP (effluent; this study) and adjacent surface water stations (for comparison, polymer types recorded in Roscher et al. (2021) were clustered according to Tab. 3.1). *) Station 53 is situated upstream of the Weser weir.

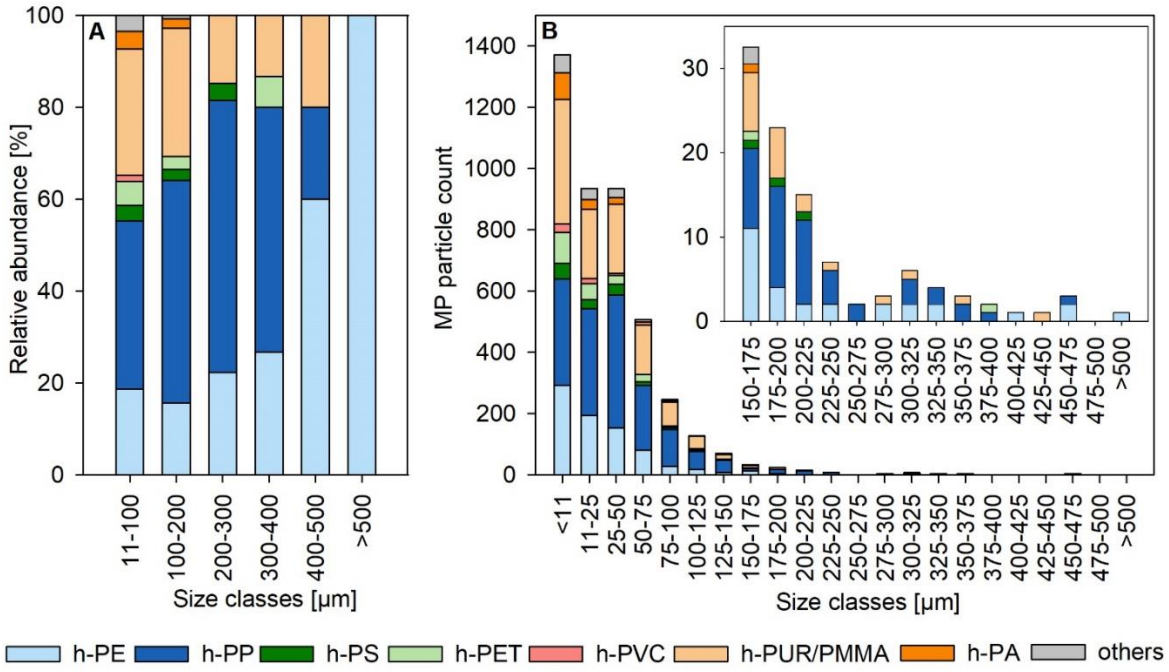

Fig. S7: A: Relative abundance of polymer types within combined S-MP size classes. B: Total MP particle counts displayed for detected polymers, presented individually for S-MP size classes (Bremen-Seehausen WWTP) (for abbreviations of harmonised polymer clusters see Tab. 3.1).

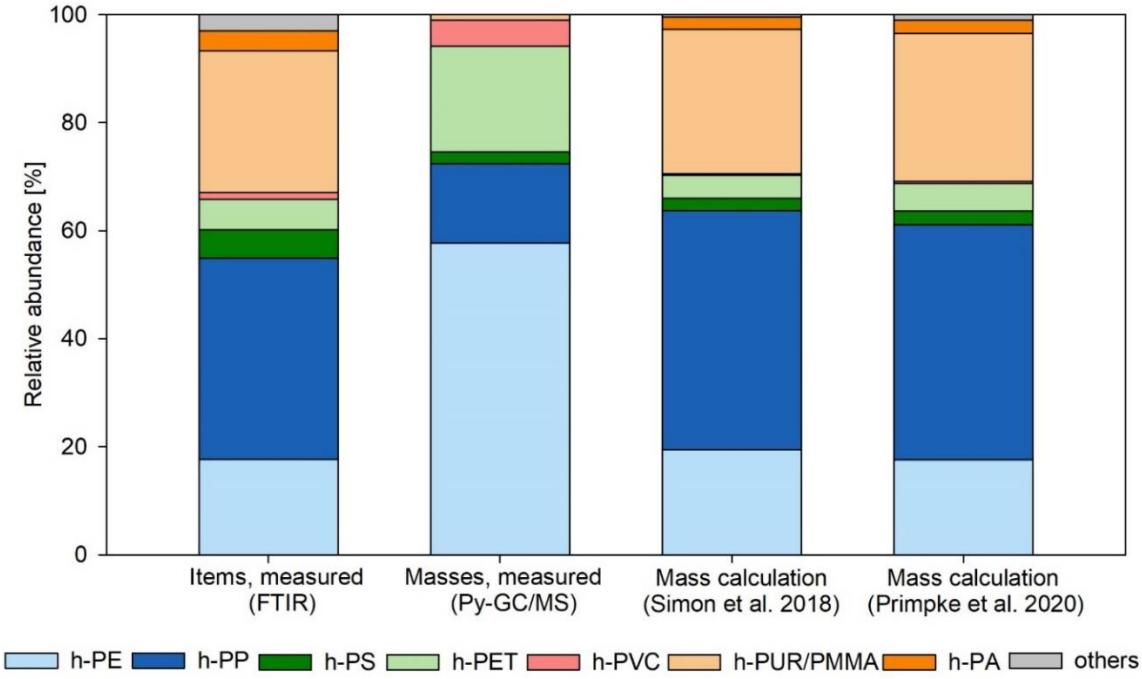

Fig. S8: Averaged polymer compositions for measured MP items and masses, as well as item-based mass calculations following and Simon et al. (2018) and Primpke et al. (2020) (Bremen-Seehausen) (for abbreviations of harmonised polymer clusters see Tab. 3.1).

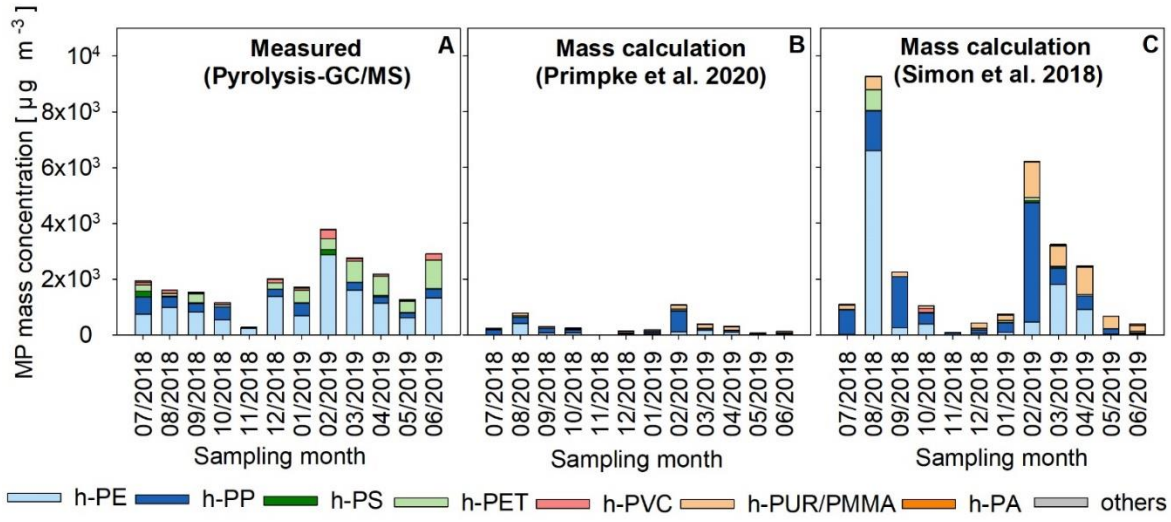

Fig. S9: Measured and calculated mass concentrations over the year, assessed for the WWTP in Bremen-Seehausen (for abbreviations of harmonised polymer clusters see Tab. 3.1).

Supplementary Data 2 for Chapter 3

Content

Excel-Files:

Supplementary Data 2.1.xlsx:
(S-MP) Blank-correction and extrapolation of S-MP fibres based on µFTIR measurements of aliquots (WWTP Bremen-Seehausen)

Supplementary Data 2.2.xlsx:
(S-MP) Blank-correction and extrapolation of S-MP particles based on µFTIR measurements of aliquots (WWTP Bremen-Seehausen).

Supplementary Data 2.3.xlsx:
(S-MP) Addition of fibres+particles and harmonisation of polymer clusters (WWTP Bremen-Seehausen).

Supplementary Data 2.4.xlsx:
(S-MP) Blank-correction and extrapolation of S-MP fibres based on µFTIR measurements of aliquots (WWTP Kassel).

Supplementary Data 2.5.xlsx:
(S-MP) Blank-correction and extrapolation of S-MP particles based on µFTIR measurements of aliquots (WWTP Kassel).

Supplementary Data 2.6.xlsx:
(S-MP) Addition of fibres+particles and harmonisation of polymer clusters (WWTP Kassel).

Supplementary Data 2.7.xlsx:
(L-MP) MP Data (Fibres and Particles) for WWTP Bremen-Seehausen and Kassel

Further files:

siMPle_database_WWTP.txt:
Adapted polymer database, used for S-MP analysis

threshold_and_metadata.csv:
Adapted spectral thresholds, used for S-MP analysis

Supplementary Material for Chapter 4

Comparison of two rapid automated analysis tools for large FTIR microplastic data sets

Sonya Moses[a]*, Lisa Roscher[b]*, Sebastian Primpke[b], Benedikt Hufnagl[c,d], Martin G. J. Löder[a], Gunnar Gerdts[b#], Christian Laforsch[a#]

[a] Department of Animal Ecology I, University of Bayreuth, Universitätsstr. 30, 95440 Bayreuth, Germany

[b] Alfred Wegener Institute Helmholtz Centre for Polar and Marine Research, Biologische Anstalt Helgoland, Kurpromenade 201, 27498 Helgoland, Germany

[c] Institute of Chemical Technologies and Analytics, Vienna University of Technology, A 1060 Vienna, Austria

[d] Purency GmbH, A 1010 Vienna, Austria

* *Shared first-authorship*

[#] *Shared senior authorship*

Corresponding authors:

Gunnar Gerdts (gunnar.gerdts@awi.de)

Christian Laforsch (christian.laforsch@uni-bayreuth.de)

Sebastian Primpke (sebastian.primpke@awi.de)

Martin Löder (martin.loeder@uni-bayreuth.de)

Keywords: automated microplastic analysis, FTIR, siMPle, Bayreuth Particle Finder (BPF), water samples

Content

Figures

Tables

Tab. S1: Background information on subsamples reanalysed in the present study, originating from samples collected in the catchment area of the River Weser and transition to the North Sea in the framework of previous studies (Roscher et al. (2021), Moses et al. (in prep.)).

Sample ID	Sampling area	North	East	SPM [mg/L]
A-01	Fulda	50°35.91	09°38.34	3.7
A-02	Eder	51°02.98	08°17.05	1.3
A-03	Eder	51°07.52	09°17.70	1.8
A-04	Fulda	51°19.46	09°31.70	6.6
A-05	Werra	51°24.99	09°40.20	5.5
A-06	Weser	51°25.81	09°38.33	6.0
A-07	Große Aue	52°34.64	09°02.29	9.6
A-08	Leine	52°41.01	09°36.12	16.5
A-09	Örtze	52°44.33	10°02.01	11.5
A-10	Wümme	53°04.54	09°12.33	7.6
B-01	Jade Bay	53°29.94	08°14.18	147.6
B-02	Jade Bay	53°27.87	08°14.00	85.6
B-03	Lower Weser	53°21.86	08°30.19	29.7
B-04	Lower Weser	53°25.46	08°29.88	47.1
B-05	Outer Weser	53°32.74	08°33.43	54.0
B-06	Outer Weser	53°35.22	08°31.12	14.3
B-07	Outer Weser	53°37.75	08°28.01	35.7
B-08	Outer Weser	53°39.27	08°24.32	29.9
B-09	North Sea	53°52.78	07°39.42	0.8
B-10	North Sea	53°59.53	07°50.61	12.8

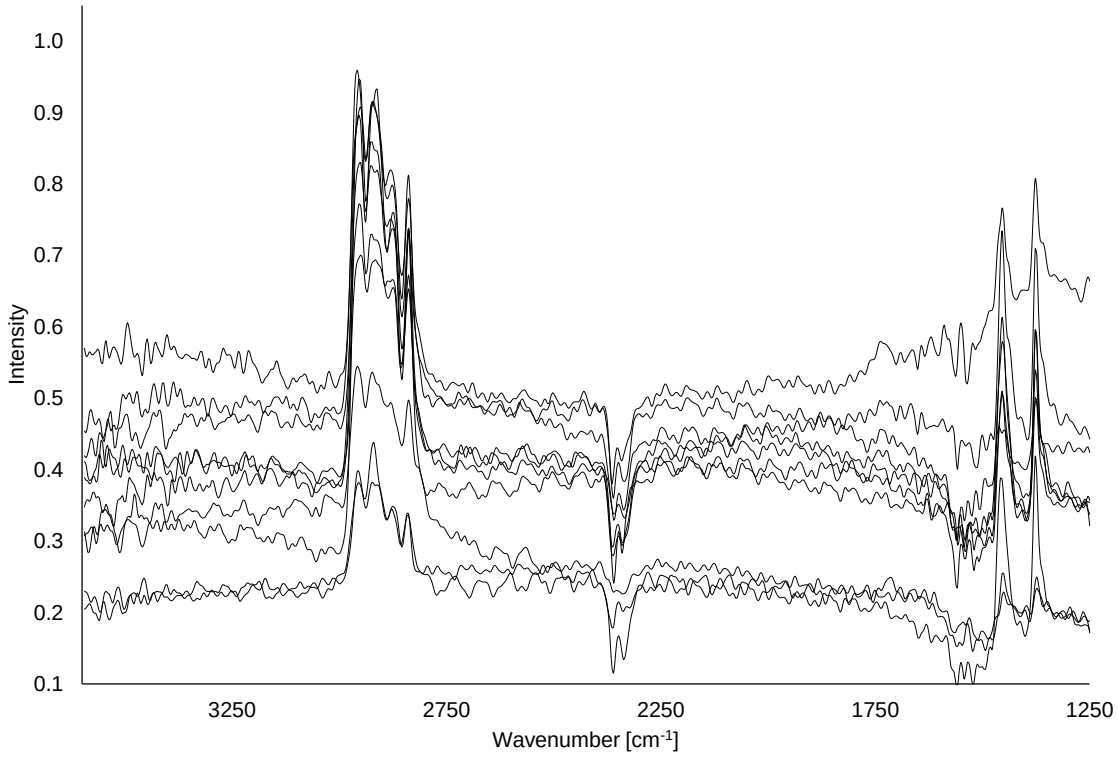

Fig. S1: Randomly selected PP-spectra (n=10) from siMPle analysis of sample B-06.

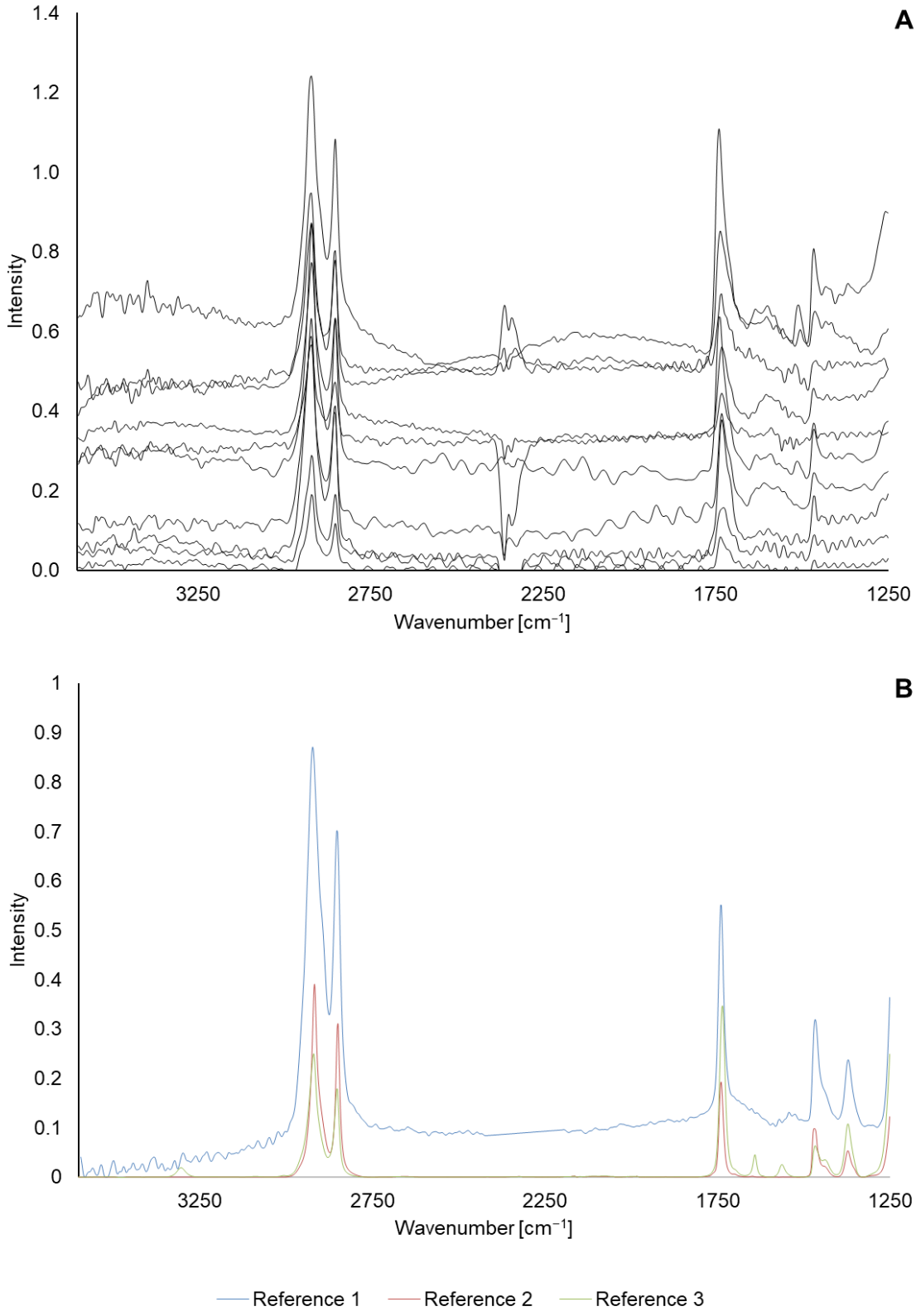

Fig. S2: A. Ten randomly selected EVA spectra, extracted from siMPle analysis (sample set A and B) and manually evaluated. B. EVA reference spectra included in siMPle database.

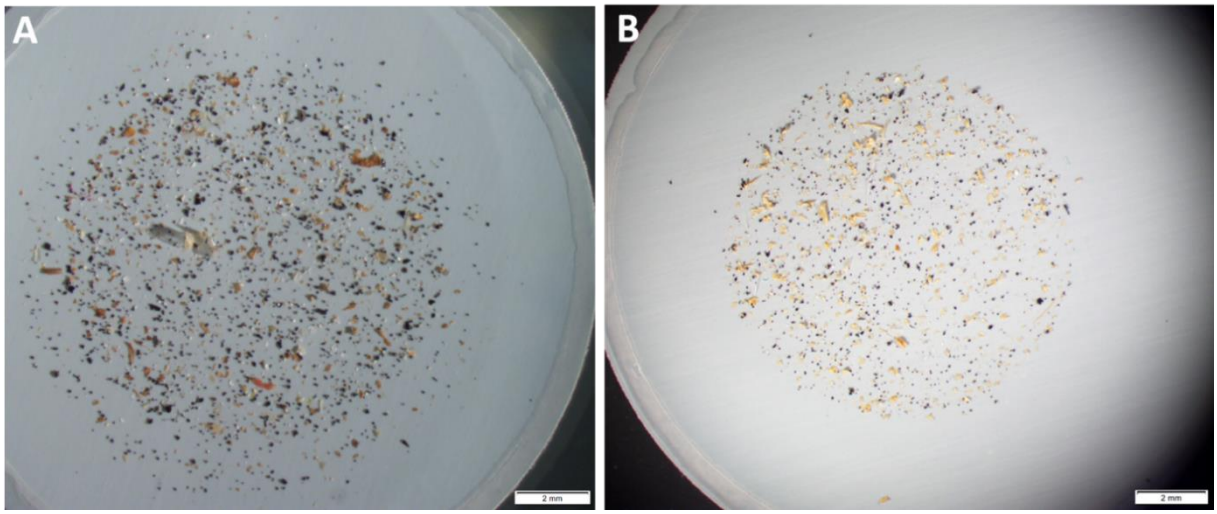

Fig. S3: Microscopy image of Anodisc filter with sample B-03 (A) and A-08 (B), showing high amounts of material with biogenic appearance.

Tab. S2: MP count of polymer types detected in sample set A after analysis with siMPle/MPAPP. The clusters A/PUR/V, CA and EVA were excluded from analysis. For abbreviations refer to Tab. 4.1 in main manuscript.

	PE	PP	PS	PC	PA	PVC	CA	PEST	A/PUR/V	PSU	PEEK	EVA	POM	∑	∑ without A/PUR/V	∑ without A/PUR/V, CA and EVA
A-01	1	4	0	0	0	0	0	0	91	0	0	4	0	100	9	5
A-02	0	1	0	0	0	0	0	1	60	0	0	1	0	63	3	2
A-03	0	11	0	0	0	0	0	0	59	0	0	1	0	71	12	11
A-04	5	8	1	0	1	0	0	0	85	1	0	2	0	103	18	16
A-05	5	9	1	0	2	1	0	4	69	0	0	2	0	93	24	22
A-06	6	14	1	0	1	0	0	4	121	0	0	7	0	154	33	26
A-07	0	3	0	0	0	0	0	0	6	0	0	0	0	9	3	3
A-08	11	76	0	0	4	0	0	5	252	0	0	25	0	373	121	96
A-09	0	3	0	0	2	0	0	1	158	0	0	5	0	169	11	6
A-10	0	3	0	0	0	0	0	1	185	0	0	8	0	197	12	4
∑	28	132	3	0	10	1	0	16	1086	1	0	55	0	1332	246	191

Tab. S3: MP count of polymer types detected in sample set A after analysis with BMF. The clusters A/PUR/V, CA and EVA were excluded from analysis. For abbreviations refer to Tab. 4.1 in main manuscript.

	PE	PP	PS	PC	PA	PVC	CA	PEST	A/PUR/V	PSU	PEEK	EVA	POM	∑	∑ without A/PUR/V	∑ without A/PUR/V, CA and EVA
A-01	3	3	0	0	0	0	0	0	3	0	0	0	0	9	6	6
A-02	0	2	0	0	0	0	0	0	0	0	0	0	0	2	2	2
A-03	0	11	0	0	0	0	0	0	1	0	0	0	0	12	11	11
A-04	0	5	1	0	0	0	0	0	0	0	0	0	0	6	6	6
A-05	1	10	1	0	0	2	0	0	0	0	0	0	1	15	15	15
A-06	2	14	2	0	0	0	0	0	0	0	0	0	0	18	18	18
A-07	0	3	0	0	0	1	0	0	0	0	0	0	0	4	4	4
A-08	8	47	1	0	3	1	0	9	0	0	0	0	0	69	69	69
A-09	0	4	0	0	0	0	0	0	0	0	0	0	0	4	4	4
A-10	0	4	0	0	0	1	0	0	0	0	0	0	0	5	5	5
∑	14	103	5	0	3	5	0	9	4	0	0	0	1	144	140	140

Tab. S4: MP count of polymer types detected in sample set B after analysis with siMPle. The clusters A/PUR/V, CA and EVA were excluded from analysis. For abbreviations refer to Tab. 4.1 in main manuscript.

	PE	PP	PS	PC	PA	PVC	CA	PEST	A/PUR/V	PSU	PEEK	EVA	POM	∑	∑ without A/PUR/V	∑ without A/PUR/V, CA and EVA
B-01	3	2	4	0	1	0	0	2	15	0	0	0	0	27	12	12
B-02	1	0	1	0	14	0	0	1	10	0	0	0	0	27	17	17
B-03	14	14	3	0	20	0	0	2	393	0	0	39	0	485	92	53
B-04	7	21	9	0	2	1	0	1	78	1	0	3	0	123	45	42
B-05	3	5	6	1	6	0	0	1	53	6	1	4	0	86	33	29
B-06	1	9	2	0	1	0	0	1	13	3	0	1	0	31	18	17
B-07	5	12	4	0	0	3	0	0	61	0	0	7	0	92	31	24
B-08	1	4	1	0	1	0	0	2	60	0	0	1	0	70	10	9
B-09	0	0	0	0	1	1	0	0	7	0	0	0	0	9	2	2
B-10	0	0	1	0	1	0	14	1	326	0	0	0	0	343	17	3
∑	35	67	31	1	47	5	14	11	1016	10	1	55	0	**1293**	**277**	**208**

Tab. S5: MP count of polymer types detected in sample set B after analysis with BMF. The clusters A/PUR/V, CA and EVA were excluded from analysis. For abbreviations refer to Tab. 4.1 in main manuscript.

	PE	PP	PS	PC	PA	PVC	CA	PEST	A/PUR/V	PSU	PEEK	EVA	POM	∑	∑ without A/PUR/V	∑ without A/PUR/V, CA and EVA
B-01	0	0	0	0	0	0	0	0	5	0	0	0	0	5	0	0
B-02	0	0	0	0	0	0	0	1	5	0	0	0	0	6	1	1
B-03	0	0	0	0	0	0	0	1	42	0	0	0	0	43	1	1
B-04	7	16	9	0	0	2	0	2	3	1	0	0	0	40	37	37
B-05	1	0	0	0	12	2	0	0	10	1	0	0	0	26	16	16
B-06	7	0	0	0	2	0	0	0	2	1	0	0	0	12	10	10
B-07	17	0	0	0	0	2	0	0	11	0	0	0	0	30	19	19
B-08	0	0	0	0	1	0	0	3	6	0	0	0	0	10	4	4
B-09	0	0	0	0	0	0	0	0	9	0	0	0	0	9	0	0
B-10	0	0	0	0	0	0	0	0	15	0	0	0	0	15	0	0
∑	32	16	9	0	15	6	0	7	108	3	0	0	0	196	88	88

References

Directive (EU) 2019/904 of the European Parliament and of the Council of 5 June 2019 on the reduction of the impact of certain plastic products on the environment.

Abel, S. M., S. Primpke, I. Int-Veen, A. Brandt, and G. Gerdts. 2021. Systematic identification of microplastics in abyssal and hadal sediments of the Kuril Kamchatka trench. Environmental Pollution **269**:116095.

Ajekwene, K. 2020. Properties and Applications of Acrylates. Pages 35-46.

Akarsu, C., H. Kumbur, K. Gökdağ, A. E. Kıdeyş, and A. Sanchez-Vidal. 2020. Microplastics composition and load from three wastewater treatment plants discharging into Mersin Bay, north eastern Mediterranean Sea. Marine Pollution Bulletin **150**:110776.

Andrade, J. M., B. Ferreiro, P. López-Mahía, and S. Muniategui-Lorenzo. 2020. Standardization of the minimum information for publication of infrared-related data when microplastics are characterized. Marine Pollution Bulletin **154**:111035.

Andrades, R., R. G. Santos, J.-C. Joyeux, D. Chelazzi, A. Cincinelli, and T. Giarrizzo. 2018. Marine debris in Trindade Island, a remote island of the South Atlantic. Marine Pollution Bulletin **137**:180-184.

Andrady, A. L. 2015. Plastics and environmental sustainability. John Wiley & Sons.

Arthur, C., J. Baker, H. Bamford, N. Barnea, R. Lohmann, and K. e. a. McElwee. 2009. Summary of the International research workshop on the occurence, effects, and fate of microplastic marine debris. National Oceanic and Athmospheric Administration Technical Memorandum NOS-OR&R-30.

ASA Spezialenzyme GmbH. 2005a. Protease A-01 (EC 3.4.21.62). Product information sheet.

ASA Spezialenzyme GmbH. 2005b. Cellulase TXL (EC 3.2.1.4). Product information sheet.

ASA Spezialenzyme GmbH. 2005c. Chitinase. Product information sheet.

Avio, C. G., L. Cardelli, S. Gorbi, D. Pellegrini, and F. Regoli. 2017. Microplastics pollution after the removal of the Costa Concordia wreck: First evidences from a biomonitoring case study. Environmental Pollution **227**:207-214.

Azizi, N., S. Nasseri, R. N. Nodehi, N. Jaafarzadeh, and M. Pirsaheb. 2022. Evaluation of conventional wastewater treatment plants efficiency to remove microplastics in terms of abundance, size, shape, and type: A systematic review and Meta-analysis. Marine Pollution Bulletin **177**:113462.

Baldwin, A., S. Corsi, and S. Mason. 2016. Plastic Debris in 29 Great Lakes Tributaries: Relations to Watershed Attributes and Hydrology. Environmental Science & Technology **50(19)**:10377–10385.

Ballent, A., P. L. Corcoran, O. Madden, P. A. Helm, and F. J. Longstaffe. 2016. Sources and sinks of microplastics in Canadian Lake Ontario nearshore, tributary and beach sediments. Marine Pollution Bulletin **110**:383-395.

Barchiesi, M., A. Chiavola, C. Di Marcantonio, and M. R. Boni. 2021. Presence and fate of microplastics in the water sources: focus on the role of wastewater and drinking water treatment plants. Journal of Water Process Engineering **40**:101787.

Barnes, D. K., F. Galgani, R. C. Thompson, and M. Barlaz. 2009. Accumulation and fragmentation of plastic debris in global environments. Philosophical Transactions of the Royal Society B: Biological Sciences **364**:1985-1998.

Bartošová, A., L. Blinová, and K. Gerulová. 2015. Characterisation of polysacharides and lipids from selected green algae species by FTIR-ATR spectroscopy. Research Papers Faculty of Materials Science and Technology Slovak University of Technology **23**:97-102.

Bashir, S. M., S. Kimiko, C.-W. Mak, J. K.-H. Fang, and D. Gonçalves. 2021. Personal Care and Cosmetic Products as a Potential Source of Environmental Contamination by Microplastics in a Densely Populated Asian City. Frontiers in Marine Science **8**:604.

Bayo, J., S. Olmos, and J. López-Castellanos. 2020. Microplastics in an urban wastewater treatment plant: The influence of physicochemical parameters and environmental factors. Chemosphere **238**:124593.

Ben-David, E. A., M. Habibi, E. Haddad, M. Hasanin, D. L. Angel, A. M. Booth, and I. Sabbah. 2021. Microplastic distributions in a domestic wastewater treatment plant: Removal efficiency, seasonal variation and influence of sampling technique. Science of the Total Environment **752**:141880.

Bergmann, M., F. Collard, J. Fabres, G. W. Gabrielsen, J. F. Provencher, C. M. Rochman, E. van Sebille, and M. B. Tekman. 2022. Plastic pollution in the Arctic. Nature Reviews Earth & Environment **3**:323–337.

Bergmann, M., S. Mützel, S. Primpke, M. B. Tekman, J. Trachsel, and G. Gerdts. 2019. White and wonderful? Microplastics prevail in snow from the Alps to the Arctic. Science Advances **5**:eaax1157.

Bian, P., Y. Liu, K. Zhao, Y. Hu, J. Zhang, L. Kang, and W. Shen. 2022. Spatial variability of microplastic pollution on surface of rivers in a mountain-plain transitional area: A case study in the Chin Ling-Wei River Plain, China. Ecotoxicology and Environmental Safety **232**:113298.

Bigalke, M., M. Fieber, A. Foetisch, J. Reynes, and P. Tollan. 2022. Microplastics in agricultural drainage water: A link between terrestrial and aquatic microplastic pollution. Science of the Total Environment **806**:150709.

Brander, S. M., V. C. Renick, M. M. Foley, C. Steele, M. Woo, A. Lusher, S. Carr, P. Helm, C. Box, and S. Cherniak. 2020. Sampling and quality assurance and quality control: a guide for scientists investigating the occurrence of microplastics across matrices. Applied Spectroscopy **74**:1099-1125.

Brandt, J., L. Bittrich, F. Fischer, E. Kanaki, A. Tagg, R. Lenz, M. Labrenz, E. Brandes, D. Fischer, and K.-J. Eichhorn. 2020. High-Throughput Analyses of Microplastic Samples Using Fourier Transform Infrared and Raman Spectrometry. Applied Spectroscopy **74**:1185-1197.

Bruge, A., M. Dhamelincourt, L. Lanceleur, M. Monperrus, J. Gasperi, and B. Tassin. 2020. A first estimation of uncertainties related to microplastic sampling in rivers. Science of the Total Environment **718**:137319.

Cabernard, L., L. Roscher, C. Lorenz, G. Gerdts, and S. Primpke. 2018. Comparison of Raman and Fourier Transform Infrared Spectroscopy for the Quantification of Microplastics in the Aquatic Environment. Environmental Science & Technology **52**:13279–13288.

Cai, M., H. He, M. Liu, S. Li, G. Tang, W. Wang, P. Huang, G. Wei, Y. Lin, B. Chen, J. Hu, and Z. Cen. 2018. Lost but can't be neglected: Huge quantities of small microplastics hide in the South China Sea. Science of the Total Environment **633**:1206-1216.

Can-Güven, E. 2021. Microplastics as emerging atmospheric pollutants: a review and bibliometric analysis. Air Quality, Atmosphere & Health **14**:203-215.

Cao, Y., Q. Wang, Y. Ruan, R. Wu, L. Chen, K. Zhang, and P. K. S. Lam. 2020. Intra-day microplastic variations in wastewater: A case study of a sewage treatment plant in Hong Kong. Marine Pollution Bulletin **160**:111535.

Carlsson, P., C. Singdahl-Larsen, and A. L. Lusher. 2021. Understanding the occurrence and fate of microplastics in coastal Arctic ecosystems: The case of surface waters, sediments and walrus (Odobenus rosmarus). Science of the Total Environment **792**:148308.

Carpenter, E. J., S. J. Anderson, G. R. Harvey, H. P. Miklas, and B. B. Peck. 1972. Polystyrene spherules in coastal waters. Science **178**:749-750.

Carpenter, E. J., and K. L. Smith, Jr. 1972. Plastics on the Sargasso sea surface. Science **175**:1240-1241.

Carr, S. A., J. Liu, and A. G. Tesoro. 2016. Transport and fate of microplastic particles in wastewater treatment plants. Water Research **91**:174-182.

Catarino, A. I., R. Thompson, W. Sanderson, and T. Henry. 2016. Development and optimisation of a standard method for extraction of microplastics in mussels by enzyme digestion of soft tissues. Environmental toxicology and chemistry / SETAC **36(4)**:947–951.

Chale, J., R. Moo-Puc, D. Robledo, and Y. Freile-Pelegrin. 2014. Hepatoprotective effect of the fucoidan from the brown seaweed Turbinaria tricostata. Journal of Applied Phycology **27**:2123–2135.

Chen, Q., Q. Wang, C. Zhang, J. Zhang, Z. Dong, and Q. Xu. 2021. Aging simulation of thin-film plastics in different environments to examine the formation of microplastic. Water Research **202**:117462.

Chen, S., L. Su, J. Chen, and J. Wu. 2013. Cutinase: characteristics, preparation, and application. Biotechnology Advances **31**:1754-1767.

Chiba, S., H. Saito, R. Fletcher, T. Yogi, M. Kayo, S. Miyagi, M. Ogido, and K. Fujikura. 2018. Human footprint in the abyss: 30 year records of deep-sea plastic debris. Marine Policy **96**:204-212.

Chouchene, K., T. Nacci, F. Modugno, V. Castelvetro, and M. Ksibi. 2022. Soil contamination by microplastics in relation to local agricultural development as revealed by FTIR, ICP-MS and pyrolysis-GC/MS. Environmental Pollution **303**:119016.

Claessens, M., L. Van Cauwenberghe, M. B. Vandegehuchte, and C. R. Janssen. 2013. New techniques for the detection of microplastics in sediments and field collected organisms. Marine Pollution Bulletin **70**:227-233.

Cohen, J. H., A. M. Internicola, R. A. Mason, and T. Kukulka. 2019. Observations and Simulations of Microplastic Debris in a Tide, Wind, and Freshwater-Driven Estuarine Environment: the Delaware Bay. Environmental Science & Technology **53**:14204-14211.

Cole, M. 2016. A novel method for preparing microplastic fibers. Scientific Reports **6**:34519.

Cole, M., P. Lindeque, C. Halsband, and T. S. Galloway. 2011. Microplastics as contaminants in the marine environment: A review. Marine Pollution Bulletin **62**:2588-2597.

Colton, J. B., F. D. Knapp, and B. R. Burns. 1974. Plastic Particles in Surface Waters of Northwestern Atlantic. Science **185**:491-497.

Conley, K., A. Clum, J. Deepe, H. Lane, and B. Beckingham. 2019. Wastewater treatment plants as a source of microplastics to an urban estuary: Removal efficiencies and loading per capita over one year. Water Research X **3**:100030.

Cowger, W., A. Gray, S. H. Christiansen, H. DeFrond, A. D. Deshpande, L. Hemabessiere, E. Lee, L. Mill, K. Munno, B. E. Ossmann, M. Pittroff, C. Rochman, G. Sarau, S. Tarby, and S. Primpke. 2020. Critical Review of Processing and Classification Techniques for Images and Spectra in Microplastic Research. Applied Spectroscopy **74**:989-1010.

Cunsolo, S., J. Williams, M. Hale, D. S. Read, and F. Couceiro. 2021. Optimising sample preparation for FTIR-based microplastic analysis in wastewater and sludge samples: multiple digestions. Analytical and Bioanalytical Chemistry **413**:3789-3799.

Cutroneo, L., A. Reboa, G. Besio, F. Borgogno, L. Canesi, S. Canuto, M. Dara, F. Enrile, I. Forioso, G. Greco, V. Lenoble, A. Malatesta, S. Mounier, M. Petrillo, R. Rovetta, A. Stocchino, J. Tesan, G. Vagge, and M. Capello. 2020. Microplastics in seawater: sampling strategies, laboratory methodologies, and identification techniques applied to port environment. Environmental Science and Pollution Research **27**:8938-8952.

Cutroneo, L., A. Reboa, I. Geneselli, and M. Capello. 2021. Considerations on salts used for density separation in the extraction of microplastics from sediments. Marine Pollution Bulletin **166**:112216.

da Silva, V. H., F. Murphy, J. M. Amigo, C. Stedmon, and J. Strand. 2020. Classification and Quantification of Microplastics (<100 μm) Using a Focal Plane Array–Fourier Transform Infrared Imaging System and Machine Learning. Analytical Chemistry **92**:13724-13733.

De-la-Torre, G. E., C. I. Pizarro-Ortega, D. C. Dioses-Salinas, J. Castro Loayza, J. Smith Sanchez, C. Meza-Chuquizuta, D. Espinoza-Morriberón, M. R. J. Rakib, M. Ben-Haddad, and S. Dobaradaran. 2022. Are we underestimating floating microplastic pollution? A quantitative analysis of two sampling methodologies. Marine Pollution Bulletin **178**:113592.

Defontaine, S., D. Sous, J. Tesan, M. Monperrus, V. Lenoble, and L. Lanceleur. 2020. Microplastics in a salt-wedge estuary: Vertical structure and tidal dynamics. Marine Pollution Bulletin **160**:111688.

Dehaut, A., A.-L. Cassone, L. Frère, L. Hermabessiere, C. Himber, E. Rinnert, G. Rivière, C. Lambert, P. Soudant, A. Huvet, G. Duflos, and I. Paul-Pont. 2016. Microplastics in seafood: Benchmark protocol for their extraction and characterization. Environmental Pollution **215**:223-233.

Demšar, J. 2006. Statistical comparisons of classifiers over multiple data sets. Journal of Machine Learning Research **7**:1-30.

Desforges, J. P. W., M. Galbraith, N. Dangerfield, and P. S. Ross. 2014. Widespread distribution of microplastics in subsurface seawater in the NE Pacific Ocean. Marine Pollution Bulletin **79**:94-99.

Devriese, L. I., M. D. van der Meulen, T. Maes, K. Bekaert, I. Paul-Pont, L. Frère, J. Robbens, and A. D. Vethaak. 2015. Microplastic contamination in brown shrimp (Crangon crangon, Linnaeus 1758) from coastal waters of the Southern North Sea and Channel area. Marine Pollution Bulletin **98**:179-187.

Dibke, C., M. Fischer, and B. M. Scholz-Böttcher. 2021. Microplastic Mass Concentrations and Distribution in German Bight Waters by Pyrolysis–Gas Chromatography–Mass Spectrometry/Thermochemolysis Reveal Potential Impact of Marine Coatings: Do Ships Leave Skid Marks? Environmental Science & Technology **55**:2285-2295.

Directive, S. F. 2013. Guidance on monitoring of marine litter in European seas. Luxembourg. doi **10**:99475.

Domogalla-Urbansky, J., P. M. Anger, H. Ferling, F. Rager, A. C. Wiesheu, R. Niessner, N. P. Ivleva, and J. Schwaiger. 2019. Raman microspectroscopic identification of

microplastic particles in freshwater bivalves (Unio pictorum) exposed to sewage treatment plant effluents under different exposure scenarios. Environmental Science and Pollution Research **26**:2007-2012.

Dong, M., Z. She, X. Xiong, and Z. Luo. 2021. Automated analysis of microplastics based on vibrational spectroscopy: Are we measuring the same metrics? Analytical and Bioanalytical Chemistry **414**:3359–3372.

dos Santos, P. R., and L. A. Daniel. 2020. A review: organic matter and ammonia removal by biological activated carbon filtration for water and wastewater treatment. International Journal of Environmental Science and Technology **17**:591-606.

Dris, R., J. Gasperi, M. Saad, C. Mirande, and B. Tassin. 2016. Synthetic fibers in atmospheric fallout: A source of microplastics in the environment? Marine Pollution Bulletin **104**:290-293.

Dris, R., H. Imhof, W. Sanchez, J. Gasperi, F. Galgani, B. Tassin, and C. Laforsch. 2015. Beyond the ocean: contamination of freshwater ecosystems with (micro-)plastic particles. Environmental Chemistry **12**:539-550.

Dubaish, F., and G. Liebezeit. 2013. Suspended Microplastics and Black Carbon Particles in the Jade System, Southern North Sea. Water Air and Soil Pollution **224**:1352.

Dümichen, E., A.-K. Barthel, U. Braun, C. G. Bannick, K. Brand, M. Jekel, and R. Senz. 2015. Analysis of polyethylene microplastics in environmental samples, using a thermal decomposition method. Water Research **85**:451-457.

Eibes, P. M., and F. Gabel. 2022. Floating microplastic debris in a rural river in Germany: Distribution, types and potential sources and sinks. Science of the Total Environment **816**:151641.

Enders, K., R. Lenz, C. A. Stedmon, and T. G. Nielsen. 2015. Abundance, size and polymer composition of marine microplastics >= 10 mu m in the Atlantic Ocean and their modelled vertical distribution. Marine Pollution Bulletin **100**:70-81.

Eriksen, M., F. Borgogno, P. Villarrubia-Gómez, E. Anderson, C. Box, and N. Trenholm. 2020. Mitigation strategies to reverse the rising trend of plastics in Polar Regions. Environment International **139**:105704.

Fischer, M., and B. Scholz-Böttcher. 2019. Microplastics analysis in environmental samples – Recent pyrolysis-gas chromatography-mass spectrometry method improvements to increase the reliability of mass related data. Analytical Methods **11**:2489-2497.

Fischer, M., and B. M. Scholz-Böttcher. 2017. Simultaneous Trace Identification and Quantification of Common Types of Microplastics in Environmental Samples by Pyrolysis-Gas Chromatography–Mass Spectrometry. Environmental Science & Technology **51**:5052-5060.

Fortin, S., B. Song, and C. Burbage. 2019. Quantifying and identifying microplastics in the effluent of advanced wastewater treatment systems using Raman microspectroscopy. Marine Pollution Bulletin **149**:110579.

Franco, A. A., J. M. Arellano, G. Albendín, R. Rodríguez-Barroso, J. M. Quiroga, and M. D. Coello. 2021. Microplastic pollution in wastewater treatment plants in the city of Cádiz: Abundance, removal efficiency and presence in receiving water body. Science of the Total Environment **776**:145795.

Free, C. M., O. P. Jensen, S. A. Mason, M. Eriksen, N. J. Williamson, and B. Boldgiv. 2014. High-levels of microplastic pollution in a large, remote, mountain lake. Marine Pollution Bulletin **85**:156-163.

Frei, S., S. Piehl, B. Gilfedder, M. Löder, J. Krutzke, L. Wilhelm, and C. Laforsch. 2019. Occurence of microplastics in the hyporheic zone of rivers. Scientific Reports **9**:1-11.

Frère, L., I. Paul-Pont, E. Rinnert, S. Petton, J. Jaffré, I. Bihannic, P. Soudant, C. Lambert, and A. Huvet. 2017. Influence of environmental and anthropogenic factors on the composition, concentration and spatial distribution of microplastics: A case study of the Bay of Brest (Brittany, France). Environmental Pollution **225**:211-222.

Frias, J. P. G. L., O. Lyashevska, H. Joyce, E. Pagter, and R. Nash. 2020. Floating microplastics in a coastal embayment: A multifaceted issue. Marine Pollution Bulletin **158**:111361.

Fu, L., J. Li, G. Wang, Y. Luan, and W. Dai. 2021. Adsorption behavior of organic pollutants on microplastics. Ecotoxicology and Environmental Safety **217**:112207.

Funck, M., M. S. M. Al-Azzawi, A. Yildirim, O. Knoop, T. C. Schmidt, J. E. Drewes, and J. Tuerk. 2021. Release of microplastic particles to the aquatic environment via wastewater treatment plants: The impact of sand filters as tertiary treatment. Chemical Engineering Journal **426**:130933.

Funck, M., A. Yildirim, C. Nickel, J. Schram, T. C. Schmidt, and J. Tuerk. 2020. Identification of microplastics in wastewater after cascade filtration using Pyrolysis-GC–MS. MethodsX **7**:100778.

Gago, J., A. Filgueiras, M. L. Pedrotti, M. Caetano, and J. Frias. 2019. Standardised protocol for monitoring microplastics in seawater. Deliverable 4.1.

Galafassi, S., L. Nizzetto, and P. Volta. 2019. Plastic sources: A survey across scientific and grey literature for their inventory and relative contribution to microplastics pollution in natural environments, with an emphasis on surface water. Science of the Total Environment **693**:133499.

Gasperi, J., S. L. Wright, R. Dris, F. Collard, C. Mandin, M. Guerrouache, V. Langlois, F. J. Kelly, and B. Tassin. 2018. Microplastics in air: Are we breathing it in? current opinion in environmental science & health **1**:1-5.

Gaylarde, C. C., J. A. B. Neto, and E. M. da Fonseca. 2021. Paint fragments as polluting microplastics: A brief review. Marine Pollution Bulletin **162**:111847.

Gerdts, G. 2018. Reaktor zur enzymatischen Mazeration biogener Bestandteile einer Partikelprobe und Verwendung des Reaktors.*in* E. P. Office, editor. https://patents.google.com/patent/EP3329994A1/de.

Gerdts, G., K. Thomas, D. Herzke, M. Haeckel, B. Scholz-Böttcher, C. Laforsch, F. Lagarde, A. M. Mahon, M. L. Pedrotti, G. de Lucia, P. Sobral, J. Gago, S. Muniategui Lorenzo, F. Norén, M. Hassellöv, T. Kögel, V. Tirelli, M. Caetano, A. Collignon, and P. Licandro. 2017. Defining the Baselines and Standards for Microplastics Analyses in European Waters (JPI-O BASEMAN). Pages 120-122.

Gerolin, C. R., F. N. Pupim, A. O. Sawakuchi, C. H. Grohmann, G. Labuto, and D. Semensatto. 2020. Microplastics in sediments from Amazon rivers, Brazil. Science of the Total Environment **749**:141604.

Gerritse, J., H. Leslie, C. De Tender, L. Devriese, and A. Vethaak. 2020. Fragmentation of plastic objects in a laboratory seawater microcosm. Scientific Reports **10**:10945.

Gilman, E., M. Musyl, P. Suuronen, M. Chaloupka, S. Gorgin, J. Wilson, and B. Kuczenski. 2021. Highest risk abandoned, lost and discarded fishing gear. Scientific Reports **11**:7195.

Goßmann, I., M. Halbach, and B. M. Scholz-Böttcher. 2021. Car and truck tire wear particles in complex environmental samples – A quantitative comparison with "traditional" microplastic polymer mass loads. Science of the Total Environment **773**:145667.

Grabemann, H.-J., I. Grabemann, and D. Eppel. 2004. Climate change and hydrodynamic impact in the Jade-Weser area: A case study. **1**:83-91.

Grabemann, I., and G. Krause. 2001. On Different Time Scales of Suspended Matter Dynamics in the Weser Estuary. Estuaries **24**:688-698.

Gündoğdu, S., C. Çevik, B. Ayat, B. Aydoğan, and S. Karaca. 2018b. How microplastics quantities increase with flood events? An example from Mersin Bay NE Levantine coast of Turkey. Environmental Pollution **239**:342-350.

Gündoğdu, S., C. Çevik, E. Güzel, and S. Kilercioğlu. 2018. Microplastics in municipal wastewater treatment plants in Turkey: a comparison of the influent and secondary effluent concentrations. Environmental Monitoring and Assessment **190**:626.

Haave, M., C. Lorenz, S. Primpke, and G. Gerdts. 2019. Different stories told by small and large microplastics in sediment - first report of microplastic concentrations in an urban recipient in Norway. Marine Pollution Bulletin **141**:501-513.

Hahn, A., G. Gerdts, C. Völker, and V. Niebühr. 2019. Using FTIRS as pre-screening method for detection of microplastic in bulk sediment samples. Science of the Total Environment **689**:341-346.

Han, M., X. Niu, M. Tang, B.-T. Zhang, G. Wang, W. Yue, X. Kong, and J. Zhu. 2020. Distribution of microplastics in surface water of the lower Yellow River near estuary. Science of the Total Environment **707**:135601.

Harris, P. T. 2020. The fate of microplastic in marine sedimentary environments: A review and synthesis. Marine Pollution Bulletin **158**:111398.

Hartmann, N. B., T. Hüffer, R. C. Thompson, M. Hassellöv, A. Verschoor, A. E. Daugaard, S. Rist, T. Karlsson, N. Brennholt, M. Cole, M. P. Herrling, M. C. Hess, N. P. Ivleva, A. L. Lusher, and M. Wagner. 2019. Are We Speaking the Same Language? Recommendations for a Definition and Categorization Framework for Plastic Debris. Environmental Science & Technology **53** 1039−1047.

He, D., X. Chen, W. Zhao, Z. Zhu, X. Qi, L. Zhou, W. Chen, C. Wan, D. Li, X. Zou, and N. Wu. 2021. Microplastics contamination in the surface water of the Yangtze River from upstream to estuary based on different sampling methods. Environmental Research **196**:110908.

Helm, P. 2017. Improving microplastics source apportionment: A role for microplastic morphology and taxonomy? Analytical Methods **9**:1328-1331.

Heredia-Guerrero, J. A., J. J. Benítez, E. Domínguez, I. S. Bayer, R. Cingolani, A. Athanassiou, and A. Heredia. 2014. Infrared and Raman spectroscopic features of plant cuticles: a review. Frontiers in plant science **5**:305-305.

Hernandez, E., B. Nowack, and D. M. Mitrano. 2017. Polyester Textiles as a Source of Microplastics from Households: A Mechanistic Study to Understand Microfiber Release During Washing. Environmental Science & Technology **51**:7036-7046.

Heß, M., P. Diehl, J. Mayer, H. Rahm, W. Reifenhäuser, J. Stark, and J. Schwaiger. 2018. Mikroplastik in Binnengewässern Süd- und Westdeutschlands. Landesanstalt für Umwelt Baden-Württemberg (LUBW).

Hesse, R. F., A. Zorndt, and P. Frohle. 2019. Modelling dynamics of the estuarine turbidity maximum and local net deposition. Ocean Dynamics **69**:489-507.

Hidalgo-Ruz, V., L. Gutow, R. C. Thompson, and M. Thiel. 2012. Microplastics in the Marine Environment: A Review of the Methods Used for Identification and Quantification. Environmental Science & Technology **46**:3060-3075.

Hidayaturrahman, H., and T.-G. Lee. 2019. A study on characteristics of microplastic in wastewater of South Korea: Identification, quantification, and fate of microplastics during treatment process. Marine Pollution Bulletin **146**:696-702.

Hildebrandt, L., T. Zimmermann, S. Primpke, D. Fischer, G. Gerdts, and D. Pröfrock. 2021. Comparison and uncertainty evaluation of two centrifugal separators for microplastic sampling. Journal of Hazardous Materials **414**:125482.

Hirt, U., M. Venohr, P. Kreins, and H. Behrendt. 2008. Modelling nutrient emissions and the impact of nutrient reduction measures in the Weser river basin, Germany. Water Science and Technology **58**:2251-2258.

Hitchcock, J. N. 2020. Storm events as key moments of microplastic contamination in aquatic ecosystems. Science of the Total Environment **734**:139436.

Hitchcock, J. N., and S. M. Mitrovic. 2019. Microplastic pollution in estuaries across a gradient of human impact. Environmental Pollution **247**:457-466.

Huang, D., X. Li, Z. Ouyang, X. Zhao, R. Wu, C. Zhang, C. Lin, Y. Li, and X. Guo. 2021. The occurrence and abundance of microplastics in surface water and sediment of the West River downstream, in the south of China. Science of the Total Environment **756**:143857.

Hufnagl, B., D. Steiner, E. Renner, M. G. J. Löder, C. Laforsch, and H. Lohninger. 2019. A methodology for the fast identification and monitoring of microplastics in environmental samples using random decision forest classifiers. Analytical Methods **11**:2277-2285.

Hufnagl, B., M. Stibi, H. Martirosyan, U. Wilczek, J. N. Möller, M. G. J. Löder, C. Laforsch, and H. Lohninger. 2022. Computer-Assisted Analysis of Microplastics in Environmental Samples Based on μFTIR Imaging in Combination with Machine Learning. Environmental Science & Technology Letters **9**:90-95.

Hurley, R. R., A. L. Lusher, M. Olsen, and L. Nizzetto. 2018. Validation of a method for extracting microplastics from complex, organic-rich, environmental matrices. Environmental Science & Technology **52**:7409-7417.

Imhof, H. K., C. Laforsch, A. C. Wiesheu, J. Schmid, P. M. Anger, R. Niessner, and N. P. Ivleva. 2016. Pigments and plastic in limnetic ecosystems: A qualitative and quantitative study on microparticles of different size classes. Water Research **98**:64-74.

Imhof, H. K., J. Schmid, R. Niessner, N. P. Ivleva, and C. Laforsch. 2012. A novel, highly efficient method for the separation and quantification of plastic particles in sediments of aquatic environments. Limnology and Oceanography-Methods **10**:524-537.

Ivleva, N. P. 2021. Chemical Analysis of Microplastics and Nanoplastics: Challenges, Advanced Methods, and Perspectives. Chemical Reviews **121**:11886-11936.

Iyare, P. U., S. K. Ouki, and T. Bond. 2020. Microplastics removal in wastewater treatment plants: a critical review. Environmental Science: Water Research & Technology **6**:2664-2675.

January, G. G., R. K. Naidoo, B. Kirby-McCullough, and R. Bauer. 2019. Assessing methodologies for fucoidan extraction from South African brown algae. Algal Research **40**:101517.

Jiang, Y., Y. Zhao, X. Wang, F. Yang, M. Chen, and J. Wang. 2020. Characterization of microplastics in the surface seawater of the South Yellow Sea as affected by season. Science of the Total Environment **724**:138375.

Jones, R. J. 2007. Chemical contamination of a coral reef by the grounding of a cruise ship in Bermuda. Marine Pollution Bulletin **54**:905-911.

Kallenbach, E. M., E. S. Rødland, N. T. Buenaventura, and R. Hurley. 2021. Microplastics in terrestrial and freshwater environments. Microplastic in the Environment: Pattern and Process:87.

Kang, P., B. Ji, Y. Zhao, and T. Wei. 2020. How can we trace microplastics in wastewater treatment plants: A review of the current knowledge on their analysis approaches. Science of the Total Environment **745**:140943.

Käppler, A., D. Fischer, S. Oberbeckmann, G. Schernewski, M. Labrenz, K. J. Eichhorn, and B. Voit. 2016. Analysis of environmental microplastics by vibrational microspectroscopy: FTIR, Raman or both? Analytical and Bioanalytical Chemistry **408**:8377-8391.

Käppler, A., M. Fischer, B. Scholz-Böttcher, S. Oberbeckmann, M. Labrenz, D. Fischer, K. Eichhorn, and B. Voit. 2018. Comparison of μ-ATR-FTIR spectroscopy and py-GCMS as identification tools for microplastic particles and fibers isolated from river sediments. Analytical and Bioanalytical Chemistry **410**:5313-5327.

Käppler, A., F. Windrich, M. G. J. Löder, M. Malanin, D. Fischer, M. Labrenz, K. J. Eichhorn, and B. Voit. 2015. Identification of microplastics by FTIR and Raman microscopy: a novel silicon filter substrate opens the important spectral range below 1300 cm(-1) for FTIR transmission measurements. Analytical and Bioanalytical Chemistry **407**:6791-6801.

Karlsson, T. M., L. Arneborg, G. Broström, B. C. Almroth, L. Gipperth, and M. Hassellöv. 2018. The unaccountability case of plastic pellet pollution. Marine Pollution Bulletin **129**:52-60.

Kasavan, S., S. Yusoff, M. F. Rahmat Fakri, and R. Siron. 2021. Plastic pollution in water ecosystems: A bibliometric analysis from 2000 to 2020. Journal of Cleaner Production **313**:127946.

Kataoka, T., Y. Nihei, K. Kudou, and H. Hinata. 2019. Assessment of the sources and inflow processes of microplastics in the river environments of Japan. Environmental Pollution **244**:958-965.

Kawai, F., T. Kawase, T. Shiono, H. Urakawa, S. Sukigara, C. Tu, and M. Yamamoto. 2017. Enzymatic hydrophilization of polyester fabrics using a recombinant cutinase Cut 190 and their surface characterization. Journal of Fiber Science and Technology **73**:8-18.

Kay, P., R. Hiscoe, I. Moberley, L. Bajic, and N. McKenna. 2018. Wastewater treatment plants as a source of microplastics in river catchments. Environmental Science and Pollution Research **25**:20264-20267.

Kedzierski, M., M. Falcou-Préfol, M.-E. Kerros, M. Henry, M. L. Pedrotti, and S. Bruzaud. 2019. A machine learning algorithm for high throughput identification of FTIR spectra: Application on microplastics collected in the Mediterranean Sea. Chemosphere **234**:242-251.

Kernchen, S., M. G. J. Löder, F. Fischer, D. Fischer, S. R. Moses, C. Georgi, A. C. Nölscher, A. Held, and C. Laforsch. 2021. Airborne microplastic concentrations and deposition across the Weser River catchment. Science of the Total Environment **818**:151812.

Kershaw, P., and C. Rochman. 2015. Sources, fate and effects of microplastics in the marine environment: part 2 of a global assessment. Reports and Studies-IMO/FAO/Unesco-IOC/WMO/IAEA/UN/UNEP Joint Group of Experts on the Scientific Aspects of Marine Environmental Protection (GESAMP) Eng No. 93.

Khan, F. R., Y. Shashoua, A. Crawford, A. Drury, K. Sheppard, K. Stewart, and T. Sculthorp. 2020. 'The Plastic Nile': First Evidence of Microplastic Contamination in Fish from the Nile River (Cairo, Egypt). Toxics **8**:22.

Kirstein, I. V., F. Hensel, A. Gomiero, L. Iordachescu, A. Vianello, H. B. Wittgren, and J. Vollertsen. 2021. Drinking plastics? – Quantification and qualification of

microplastics in drinking water distribution systems by µFTIR and Py-GCMS. Water Research **188**:116519.

Klingelhöfer, D., M. Braun, D. Quarcoo, D. Brüggmann, and D. A. Groneberg. 2020. Research landscape of a global environmental challenge: Microplastics. Water Research **170**:115358.

Klöckner, P., T. Reemtsma, P. Eisentraut, U. Braun, A. S. Ruhl, and S. Wagner. 2019. Tire and road wear particles in road environment – Quantification and assessment of particle dynamics by Zn determination after density separation. Chemosphere **222**:714-721.

Knight, L. J., F. N. F. Parker-Jurd, M. Al-Sid-Cheikh, and R. C. Thompson. 2020. Tyre wear particles: an abundant yet widely unreported microplastic? Environmental Science and Pollution Research **27**:18345-18354.

Koelmans, A. A., M. Kooi, K. L. Law, and E. Van Sebille. 2017. All is not lost: deriving a top-down mass budget of plastic at sea. Environmental Research Letters **12**:114028.

Koelmans, A. A., N. H. M. Nor, E. Hermsen, M. Kooi, S. M. Mintenig, and J. De France. 2019. Microplastics in freshwaters and drinking water: Critical review and assessment of data quality. Water Research **155**:410-422.

Kögel, T., Ø. Bjorøy, B. Toto, A. M. Bienfait, and M. Sanden. 2020. Micro- and nanoplastic toxicity on aquatic life: Determining factors. Science of the Total Environment **709**:136050.

Kooi, M., E. H. v. Nes, M. Scheffer, and A. A. Koelmans. 2017. Ups and Downs in the Ocean: Effects of Biofouling on Vertical Transport of Microplastics. Environmental Science & Technology **51**:7963-7971.

Koongolla, J. B., A. Andrady, P. T. P. Kumara, and C. Gangabadage. 2018. Evidence of microplastics pollution in coastal beaches and waters in southern Sri Lanka. Marine Pollution Bulletin **137**:277-284.

Krämer, K., A. Lefebvre, M. Becker, G. Herrling, and C. Winter. 2019. Long-term dune dynamics in the Lower Weser Estuary.*in* MARID IV, Bremen, Germany.

Kroon, F., C. Motti, S. Talbot, P. Sobral, and M. Puotinen. 2018. A workflow for improving estimates of microplastic contamination in marine waters: A case study from North-Western Australia. Environmental Pollution **238**:26-38.

Kühn, S., J. A. van Franeker, A. M. O'Donoghue, A. Swiers, M. Starkenburg, B. van Werven, E. Foekema, E. Hermsen, M. Egelkraut-Holtus, and H. Lindeboom. 2020. Details of plastic ingestion and fibre contamination in North Sea fishes. Environmental Pollution **257**:113569.

Kukulka, T., G. Proskurowski, S. Moret-Ferguson, D. W. Meyer, and K. L. Law. 2012. The effect of wind mixing on the vertical distribution of buoyant plastic debris. Geophysical Research Letters **39**:L07601.

Laermanns, H., G. Reifferscheid, J. Kruse, C. Földi, G. Dierkes, D. Schaefer, C. Scherer, C. Bogner, and F. Stock. 2021. Microplastic in Water and Sediments at the Confluence of the Elbe and Mulde Rivers in Germany. Frontiers in Environmental Science **9**.

Lam, T. W. L., L. Fok, L. Lin, Q. Xie, H.-X. Li, X.-R. Xu, and L. C. Yeung. 2020. Spatial variation of floatable plastic debris and microplastics in the Pearl River Estuary, South China. Marine Pollution Bulletin **158**:111383.

Lapointe, M., J. M. Farner, L. M. Hernandez, and N. Tufenkji. 2020. Understanding and Improving Microplastic Removal during Water Treatment: Impact of Coagulation and Flocculation. Environmental Science & Technology **54**:8719-8727.

Lebreton, L. C. M., J. van der Zwet, J. W. Damsteeg, B. Slat, A. Andrady, and J. Reisser. 2017. River plastic emissions to the world's oceans. Nature Communications **8**:15611.

Lechner, A., H. Keckeis, F. Lumesberger-Loisl, B. Zens, R. Krusch, M. Tritthart, M. Glas, and E. Schludermann. 2014. The Danube so colourful: A potpourri of plastic litter outnumbers fish larvae in Europe's second largest river. Environmental Pollution **188**:177-181.

Lechner, A., and D. Ramler. 2015. The discharge of certain amounts of industrial microplastic from a production plant into the River Danube is permitted by the Austrian legislation. Environmental Pollution **200**:159-160.

Legendre, P., and E. D. Gallagher. 2001. Ecologically meaningful transformations for ordination of species data. Oecologia **129**:271-280.

Lenz, R., K. Enders, C. A. Stedmon, D. M. A. Mackenzie, and T. G. Nielsen. 2015. A critical assessment of visual identification of marine microplastic using Raman spectroscopy for analysis improvement. Marine Pollution Bulletin **100**:82-91.

Lindeque, P. K., M. Cole, R. L. Coppock, C. N. Lewis, R. Z. Miller, A. J. R. Watts, A. Wilson-McNeal, S. L. Wright, and T. S. Galloway. 2020. Are we underestimating microplastic abundance in the marine environment? A comparison of microplastic capture with nets of different mesh-size. Environmental Pollution **265**:114721.

Liu, F., K. B. Olesen, A. R. Borregaard, and J. Vollertsen. 2019. Microplastics in urban and highway stormwater retention ponds. Science of the Total Environment **671**:992-1000.

Liu, W., J. Zhang, H. Liu, X. Guo, X. Zhang, X. Yao, Z. Cao, and T. Zhang. 2021. A review of the removal of microplastics in global wastewater treatment plants: Characteristics and mechanisms. Environment International **146**:106277.

Liu, Y., J. Zhang, C. Cai, Y. He, L. Chen, X. Xiong, H. Huang, S. Tao, and W. Liu. 2020. Occurrence and characteristics of microplastics in the Haihe River: An investigation of a seagoing river flowing through a megacity in northern China. Environmental Pollution **262**:114261.

Löder, M., H. Imhof, M. Ladehoff, L. Löschel, C. Lorenz, S. Mintenig, S. Piehl, S. Primpke, I. Schrank, C. Laforsch, and G. Gerdts. 2017. Enzymatic Purification of Microplastics in Environmental Samples. Environmental Science & Technology **51**:14283−14292.

Löder, M. G., and G. Gerdts. 2015. Methodology used for the detection and identification of microplastics—A critical appraisal. Pages 201-227 Marine anthropogenic litter. Springer.

Löder, M. G. J., M. Kuczera, S. Mintenig, C. Lorenz, and G. Gerdts. 2015. Focal plane array detector-based micro-Fourier-transform infrared imaging for the analysis of microplastics in environmental samples. Environmental Chemistry **12**:563-581.

Lorenz, C., L. Roscher, M. S. Meyer, L. Hildebrandt, J. Prume, M. G. J. Löder, S. Primpke, and G. Gerdts. 2019. Spatial distribution of microplastics in sediments and surface waters of the southern North Sea. Environmental Pollution **252B**:1719-1729.

Lusher, A., I. L. Bråte, K. Munno, R. Hurley, and N. Welden. 2020. EXPRESS: Is It or Isn't It: The Importance of Visual Classification in Microplastic Characterization. Applied Spectroscopy **74**:1139–1153.

Lv, X., Q. Dong, Z. Zuo, Y. Liu, X. Huang, and W.-M. Wu. 2019. Microplastics in a municipal wastewater treatment plant: Fate, dynamic distribution, removal efficiencies, and control strategies. Journal of Cleaner Production **225**:579-586.

Ma, P., m. Wei Wang, H. Liu, y. Feng Chen, and J. Xia. 2019. Research on ecotoxicology of microplastics on freshwater aquatic organisms. Environmental Pollutants and Bioavailability **31**:131-137.

Mai, L., L.-J. Bao, L. Shi, L.-Y. Liu, and E. Y. Zeng. 2018. Polycyclic aromatic hydrocarbons affiliated with microplastics in surface waters of Bohai and Huanghai Seas, China. environmental pollution **241**:834-840.

Mani, T., and P. Burkhardt-Holm. 2020. Seasonal microplastics variation in nival and pluvial stretches of the Rhine River – From the Swiss catchment towards the North Sea. Science of the Total Environment **707**:135579.

Mani, T., A. Hauk, U. Walter, and P. Burkhardt-Holm. 2015. Microplastics profile along the Rhine River. Scientific Reports **5**:17988.

Mani, T., S. Primpke, C. Lorenz, G. Gerdts, and P. Burkhardt-Holm. 2019. Microplastic pollution in benthic midstream sediments of the Rhine River. Environmental Science & Technology **53**:6053-6062.

Manjunatha, S., and S. Girisha. 2021. Characterization of microalgal biomass through fourier transforms infrared (FT-IR) spectroscopy. **6**:57-60.

Mansa, R., and S. Zou. 2021. Thermogravimetric analysis of microplastics: A mini review. Environmental Advances **5**:100117.

Mao, Y., H. Li, W. Gu, G. Yang, Y. Liu, and Q. He. 2020. Distribution and characteristics of microplastics in the Yulin River, China: Role of environmental and spatial factors. Environmental Pollution **265**:115033.

Mári, Á., G. Bordós, S. Gergely, M. Büki, J. Háhn, Z. Palotai, G. Besenyő, É. Szabó, A. Salgó, B. Kriszt, and S. Szoboszlay. 2021. Validation of microplastic sample preparation method for freshwater samples. Water Research **202**:117409.

Masura, J., J. Baker, G. Foster, and C. Arthur. 2015. Laboratory Methods for the Analysis of Microplastics in the Marine Environment: Recommendations for quantifying synthetic particles in waters and sediments.

Menéndez-Manjón, A., R. Martínez-Díez, D. Sol, A. Laca, A. Laca, A. Rancaño, and M. Díaz. 2022. Long-Term Occurrence and Fate of Microplastics in WWTPs: A Case Study in Southwest Europe. Applied Sciences **12**:2133.

Michielssen, M. R., E. R. Michielssen, J. Ni, and M. B. Duhaime. 2016. Fate of microplastics and other small anthropogenic litter (SAL) in wastewater treatment plants depends on unit processes employed. Environmental Science: Water Research & Technology **2**:1064-1073.

Mintenig, S. M., I. Int-Veen, M. G. J. Löder, S. Primpke, and G. Gerdts. 2017. Identification of microplastic in effluents of waste water treatment plants using focal plane array-based micro-Fourier-transform infrared imaging. Water Research **108**:365-372.

Mintenig, S. M., M. Kooi, M. W. Erich, S. Primpke, P. E. Redondo- Hasselerharm, S. C. Dekker, A. A. Koelmans, and A. P. van Wezel. 2020. A systems approach to understand microplastic occurrence and variability in Dutch riverine surface waters. Water Research **176**:115723.

Möhlenkamp, P., A. Purser, and L. Thomsen. 2018. Plastic microbeads from cosmetic products: an experimental study of their hydrodynamic behaviour, vertical transport and resuspension in phytoplankton and sediment aggregates. Page 61.

Möller, J. N., I. Heisel, A. Satzger, E. C. Vizsolyi, S. J. Oster, S. Agarwal, C. Laforsch, and M. G. Löder. 2022. Tackling the challenge of extracting microplastics from soils: a protocol to purify soil samples for spectroscopic analysis. Environmental Toxicology and Chemistry **41**:844-857.

Moore, R. C., L. Loseto, M. Noel, A. Etemadifar, J. D. Brewster, S. MacPhee, L. Bendell, and P. S. Ross. 2020. Microplastics in beluga whales (Delphinapterus leucas) from the Eastern Beaufort Sea. Marine Pollution Bulletin **150**:110723.

Moses, S. R., M. G. J. Löder, F. Herrmann, and C. Laforsch. in prep. Seasonal variations of the microplastic pollution in the German River Weser

Moses, S. R., L. Roscher, S. Primpke, B. Hufnagl, M. G. J. Löder, G. Gerdts, and C. Laforsch. 2023. Comparison of two rapid automated analysis tools for large FTIR microplastic datasets. Analytical and Bioanalytical Chemistry:1-13lytical

Murphy, F., C. Ewins, F. Carbonnier, and B. Quinn. 2016. Wastewater Treatment Works (WwTW) as a Source of Microplastics in the Aquatic Environment. Environmental Science & Technology **50**:5800-5808.

Naji, A., S. Azadkhah, H. Farahani, S. Uddin, and F. R. Khan. 2021. Microplastics in wastewater outlets of Bandar Abbas city (Iran): A potential point source of microplastics into the Persian Gulf. Chemosphere **262**:128039.

Napper, I. E., A. Baroth, A. C. Barrett, S. Bhola, G. W. Chowdhury, B. F. R. Davies, E. M. Duncan, S. Kumar, S. E. Nelms, M. N. Hasan Niloy, B. Nishat, T. Maddalene, R. C. Thompson, and H. Koldewey. 2021. The abundance and characteristics of microplastics in surface water in the transboundary Ganges River. Environmental Pollution **274**:116348.

Napper, I. E., and R. C. Thompson. 2016. Release of synthetic microplastic plastic fibres from domestic washing machines: Effects of fabric type and washing conditions. Marine Pollution Bulletin **112**:39-45.

Negrete Velasco, A. d. J., L. Rard, W. Blois, D. Lebrun, F. Lebrun, F. Pothe, and S. Stoll. 2020. Microplastic and Fibre Contamination in a Remote Mountain Lake in Switzerland. Water **12**:2410.

Norén, F. 2007. Small plastic particles in coastal swedish waters. KIMO Sweden, N-Research, Lysekil, Sweden.

Obbard, R., S. Sadri, Y.-Q. Wong, A. Khitun, I. Baker, and R. Thompson. 2014. Global warming releases microplastic legacy frozen in Arctic Sea ice. Earth's Future **2**:315-320.

Papenmeier, S., K. Schrottke, and A. Bartholomä. 2014. Over time and space changing characteristics of estuarine suspended particles in the German Weser and Elbe estuaries. Journal of Sea Research **85**:104-115.

Park, H.-J., M.-J. Oh, P.-G. Kim, G. Kim, D.-H. Jeong, B.-K. Ju, W.-S. Lee, H.-M. Chung, H.-J. Kang, and J.-H. Kwon. 2020a. National Reconnaissance Survey of Microplastics in Municipal Wastewater Treatment Plants in Korea. Environmental Science & Technology **54**:1503-1512.

Park, T.-J., S.-H. Lee, M.-S. Lee, J.-K. Lee, S.-H. Lee, and K.-D. Zoh. 2020b. Occurrence of microplastics in the Han River and riverine fish in South Korea. Science of the Total Environment **708**:134535.

Paul, A., L. Wander, R. Becker, C. Goedecke, and U. Braun. 2019. High-throughput NIR spectroscopic (NIRS) detection of microplastics in soil. Environmental Science and Pollution Research **26**:7364-7374.

Peeken, I., S. Primpke, B. Beyer, J. Gütermann, C. Katlein, T. Krumpen, M. Bergmann, L. Hehemann, and G. Gerdts. 2018. Arctic sea ice is an important temporal sink and means of transport for microplastic. Nature Communications **9**:1505.

Peng, G., B. Xu, and D. Li. 2022. Gray Water from Ships: A Significant Sea-Based Source of Microplastics? Environmental Science & Technology **56**:4-7.

Pfeiffer, F., and E. K. Fischer. 2020. Various Digestion Protocols Within Microplastic Sample Processing—Evaluating the Resistance of Different Synthetic Polymers and the Efficiency of Biogenic Organic Matter Destruction. Frontiers in Environmental Science **8**:572424.

Pham, D. N., L. Clark, and M. Li. 2021. Microplastics as hubs enriching antibiotic-resistant bacteria and pathogens in municipal activated sludge. Journal of Hazardous Materials Letters **2**:100014.

Piehl, S., E. C. Atwood, M. Bochow, H. K. Imhof, J. Franke, F. Siegert, and C. Laforsch. 2020. Can Water Constituents Be Used as Proxy to Map Microplastic Dispersal Within Transitional and Coastal Waters? Frontiers in Environmental Science **8**:92.

Piehl, S., R. Hauk, E. Robbe, B. Richter, F. Kachholz, J. Schilling, R. Lenz, D. Fischer, F. Fischer, M. Labrenz, and G. Schernewski. 2021. Combined Approaches to Predict Microplastic Emissions Within an Urbanized Estuary (Warnow, Southwestern Baltic Sea). Frontiers in Environmental Science **9**:616765.

Piperagkas, O., and N. Papageorgiou. 2021. Changes in (micro and macro) plastic pollution in the sediment of three sandy beaches in the Eastern Mediterranean Sea, in relation to seasonality, beach use and granulometry. Marine Pollution Bulletin **173**:113014.

PlasticsEurope. 2020. Plastics - the Facts 2020. An analysis of European plastics production, demand and waste data.

Porter, A., B. P. Lyons, T. S. Galloway, and C. Lewis. 2018. Role of Marine Snows in Microplastic Fate and Bioavailability. Environmental Science & Technology **52**:7111-7119.

Primpke, S., S. H. Christiansen, W. Cowger, H. De Frond, A. Deshpande, M. Fischer, E. B. Holland, M. Meyns, B. A. O'Donnell, B. E. Ossmann, M. Pittroff, G. Sarau, B. M. Scholz-Böttcher, and K. J. Wiggin. 2020a. Critical Assessment of Analytical Methods for the Harmonized and Cost-Efficient Analysis of Microplastics. Applied Spectroscopy **74**:1012-1047.

Primpke, S., R. K. Cross, S. M. Mintenig, M. Simon, A. Vianello, G. Gerdts, and J. Vollertsen. 2020b. Toward the Systematic Identification of Microplastics in the Environment: Evaluation of a New Independent Software Tool (siMPle) for Spectroscopic Analysis. Applied Spectroscopy **74**:1127-1138.

Primpke, S., P. Dias, and G. Gerdts. 2019. Automated Identification and Quantification of Microfibres and Microplastics. Analytical Methods **11**:2138-2147.

Primpke, S., M. Fischer, C. Lorenz, G. Gerdts, and B. Scholz-Böttcher. 2020c. Comparison of pyrolysis gas chromatography/mass spectrometry and hyperspectral FTIR imaging spectroscopy for the analysis of microplastics. Analytical and Bioanalytical Chemistry **412**:8283–8298.

Primpke, S., M. Godejohann, and G. Gerdts. 2020d. Rapid Identification and Quantification of Microplastics in the Environment by Quantum Cascade Laser-Based Hyperspectral Infrared Chemical Imaging. Environmental Science & Technology **54**:15893-15903.

Primpke, S., C. Lorenz, R. Rascher-Friesenhausen, and G. Gerdts. 2017. An automated approach for microplastics analysis using focal plane array (FPA) FTIR microscopy and image analysis. Analytical Methods **9**: 1499-1511.

Primpke, S., M. Wirth, C. Lorenz, and G. Gerdts. 2018. Reference database design for the automated analysis of microplastic samples based on Fourier transform infrared (FTIR) spectroscopy. Analytical and Bioanalytical Chemistry **410**:5131-5141.

Provencher, J. F., G. A. Covernton, R. C. Moore, D. A. Horn, J. L. Conkle, and A. L. Lusher. 2020. Proceed with caution: The need to raise the publication bar for microplastics research. Science of the Total Environment **748**:141426.

Ramírez-Álvarez, N., L. M. Rios Mendoza, J. V. Macías-Zamora, L. Oregel-Vázquez, A. Alvarez-Aguilar, F. A. Hernández-Guzmán, J. L. Sánchez-Osorio, C. J. Moore, H. Silva-Jiménez, and L. F. Navarro-Olache. 2020. Microplastics: Sources and distribution in surface waters and sediments of Todos Santos Bay, Mexico. Science of the Total Environment **703**:134838.

Rasmussen, L. A., L. Iordachescu, S. Tumlin, and J. Vollertsen. 2021. A complete mass balance for plastics in a wastewater treatment plant - Macroplastics contributes more than microplastics. Water Research **201**:117307.

Renner, G., A. Nellessen, A. Schwiers, M. Wenzel, T. Schmidt, and J. Schram. 2018. Data Preprocessing & Evaluation used in the Microplastics Identification Process: A Critical Review & Practical Guide. TrAC Trends in Analytical Chemistry **111**:229-238.

Renner, G., P. Sauerbier, T. C. Schmidt, and J. r. Schram. 2019. Robust automatic identification of microplastics in environmental samples using FTIR microscopy. Analytical Chemistry **91**:9656-9664.

Renner, G., T. C. Schmidt, and J. Schram. 2017. A New Chemometric Approach for Automatic Identification of Microplastics from Environmental Compartments Based on FT-IR Spectroscopy. Analytical Chemistry **89**:12045-12053.

Rillig, M. C. 2012. Microplastic in Terrestrial Ecosystems and the Soil? Environmental Science & Technology **46**:6453-6454.

Rillig, M. C., and A. Lehmann. 2020. Microplastic in terrestrial ecosystems. Science **368**:1430-1431.

Rist, S., A. Vianello, M. H. S. Winding, T. G. Nielsen, R. Almeda, R. R. Torres, and J. Vollertsen. 2020. Quantification of plankton-sized microplastics in a productive coastal Arctic marine ecosystem. Environmental Pollution **266**:115248.

Rögener, F., S. Theus, A. Chusov, and J. Lednova. 2021. How Membrane Bioreactor Technology Can Help to Solve Both, German and Russian Wastewater Problems. Pages 89-100 Towards Water Secure Societies. Springer.

Roscher, L., A. Fehres, L. Reisel, M. Halbach, B. Scholz-Böttcher, M. Gerriets, T. H. Badewien, G. Shiravani, A. Wurpts, S. Primpke, and G. Gerdts. 2021. Microplastic pollution in the Weser estuary and the German North Sea. Environmental Pollution **288**:117681.

Roscher, L., M. Halbach, M. T. Nguyen, M. Hebeler, F. Luschtinetz, B. M. Scholz-Böttcher, S. Primpke, and G. Gerdts. 2022. Microplastics in two German wastewater treatment plants: Year-long effluent analysis with FTIR and Py-GC/MS. Science of the Total Environment **817**:152619.

Rummel, C. D., M. G. J. Löder, N. F. Fricke, T. Lang, E.-M. Griebeler, M. Janke, and G. Gerdts. 2016. Plastic ingestion by pelagic and demersal fish from the North Sea and Baltic Sea. Marine Pollution Bulletin **102**:134-141.

Russell, M., and L. Webster. 2021. Microplastics in sea surface waters around Scotland. Marine Pollution Bulletin **166**:112210.

Ryan, P. G. 2018. Entanglement of birds in plastics and other synthetic materials. Marine Pollution Bulletin **135**:159-164.

Ryan, P. G., C. J. Moore, J. A. Van Franeker, and C. L. Moloney. 2009. Monitoring the abundance of plastic debris in the marine environment. Philosophical Transactions of the Royal Society B: Biological Sciences **364**:1999-2012.

Saeed, T., N. Aljandal, A. Mutairi, and H. Taqi. 2020. Microplastics in Kuwait marine environment: Results of first survey. Marine Pollution Bulletin **152**:110880.

Saliu, F., G. Biale, C. Raguso, J. La Nasa, I. Degano, D. Seveso, P. Galli, M. Lasagni, and F. Modugno. 2022. Detection of plastic particles in marine sponges by a combined infrared micro-spectroscopy and pyrolysis-gas chromatography-mass spectrometry approach. Science of the Total Environment **819**:152965.

Sanchez, W., C. Bender, and J.-M. Porcher. 2014. Wild gudgeons (Gobio gobio) from French rivers are contaminated by microplastics: Preliminary study and first evidence. Environmental Research **128**:98-100.

Scherer, C., A. Weber, S. Lambert, and M. Wagner. 2018. Interactions of microplastics with freshwater biota. Pages 153-180 Freshwater microplastics. Springer, Cham.

Scherer, C., A. Weber, F. Stock, S. Vurusic, H. Egerci, C. Kochleus, N. Arendt, C. Foeldi, G. Dierkes, M. Wagner, N. Brennholt, and G. Reifferscheid. 2020. Comparative assessment of microplastics in water and sediment of a large European river. Science of the Total Environment **738**:139866.

Schmidt, C., R. Kumar, S. Yang, and O. Büttner. 2020. Microplastic particle emission from wastewater treatment plant effluents into river networks in Germany: Loads, spatial patterns of concentrations and potential toxicity. Science of the Total Environment **737**:139544.

Schmidt, L. K., M. Bochow, H. K. Imhof, and S. E. Oswald. 2018. Multi-temporal surveys for microplastic particles enabled by a novel and fast application of SWIR imaging spectroscopy – Study of an urban watercourse traversing the city of Berlin, Germany. Environmental Pollution **239**:579-589.

Schöneich-Argent, R. I., K. Dau, and H. Freund. 2020. Wasting the North Sea? – A field-based assessment of anthropogenic macrolitter loads and emission rates of three German tributaries. Environmental Pollution **263**:114367.

Schönlau, C., T. M. Karlsson, A. Rotander, H. Nilsson, M. Engwall, B. van Bavel, and A. Kärrman. 2020. Microplastics in sea-surface waters surrounding Sweden sampled by manta trawl and in-situ pump. Marine Pollution Bulletin **153**:111019.

Schrank, I., M. G. J. Löder, H. K. Imhof, S. R. Moses, M. Heß, J. Schwaiger, and C. Laforsch. 2022. Riverine microplastic contamination in southwest Germany: A large-scale survey. Frontiers in Earth Science **10**:794250.

Schrottke, K., M. Becker, A. Bartholomä, B. Flemming, and D. Hebbeln. 2006. Fluid mud dynamics in the Weser estuary turbidity zone tracked by high-resolution side-scan sonar and parametric sub-bottom profiler. Geo-Mar. Lett. **26**:185-198.

Schwaferts, C., R. Niessner, M. Elsner, and N. P. Ivleva. 2019. Methods for the analysis of submicrometer- and nanoplastic particles in the environment. TrAC Trends in Analytical Chemistry **112**:52-65.

Schymanski, D., B. E. Oßmann, N. Benismail, K. Boukerma, G. Dallmann, E. von der Esch, D. Fischer, F. Fischer, D. Gilliland, K. Glas, T. Hofmann, A. Käppler, S. Lacorte, J. Marco, M. E. L. Rakwe, J. Weisser, C. Witzig, N. Zumbülte, and N. P. Ivleva. 2021. Analysis of microplastics in drinking water and other clean water samples with micro-Raman and micro-infrared spectroscopy: minimum requirements and best practice guidelines. Analytical and Bioanalytical Chemistry **413**:5969-5994.

Serranti, S., R. Palmieri, G. Bonifazi, and A. Cózar. 2018. Characterization of microplastic litter from oceans by an innovative approach based on hyperspectral imaging. Waste Management **76**:117-125.

Sevillano-González, M., J. González-Sálamo, F. J. Díaz-Peña, C. Hernández-Sánchez, S. Catalán Torralbo, A. Ródenas Seguí, and J. Hernández-Borges. 2022. Assessment

of microplastic content in Diadema africanum sea urchin from Tenerife (Canary Islands, Spain). Marine Pollution Bulletin **175**:113174.

Sewwandi, M., O. Hettithanthri, S. M. Egodage, A. A. D. Amarathunga, and M. Vithanage. 2022. Unprecedented marine microplastic contamination from the X-Press Pearl container vessel disaster. Science of the Total Environment **828**:154374.

Shan, J., J. Zhao, Y. Zhang, L. Liu, F. Wu, and X. Wang. 2019. Simple and rapid detection of microplastics in seawater using hyperspectral imaging technology. Analytica Chimica Acta **1050**:161-168.

Shim, W. J., S. H. Hong, and S. Eo. 2018. Chapter 1 - Marine Microplastics: Abundance, Distribution, and Composition. Pages 1-26 *in* E. Y. Zeng, editor. Microplastic Contamination in Aquatic Environments. Elsevier.

Shim, W. J., S. H. Hong, and S. E. Eo. 2017. Identification methods in microplastic analysis: a review. Analytical Methods **9**:1384-1391.

Shim, W. J., Y. K. Song, S. H. Hong, and M. Jang. 2016. Identification and quantification of microplastics using Nile Red staining. Marine Pollution Bulletin **113**:469-476.

Siegfried, M., A. A. Koelmans, E. Besseling, and C. Kroeze. 2017. Export of microplastics from land to sea. A modelling approach. Water Research **127**:249-257.

Silvestrova, K., and N. Stepanova. 2021. The distribution of microplastics in the surface layer of the Atlantic Ocean from the subtropics to the equator according to visual analysis. Marine Pollution Bulletin **162**:111836.

Simon, M., N. van Alst, and J. Vollertsen. 2018. Quantification of microplastic mass and removal rates at wastewater treatment plants applying Focal Plane Array (FPA)-based Fourier Transform Infrared (FT-IR) imaging. Water Research **142**:1-9.

Sobhani, Z., M. Al Amin, R. Naidu, M. Megharaj, and C. Fang. 2019. Identification and visualisation of microplastics by Raman mapping. Analytica Chimica Acta **1077**:191-199.

Song, J., E. Jongmans-Hochschulz, N. Mauder, C. Imirzalioglu, A. Wichels, and G. Gerdts. 2020. The Travelling Particles: Investigating microplastics as possible transport vectors for multidrug resistant E. coli in the Weser estuary (Germany). Science of the Total Environment **720**:137603.

Song, Y. K., S. H. Hong, S. Eo, and W. J. Shim. 2021a. A comparison of spectroscopic analysis methods for microplastics: Manual, semi-automated, and automated Fourier transform infrared and Raman techniques. Marine Pollution Bulletin **173**:113101.

Song, Y. K., S. H. Hong, M. Jang, J. H. Kang, O. Y. Kwon, G. M. Han, and W. J. Shim. 2014. Large Accumulation of Micro-sized Synthetic Polymer Particles in the Sea Surface Microlayer. Environmental Science & Technology **48**:9014-9021.

Song, Z., K. Liu, X. Wang, N. Wei, C. Zong, C. Li, C. Jiang, Y. He, and D. Li. 2021b. To what extent are we really free from airborne microplastics? Science of the Total Environment **754**:142118.

Sooksai, T., W. Bankeeree, U. Sangwatanaroj, P. Lotrakul, H. Punnapayak, and S. Prasongsuk. 2019. Production of cutinase from Fusarium falciforme and its application for hydrophilicity improvement of polyethylene terephthalate fabric. 3 Biotech **9**:389.

Stanev, E. V., B. Jacob, and J. Pein. 2019. German Bight estuaries: An inter-comparison on the basis of numerical modeling. Continental Shelf Research **174**:48-65.

Stelfox, M., J. Hudgins, and M. Sweet. 2016. A review of ghost gear entanglement amongst marine mammals, reptiles and elasmobranchs. Marine Pollution Bulletin **111**:6-17.

Stock, F., C. Kochleus, B. Bänsch-Baltruschat, N. Brennholt, and G. Reifferscheid. 2019. Sampling techniques and preparation methods for microplastic analyses in the aquatic environment – A review. TrAC Trends in Analytical Chemistry **113**:84-92.

Stolte, A., S. Forster, G. Gerdts, and H. Schubert. 2015. Microplastic concentrations in beach sediments along the German Baltic coast. Marine Pollution Bulletin **99**:216-229.

Suaria, G., V. Perold, J. R. Lee, F. Lebouard, S. Aliani, and P. G. Ryan. 2020. Floating macro- and microplastics around the Southern Ocean: Results from the Antarctic Circumnavigation Expedition. Environment International **136**:105494.

Sun, J., X. Dai, Q. Wang, M. C. van Loosdrecht, and B.-J. Ni. 2019. Microplastics in wastewater treatment plants: Detection, occurrence and removal. Water Research **152**:21-37.

Szewc, K., B. Graca, and A. Dołęga. 2021. Atmospheric deposition of microplastics in the coastal zone: Characteristics and relationship with meteorological factors. Science of the Total Environment **761**:143272.

Tagg, A. S., M. Sapp, J. P. Harrison, C. J. Sinclair, E. Bradley, Y. Ju-Nam, and J. J. Ojeda. 2020. Microplastic Monitoring at Different Stages in a Wastewater Treatment Plant Using Reflectance Micro-FTIR Imaging. Frontiers in Environmental Science **8**:145.

Talbot, R., and H. Chang. 2022. Microplastics in freshwater: A global review of factors affecting spatial and temporal variations. Environmental Pollution **292**:118393.

Talvitie, J., A. Mikola, A. Koistinen, and O. Setälä. 2017a. Solutions to microplastic pollution – Removal of microplastics from wastewater effluent with advanced wastewater treatment technologies. Water Research **123**:401-407.

Talvitie, J., A. Mikola, O. Setälä, M. Heinonen, and A. Koistinen. 2017b. How well is microlitter purified from wastewater? – A detailed study on the stepwise removal of microlitter in a tertiary level wastewater treatment plant. Water Research **109**:164-172.

Tanaka, K., and H. Takada. 2016. Microplastic fragments and microbeads in digestive tracts of planktivorous fish from urban coastal waters. Scientific Reports **6**:34351.

Teichert, S., M. G. J. Löder, I. Pyko, M. Mordek, C. Schulbert, M. Wisshak, and C. Laforsch. 2021. Microplastic contamination of the drilling bivalve Hiatella arctica in Arctic rhodolith beds. Scientific Reports **11**:14574.

Tekman, M. B., C. Wekerle, C. Lorenz, S. Primpke, C. Hasemann, G. Gerdts, and M. Bergmann. 2020. Tying up Loose Ends of Microplastic Pollution in the Arctic: Distribution from the Sea Surface through the Water Column to Deep-Sea Sediments at the HAUSGARTEN Observatory. Environmental Science & Technology **54**:4079-4090.

ter Halle, A., L. Ladirat, X. Gendre, D. Goudouneche, C. Pusineri, C. Routaboul, C. Tenailleau, B. Duployer, and E. Perez. 2016. Understanding the Fragmentation Pattern of Marine Plastic Debris. Environmental Science & Technology **50**:5668-5675.

Turner, A. 2010. Marine pollution from antifouling paint particles. Marine Pollution Bulletin **60**:159-171.

Turner, A. 2021. Paint particles in the marine environment: An overlooked component of microplastics. Water Research X **12**:100110.

Uurasjärvi, E., S. Hartikainen, O. Setälä, M. Lehtiniemi, and A. Koistinen. 2020. Microplastic concentrations, size distribution, and polymer types in the surface waters of a northern European lake. Water Environment Research **92**:149-156.

van Den Dool, H., and P. D. Kratz. 1963. A generalization of the retention index system including linear temperature programmed gas—liquid partition chromatography. Journal of Chromatography A **11**:463-471.

van der Molen, J., S. M. van Leeuwen, L. L. Govers, T. van der Heide, and H. Olff. 2021. Potential Micro-Plastics Dispersal and Accumulation in the North Sea, With Application to the MSC Zoe Incident. Frontiers in Marine Science **8**:607203.

van Emmerik, T., and A. Schwarz. 2020. Plastic debris in rivers. Wiley Interdisciplinary Reviews: Water **7**:e1398.

van Wijnen, J., A. M. Ragas, and C. Kroeze. 2019. Modelling global river export of microplastics to the marine environment: Sources and future trends. Science of the Total Environment **673**:392-401.

Veerasingam, S., M. Mugilarasan, R. Venkatachalapathy, and P. Vethamony. 2016. Influence of 2015 flood on the distribution and occurrence of microplastic pellets along the Chennai coast, India. Marine Pollution Bulletin **109**:196-204.

Wagner, M., C. Scherer, D. Alvarez-Muñoz, N. Brennholt, X. Bourrain, S. Buchinger, E. Fries, C. Grosbois, J. Klasmeier, T. Marti, S. Rodriguez-Mozaz, R. Urbatzka, A. D. Vethaak, M. Winther-Nielsen, and G. Reifferscheid. 2014. Microplastics in freshwater ecosystems: what we know and what we need to know. Environmental Sciences Europe **26**:12.

Wagner, S., P. Klöckner, B. Stier, M. Römer, B. Seiwert, T. Reemtsma, and C. Schmidt. 2019. Relationship between Discharge and River Plastic Concentrations in a Rural and an Urban Catchment. Environmental Science & Technology **53**:10082-10091.

Waldschläger, K., and H. Schüttrumpf. 2019. Erosion behavior of different microplastic particles in comparison to natural sediments. Environmental Science & Technology **53**:13219-13227.

Waller, C. L., H. J. Griffiths, C. M. Waluda, S. E. Thorpe, I. Loaiza, B. Moreno, C. O. Pacherres, and K. A. Hughes. 2017. Microplastics in the Antarctic marine system: An emerging area of research. Science of the Total Environment **598**:220-227.

Wang, G., J. Lu, Y. Tong, Z. Liu, H. Zhou, and N. Xiayihazi. 2020. Occurrence and pollution characteristics of microplastics in surface water of the Manas River Basin, China. Science of the Total Environment **710**:136099.

Wang, T., J. Wang, Q. Lei, Y. Zhao, L. Wang, X. Wang, and W. Zhang. 2021a. Microplastic pollution in sophisticated urban river systems: Combined influence of land-use types and physicochemical characteristics. Environmental Pollution **287**:117604.

Wang, T., X. Zou, B. Li, Y. Yao, Z. Zang, Y. Li, W. Yu, and W. Wang. 2019. Preliminary study of the source apportionment and diversity of microplastics: Taking floating microplastics in the South China Sea as an example. Environmental Pollution **245**:965-974.

Wang, Z., Y. Zhang, S. Kang, L. Yang, H. Shi, L. Tripathee, and T. Gao. 2021b. Research progresses of microplastic pollution in freshwater systems. Science of the Total Environment **795**:148888.

Weisser, J., I. Beer, B. Hufnagl, T. Hofmann, H. Lohninger, N. P. Ivleva, and K. Glas. 2021. From the Well to the Bottle: Identifying Sources of Microplastics in Mineral Water. Water **13**:841.

Weithmann, N., J. N. Möller, M. G. J. Löder, S. Piehl, C. Laforsch, and R. Freitag. 2018. Organic fertilizer as a vehicle for the entry of microplastic into the environment. Science Advances **4**:eaap8060.

Werbowski, L. M., A. N. Gilbreath, K. Munno, X. Zhu, J. Grbic, T. Wu, R. Sutton, M. D. Sedlak, A. D. Deshpande, and C. M. Rochman. 2021. Urban Stormwater Runoff: A

Major Pathway for Anthropogenic Particles, Black Rubbery Fragments, and Other Types of Microplastics to Urban Receiving Waters. ACS ES&T Water **1**:1420-1428.
Westad, F., and F. Marini. 2015. Validation of chemometric models – A tutorial. Analytica Chimica Acta **893**:14-24.
Winterwerp, J. C. 2002. On the flocculation and settling velocity of estuarine mud. Continental Shelf Research **22**:1339-1360.
Wolff, S., J. Kerpen, J. Prediger, L. Barkmann, and L. Müller. 2019. Determination of the microplastics emission in the effluent of a municipal waste water treatment plant using Raman microspectroscopy. Water Research X **2**:100014.
Wolff, S., F. Weber, J. Kerpen, M. Winklhofer, M. Engelhart, and L. Barkmann. 2020. Elimination of microplastics by downstream sand filters in wastewater treatment. Water **13**:33.
Wong, G., L. Löwemark, and A. Kunz. 2020. Microplastic pollution of the Tamsui River and its tributaries in northern Taiwan: Spatial heterogeneity and correlation with precipitation. Environmental Pollution **260**:113935.
Wright, L. S., I. E. Napper, and R. C. Thompson. 2021. Potential microplastic release from beached fishing gear in Great Britain's region of highest fishing litter density. Marine Pollution Bulletin **173**:113115.
Xu, Q., R. Xing, M. Sun, Y. Gao, and L. An. 2020. Microplastics in sediments from an interconnected river-estuary region. Science of the Total Environment **729**:139025.
Yin, L., C. Jiang, X. Wen, C. Du, W. Zhong, Z. Feng, Y. Long, and Y. Ma. 2019. Microplastic Pollution in Surface Water of Urban Lakes in Changsha, China. International Journal of Environmental Research and Public Health **16**:1650.
Yong, C. Q. Y., S. Valiyaveettil, and B. L. Tang. 2020. Toxicity of microplastics and nanoplastics in mammalian systems. International Journal of Environmental Research and Public Health **17**:1509.
Zhang, H., Q. Zhou, Z. Xie, Y. Zhou, C. Tu, C. Fu, W. Mi, R. Ebinghaus, P. Christie, and Y. Luo. 2018a. Occurrences of organophosphorus esters and phthalates in the microplastics from the coastal beaches in north China. Science of the Total Environment **616-617**:1505-1512.
Zhang, J., K. Tian, C. Lei, and S. Min. 2018b. Identification and quantification of microplastics in table sea salts using micro-NIR imaging methods. Analytical Methods **10**:2881-2887.
Zhang, L., J. Liu, Y. Xie, S. Zhong, B. Yang, D. Lu, and Q. Zhong. 2020. Distribution of microplastics in surface water and sediments of Qin river in Beibu Gulf, China. Science of the Total Environment **708**:135176.
Zhang, L., Y. Xie, S. Zhong, J. Liu, Y. Qin, and P. Gao. 2021a. Microplastics in freshwater and wild fishes from Lijiang River in Guangxi, Southwest China. Science of the Total Environment **755**:142428.
Zhang, X., S. Li, Y. Liu, K. Yu, H. Zhang, H. Yu, and J. Jiang. 2021b. Neglected microplastics pollution in the nearshore surface waters derived from coastal fishery activities in Weihai, China. Science of the Total Environment **768**:144484.
Zhao, S., E. R. Zettler, R. P. Bos, P. Lin, L. A. Amaral-Zettler, and T. J. Mincer. 2022. Large quantities of small microplastics permeate the surface ocean to abyssal depths in the South Atlantic Gyre. Global Change Biology **28**:2991-3006.
Zhao, S., L. Zhu, L. Gao, and D. Li. 2018. Chapter 2 - Limitations for Microplastic Quantification in the Ocean and Recommendations for Improvement and Standardization. Pages 27-49 *in* E. Y. Zeng, editor. Microplastic Contamination in Aquatic Environments. Elsevier.

Zhao, S., L. Zhu, and D. Li. 2015a. Microplastic in three urban estuaries, China. Environmental Pollution **206**:597-604.

Zhao, Z., Z. Xie, J. Tang, R. Sturm, Y. Chen, G. Zhang, and R. Ebinghaus. 2015b. Seasonal variations and spatial distributions of perfluoroalkyl substances in the rivers Elbe and lower Weser and the North Sea. Chemosphere **129**:118-125.

Zheng, Y., J. Li, C. Sun, W. Cao, M. Wang, F. Jiang, and P. Ju. 2021. Comparative study of three sampling methods for microplastics analysis in seawater. Science of the Total Environment **765**:144495.

Zorndt, A., T. Schlurmann, and I. Grabemann. 2012. The influence of extreme events on hydrodynamics and salinities in the weser estuary in the context of climate impact research. Coastal Engineering Proceedings **1**.

Additional publications

Cabernard, L., L. Roscher, C. Lorenz, G. Gerdts, and S. Primpke. 2018. Comparison of Raman and Fourier Transform Infrared Spectroscopy for the Quantification of Microplastics in the Aquatic Environment. Environmental Science & Technology **52**:13279–13288. https://pubs.acs.org/doi/10.1021/acs.est.8b03438

Lorenz, C., L. Roscher, M. S. Meyer, L. Hildebrandt, J. Prume, M. G. J. Löder, S. Primpke, and G. Gerdts. 2019. Spatial distribution of microplastics in sediments and surface waters of the southern North Sea. Environmental Pollution **252B**:1719-1729. https://doi.org/10.1016/j.envpol.2019.06.093

Lorenz, C., M. Schafberg, L. Roscher, M. S. Meyer, S. Primpke, U. R. Kraus, and G. Gerdts. 2021. Paraffin and other petroleum waxes in the southern North Sea. Marine Pollution Bulletin **162**:111807. https://doi.org/10.1016/j.marpolbul.2020.111807

Acknowledgements

First of all, I am extremely grateful for the support and advice provided to me by my PhD committee over the last years. I would like to kindly thank the Chair of my committee, Professor Matthias Ullrich, for his steady support and advice, also with respect to administrational aspects of the PhD, and Professor Laurenz Thomsen for his scientific input during the committee meetings. My supervisors at the AWI on Helgoland Dr. Gunnar Gerdts and Dr. Sebastian Primpke were always there for fruitful discussions and helpful advice in challenging situations.

A huge 'thank you' goes to the *Microbial Ecology* working group situated on Helgoland, led by Dr. Gunnar Gerdts and Dr. Antje Wichels. Corona did not always make it easy, but it was a pleasure to conduct my thesis in this group. I felt supported and at home, and highly appreciate the motivating words in difficult situations. In terms of hands-on support but also inspiring discussions, I especially thank the master's students Lorenz Reisel, Annika Fehres and Minh Trang Nguyen, as well as our technical assistant Hannah Jebens. Furthermore I would like to thank the *Haustechnik* team of the AWI on Helgoland, for the technical support, such as building or repairing tools or transporting tons of sampling equipment over the island. Also, I would like to thank the crew of the research vessel Uthörn for their help during the sampling campaign.

I would further like to thank the BMBF for supporting this work financially, as well as the partners and stakeholders within the project FONA PLAWES for the fruitful cooperation, exchange of ideas and constructive discussions.

Without the unconditional support of family and friends, I couldn't have done it. My family was understanding, and positive throughout the whole time, providing a safe haven whenever I needed it. I would also like to thank Lisa (*Böller*) for being there for me, and supporting me during the last years with an open ear and her faith in me. Last, but not least, I would like to thank Nick for being there for me, no matter what – thank you for your unlimited support and patience.